An integrated view of changing nutrient availability in model species:

The role of signaling in the plant response

Memoria presentada por **Beatriz Royo Castillejo** para optar al Grado de Doctora con mención de "Doctor Internacional"

Beatriz Royo Castillejo

Pamplona, mayo 2017

A Javi

A Haizea

A mi familia

Quisiera agradecer al Grupo de Fisiología Vegetal y Agrobiología del Departamento de Ciencias del Medio Natural de la Escuela Técnica Superior de Ingenieros Agrónomos de la Universidad Pública de Navarra (UPNA), y al Instituto de Agrobiología, IdAB (CSIC-UPNA-Gobierno de Navarra), en especial a mis directores, el Dr. José F. Morán y a la Dra. Raquel Esteban por darme la oportunidad de realizar este trabajo. Así mismo me gustaría dar las gracias a:

- Al Department of Plant Science de la Universidad de Oxford (Reino Unido), especialmente al Professor George R. Ratcliffe y al Dr. Jagadis K. Gupta por darme la oportunidad de realizar una estancia en su laboratorio.
- Al Departamento de Bioquímica y Biología Molecular de la Universidad de Córdoba, en especial al Dr. Emilio Fernández por permitirme realizar una estancia en el grupo Biología Molecular de la Asimilación de Nitrato en Algas.
- A la Dra. Esther González y a la Dra. Estíbaliz Larrainzar por cederme desinteresandamente semillas de *Medciago truncatula.*

La autora de la tesis doctoral ha disfrutado una ayuda para la Formación de Personal Investigador (FPI) (BES-2011-044363). Asimismo, ha disfrutado de las ayudas EEBB-I-13-06475 y : EEBB-I-14-00560 del Ministerio de Ciencia e Innovación (MICINN) del Gobierno de España para la realización de sendas estancias en las Universidades de Oxford y Córdoba. Además la autora también ha disfrutado de una beca para la asistencia al XX Congreso de la Sociedad Española de Fisiología Vegetal celebrado en Toledo (2015). La directora de la presente tesis doctoral ha disfrutado de JAE-Doc-2011-046 contrato del CSIC "Junta para la Ampliación de Estudios" y co-financidado por el Fondo Social Europeo y un contrato Juan de la Cierva-Incorporación IJCI-2014-21452. Este trabajo de investigación ha recibido financiación de proyectos de investigación AGL2010-16167; AGL2014-52396 del Ministerio de Economía y Competitividad (MINECO) del Gobierno de España, y la Ayuda Intra-Europea Marie Curie para el Desarrollo Profesional dentro del 7º Programa Marco de la Comunidad Europea.

Resumen

Las plantas tienen que hacer frente a situaciones cambiantes en cuanto a la disponibilidad de nutrientes, por ese motivo en la presente tesis se ha estudiado la respuesta de (i) *Arabidopsis thaliana* frente a la deficiencia de fósforo, y de (ii) *Medicago truncatula* expuesto a diferentes fuentes de N. En este sentido, la deficiencia de fosfato afecta al transporte de electrones mediado por el citocromo *c* en la cadena de transporte de electrones de la mitocondria, con lo que las plantas habitualmente aumentan el flujo de electrones a través de la oxidasa alternativa (AOX). Con el objetivo de discernir si esta respuesta está unida a un aumento en la producción de óxido nítrico (NO) bajo la deficiencia de fosfato, se crecieron axénicamente plántulas wild type (WT) y doble mutantes de la nitrato reductasa (*nia)* de *Arabidopsis thaliana* durante 15 días en un medio que contenía una concentración de fosfato inorgánico de 0 ó 1 mM. La deficiencia de fosfato produjo un aumento de la producción de NO en las raíces WT, y a su vez también incrementó la cantidad de AOX así como la capacidad de consumir electrones de la vía alternativa en plántulas WT. Sin embargo, bajo el mismo tratamiento las mutantes *nia* no fueron capaces de estimular la producción de NO ni la expresión de la AOX, y como consecuencia se alteró el crecimiento de estas plántulas que exhibieron un fenotipo diferente. La adición de *S*-nitrosoglutatión en el medio de cultivo sin fosfato, en cierto modo restituyó el fenotipo de los mutantes *nia*, al mismo tiempo que aumentó la capacidad respiratoria asociada a la AOX. De esta manera, se puede concluir que el NO es necesario para la inducción de la vía alternativa de respiración en situaciones en las que la disponibilidad del fosfato es limitada. En la segunda parte de esta tesis, mediante la utilización de condiciones axénicas se ha identificado la respuesta temprana así como el comportamiento de *Medicago truncatuala* frente a la utilización de amonio y urea como únicas fuentes de N en comparación con la nutrición nítrica. Tanto el amonio como la urea afectaron a la arquitectura radicular, observándose cambios en el ratio de crecimiento de la raíz principal, en el desarrollo de las raíces laterales, así como alternaciones en el punto de inserción de la raíz. El contenido de auxinas disminuyó en raíces tratadas con amonio y urea, mientras que respecto a la parte aérea únicamente se vieron afectadas las plantas crecidas en amonio. El análisis de fluorescencia de la clorofila *a* mostró que mientras el aporte de amonio afectó al fotosistema II, la urea no perjudicó la actividad fotosintética. En raíces, tanto el amonio como la urea afectaron de forma moderada las isoenzimas plastidiales de la actividad superóxido dismutasa. Por otro lado, la exposición a bajas dosis (1mM) de amonio y urea no tuvo efectos en el metabolismo ni en la señalización del N. Bajo estas condiciones, se observó una inducción de las acuaporinas así como cambios en el metabolismo de los fenilpropanoides de las raíces indicando que la absorción de N del medio por las plantas

está mediada por un adecuado mecanismo de detección. Sin embargo, altas dosis (25mM) de N produjeron cambios moderados en las plantas pero no se observaron signos de toxicidad ni estrés nitro-oxidativo. El contenido de aminoácidos libres y de ureidos se vio afectado a altas concentraciones de N, observándose como resultado un aumento en la producción de amidas así como la activación del ciclo GABA para compensar el exceso de N asimilado bajo nutrición amoniacal. Las raíces crecidas con amonio produjeron las mismas cantidades de NO que las raíces nítricas, indicando que dicho NO podría estar implicado en la respuesta de *M. truncatula* a altas concentraciones de amonio. En general, nuestros resultados indicaron que las distintas fuentes de N no tuvieron efectos remarcables en *M. truncatula* crecido a bajas dosis, con excepción de la distinta respuesta fenotípica encontrada en las raíces. En conjunto, estos datos demuestran que tanto el ácido 3-indolacético y el rendimiento fotosintético son componentes importantes en la respuesta de *M. truncatula* crecida con amonio o urea como fuentes exclusivas de N. Además, otras piezas clave en la tolerancia de *M. truncatula* frente a la nutrición con amonio y urea son la redistribución del N asimilado, la disponibilidad de un mecanismo de detección muy específico de la fuente de N a nivel de pared celular y membrana plasmática, así como el papel que el NO puede estar desempeñando.

Summary

The present thesis is focused on the responses of (i) *Arabidopsis thaliana* to phosphate starvation, and (ii) *Medicago truncatula* to different N sources. In this sense, phosphate starvation compromises electron flow through the cytochrome pathway of the mitochondrial electron transport chain, and plants commonly respond to phosphate deprivation by increasing flow through the alternative oxidase (AOX). To test whether this response is linked to the increase in nitric oxide (NO) production that also increases under phosphate starvation, *Arabidopsis thaliana* seedlings (wild type, WT and nitrate reductase double mutant *nia*) were grown for 15 days on media containing either 0 or 1mM inorganic phosphate. Phosphate deprivation increased NO production in WT roots, and the AOX level and the capacity of the alternative pathway to consume electrons in WT seedlings; whereas the same treatment failed to stimulate NO production and AOX expression in the *nia* mutant, and the plants had an altered growth phenotype. The NO donor *S*-nitrosoglutathione rescued the growth phenotype of the *nia* mutants under phosphate deprivation to some extent, and it also increased the respiratory capacity of AOX. It is concluded that NO is required for the induction of the AOX pathway when seedlings are grown under phosphate-limiting conditions. Regarding the second part of this thesis, it was focused on the early identification of stress response and plant performance of *Medicago truncatula* growing in axenic medium with ammonium or urea as the sole source of nitrogen, with respect to nitrate-based nutrition. Both ammonium and ureic nutrition severely affected the root system architecture, resulting in changes in the main elongation rate, lateral root development, and insert position from the root base. The auxin content decreased in both urea- and ammonium-treated roots; however, only the ammonium-treated plants were affected at the shoot level. The analysis of chlorophyll *a* fluorescence transients showed that ammonium affected photosystem II, but urea did not impair photosynthetic activity. Superoxide dismutase isoenzymes in the plastids were moderately affected by urea and ammonium in the roots. Low dose (1mM) of ammonium or urea did not affect the metabolism and signalling of N. Under this scenario, there was an up-regulation of aquaporins and the modulation of phenylpropanoids metabolism on roots, allowing an accurate sensing mechanism through which plants uptake and assimilated the N of the medium. However, high doses of N (25mM) provoke moderate changes without signals of toxicity or nitro-oxidative stress. High N dose led to changes in the free amino acids and ureides contents, and as a result, an enhancement of amides and an activation of the GABA shunt under ammonium nutrition counterbalance the excess of N assimilated by those plants. Nitric oxide of ammonium roots reached the levels observed under nitrate indicating its possible role on the response to high ammonium by *M. truncatula*. Overall, our results showed that low N doses from different sources had no remarkable effects on *M. truncatula*, with the exception of the differential phenotypic root response. Taken together, these data demonstrate that both the indole-3-acetic acid pool and performance index are important components of the response of *M. truncatula* under ammonium or urea as the sole N source. In addition, the re-distribution of assimilated N compounds, a high specific sensing machinery at cell wall and plasmatic membrane level together with a NO-mediated molecular response in roots are essential players of ammonium or urea tolerance in *M. truncatula*.

Preface

Beatriz Royo was the author of this thesis. She was the main responsible of the experimental designs, analytical and physiological measurements, data collection and processing and elaboration of results. Dr. Jagadis K. Gupta supervised the publication of *Arabidopsis* (Royo et al., 2015), which corresponds with chapter 4.1 and chapter 5.1. Dr. Raquel Esteban thoroughly participated in the processing of OJIP and RSA data showed in chapter 4.2, and she also supervised the elaboration of the manuscript originated in this section. All co-authors of the papers contributed in the experimental designs and in the discussion of the articles.

The introduction, aims, materials and methods, and conclusions refer to the thesis as a whole, whereas the results and discussion chapters are divided in four sections. Thus, the results described in chapters 4.1 and 4.2, and further discussed in chapters 5.1 and 5.2 in this thesis have been respectevely extracted from the original papers already published:

- Royo B, Moran JF, Ratcliffe RG, Gupta KJ. Nitric oxide induces the alternative oxidase pathway in *Arabidopsis* seedlings deprived of inorganic phosphate. Journal of Experimental Botany. 2015; 66(20): 6273-6280. doi:10.1093/jxb/erv338.

- Esteban R, Royo B, Urarte E, Zamarreño ÁM, Garcia-Mina JM, Moran JF. Both free indole-3-acetic acid and photosynthetic performance are important players in the response of *Medicago truncatula* to urea and ammonium nutrition under axenic conditions. Frontiers in Plant Science. 2016; 7: 140. doi:10.3389/fpls.2016.00140.

Contents

Chapter 1:

INTRODUCTION

1.1. A journey across plant mineral nutrition history

Plant nutrition is the study of the chemical elements necessary for the plant growth, plant metabolism and their external supply and survival. Briefly, plants effectively absorb the mineral elements due to their system of roots. They have the ability to uptake the inorganic ions, even present at low concentration in soils. Once the mineral elements have been absorbed by roots, they are transported to the various part of the plant to be utilized in the multiple biological functions (e.g. photosynthesis, respiration, growth…) of the plants.

The concept of "essential element" was first described in 1804, when De Saussure introduced the idea that "some but not all elements are indispensable for plant growth". Next, Arnon and Stout (1939) and Eptein (1999), defined an essential element as "one whose absence prevents a plant from completing its life cycle or one that has a clear physiological role". Controversially, mineral nutrients have usually been classified as macronutrient (nitrogen, phosphorus, potassium, calcium, sulfur and magnesium) and micronutrient or trace minerals (boron, chlorine, manganese, iron, zinc, copper, molybdenum, nickel and cobalt) in agreement with their relative concentration in plant tissues. Nevertheless, this classification is difficult to justify physiologically and, as showed in Table 1.1, an alternative classification in accordance to their biochemical and physiological function was then proposed (Mengel and Kirkby, 1987). In general, an essential element is defined as an element, which is part of an essential molecule inside the plant and with its absence the plant cannot complete a normal life cycle. In this way, two of the most important mineral nutrients for plants are **nitrogen** (N) and **phosphorus** (P), which both participate in carbon compounds and energy metabolism. Nitrogen is the constituent of many plant cell components and biomolecules. Therefore, since N is the most important mineral nutrient for plant development, it is required in larger amounts. The element phosphorus plays a key role in photosynthesis, respiration and energetic metabolism; and it also participates in the structure of plant membranes.

Table 1.1. *Classification of plant mineral nutrients according to biochemical function.*

Nutrient	Function	Essentiality
Group 1: Nutrients that are part of carbon compounds		
N	Constituent of amino acids, amides, proteins, nucleic acids, nucleotides, coenzymes, hexoamines, etc.	Macronutrient
S	Component of cysteine, cystine, methionine, and proteins. Constituent of lipoic acid, coenzyme A, thiamine pyrophosphate, glutathione, biotin, adenosine-5'-phosphosulfate, and 3-phosphoadenosine.	Macronutrient
Group 2: Nutrients that are important in energy storage or structural integrity		
P	Component of sugar phosphates, nucleic acids, nucleotides, coenzymes, phospholipids, phytic acid, etc.Has a key role in reactions that involve ATP.	Macronutrient
Si	Deposited as amorphous silica in cell walls. Contributes to cell wall mechanical properties, including rigidity and elasticity.	Beneficial element
B	Complexes with mannitol, mannan, polymannuronic acid, and other constituents of cell walls. Involved in cell elongation and nucleic acid metabolism.	Micronutrient
Group 3: Nutrients that remain in ionic form		
K	Required as a cofactor for more than 40 enzymes. Principal cation in establishing cell turgor and maintaining cell electroneutrality.	Macronutrient
Ca	Constituent of the middle lamella of cell walls. Required as a cofactor by some enzymes involved in the hydrolysis of ATP and phospholipids. Acts as a second messenger in metabolic regulation.	Macronutrient
Mg	Required by many enzymes involved in phosphate transfer. Constituent of the chlorophyll molecule.	Macronutrient
Cl	Required for the photosynthetic reactions involved in O_2 evolution.	Micronutrient
Mn	Required for activity of some dehydrogenases, decarboxylases, kinases, oxidases, and peroxidases. Involved with other cation-activated enzymes and photosynthetic O_2 evolution.	Micronutrient
Na	Involved with the regeneration of phosphoenolpyruvate in C4 and CAM plants. Substitutes for potassium in some functions.	Beneficial element
Group 4: Nutrients that are involved in redox reactions		
Fe	Constituent of cytochromes and non-heme iron proteins involved in photosynthesis, N_2 fixation, and respiration.	Micronutrient
Zn	Constituent of alcohol dehydrogenase, glutamic dehydrogenase, carbonic anhydrase, etc.	Micronutrient
Cu	Component of ascorbic acid oxidase, tyrosinase, monoamine oxidase, uricase, cytochrome oxidase, phenolase, laccase, and plastocyanin.	Micronutrient
Ni	Constituent of urease. In N_2-fixing bacteria, constituent of hydrogenases.	Micronutrient
Mo	Constituent of nitrogenase, nitrate reductase, and xanthine dehydrogenase.	Micronutrient

Source: Taiz and Zieger, 2006.

Thus, the availability of N and P in soils affects plant growth, and limits the productivity in agricultural ecosystems due to their involvement in key functions in plants (Fig. 1.1). An interaction between the soil mineral matrix, plants and microbes is needed for a correct functioning of soils. Actually, as a result of the industrial farming, soils suffer several alterations including compaction, loosening of significant amounts of organic matter, and the decay of their fertility. Hence, the availability of nutrients for plants, as phosphate and nitrogen, has been endangered and thereby the use of mineral N and P fertilizers augmented. This abusive utilization of mineral fertilizers and manures continues increasing, tough the productivity of crops is suffering a continuous decline. Moreover, as a consequence of the high input of fertilizers, an over-accumulation of N often occurs. In this context, it is interesting to understand how plants utilizes the nutrients, and also the mechanism which plants deal with nutritional stresses such as P deficiency and high inputs of N. Thus, by means of axenic cultures (as in the present work), the modeling of plant growth to these environmental changing conditions is able.

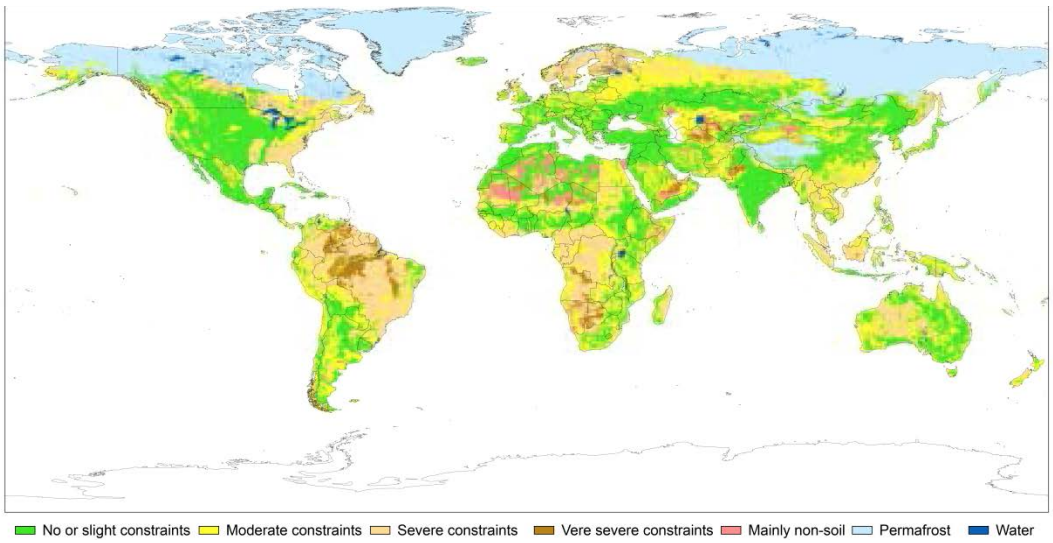

Figure 1.1. ***Nutrient restriction in soil.*** The compromised availability of nutrients in world soils is illustrated in the map (illustration from Fischer et al., 2008).

1.2. Phosphorus: an important player on plants´ metabolism

Phosphorus (P) is one of the most important nutrients for plant growth and development, which plays an important role in energy metabolism, and it is also required for the formation of cellular components as nucleic acids, membranes, and ATP. In addition, P is a key component for the regulation of many enzymatic reactions and in signal transduction processes (Marchsner, 2012).

The amount of P present in soils is usually high, but it is mainly found as immobile and unavailable forms for plants uptake (Holford, 1997). One part of this unavailable P may exchange with soil solution turning it accessible to plants, but it is mainly moved through the soil by diffusion. Plants preferably acquire and assimilate inorganic P (Pi) as orthophosphate ($H_2PO_4^-$; HPO_4^{2-}); the form of Pi that commonly occurs at 6.5, the typical soil pH. However, the usual low availability of P in the bulk soil, together with the low rate of P diffusion and the leaching, mineralization and fixation restrict plant uptake and create a zone around the root that is depleted in P. As a result, Pi becomes one of the most frequently limiting nutrients for plant growth. The entrance of Pi into the roots, as well as its movement within the cell and around the whole plant, is mediated by a wide variety of transporters. Thus, the acquisition of Pi from the external soil solution across the plasma membrane requires a high-affinity, energy driven transport mechanism (Schachtman, 1998; Smith, 2002), whereas its distribution along the plant is carried out by low-affinity transporters.

Since the low Pi present in soils leads to an inadequate P absorption, plants have developed highly specialized mechanisms to improve the uptake, utilization and conservation of Pi (Fig. 1.2). Examples of some of the major adaptive modifications to improve Pi acquisition include an increase in the root:shoot ratio; changes in root morphology and architecture; increased capacity for Pi uptake; induction of high-affinity to Pi transporters; enhanced Pi use efficiency, as well as a reallocation of Pi among organs, tissues and sub-cellular compartments; secretion of acid phosphatases and organic acids; decreased uptake of nitrate; and changes in carbon metabolism (Raghothama, 1999; Vance *et* al., 2003; Plaxton and Tran, 2011; Liang *et al.*, 2014).

Phosphate deficiency

Although all the mechanisms explained in the previous section for P uptake, plants may suffer from phosphate deficiency, which may reduce plant growth and yield (Wissuwa *et al.*, 2005). In response to Pi starvation, respiration undergoes several modifications including an increased consumption of inorganic pyrophosphate to conserve ATP, the reorganization of glycolysis and the induction of the alternative

pathway of mitochondrial electron transport (Vance *et al.*, 2003; Plaxton and Tran, 2011).

Induction of the alternative pathway under Pi limiting conditions

Under phosphate deficiency, the synthesis of ATP coupled to the TCA cycle is restricted but plants still continue to respire by the induction of the alternative pathway (Rychter and Mikulska, 1990; Parsons et al., 1999; Gonzalez-Meler et al., 2001). The electron transport steps catalyzed by the alternative NADH dehydrogenases and the alternative oxidase (AOX) do not pump protons across the inner mitochondrial membrane and so provide a non-energy conserving alternative to the cytochrome pathway (Millar *et al.*, 2011). The importance of these pathways under Pi starvation has been shown in numerous studies in different plant species and tissues, including bean roots (Rychter and Mikulska, 1990; Wanke *et al.*, 1998), leaves of bean and *Gliricidia sptium* (Gonzàlez-Meler *et al.*, 2001), tobacco suspensions (Parsons *et al.*, 1999) and *Arabidopsis* seedlings (Vijayraghavan and Soole, 2010). Further, observations in *Phaseolus vulgaris* mitochondria showed increased AOX activity and decreased cytochrome *c* oxidase (COX) activity when isolated from roots of plants grown on a Pi-deficient medium (Rychter *et al.*, 1992; Juszczuk *et al.*, 2001). In the same way, a Pi limitation caused a strong increase in AOX protein and the capacity for cyanide-resistant respiration on cell suspension cultures of *Nicotiana tabacum*, (Parsons *et al.*, 1999; Sieger *et al.*, 2005). In addition, Gonzàlez-Meler *et al.* (2001) observed that the activity of the AOX pathway increased in leaves of *P. vulgaris* and *G. sptium*, but not in tobacco.

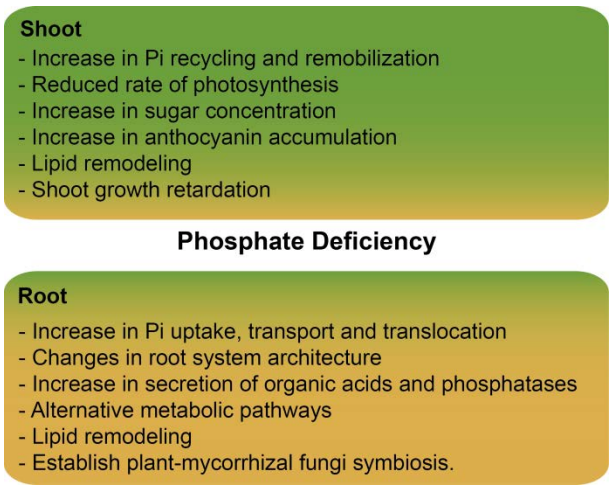

Figure 1.2. ***Effects of phosphate deficiency in plants.*** Shoot and root specific responses to Pi deficiency.

1.3. Nitrogen: another essential element in the plants´ metabolism

In nature, nitrogen becomes essential as it is present in a wide number of essential biomolecules, like amino acids and nucleotides, and it is also a component of coenzymes and products of the secondary metabolism. Plants need N for their optimal growth and development. Nitrogen fertilizers for crops typically contain ammonium (NH_4^+) and nitrate (NO_3^-) salts (applied primarily as ammonium nitrate, ammonium sulfate and ammonium phosphate in solid form or in solution), urea ($CO(NH_2)_2$) or anhydrous ammonia (a gas produced by a modified Haber–Bosch process, injected under the soil surface) (Bittsánszky *et al.*, 2015). Although its absorption and assimilation implies higher energy consumption, NO_3^- turns as the most commonly uptaken N source by roots. Roots are also able to uptake N in other forms different from nitrate, as NH_4^+, urea, molecular nitrogen (N_2) in symbiosis with nitrogen-fixing bacteria, or amino acids under particular conditions of soil composition. Ammonium is the form of N preferably uptaken at low concentrations, but it becomes toxic above certain threshold (Britto and Kronzucker, 2002). Indeed, NH_4^+ sensitivity of plants is a worldwide problem leading to physiological and morphological disorders affecting plant development (Li *et al.*, 2014; Bittsánszky *et al.*, 2015). Urea is the most commonly used fertilizer and its uptake by plants can be i) in the form of NH_4^+ resulting from the action of soil ureases, or ii) directly by transporters. Whatever the source of N is, only ammonium can be incorporated into amino acids and amides (Lea and Miflin, 2011). Thus, the utilization of NO_3^-; NH_4^+; and urea, the most common N sources utilized in agriculture, lead to an elevate intracellular accumulation of NH_4^+, therefore it is indispensable to understand and elucidate the mechanism by which plants face NH_4^+ toxicity, and to less extend urea toxicity.

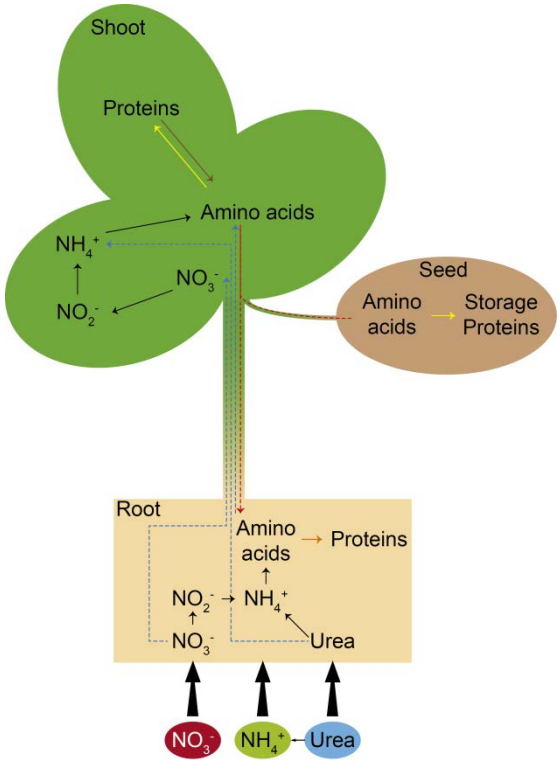

Figure 1.3. ***Nitrogen management in plants.*** The uptake, assimilation, and transport of nitrogen among the whole plant are illustrated. Nitrate and urea can be either assimilated (→) on root or shoot after their translocation through the xylem stream (→), further NH_4^+ is assimilated into amino acids. The synthesized amino acids are used to synthetize proteins in roots (→), shoots or seeds (→), after their transport on the phloem (→). Proteins can also be degraded (→) back to amino acids, and re-translocated through the phloem stream to roots (→).

Nitrate assimilation and metabolism

Nitrate is absorbed by roots and further assimilated into organic nitrogen compounds. Once it enters into the cells, NO_3^- is assimilated to NH_4^+ in a two steps process occurring in both roots and shoots (Fig. 1.3). When the amount of NO_3^- available for roots is small, its reduction takes place in the roots; whereas the absorbed NO_3^- is transported and assimilated into the shoot at higher dose (Marschener, 2012). Initially, nitrate is first reduced to nitrite (NO_2^-) in the cytosol by the enzyme nitrate reductase (NR) (Oaks, 1994; Meyer and Stitt, 2001). Then, since nitrite is a toxic ion, it is immediately translocated into the plastids in roots and into the chloroplasts in leaves, where the nitrite reductase (NiR) catalyzes the reduction of NO_2^- to NH_4^+.

Cytosolic NR is composed of two identical monomers, each associated with three prosthetic groups: a flavin adenine dinucleotide (FAD), a heme, and a

molybdenum cofactor (MoCo) (Figure 1.4). Nitrate reductase has two active sites. Hence, one for NAD(P)H to donate electrons and another for NO_3^- reduction. Specifically, NAD(P)H binds at the FAD-binding region initiating the transfer a two electron from the carboxyl (C) terminus via the heme to MoCo, where NO_3^- is normally reduced.

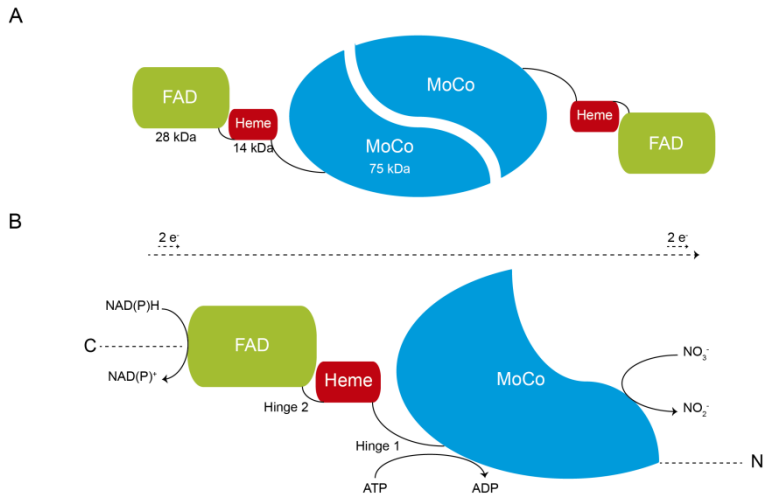

Figure 1.4. ***Structural and functional scheme for nitrate reductase.*** **(A)** Homodimeric structure of nitrate reductase showing the three prosthetic groups: FAD, heme, and Moco. (**B**) The transfer of two electrons from the C-terminus starts when NAD(P)H binds at the FAD region, and as the electrons reach the MoCo group at the N-terminus the nitrate reduction takes place.

Nitrite reductase is a single polypeptide containing an iron-sulfur cluster (Fe_4S_4) and a specialized heme as prosthetic groups (Siegel and Wilkerson, 1989) which reduce directly NO_2^- to NH_4^+. The electrons used are supplied by the reduced ferredoxin derived from photosynthetic electron flow in the chloroplast under light conditions, and from NAD(P)H in non-green tissues (Tischner and Kaiser, 2007). This enzyme may be induced by NO_3^- and light but repressed by asparagine (ASN) and glutamine (GLN), the end products of N assimilation.

Ammonium assimilation and metabolism

The uptake of NH_4^+ by roots is mediated by transporters, and once inside the plant cell it is distributed to intracellular compartments also via different classes of transporters. As proposed recently, the transport of NH_4^+ across the cell membrane is mainly in the form of ammonia gas (NH_3), but it also enters the cell as NH_4^+ through high-affinity ammonium transporters (AMT) and non-specific cation channels (Coskun *et al.*, 2013). Hence, before its transport across the membrane, NH_4^+ has to be deprotonated and then NH_3 can enter the cell by diffusion. In addition, NH_3 and H_2O

molecular structures are pretty similar, thus the transport across plasma membrane might be also mediated by aquaporins (Bertl and Kaldenhoff, 2007; Coskun *et al.*, 2013; Kirscht *et al.*, 2016). As the transport of NH_4^+ across AMT takes place at low NH_4^+ concentrations, the transport of NH_3/ NH_4^+ across both AQP and non-specific cation channels appears to be the cause of toxicity at high concentrations of NH_4^+ (Pantoja, 2012; Bittsánszky *et al.*, 2015).

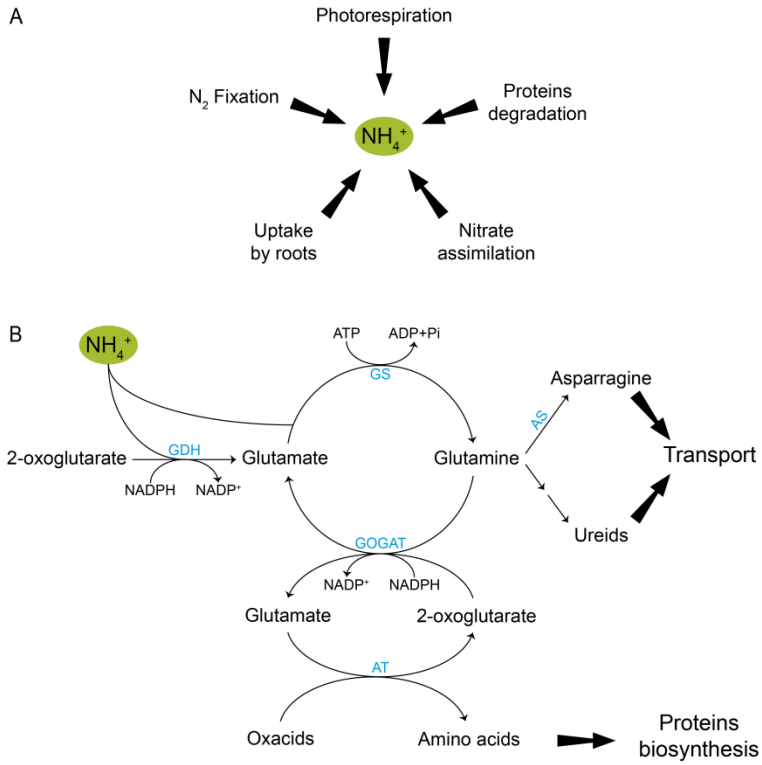

Figure 1.5. ***Ammonium metabolism in plants.*** The NH_4^+ is accumulated inside the plant cells as a result of different metabolic processes (**A**), and further it is mainly assimilated by the GS-GOGAT cycle or alternatively by the GDH enzyme (**B**). The enzymes involved in the assimilation of NH_4^+ are typed in blue. AS: asparagine synthetase; AT: aminotransferases; GDH: glutamate dehydrogenase; GOGAT: glutamate synthase; GS: glutamine synthetase.

The NH_4^+ contained in plant cells is mainly produced in some metabolic processes as i) reduction of NO_3^- and atmospheric N_2 fixation; ii) photorespiration; and iii) catabolism of proteins (Fig. 1.5A).

The accumulation of NH_4^+ inside the cell can be toxic thereby; it is rapidly assimilated into amino acids. Thus, NH_4^+, taken up from the rhizosphere, is generally assimilated via the called GS-GOGAT cycle (Fig. 1.5B). First, one molecule of NH_4^+ is combined with glutamate to produce glutamine by the enzyme glutamine synthetase (GS). This reaction implies the consumption of one molecule of ATP. Next, the

enzyme glutamate synthase (GOGAT) catalyzes the transamination of that glutamine to two molecules of glutamate. Both amino acids, glutamine and glutamate, are precursors of other N compounds, like ureides, the others amino acids and their concomitant proteins. Two classes of both enzymes are present in plants and they are involved in the assimilation of NH_4^+ coming from different origins. Glutamine synthetase is divided into cytosolic and plastidic/chloroplstic, while GOGAT enzyme is classified depending on their electrons donor (NADH or Fd) (Lam *et al.*, 1996).

Additionally to the GS-GOGAT cycle, NH_4^+ can be assimilated via an alternative pathway that involves the glutamate dehydrogenase (GDH) enzyme that catalyzes a reversible reaction where the synthesis or deamination of glutamate.

Ammonium toxicity

Plants are able to accumulate and translocate high levels of nitrate without deleterious effects. Nitrate should be reduced to NH_4^+ prior to be assimilated into organic compounds, with resultant consumption of energy. On the contrary, since NH_4^+ can be assimilated directly, it takes place with a lower energy cost. Therefore, for the plant economy, NH_4^+ may be thought of as a favorable N nutrient. However, the presence of NH_4^+ as the only N source is paradoxically toxic to most plants, as long as, high levels of ammonium dissipate the required transmembrane proton gradients for essential processes for plant development such as photosynthesis and respiration. In this way, plant response depends on the concentration and the relative tolerance capacity of the plant species or variety (Gerendás *et al.*, 1998; Cruz *et al.*, 2011; Li *et al.*, 2014: Esteban *et al.*, 2016).

Phenotypic symptoms of NH_4^+ toxicity usually include reduced plant growth, changes in root architecture, decreases in the root/shoot ratio and leaf chlorosis (Britto and Kronzucker, 2002). As reviewed in Esteban *et al.* (2016), the excess of NH_4^+ causes changes in ion balance by the inhibition of cations (K^+, Mg^{2+} or Ca^{2+}) uptake; intracellular alkalinization and extracellular acidification; the inhibition of root respiration and stimulation of photorespiration; interference with photosynthetic activity; the altered expression/activity of NH_4^+ assimilating enzymes; the disruption of hormonal homeostasis; and high energy cost to maintain low levels of cytosolic NH_4^+ content. An increased oxidative stress has also been reported in NH_4^+-fed plants, such as *Arabidopsis* (Podgórska *et al.*, 2013; Podgórska and Szal, 2015); and consequently plant cells undergo changes in the homeostasis of reactive oxygen species (ROS) (Medici *et al.*, 2004; Patterson *et al.*, 2010). However, in another study, it was concluded that the NH_4^+-generated stress in spinach and pea plants was not oxidative stress (Domínguez-Valdivia *et al.*, 2008). Hence, the relationship of NH_4^+ with oxidative

stress in plants is still under debate (Bittsánszky *et al.*, 2015). NH_4^+-fed plants also exhibited increased lipid peroxidation and enhanced glutathione-ascorbate cycle enzyme activity. The origin of all these effects is still unclear. They may be a cascade-type response or solely the summation of several plant responses to NH_4^+ or to one product of its metabolism. Some studies have suggested that NH_4^+ is locally sensed by mechanism which employs similar regulatory modules than those involved in nitrate sensing (Lima *et* al., 2010; Rogato *et al.*, 2010).

To mitigate the detrimental effects of NH_4^+, plants cells tend to assimilate it close to the site where it is absorbed or generated, and immediately store any excess in their vacuoles. What is more, an accurate balance among the uptake, production, and consumption of NH_4^+ has to be also maintained (Bittsánszky *et* al., 2015).

Mechanism of tolerance

During the last decades, the causes of NH_4^+ sensitivity/tolerance has been largely studied, though the plant traits that are responsible for NH_4^+ sensitivity or tolerance remain still unclear. In addition, the availability of sequenced genomes of both sensitive and tolerant model plants, such as *A. thaliana*, rice, and *M. truncatula*, has allowed carrying out "omic" studies providing new insights into the knowledge.

Accordingly, it is possible to counterbalance NH_4^+ toxicity interfering in several environmental factors including high light intensity and increased CO_2 concentrations (Ariz *et* al., 2013; Setién *et al.*, 2013; Vega-Mas *et al.*, 2015). Through the supply of either organic or inorganic carbon it is possible to reverse C-starvation, a common symptom exhibited by plants grown under NH_4^+ nutrition (Roosta *et al.*, 2007). Several studies have also demonstrated that high concentrations of K^+ can alleviate NH_4^+toxicity symptoms in sensitive species as barley, and even enhance the tolerance in rice, a very tolerant plant (Szczerba *et al.*, 2008; Balkos *et al.*, 2010). Furthermore, a shift in the pH of the growth solution mitigates the toxic effect on *A. thaliana* (Zheng *et al.*, 2015). A usual practice in agriculture is the use of NH_4NO_3 or urea to counterbalance the toxic effect of NH_4^+, since the presence of low doses of NO_3 alkalinizes the rhizosphere.

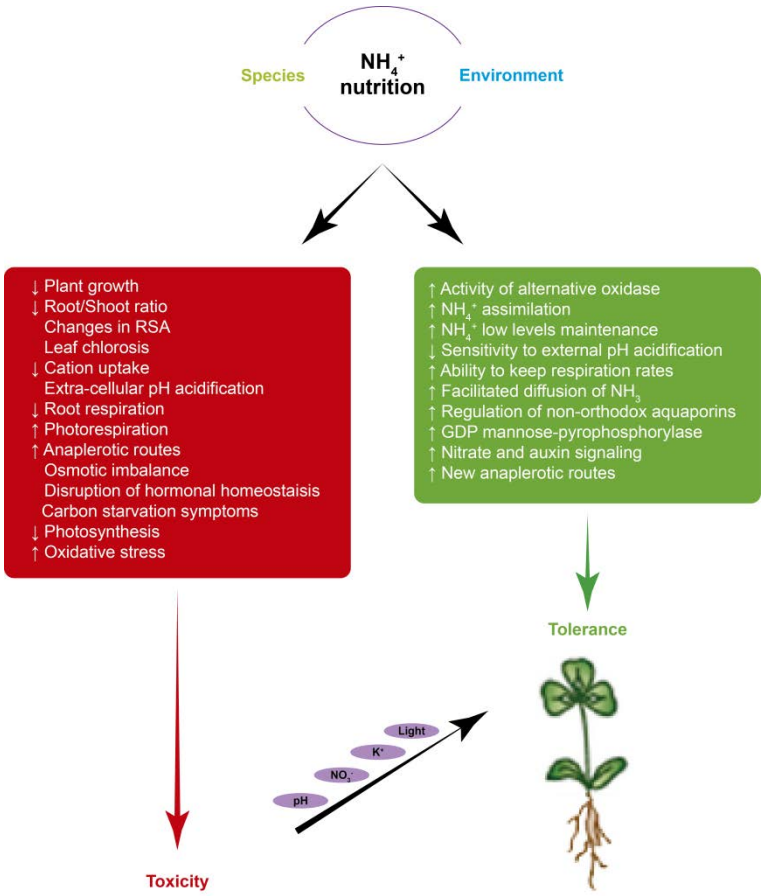

Figure 1.6. ***Ammonium toxicity and tolerance in plants.*** The tolerance or sensitivity to NH_4^+ toxicity depends on several environmental factors and the species used. The green box shows the theories of NH_4^+ tolerance. The red box shows the main symptoms of NH_4^+ toxicity in plants. The modification of factors such as pH, light, NO_3^- and K^+ might increase NH_4^+ tolerance.

Recently, "omic" studies have confirmed the involvement of oxidative metabolism in the response to NH_4^+ nutrition. Here, a novel antioxidant regulatory enzyme involved in the improvement of plant tolerance to NH_4^+ in both tolerant and sensitive species has been detected (Xie *et al.*, 2014).

Additionally, nitrate also plays an important role in NH_4^+ tolerance, since it participates in the regulation of endogenous auxin in root cells (Krouk *et al.*, 2010). It is known that auxin stimulate lateral root development, but whether auxin signaling is NO_3^-- dependent or independent is still uncertain. Nitric oxide can also promote the formation of lateral and adventitious roots, an effect that is related with an increase on auxin signaling, as demonstrated using *A. thaliana* mutant plants (Flores *et al.*, 2008). To date, the origin of NO in plants grown exclusively with NH_4^+ or urea is unfortunately unknown. Taking these together, the study of the signaling mechanism in NH_4^+-grown

plants complemented with NO_3^-, as well as the search on the NO origin is required for a better understanding of the mechanism of NH_4^+ tolerance.

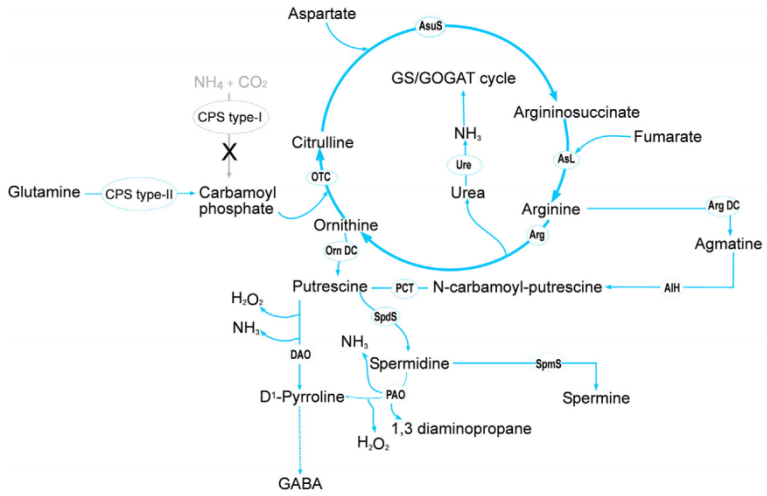

Figure 1.7. ***The "urea cycle" in plants.*** Carbamoyl phosphate is synthesized from glutamine, but not from NH_4^+ in plants. Arginine and ornithine can be used as the precursors of polyamines synthesis. Inter-conversions of polyamines give rise to NH_4^+ and H_2O_2 molecules that result from oxidases catalysis. The enzymes are represented inside a circle as: agmatine imidohydrolase (AIH), argininosuccinate lyase (AsL), arginase (ARG), arginine decarboxylase (Arg DC), argininosuccinate synthase (AsuS), diamine oxidase (DAO), ornithine decarboxylase (Orn DC), transcarbamylase (OTC), polyamine oxidase (PAO), putrescine carbamoyl transferase (PCT), spermidine synthase (SpdS), spermine synthase (SpmS), urease (Ure) (illustration from Esteban *et al.*, 2016).

Finally, as described by Allen *et al.* (2011) a "urea cycle" that serves as a distribution and repackaging hub for inorganic carbon and nitrogen that contributes significantly to the metabolic response to episodic nitrogen availability has been described in diatoms. In other words, an excess of NH_4^+ inside the cells can be diminished by activation of the urea cycle. Nevertheless, plants are not able to synthesize urea directly from NH_4^+, and consequently the high internal accumulation of NH_4^+ produced under stress conditions would not be reduced. In contrast, plants can utilize glutamine as source of NH_3 to produce carbamoyl phosphate, the molecule which first introduces the NH_3 in the urea cycle (Zhou *et al.*, 2000). As showed in Figure 1.7, the urea cycle produce arginine that further can be degraded to urea and ornithine (Orn), or serve as substrate to form argmatine. Both, ornithine and argmatine are precursors of the polyamines synthesis, and the inter-conversion of polyamines release NH_4^+ and H_2O_2. In addition, the γ-aminobutyric acid can be produced from putrescine, the immediately polyamine originated from the amino acids cited previously. Therefore, since the synthesis of polyamines can be either a sink or a source of NH_4^+, the importance of this pathway in plants is still unclear.

Urea assimilation and metabolism

In the same way that nitrate, urea must be hydrolyzed to NH_4^+ before it can be assimilated into amino acids. The assimilation takes place then after its hydrolysis to NH_3 and carbon dioxide (CO_2). In this way, it is traditionally believed that urea present in soils is mainly taken up as NH_4^+ and NO_3^- after the action of soil microorganisms. Then, urea is first hydrolyzed by the enzyme urease (Watson *et al.*, 1994) into NH_4^+ and further converted into NO_3^- by nitrification (Hollocher, 1981; Costa *et al.*, 2006; Van Kessel *et al.*, 2015). Recently, the direct uptake of urea was described and two mechanisms proposed: a high affinity active transport and a low affinity passive transport mediated by major intrinsic proteins (MIPs) (Witte, 2011; Yang *et* al., 2015; Pinton *et al.*, 2015). Urea is also an important N metabolite in plants since it takes part on arginine (Arg) and ureides metabolisms. Arginine catabolism produces Orn and urea in the mitochondrial matrix. Then urea is transported to the cytosol where most plants possess urease activity that hydrolyze urea to produce NH_3 and carbamate (Carter *et al.*; 2009). This reaction occurs in the cytosol and the NH_4^+ generated is assimilated by the GS-GOGAT cycle. On the other hand, Orn can be either converted to glutamate in the mitochondria or to putrescine and other polyamines. Taken as a whole, these reactions constitute the so called "urea cycle" (Fig. 1.7), which importance in plants is still uncertain (Pollaco and Holland, 1993; Esteban *et al.*, 2016).

Urea stress

Urea-fed plants also accumulate high amounts of NH_4^+ leading to a harmful effect. Although significant advances have been made in the urea field, its possible toxicity is also a matter of debate (Gerendás *et al.*, 1998; Witte *et al.*, 2002; Mérigout *et al.*, 2008; Zanin *et al.*, 2014, 2015). Already in 1962, Court *et al.* observed clear symptoms of damage in maize seedlings when supplying urea as fertilizer, such as necrosis at the leaf tip, loss of turgidity, reduction of the plant yield, and even the death. At that point, they suggested that the phytotoxicity due to urea may be caused by the accumulation of high levels of NH_4^+ and NO_2^- in soils (Court *et al.*, 1964). In general, similar effects on plants to those described for NH_4^+ have been reported for urea, but with a lower intensity (Houdusse *et al.*, 2005). Under axenic conditions (as the one present here), the hydrolysis of urea in the medium is avoided; then urea is incorporated without hydrolysis inside the plant, which eventually may lead to an accumulation of considerable amounts of urea in plants, and consequently drive to alterations in the turnover of "urea cycle" (Gerendas *et al.*, 1998). The physiological aspects of urea acquisition in plants grown under axenic conditions have only been investigated in *Arabidopsis* and rice (Wang et al., 2013; Yang et al., 2015). Thereby the

role of urea as an accessible N source and its use by plants represents still an important gap in our knowledge.

1.4. Main stress adaptations or indicators in detail

Root system architecture (RSA) changes

Any modification in soils dynamism directly affects plant development, and the adaptation of roots to the stressing environmental changes becomes essential to the survival of the plant. As the first sensing mechanism, the root system architecture (RSA) performance is modulated to ensure the correct uptake of nutrients and also to avoid stressful, toxic and physical soil barriers. As cited earlier, a stunted of root growth is the most visible phenotypic change related to ammonium accumulation inside the cells (Gerendas *et al.*, 1997; Wiesler F, 1997; Britto and Kronzucker, 2002). Exposure to ammonium principally target RSA development affecting elongation, gravitropism and lateral root branching (Li *et al.*, 2010; Lima *et al.*, 2010; Zou *et al.*, 2013), furthermore the response to ammonium nutrition has been described to be highly localized in the root tip (Li *et al.*, 2010).

The most apparent effect of NH_4^+ in the RSA is the inhibition of root elongation that has been largely attributed to the presence of auxins (Cao *et al.*, 1993), but studies with auxin-resistant mutants have supported the idea that the reduction of root elongation is uncoupled from auxin pathways (Liu *et al.*, 2013). Based on length assays, it has been identified an *Arabidopsis* mutant hypersensitive to NH_4^+ (*hsn1-1*) which is not able to produce GDP-mannose essential for the N- glycosylation of root proteins, but how this compound affects NH_4^+ sensitivity is still unclear (Qin *et al.*, 2008; Kempinski *et al.*, 2011). Independently of root elongation, root gravitropism is also reduced under NH_4^+ nutrition and, in this case, the distribution of auxin in the root might be involved (Zou *et al.*, 2012). Several studies have described the implication of the auxin exporter PIN2 in the response to diverse stresses (Jasik *et al.*, 2013). For instance, the degradation of PIN2, which has been observed under NH_4^+ stress, enables roots to override gravity to avoid toxic areas of soil (Zou *et al.*, 2013). In a similar way to the primary root, lateral root elongation is suppressed, nevertheless both lateral root initiation and higher branching are enhanced by NH_4^+ (Lima *et al.*, 2010; Li *et al.*, 2010). Moreover, the involvement of NH_4^+-transporters has been studied and the results suggested that NH_4^+ locally stimulates the formation of lateral roots (Lima *et al.*, 2010).

Redox balance: oxidants and antioxidants

Reactive oxygen and nitrogen species (ROS and RNS) are generated in biological systems and play a key role in cellular signaling. Environmental stress induces the accumulation of ROS and RNS, which can cause severe oxidative damage to the plants, resulting in loss of physiological capacity and eventual cell death. However, these molecules also present regulatory functions in many physiological processes, such as stomatal closure, germination, root development, gravitropism, and programmed cell death. However, under certain conditions, the levels of ROS and RNS inside the cell may increase provoking the disruption of the cell redox homeostasis (Halliwell and Gutteridge, 2007). In plants, ROS and RNS are by-products of plant metabolism and sites for their origin include chloroplasts, mitochondria, peroxisomes, the endoplasmic reticulum, and plasma membranes (Gupta and Igamberdiev, 2013).

ROS production

The group of molecules enclosed as ROS include several free radicals such as superoxide ($O_2^{\cdot-}$), hydroxyl, and molecular forms as hydrogen peroxide (H_2O_2) and singlet oxygen. Superoxide and hydrogen peroxide are the most important ROS in plants since they play an essential role in signaling; and besides they are the most abundant (Zorov *et al.*, 2014). In aerobic metabolism, the production of ROS is inevitable and is mainly associated with the leakage of electrons onto O_2. In plant cells, different sites of ROS production have been detected, including several organelles and plasma membrane (Corpas *et al.,* 2001; Foreman *et al.,* 2003; Asada K, 2006; Sagi and Flurh, 2006; Marino *et al.,* 2012). In chloroplast, $O_2^{\cdot-}$ is produced at photosystems I and II, whereas in plasma membrane is generated by the activity of NADPH oxidases. In both organelles, the enzyme superoxide dismutase (SOD) converts the $O_2^{\cdot-}$ to H_2O_2. Moreover, the cytochrome P-450 generates the $O_2^{\cdot-}$ anion in the endoplasmic reticulum (Mittler R, 2002). In peroxisomes, ROS are produced by the activity of various enzymes such as acyl-CoA oxidase and xanthine oxidase (XO). Finally, the production of ROS in mitochondria takes place at the ETC. In Figure 1.8, the compartmentalization of ROS production is depicted.

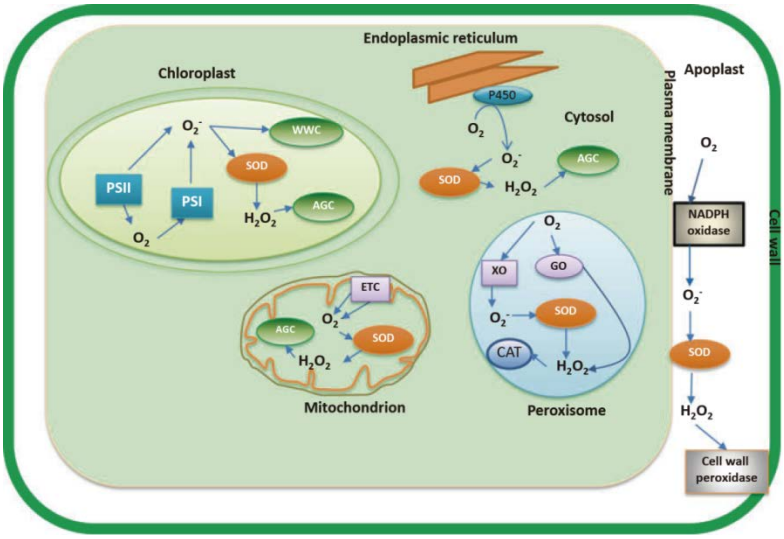

Figure 1.8. ***ROS-generating pathways in various compartments of plant cell.*** In chloroplasts superoxide production takes place at PSI and PSII; it is converted by SOD to hydrogen peroxide which is scavenged in the ascorbate–glutathione cycle (AGC), also the water–water cycle (WWC) is involved. In plasma membrane NADPH oxidase generates superoxide which is converted by SOD to hydrogen peroxide and the latter is used by cell wall peroxidase. In mitochondria the complexes I and III are sites for ROS production, SOD and AGC are scavengers. In peroxisomes, glycolate oxidase (GO), acyl-CoA oxidase and xanthine oxidase (XO) are major sites of ROS production, catalase (CAT) and SOD are scavengers. In endoplasmic reticulum cytochome P-450 generates superoxide which is scavenged via cytosolic SOD and AGC. (from Gupta and Igamberdiev, 2013)

In mitochondria, two pathways of electron transport operate: the cytochrome pathway (COX), which leads to the production of ATP via the complexes III and IV; and the alternative cyanide-resistant pathway. The electron transfer across the alternative pathway is mediated by the enzyme alternative oxidase (AOX) and the lack of proton pumping sites results in the no production of ATP by this pathway. When the rate of electron transfer exceeds the capacities of COX and AOX pathways, ROS are produced (Møller, 2001; Rhoads *et al.*, 2006). The most common sites of ROS production in mitochondria are complexes I and III, but recently have been demonstrated that the activity SDH in complex II also contributes to mitochondrial ROS production (Jardim-Messeder *et al.*, 2015). The leakage of electrons onto O_2 is intensified under stress situations and an overproduction of ROS takes place which is mitigated by antioxidant systems. However, ROS production becomes deleterious when their levels reach certain threshold that antioxidant systems cannot alleviate.

In addition to intracellular ROS produced in organelles and those originated in plasma-membrane, many studies have demonstrated that ROS are also produced in the plant cell wall in a highly regulated manner developing distinct functions (Passardi *et al.,* 2004; Cona *et al.,* 2006; Müller *et al.*, 2009; Novo-Uzal *et al.*, 2013). As reviewed in

Kärkönen and Kuchitsu (2015), the apoplastic production of ROS in plants is mediated by several enzymes comprising amine oxidases, quinone reductases, lipoxygenases, class III peroxidases and oxalate oxidases, as well as the previously mentioned NADPH oxidases.

RNS production: The origin of NO and the interaction with ROS

Nitric oxide (NO), the main RNS, is a free radical that participates in energy metabolism, signal transduction processes and in plant growth and development (Gupta *et al.*, 2011), and it also modulates the response to certain biotic and environmental stress conditions (Wendehenne *et al.*, 2004; Baudouin, 2011). Other RNS are derivative molecules of NO, such as peroxynitrite ($ONOO^-$) and nitrogen oxides (NO_2 and N_2O_3) that are formed when NO reacts with the superoxide anion and molecular oxygen respectively (Radi *et al.*, 2004; Brown, 2007). As described by Gupta et al 2011, NO can be produced specifically in various compartments by both reductive and oxidative pathways in order to fulfill the needs required. The reductive pathways are mediated by plasma membrane and mitochondrial Nitrite: NO reductase (PM Ni-NOR and Mt Ni-NOR), cytosolic nitrate reductase (NR) and xanthine oxidoreductase (XOR), whereas the oxidative pathways are dependent on polyamines, hydroxylamine and L-arginine.

The involvement of NO in plant processes is determined by the subcellular localization of its synthesis. Thus, the production of NO by mitochondria may be particularly higher than that produced in every other compartments (Gupta *et al.*, 2011). Under certain stresses, mitochondrial NO production increases specially in roots indicating that mitochondria, as an important source of NO, may be a major target for the actions of NO and other RNS.

The cytosolic production of NO is responsibility of the NR. Nitrate reductase activity catalyzes, as mentioned earlier, the reduction of NO_3^- to NO_2^- (see Figure 1.3B), but it can furthermore reduce NO_2^- to NO (Dean and Harper, 1988). The reduction of NO_3^- to NO_2^- implies the transfer of two electrons, but otherwise two different one-electron transfers may take place at the MoCo domain, one to produce $O_2^{\cdot-}$ and another to release NO (Kaiser *et al.*, 2011). Superoxide anion and NO production may occur simultaneously, and as a result of their interaction, the highly reactive specie peroxynitrite can be formed (Yamasaki and Sakihama, 2000). This NO production is dependent of high levels of NO_2^-, and is also affected by pH. Hence, a decline on cytosolic pH leads to inhibit the NiR activity, as a consequence an accumulation of NO_2^- takes place and NO synthesis is induced. In *Arabidopsis thaliana*, NR is encoded by the two genes *Nia1* and *Nia2*, so NR mutants in both genes are

defective in NO production. As cited in Gupta and Igamberdiev (2013), NR-dependent NO plays a key role under both biotic and abiotic stresses such as bacterial pathogenesis, fungi infection, heavy metal exposure, hypoxia and cold.

In the hypoxic plant cell, cytochrome *c* oxidase (COX) is the major site of NO production in mitochondria where the reduction of cytosolic NO_2^- occurs in complexes III and IV of the ETC (Planchet et al. 2005; Stoimenova et al. 2007). Moreover, NO can also bind competitively to the ferrous-heme group at the O_2-binding center of complex IV and as a result COX can be inhibited. This binding improves oxidative phosphorylation capacity because it keeps oxygen concentration above certain levels. In this transition from hypoxia to normoxia, COX can also scavenge NO back to nitrite suggesting that mitochondria produces and sinks NO (Gupta et al 2005; Brunori *et* al., 2006).

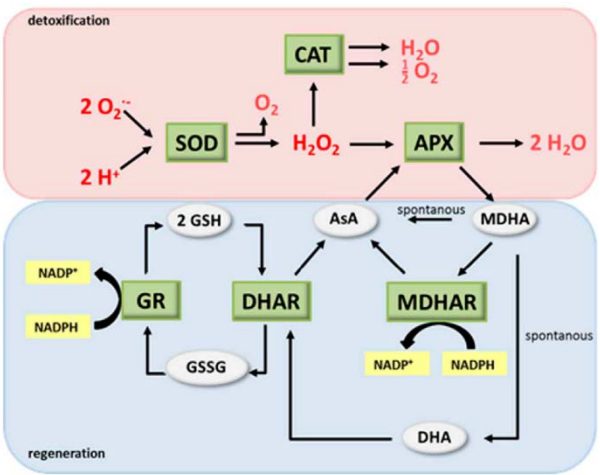

Figure 1.9. ***The Foyer-Halliwey-Asada cycle.*** The antioxidant system is composed of: a detoxification pathway that mitigates ROS levels; and the regeneration pathway where the antioxidant molecules are recycled. Ascorbate (AsA), ascorbate peroxidase (APX), catalase (CAT), dehydroascorbate (DHA), DHA reductase (DHAR), glutathione reductase (GR), glutathione (GSH), glutathione disulphide (GSSG), monodehydroascorbate (MDHA), MDHA resductase (MDHAR), and superoxide dismutase (SOD). (illustration from Groβ *et al.*, 2013)

Antioxidant barriers

The overproduction of ROS and RNS lead to damage the cell, and the interaction of both species produce the called nitro-oxidative stress being proteins the most frequently affected molecules. For instance, the interplay between $O_2^{\cdot-}$ and NO generates the powerful oxidant $ONOO^-$ which mediates the broadly studied tyrosine nitration of proteins that usually involves the loss of their function Cecconi *et al.*, 2009; Chaki *et al.*, 2011; Holzmeister *et al.*, 2015; Arora *et al.*, 2016; Mata-Pérez *et al.*, 2016).

In this context, the protection against oxidizing molecules is essential for mitigating the oxidative, as well as, the nitro-oxidative damage, and involves an extensive network of antioxidant compounds that includes non-enzymatic and enzymatic ROS scavengers (Fig. 1.9).

Non-enzymatic antioxidants, as ascorbate and glutathione, α-tocopherol, carotenoids and xanthophylls can detoxify ROS directly, or they can reduce the substrates for antioxidant enzymes (for more details see Mittler R, 2002; Das and Roychoudhury, 2014).

The enzymatic antioxidant defense is mainly mediated by three groups of enzymes: superoxide dismutases, catalases, and peroxidases. As previously cited, the enzyme SOD efficiently catalyzes the dismutation of two molecules of $O_2^{\cdot-}$ to yield one molecule of O_2 and one molecule of H_2O_2; therefore, this activity constitute a frontline in the defense against ROS (Halliwell and Gutteridge, 2007). The H_2O_2 produced by SODs can also be responsible of oxidative damage, and therefore cells require its scavenging. Plants possess multiples catalases mainly localized into peroxisomes, which catalyze the reduction of H_2O_2 to water. Moreover, peroxidases, like catalases, are also able to degrade H_2O_2. This activity includes a wide number of enzymes, such as class III peroxidases, which are mainly located in the cell wall and the vacuole. Additionally, since peroxidases can function in both ROS-consuming and ROS-generating reactions, the ROS produced by peroxidases paradoxically are suggested to play an important role, for example in cell wall loosening, stiffening and cross-linking (Passardi *et al.*, 2004; Kärkönen and Kuchitsu, 2015).

Chapter 2:

aIMS

General objective

The general purpose of this thesis was to study in deep **the physiological, metabolic and signaling changes** produced in the response to two nutritional status (**phosphate deprivation and ammonium and urea nutrition**) of two model species (*Arabidopsis thaliana* and *Medicago truncatula*) in axenic cultures. These kind of cultures are of great interest because it allows the modeling of the plants response, as the growth of other organisms, such as bacteria and/or fungus, are avoided. The nutritional stress provoked in plants due to phosphate deprivation and ammonium and urea nutrition produce an alteration on the RNS-mediated signaling response, which will be investigated and whose study could allow discerning the implication of NO in the defense mechanism. In addition, the use of ammonium and urea as the only source of N may permit understand the mechanism by which plants face the ammonium- or ureic-induced "stress". The central aim was, therefore, developed through two major and consecutive goals (see details below).

Specific objectives

1. The goal of this study was to investigate the effect of inorganic phosphate deprivation in *Arabidopsis thaliana* seedlings (Chapter 4.1)

   Arabidopsis thaliana wild type and mutant seedlings were grown in axenic culture with or without inorganic phosphate. Growth, inorganic phosphorous content, nitric oxide, nitrite, superoxide, hydrogen peroxide, respiration and alternative oxidase (AOX) protein were measured. In the chapter 4.1, the induction of the AOX pathway by nitric oxide will be discussed under the deprivation of inorganic phosphate.

2. The specific objective of this part was to study the differential effect of distinct nitrogen nutrition (ammonia and urea) in comparison to nitrate in *Medicago truncatula* plants (Chapters 4.2, 4.3 and 4.4)

   Medicago truncatula plants were grown in nitrate, ammonium or urea as a sole nitrogen source in axenic conditions. Firstly, the physiological response to the differential effect of ammonia and ureic nutrition respect to nitrate were characterized using growth, root system architecture (RSA), photosynthesis, auxin contents, superoxide dismutase (SOD) activity and antioxidant metabolites measurements (Chapter 4.2.)

In addition, using the same nutrition comparison, the effect on N metabolism and signaling was studied by the content of several molecules of importance as anions, cations, amino acids and ureids, besides to xanthine oxide reductase (XOR) activities, and some reactive species as nitric oxide, superoxide and hydrogen peroxide (Chapter 4.3).

Finally, a proteomic approach of roots response to the differential nutrition was performed using the iTRAQ-based methodology in order to investigate the proteomic changes in *M. truncatula* to differential N sources (Chapter 4.4).

In the chapters 4.2, 4.3 and 4.4, an attempt to model the response of *M. truncatula* to ammonium and ureic nutrition as only N source is achieved.

Chapter 3:

MATERIAL and METHODS

3.1. Plant material, growth conditions and experimental design

3.1.1. *Arabidopsis thaliana*

Arabidopsis thaliana (L.) Heynh. (Brassicaceae) produces few leaves that form a flat rosette with thin, long, and highly branched roots. This plant is the most widely used organism in plant biology and genetics research. The success of this annual crucifer and its use as model plant is due to its relative short life cycle, the prolific production of seeds, and its small genome. In fact, as the genome of *A. thaliana* is totally sequenced, the generation of mutants can be easily produced. This species was used for fulfilling the first specific aim of this thesis (Chapter 2); to investigate the effect of inorganic phosphate deprivation. Seedlings of wild type ecotype Columbia-0 (WT) and nitrate reductase double mutant (*nia1,2*) were used to achieve this specific objective.

Wild-type (WT) and nitrate reductase double mutant (*nia1,2*) seeds of *A. thaliana* were surface-sterilized with 10% (v/v) sodium hypochlorite (NaClO) and washed three times with sterile deionized water. Then, the sterilized seeds were transferred to square Petri dishes containing the nutritive solution (Loque *et al.* 2003), as showed in Table 3.1., supplemented with 1% (w/v) sucrose and 100 mg/l Murashige and Skoog (MS) vitamin powder (Fig. 3.1A). Next, plates were kept overnight at 4 ºC to break dormancy, and then relocated vertically into a growth chamber at 18 ºC, 60-70% relative humidity and a long day photoperiod (16/8 h day/night).

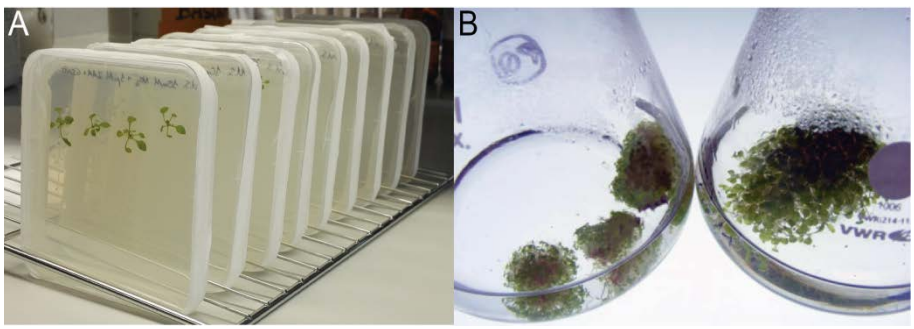

Figure 3.1. Arabidopsis thaliana *growth.* *A. thaliana* seedlings grown in vertically placed plates (**A**), and in liquid (**B**) modified MS medium.

For experiments with mitochondria seedlings were grown in liquid culture on a half strength medium without agar (Fig. 3.1B). The 100 ml beakers containing 25 ml of autoclaved medium were placed in a rotatory incubator at 18 ºC with a 16/8 h day/night photoperiod and continuous shaking at 60 rpm.

Table 3.1. ***Nutritive solution modified from Loque et al. (2003) for*** **A. thaliana** ***growth under axenic conditions.*** Macronutrients, micronutrients and nitrogen source employed in the medium for axenic culture. Final agar concentration was 1% (w/v).

Nutrients	Concentration
Macronutrients	**mM**
CaCl2	0.25
$MgSO_4$	1
KH_2PO_4	0 or 1
KCl	0.05
FeEDTA	0.1
Micronutrients	**µM**
Mn SO_4	10
$CuSO_4$	1.5
Zn SO_4	2
H_3BO_3	100
Na_2MoO_4	0.1
Na_2SiO_3	100
Nitrogen	**mM**
NH_4NO_3	1

In both cases, pH was adjusted to 5.8 and two different scenarios were carefully studied: the presence (+P) and the absence (-P) of inorganic phosphate (Pi). For control plants 1 mM PO_4^- was supplied whereas phosphate deficient plants were grown without supplying Pi (0 mM PO_4^-).

Finally, *A. thaliana* plants were harvested 15 days after germination, used fresh or frozen in liquid N_2 and stored at -80 ºC until use.

3.1.2. *Medicago truncatula*

Medicago truncatula Gaertn (Fabaceae) is also a model plant among legumes, a large family of plants with enormous agronomical importance. As in the case of *A. thaliana*, this species was chosen as a model plant because of its short life cycle with high production of seeds, and its small sequenced genome (Tang *et al.* 2014). In contrast with *A. thaliana*, legumes possess the ability of form symbiotic relations with nitrogen fixing bacteria. Thus, this species is commonly used to studying the fixation of the atmospheric nitrogen (N_2). Indeed, legumes suffer from phenotypic and physiological changes when cultured under different N sources (Dominguez-Valdivia et al., 2008; Ariz et al., 2011a). Therefore, to achieve the second specific aim of this

thesis (Chapter 2) of studying the differential effect of distinct nitrogen nutrition, i.e. ammonia and urea, in comparison to nitrate under axenic culture, this species was chosen due to the following reasons: (i) its tolerance to ammonium nutrition (while the effect associated with urea nutrition reminds unknown) and (ii) the ability of this plant to grow in axenic cultures, allowing the exclusion of contaminating bacteria and avoiding nodulation and the interference with other organisms.

Medicago truncatula (ecotype *Jemalong A17*) seeds were scarified and surface-sterilized under a laminar flow cabinet. For scarification, seeds were incubated in 95% sulfuric acid for 8 min and rinsed with sterile deionized water. After that, seeds were sterilized with 50% (v/v) NaClO for 5 min, and then rinsed with sterile water until pH was above 6. In order to synchronize germination, seeds were kept overnight in sterile water at 4 ºC in darkness. Then, they were subsequently germinated in Petri dishes containing 0.4% (w/v) plant agar for 72 h at 14 ºC, also in darkness (Fig. 3.2B and C). Seedlings were transferred in a laminar flow cabinet to glass pots containing 100 ml of Fahraeus medium with 5 g l^{-1} of Phytagel™ (Sigma-Aldrich) as nutrient solution (Table 3.2 and Fig. 3.2D). Nitrogen was supplied either as NO_3^- using $Ca(NO_3)_2$, as NH_4^+ using $(NH_4)_2SO_4$, or as urea (Table 3.3). In addition, seedlings used to determine the root system architecture were transferred to plates containing the same medium and placed vertically in the growth chamber (Fig. 3.2E).

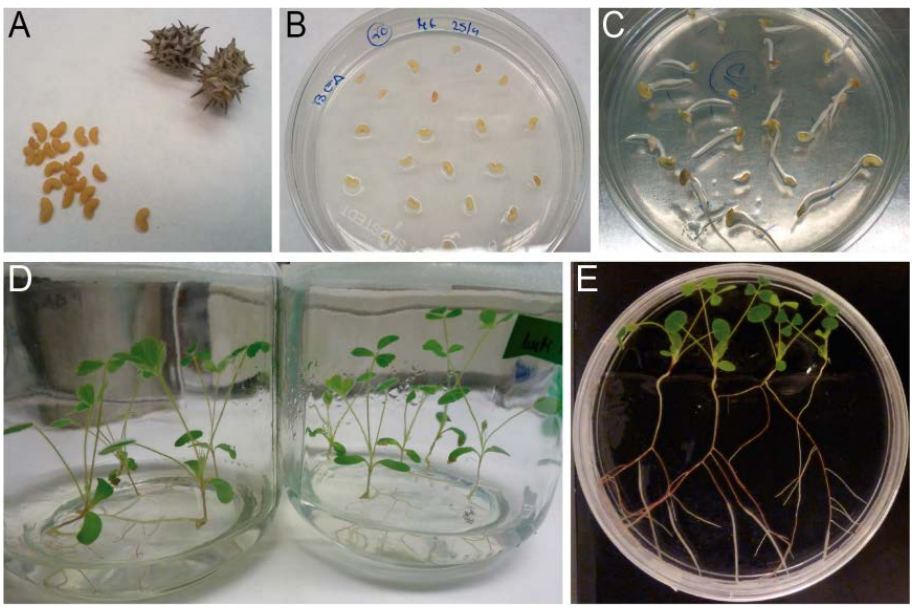

Figure 3.2. Medicago truncatula *sterilization, germination and growth.* Images of fresh (**A**), sterilized (**B**), and germinated (**C**) seeds of *M. truncatula*, and seedlings grown on (**D**) glass pots and € plates containing solid Fahraeus medium.

Table 3.2. ***Fahraeus nutritive solution for*** **Medicago truncatula** ***growth under axenic conditions.*** Macro- and micronutrients employed in the Fahraeus solution for axenic culture. Phytagel™ was added to a final agar concentration of 0.5% (w/v).

Nutrients	Concentration
Macronutrients	**mM**
$CaCl_2$	0.9
$MgSO_4$	0.5
KH_2PO_4	0.7
Na_2HPO_4	0.8
Ferric citrate	0.02
Micronutrients	**µM**
$MnCl_2$	0.8
$CuSO_4$	0.6
$ZnCl_2$	0.7
H_3BO_3	1.6
Na_2MoO_4	0.5

To study the differential effect of nitrogen, plants were grown under two different conditions. In particular, plants were grown with a low supply of N (1 mM) or at high N supply (25 mM) (Table 3.3).

In addition, in order to compensate the Ca^{+2} supplied with the NO_3^- treatment, the ammonium- and urea-fed plants were supplemented with 0.5 or 12.5 mM $CaSO_4$ when growing in low and high N concentration, respectively (Table 3.3).

Table 3.3. ***Nitrogen sources used in plants growth under axenic conditions.*** Calcium sulfate was added to the mediums containing NH_4^+ or urea as N source to equilibrate the content of calcium ion respect to nitric mediums.

Nitrogen Source	N Concentration	$CaSO_4 \cdot 2H_2O$
Nitrate	**mM**	**mM**
$Ca(NO_3)_2$	1	-
	25	-
Ammonium	**mM**	**mM**
$(NH_4)_2SO_4$	1	0.5
	25	12.5
Urea	**mM**	**mM**
$CO(NH_2)_2$	1	0.5
	25	12.5

Plants were cultured for 15 days in a growth chamber at 24.5/22 ºC (day/night) under 80% relative humidity with a 16/8 h photoperiod and a photosynthetically active

radiation of 70 µmols m^{-2} s^{-1}. During harvest, roots and shoots (0.1-0.2 g) were separately collected, frozen in liquid N_2 and kept at -80 ºC until use.

When preparing the Fahraeus axenic media for *M. truncatula* growth, the process of autoclaving the solutions differently affects the pH (Chapters 4.2, 4.3 and 4.4). As the pH at day 0 should be around 6.5 in all mediums, it was carefully controlled before, as well as after autoclaving as follows: pH of calcium and nitrogen sources were adjusted at 6.5 before sterilizing. The $CaCl_2$ and N sources were sterilized by filtering through cellulose acetate filters and $CaSO_4$ was sterilized by autoclaving in a separate bottle. Then, all of them were added to the rest of medium after autoclaving under a sterile laminar flow cabinet. This process allowed us to maintain a specific pH close to 6.5 at time of sowing for *M. truncatula* seeds (see Chapter 4.2, Fig.4.10).

In order to facilitate the understanding of the structure of the results (Chapter 4) from this thesis, the experimental design followed is depicted in Figure 3.3.

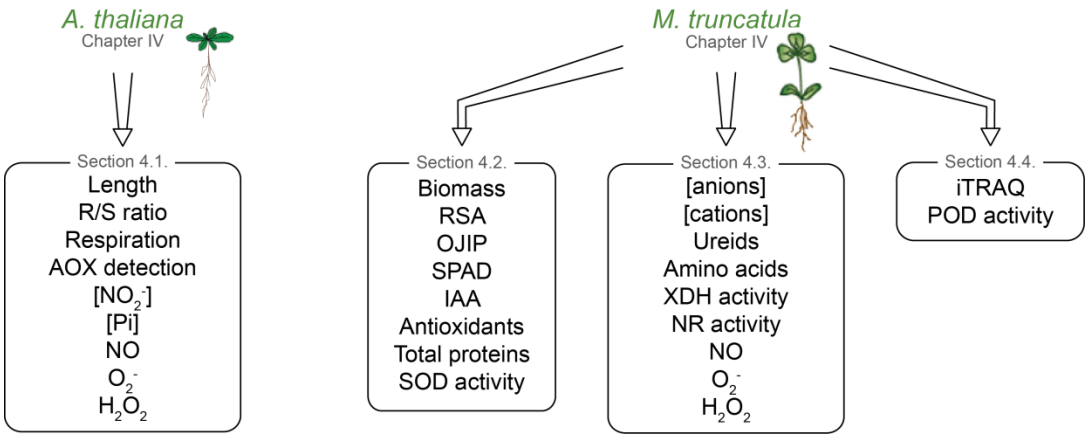

Figure 3.3. ***Experimental design.*** A schema showing the structure of the results (Chapter 4) and the parameters measured in *A. thaliana* and *M. truncatula plants,* respectively.

3.2. Morphological and physiological measurements

3.2.1. Total biomass (Chapter 4.2.)

To determine the fresh weight (FW) of both the roots and shoots, fifteen plants from each treatment were randomly selected at harvest, blotted with soft paper to remove any surface moisture and weighted. After obtaining the fresh weight, the same plant material was weighted after drying at 80 ºC for 48 h to obtain the dry weight (DW).

3.2.2. Length measurement of *A. thaliana plants* (Chapter 4.1.)

The length of roots and shoots of vertically grown *A. thaliana* seedlings were measured from photographs taken at 8 and 15 days after germination with the free software program ImageJ v1.47 (developed by Rasband, WS; National Institutes of Health, Bethesda, MD, USA; and available at http://rsbweb.nih.gov/ij/).

3.2.3. Root system architecture analysis (RSA) (Chapter 4.2.)

Root growth and architecture quantification was performed using the semi-automated image analysis software SmartRoot (Lobet *et al.* 2011). This software represents the roots as vectors, which serve to estimate the roots length, diameter and insertion angle from primary root base, as well as the accumulated length of lateral roots or the inter-branch distance (Fig. 3.4).

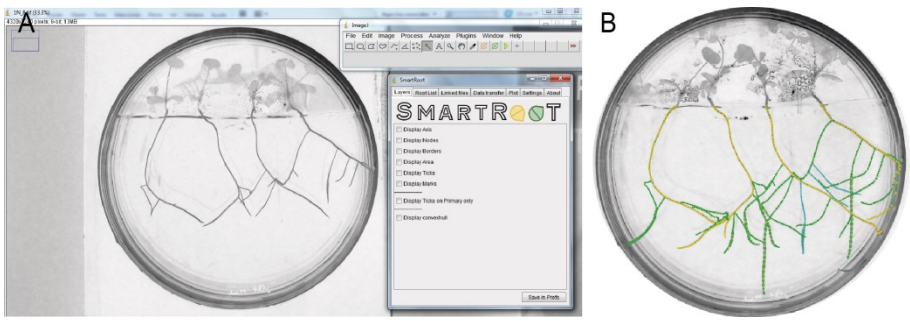

Figure 3.4. ***SmartRoot software used for root system architecture analysis.*** SmartRoot program appearance and running as an ImageJ plugin (**A**), and a representative image of *M. truncatula* growth analyzed (**B**).

In our study, four *M. truncatula* plants grew vertically on plates were photographed every 4 days for 15 days. Pictures were used to measure the growth rates, the accumulated length of lateral roots and their position of insertion from the root base. The architectural description of the root system under the different N sources was established in a dataset.

3.2.4. Respiration measurement (Chapter 4.1.)

Respiration rates were determined using a Clark type oxygen electrode (Oxygrapg, Hansatech, United Kingdom) and the software Oxygen32 was used to monitor the respiration reactions. The Clark electrode consists in an electrochemical cell composed of two electrodes (Ag and Pt) immersed in a 50% satured KCl electrolyte solution. When applying 700 mV, the electrolyte solution is ionized and a series of electrochemical reaction start (Fig. 3.5.). Firstly, the Ag electrode (anode) reacts with the chloride ion forming silver chloride (AgCl) and releasing electrons. Secondly, those electrons will reduce the oxygen present in the Pt electrode (cathode). Since oxygen is consumed during the electrochemistry, the magnitude of the current flow is related to the oxygen concentration (Clark 1956).

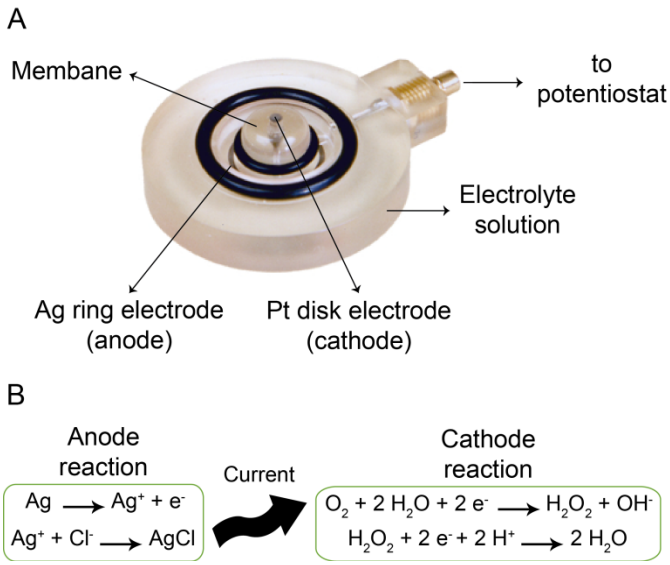

Figure 3.5. ***Clark type electrode.*** The different components of a Clark type electrode used for respiration measurements (**A**), and a schema of the reaction that occurs inside the cell (**B**) is illustrated. The current flow generated to produce the electrochemical consumption of oxygen in the cathode is used to measure the respiration rates.

First of all, calibration of the electrode was conducted using sodium dithionite ($Na_2S_2O_4$) to remove the oxygen and establish the zero. Subsequently, to establish the 100% of electric signal corresponding to an oxygen concentration of 250 µM O_2 at 25 ºC, distilled air saturated water was used.

Following, fresh plants (~50 mg) were placed in a darkened oxygen electrode chamber that contained 2 ml of 100 mM HEPES pH 7.6 buffer. Approximately after 8 min of reaction, a decrease of current corresponding to total respiration was observed. Then, 1 mM final KCN was added to measure AOX-linked respiration and the

reaction monitored during 6 min. Finally, AOX activity was blocked with 2 mM final concentration of salicylhydroxamic acid (SHAM) and residual respiration was scanned. The difference between the total respiration and the alternative was taken as the cytochromic respiration.

3.2.5. Determination of leaf chlorophyll fluorescence kinetics and content (Chapter 4.2.)

3.2.5.1. Chlorophyll *a* fluorescence

Chlorophyll *a* fast fluorescence transients (OJIP) of *M. truncatula* leaves were measured using a FluorPen FP 100 (Photon System Instrument, Brno, Czech Republic). The flow of energy through photosystem II is a highly sensitive signature of photosynthesis (Strasser *et al.*, 2000 and 2004; Stirbet and Govindiee, 2011), therefore the OJIP technique allows an estimation of photosynthetic performance. First, leaves were dark-adapted for 14 h to allow the complete relaxation or oxidation of reaction centers in order to determine the minimal fluorescence intensity (F_0). For excitation, bandpass filters of light emitting diodes with 697 to 750 nm provided of 3000 μmol photons m^{-2} s^{-1} at leaf sample and fluorescence transients were induced and recorded during 2 s at a frequency of 10 μs, 100 μs, 1 ms and 10 ms for the time intervals of 10-600 μs, 0.6-14 ms, 14-100 ms and 0.1-2 s, respectively. The fluorescence values at 40 μs (F_o, step 0, all reaction centers of the photosystem II are open), 100 μs (F_{100}), 300 μs (F_{300}), 2ms (step J), 30 ms (step I) and maximal (F_M, step P, closure of all reaction centers) were taken into consideration. Following the formulas derived from Strasser *et al.* (2000; 2004) based on the theory of energy fluxes in biomembranes, the cardinal points of the OJIP curve and derived parameters were calculated with the Fluorpen 2.0 software.

In this thesis, the fluorescence parameters derived from the extracted data and (i) normalized signals as V_j (F_j-F_o/F_M-F_o) and V_i (F_i-F_o/F_M-F_o), (ii) quantum yields and efficiencies, (iii) the specific fluxes per active reaction centre (RC) for absorption (ABS/RC), trapping (TR_0/RC), electron transport (ET_0/RC), and dissipation (DI_0/RC) have been considered. The performance index (Pi_{Abs}) represents the potential performance index for energy conservation from photons absorbed by photosystem II to the reduction of intersystem electron acceptors. Thus, the Pi_{Abs} has also been analyzed but not the events relative to photosystem I (Zubek *et al.*, 2009).

The formulas used to calculate the above described parameters and detailed information are showed in Table 3.4.

Table 3.4. *Definition of terms and formulae of the OJIP-test parameters used for the analysis of the chlorophyll a fluorescence transients following the formulas of Strasser* **et al.** *(2000, 2004).*

Data extracted from the recorded fluorescence transient OJIP		
F_t		Fluorescence at time t after onset of actinic illumination
F_o	$= F_{40\mu s}$	Minimal fluorescence intensity at 40 μs, when all reaction centers (RCs) are open
F_j	$=F_{2ms}$	Fluorescence value at 2 ms (J-level)
F_i	$=F_{30ms}$	Fluorescence value at 30 ms (I-level)
F_M	$=F_p=F_{1s}$	Maximal fluorescence intensity, when all RCs are closed
M_0	$4(F_{300\mu s}–F_0)/(F_M–F_0)$	Initial slope of the fluorescence transient
S_M	$Area/(F_M-F_o)$	Normalized area (assumed proportional to the number of reduction and oxidation of one Q_A^-molecule during the fast OJIP transient, and therefore related to the number of electron carriers per electron transport chain)
Fluorescence parameters derived from the extracted data		
V_t	$=(F_t-F_0)/(F_M-F_0)$	Relative variable chlorophyll (Chl) fluorescence at time t (from F_0 to F_M)
V_j	$=(F_J-F_O)/(F_M-F_0)$	Relative variable Chl fluorescence at 2 ms (at the J-step)
V_i	$=(F_i-F_O)/(F_M-F_0)$	Relative variable Chl fluorescence at 30 ms (at the I-step)
Specific energy fluxes per RC TR, ABS and ET denote the trapped, the absorbed excitation energy fluxes and the electron transport rate respectively		
ABS/RC	$(M_0/V_J)\cdot F_M/(F_M–F_0)$	Specific flux for absorption: absorption flux per RC. Also a measure of PSII apparent antenna size
TRo/RC	M_0/V_J	Specific flux for trapping: trapped energy flux per RC resulting in the reduction of QA to QA^-
ETo/RC	$(M_0/V_J)(1–V_J)$	Specific flux for electron transport: electron transport flux per RC
DIo/RC	$(M_0/V_J)(F_0/F_V)$	Specific flux for dissipation: the excitation energy dissipated, mainly as heat and less as fluorescence emission per RC

Table 3.4. *Continuation*

Quantum yields or flux ratio		
φ_{Po}	F_v/F_M	The maximum quantum yield of primary photochemistry: represents the probability that an absorbed photon is trapped by the RC and used for primary photochemistry.
Ψ_o	$1 - V_J$	The efficiency with which a trapped exciton can move an electron into the electron transport chain further than QA.
φ_{Eo}	$(1–(F_0/F_M))\cdot \Psi_o$	The quantum yield of electron transport: represents the probability that an absorbed photon moves an electron into the electron transport chain
φ_{Do}	$1– \varphi_{Po}–(F_0/F_M)$	The quantum yield for energy dissipation
PI_{Abs}	$[RC/ABS][TR_0/(ABS-TR_0)][ET_0/(TR_0-ET_0)]$	Performance index (potential) for energy conservation from photons absorbed by photosystem II to the reduction of intersystem electron acceptors.

3.2.5.2. Chlorophyll content by SPAD measurements

A chlorophyll meter SPAD-502 (Minolta, Japan) was used to obtain the relative content of chlorophyll in leaves (SPAD index) of *M.truncatula* plants at harvest moment. The device is based on two light-emiting diodes and a silicon photodiode receptor, and measures leaf transmittance in the red (600-700 nm) and in the near infrared regions of the visible spectra. To determine the amount of chlorophylls in the samples, the instrument uses these transmittance values to derive a relative SPAD value that is proportional to the chlorophyll content (Richardson *et* al., 2002; Ling *et al.*, 2010; Kalaji *et al.*, 2014).

3.3. Isolation of *A. thaliana* root mitochondria (Chapter 4.1.)

Mitochondria for AOX protein detection by western-blot were isolated from 10g of fresh weight of 15 days old *A. thaliana* seedlings grown on liquid culture. The isolation was carried out as described in (Day *et al.*, 1985; Sweetlove *et al.*, 2007) and all the proceeding was conducted at 4ºC. Briefly, seedlings were homogenized with a pestle and mortar in 200 ml of cold grinding medium (Table 3.5), followed by two 10 s bursts separated by 5-10 s in a blender. The homogenate was filtered through two layers of Miracloth (GE Healthcare) and centrifuged at 1500 *g* for 5 min. The resulting supernatant was then centrifuged at 12000 *g* for 15 min and the mitochondria-containing pellet was washed by repeating the two centrifugation step twice in the washing medium (Table 3.5). The obtained pellet of crude organelles was carefully resuspended in 4 ml of wash medium and gently layered over a 15 ml of a

discontinuous Percoll gradient composed of the following layers: 3 ml of 60% (v/v), 4 ml of 45% (v/v), 4 ml of 28% (v/v) and 4 ml of 5% (v/v), all containing 250 mM sucrose, 20 mM HEPES pH 7.6, and 0.1% BSA. Then, the gradient was centrifuged at 40000 *g* for 45 min and the mitochondrial fraction was seen as a yellow-brownish band at the interface between the 45 and 28% (v/v) layers (Figure 3.6A). After removal of the upper layers of the density gradient, the mitochondrial band was collected and diluted 5-fold with the same washing buffer prior to an additional centrifugation step at 24000 *g* for 10 min three more times, in order to remove the Percoll (Fig. 3.6B and 3.6C).

Table 3.5. Composition of grinding and washing mediums used for mitochondria isolation.

Grinding medium	Washing medium
0.3 M sucrose	0.3M sucrose
25mM tetrasodium pyrophosphate	0. 1% (w/v) BSA
1% (w/v) PVP-40	2mM $MgCl_2$
2mM EDTA	1mM EDTA
10mM KH_2PO_4	0.1mM KH_2PO_4
1% (w/v) BSA	20mM HEPES pH 7.6
20mM ascorbic acid	
100mM HEPES pH 7.6	

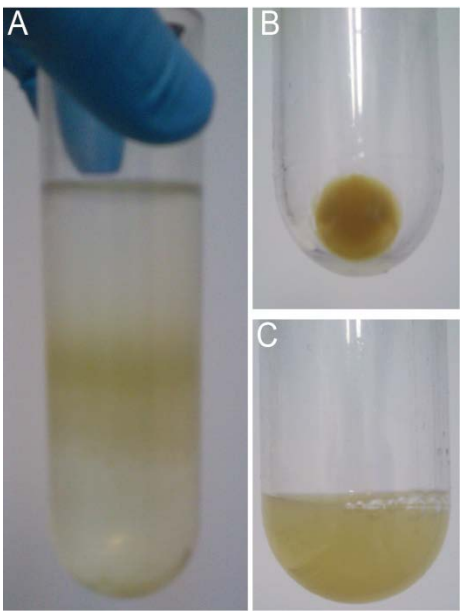

Figure 3.6. ***Isolation of* A. thaliana *root mitochondria.*** Mitochondrial fraction appeared as a yellow-brownish band in the Percoll gradient (**A**), pellet containing the mitochondrial fraction obtained after centrifugation (**B**), and resuspended mitochondria used to detect de AOX protein by immunoblotting (**C**) (see Chapter 3, section 3.5.3. and Chapter 4, section 4.1.4).

3.4. Analytical measurements

3.4.1. Determination of soluble inorganic ionic contents

3.4.1.1. Ionic content determination by chromatography (Chapter 4.3.)

Inorganic ionic content determination from *M. truncatula* roots and shoots were measured with the isocratic ion chromatography technique using a DIONEX-DX500 ion chromatograph (Dionex Corporation, CA, USA). The ion detection was done by conductivity. The cellular soluble ionic fraction was obtained by centrifugation (16000 *g*, 30 min) of root or leaves tissues from frozen plant (0.2 g) previously incubated in 1 ml milli-Q water at 80 ºC in a bath for 5 min (Ariz *et al.* 2011). The stored supernatants at -20 ºC were diluted 1:10 for injection with an AS40 autosampler (Dionex) and a 1.5 ml min^{-1} flow of solvent composed by 30% 100 mM NaOH and 70% milli-Q water was applied for 15 min.

Soluble anions (NO_3^-, NO_2^-, PO_4^{-3}, SO_4^{-2}, and Cl^-) were determined by gradient separation with Ion Pac AS-11 column and suppressor column ASRS (4 mm) connected to an ion trap ATC-3 protecting column, and a pre-column Ion Pac AG-11.Soluble cations (Na^+, K^+, Ca^{+2}, Mg^{+2}, and NH_4^+) determination was carried out by isocratic elution with 20 mM metanosulphonic acid solute as eluent with Ion Pac CG12A and Ion Pac CS12A columns for 13 min, and suppressed conductivity detection (ED 40 Dionex).

The sum of either anions or cations was used to represent total anions (A^-) or cations (C^+), and the C+/A- ratio.

3.4.1.2. Nitrite determination by the Griess method (Chapter 4.1.)

For the detection of nitrite in *M. truncatula* roots following this assay, the supernatants obtained in the extraction for ion chromatography (Chapter 3, section 3.4.1.1) were used.

Nitrite contents from *A. thaliana* and *M. truncatula* roots were measured by the Griess colorimetric assay (Planchet *et al.* 2005). *Arabidopsis thaliana* root samples (0.1 g FW) were ground in 25 mM HEPES buffer pH 7.6 and then crentrifuged at 13000 *g* for 12 min. Aliquots (100 µl) of the supernatants obtained were mixed with a solution composed of 10 µM zinc acetate, 0.02% (w/v) N-(1)-(naphthyl) ethylenediaminedihydrochloride (NEDA) and 1% (w/v) sulphanilamide. After 25 min of incubation at room temperature, samples were cleared by centrifugation at 16000 *g*

for 5 min. The nitrite content from the supernatant was determined spectrophotometrically at 540 nm. **3.4.1.3. Inorganic phosphate (Chapter 4.1.)**

Free Pi content was measured by a colorimetric assay as described in Bozzo *et al.* (2006). In brief, 0.1 g of frozen plant tissues were ground in 0.5 mL of 10% perchloric acid and centrifuged at 13000 rpm for 10 min. Then, the supernatant was neutralized with 5 M KOH and the precipitate was removed by centrifugation. Thus, an aliquot of the supernatant was added to 100 µl of a freshly prepared assay solution containing a 4:1 mixture of 10% (v/v) ascorbate and 10mM ammonium molybdate in 15 mM zinc acetate pH 5.0. Finally, samples were incubated for 60 min at 37 ºC and Pi was determinate by measuring the absorbance at 720nm.

3.4.2. Total soluble proteins (Chapters 4.2. and 4.4.)

Total soluble proteins were quantified from roots and shoots as described in Bradford (1976) by using the extracts obtained for the different enzymatic determinations. Shortly, the protein content was estimated in a mixture composed of 60 µl of diluted extract (1:25 and 1:50 in roots, and 1:50 and 1:75 in shoots) and 200 µl of Bradford reagent (Bio-Rad, Watford, UK) added in microplates, and bovine serum albumin (BSA) was used as standard. After 5 min of incubation at room temperature, the absorbance at a wavelength of 595 nm was read in a microplate reader (SpectraMax 340pc, Molecular Devices).

3.4.3. Aminoacids (Chapter 4.3.)

Amino acids determination from roots and shoots of *M. truncatula* seedlings was performed using high-performance capillary electrophoresis in a Beckman Coulter PA-800 apparatus (Beckman Coul-ter, Inc., Brea, CA) with laser-induced fluorescence detection (argon ion: 488 nm). Frozen plant tissues (0.1 g) were ground with mortar and pestle using liquid N_2. Powdered samples were homogenized with 1.5 ml of 1 M HCl, incubated in ice for 10 min and centrifuged (13000 *g*, 10 min, 4ºC). The obtained supernatant was neutralized with NaOH and stored at -80 ºC until analyzed. Amino acids were derivatized with fluorescein isothiocyanate (FITC) dissolved in 20 mM acetone/borate pH 10 at room temperature between 12 and 16 h. Single amino acids were separated using a 50 µm i.d. × 43/53.2 cm fused silica capillary at a voltage of 30 kV and a temperature of 20 ºC. A pressurized method (5 s, 0.5 psi) was used to inject the samples, and a solution composed by 80 mM borax and 45 mM alfa-cyclodextrin at pH 9.2 was used as migration buffer. Norvaline and homoglutamic acid were used as internal standards.

3.4.4. Ureides (Chapter 4.3.)

The concentration of ureides was analyzed by the colorimetric assay described by Vogels and Van der Drift (1970). In this method, a chemical transformation of ureides to glyoxylate is needed prior to their independent determination (Figure 3.7.). Thus, allantoin, allantoate, ureidoglycolate and glyoxylate were quantified, and the total ureides content correspond to the sum of them.

Briefly, 0.1 g of plant tissue was homogenized in 50 mM Tris-HCl pH 7.8, 100 mM $MgSO_4$ and 0.15 % (w/v) deoxycholic acid, centrifuged to remove cell debris and the obtained extract was used immediately. Allantoin was transformed to allantoate by incubation in 0.5 M NaOH at 100ºC for 10 min, and cooled in ice. Both, present and produced, allantoate were transformed to glyoxylate by incubating with 0.65 N HCl at 100 ºC for 10 min and subsequently kept in ice. Ureideoglycolate content was measured after its transformation to glyoxylate by incubating the extract in 0.4 M sodium phosphate buffer pH 7.0 at 100 ºC for 10 min. After cooling the samples at 4 ºC, a solution of 0.33% (w/v) phenylhydrazine-HCl was added.

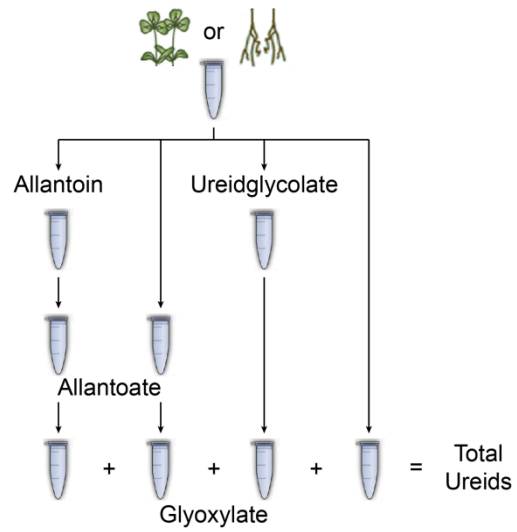

Figure 3.7. ***The processing chart for quantification of ureides.*** The schema shows the procedure followed for the extraction, transformation and analysis of the ureides of *M. truncatula* tissues.

Finally, the glyoxylate present in the extracts as well as the obtained from the allantoin, allantoate and ureidoglyocolate transformation was measured as follows. The glyoxylate containing extracts were mixed with 0.4 M sodium phosphate pH 7.0 and 0.33% (w/v) phenylhydrazine-HCl. After 10 min at room temperature, 12 N HCl and 1.6% (w/v) potassium ferricyanide were added prior to incubate 15 min at room temperature. The content of glyoxylate in the mixtures was estimated

spectrophotometrically at 520 nm, and the molar extinction coefficient of the end product glyoxylate diphenylformazan was used ($\mathfrak{E}$ = 42.36 $mM^{-1}cm^{-1}$).

3.4.5. Indole-3-acetic acid content (Chapter 4.2.)

The concentration of indole-3-acetic acid (IAA) was analyzed in shoot and root extracts using high performance liquid chromatography-electrospray-mass spectrometry (HPLC-ESI-MS/MS) as described in Jauregui et al. (2015). For the extraction, 0.3 g of frozen plant tissues were homogenized with 4 ml of precooled 90:9:1 (v/v/v) methanol:water:formic acid with 2.5m*M* sodium diethyldithiocarbamate. The internal standards $^{2}H_5$-IAA (D-IAA) was added to the extraction medium deuterium-labeled from a stock solution of 2000 ng ml^{-1} of D-IAA in methanol. Then, homogenized samples were shaken for 60 min at 2000 rpm at room temperature in a Multi Reax shaker (Heidolph Instruments, Schwabach, Germany). Secondly, samples were centrifuged at 11000 rpm for 10 min using a Centrikon T-124 (Kontron Instruments, Cumbernauld, UK) to separate the solids, and further re-extracted by shaking with 3 ml of extraction buffer for 20 min. Next, supernatants were passed through a Strata C18-E cartridge (Phenomenex, Torrance, CA, USA). Finally, 5 ml of diethyl ether was used to hormones extraction, and the organic phase was evaporated to dryness. Before injection into the quantification system, the residue was redissolved in 250 µl of 40:60 (v/v) methanol:0.4% acetic acid and centrifuged at 3750 g for 10 min. Hormones were quantified by HPLC-ESI-MS/MS using an HPLC (2795 Alliance HT; Waters Co., Milford, MA, USA) coupled to a 3200 Q-TRAP LC/MS/MS System (Applied Biosystems/MDS Sciex, Ontario, Canada), equipped with an electrospray interface. A reverse-phase column (Synergi 4 mm Hydro-RP 80A, 150×2 mm; Phenomenex) was used. The detection and quantification of the hormone was carried out using multiple reactions monitoring in the negative-ion mode, employing multilevel calibration curves with the internal standards as described in Jauregui et al. (2015).

3.4.6. Reactive Oxygen and Nitrogen Species determination

The levels of the reactive nitrogen and oxygen species (RNS; ROS) nitric oxide (NO), superoxide (O_2^-) and hydrogen peroxide (H_2O_2) were determined as follow (Fig. 3.8).

3.4.6.1. Nitric oxide measurement (Chapters 4.1. and 4.3.)

a) Nitric oxide detection by fluorescence bioimaging

Nitric oxide was detected using the cell-permeable fluorescence indicator 4,5-diaminofluorescein diacetate (DAF-2DA) (Sigma). Once DAF-2DA is inside the cell, cellular esterases transform the probe into DAF-2 preventing the diffusion of the molecule from the cell. Thus, in the presence of oxygen DAF-2 reacts with NO and the highly fluorescent molecule trizaolofluorescein (DAF-2T) was formed (Kojima *et* al. 1998).Roots were incubated in 1 ml of 2.5 mM HEPES buffer and 10 μM DAF-2DA at pH 7.6 in darkness. Incubation time was adapted to the species studied. Thus, *A. thaliana* roots were incubated for 15 min, while incubation period of *M. truncatula* roots was 30 min. Immediately; roots were washed with 2.5 mM HEPES pH 7.6 buffer in order to remove the excess of fluorescence around the tissues (Fig. 3.8A). The formation of DAF-2T was visualized using a Leica M165-FC fluorescence microscope upon excitation at 488 nm with an Argon 2 laser. Finally, fluorescence emission was recorded using a 505-530 nm band-pass filter coupled with a 515 nm long-pass filter. Images were taken with Leica DFC310-FX camera and further analyzed using ImageJ software for NO quantification (Fig. 3.8A). To demonstrate NO was being measured, 200 μM of the NO scavenger cPTIO was used as control.

b) Nitric oxide determination by the Griess method (Chapter 4.1.)

As recommended in Gupta and Igamberdiev (2013), in the case of *A. thaliana* roots, NO was measured using a second method: the gas phase Griess assay. As can be seen in Figure 3.8B, the NO released from plants is first oxidized to NO_2 in the air stream, and then converted to NO_2^- in the detection solution forming an adduct that could be detected spectrophotometrically. As described in Gupta *et al.* 2014, roots (0.5 g FW) were incubated in 25 mM HEPES buffer pH 7.6 containing 0.5 mM NO_2^-, and the NO emitted by roots over 30 min was swept by a stream of air into a solution containing 0.02% (w/v) N-(1)-(naphthyl) ethylenediaminedihydrochloride (NEDA) and 1% (w/v) sulphanilamide. The estimation of the NO produced by *A. thaliana* roots was read by measuring the absorbance at 540 nm.

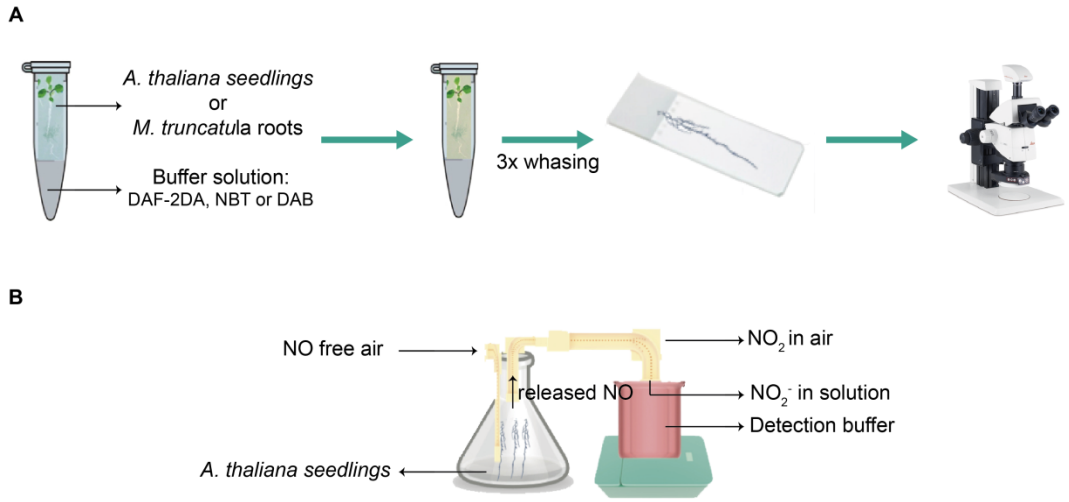

Figure 3.8. ***Reactive nitrogen and oxygen species detection.*** Experimental procedure to detect (**A**) nitric oxide, superoxide and hydrogen peroxide by bioimaging in *A. thaliana* and *M. truncatula* roots using the fluorescence probe DAF-2DA, NBT and DAB staining, respectively; and (**B**) nitric oxide by the gas phase Griess method in *A. thaliana* roots.

3.4.6.2. Superoxide and hydrogen peroxide detection (Chapters 4.1. and 4.3.)

Superoxide (O_2^-) and hydrogen peroxide (H_2O_2) levels were in vivo estimated in seedlings using the nitroblue tetrazolium chloride (NBT) and the 3,3'-diaminobenzidine (DAB) staining methods respectively as follows (Jambunathan, 2010; Fig. 3.8A):

a) O_2^- quantification

Seedlings were immersed in a 0.1% (w/v) NBT solution for 24 h and destained with 96% (v/v) ethanol at 40 ºC. Images were taken using a Leica M165-FC microscope coupled with a Leica DFC310-FX camera.

b) H_2O_2 quantification

Seedlings were incubated in 1 mg/ml 3,3'-diaminobenzidine (DAB) pH 3.8 staining solution for 24 h. After destaining the tissues at 40 ºC using 96% (v/v) ethanol, photographs were taken with a Leica M165-FC microscope coupled and a Leica DFC310-FX camera.

Images were analyzed using the software ImageJ to quantify the blue (O_2^-) or brown (H_2O_2) staining. Thus, the number of pixels in the intensity range of each ROS color was quantified.

3.4.7. Small antioxidant molecules (Chapter 4.2.)

Ascorbate (ASC), glutathione (GSH) and homoglutathione (hGSH), as representative reduced and oxidized forms of the small antioxidants, were measured in roots and shoots just as described in Zabalza *et al.* (2007). Briefly, frozen tissue samples (0.2 g) were powdered with mortar and pestle using liquid nitrogen and then homogenized with 2 ml of an extraction medium composed of 2% metaphosphoric acid and 1mM EDTA. Subsequently, the homogenate was centrifuged for 2 min at 4400 *g* at 4 ºC and filtered. The antioxidant metabolite content were analyzed by high-performance capillary electrophoresis (HPCE) in a Beckman Coulter P/ACE system 5500 (Fullerton, CA, USA) using a capillary tubing (50 μm; 30/37cm long) applying a potencial of 15kV. The UV detection was made with a diode array detector by setting wavelength at 200 and 256 nm. Hence, the detection of reduced ASC, GSH and hGSH were carried out directly by injecting an aliquot of tissue extract in the HPCE, and using standards as reference. However, to measure the dehydroascorbate (DHA), oxidized glutathione (GSSG) and oxidized hGSH (hGSSG) metabolites, the reduction with DTT of the extracts was needed (Davey *et al.* 2003) prior to the injection in the HPCE. Next, total ASC, GSH and hGSH were analyzed from the reduced samples, and then DHA, GSSG and hGSSG contents were obtained by subtracting the content of the reduced corresponding form from the total antioxidant content. In addition, the ratio between the reduced form (ASC, GSH, hGSH) and the total antioxidant content was determined as an indicator of the plants redox status. Regarding the plant redox state, GSH and hGSH are analogous molecules so we have considered both metabolites together.

3.5. Enzymatic activities determination

3.5.1. In-gel activity assays (Chapters 4.2. and 4.3.)

3.5.1.1. Superoxide dismutase (EC 1.15.1.1)

Superoxide dismutase (SOD) activity of *M. truncatula* roots and shoots were estimated in-gel as described by Beauchamp and Fridovich (1971) and Asensio *et al.* (2011; 2012). These assays are based on the inhibition of the reduction of nitroblue tetrazolium (NBT) by SOD due to the O_2^- radicals generated photochemically. The identification of the different SOD isoforms was made according to known mobility of the enzyme on native gels.

Frozen samples (0.2 - 0.3 g FW) were homogenated with cold extraction buffer (50 mM potassium phosphate pH 7.8, 0.1 mM EDTA, 0.1 % (v/v) Triton X-100 and 1% (w/v) PVP-10), filtered through Miracloth (Calbiochem) and centrifuged at 4 ºC for 20 min at 22000 *g*. Supernatants containing the SOD isoenzymes were separated on

15% (w/v) native PAGE, and the electrophoresis process was run for 2 h at 200 V in the cold room. In this way, the mobility of SODs into the gels was improved by increasing the electrophoresis time one hour after the bromophenol blue reaches the end of the gel. After the separation, gels were kept in reaction buffer for 30 min, and then transferred to reaction buffer supplemented with 0.5 mM NBT and incubated for 20 min. Further, gels were incubated in 0.03 mM riboflavin and 0.2% (v/v) TEMED for 20 min. Finally, they were exposed to white light until SOD bands were visualized.

For the identification of the different SOD isoforms, gels were pre-incubated with 3 mM KCN or 5 mM H_2O_2 for 1 h (Asensio *et al.* 2011; 2012) before NBT and riboflavin-TEMED incubations.

All incubations were performed in darkness. Quantification of SOD isoforms was performed using the software ImageJ.

3.5.1.2. Xanthine dehydrogenase (EC 1.17.1.4., formally EC 1.1.1.204)

In-gel xanthine dehydrogenase (XDH) activity was assayed in roots and shoots of *M. truncatula*. The determination of XDH is based on the enzymatic reduction of a tetrazolium salt to its insoluble formazan, which has a purple color. Concisely, frozen plant tissues (0.1-0.2 g) were grounded with 100 mM potassium phosphate pH 7.5, 5 mM DTT and 2 mM EDTA pH 8.0 in a precooled mortar and pestle. The extracts were sonicated in an ultrasonic water bath and centrifuged for 20 min at 20000 *g* and 4 ºC, and supernatants were used to perform the assay. After the extraction, protein extracts (30 μg of roots or 50 μg of shoots) were loaded on 7.5 % (w/v) native PAGE in the cold room. The electrophoresis was run for 90 min at 150 V. Subsequently, gels were equilibrated in 250 mM TRIS-HCl pH 8.5 for 15 min and further stained for 1 hour in darkness. The staining solution was composed by 10 ml of 250 mM Tris-HCl pH 8.5, 50 mg of hypoxanthine, 4-8 mg of 3-(4,5 dimethylethiazol-2-yl)-2,5-diphenyltetrazoliumbromide (MTT) and 50 μl of 10 mg/ml phenazine methosulfate (PMS). After staining, gels were washed several times with distilled water in order to stop the reaction and remove the background. The ≈300 kDa bands were quantified using the ImageJ software.

3.5.2. Spectrophotometric activity assay (Chapter 4.4.)

3.5.2.1. Nitrate reductase (EC 1.6.6.1)

Nitrate reductase (NR) activity was assayed in *M. truncatula* roots as described previously in Gonzalez *et al.* (2001) with some modifications. Root tissues (0.2 g) were ground to powder with mortar and pestle and homogenated with 50 mM HEPES pH 7.5, 2 mM EDTA and 5 mM DTT extraction buffer. After filter through one layer of Miracloth (Calbilochem), the homogenate was centrifuged at 4 ºC for 5 min at 12000 *g*, and the maximal and actual NR activity were measured. Firstly, 30 µl of supernatant were pre-incubated in 300 µl of reaction buffer for 10 min at 30 ºC, and following the reaction was started with the addition of 5 mM KNO_3 and 0.2 mM NADH. The reaction buffer was composed of 50 mM HEPES pH 7.5, 10 mM EDTA, 5 mM AMP and 10 µM FAD for maximal NR, and 50 mM HEPES pH 7.5, 20 mM $MgCl_2$ and10 µM FAD for actual NR. After a further 30 min, samples were heated for 5 min at 100 ºC, gently shaken and incubated on ice to stop the reaction. Secondly, samples were centrifuged at 4 ºC for 5 min at 12000 *g*. Finally, 300 µl of supernatant were mixed with equal quantities of 0.02% (w/v) N-(1)-(naphthyl) ethylenediaminedihydrochloride (NEDA) and 1% (w/v) sulphanilamide and incubated 15 min at room temperature. The absorbance of the nitrite produced was read at 540 nm.

3.5.2.2. Peroxidase (EC 1.11.1.)

Peroxidase (POD) activity was measured in roots from *M. truncatula* plants. For the extraction, 0.1-0.2 g of frozen tissues were homogenized at 4 ºC with a medium containing 50 mM potassium phosphate buffer at pH 6.0, 1 mM EDTA, 2 mM DTT, 0.5% (v/v) TRITON and 1.5% (w/v) PVPP. Enzyme crude extracts were obtained by centrifugation at 16000 *g* for 20 min at 4ºC.

Two different POD activities were measured using these extracts: guaiacol peroxidase (GP), and ferulic acid peroxidase (FP).

Guaiacol peroxidase activity assay was adapted from Stasolla and Yeung (2007). Thus, oxidation of guaiacol was spectrophotometrically monitored at 25ºC for 2 min at a wavelength of 470 nm (ε=26.6 $mM^{-1}cm^{-1}$). The reaction was followed after the addition of 10 µl of enzyme extract to a mixture that contained 50 mM sodium phosphate pH 6.0, 1 mM guaiacol and 5 mM H_2O_2.

The ferulic acid (FA) activity was estimated as described in Cordoba-Pedregosa *et al.* (1996). As FA is a substrate for cell wall forming PODs, FP was estimated by following the oxidation of FA at 310 nm for 2 min (16.3 mM^{-1} cm^{-1}). The reaction was

initiated by adding 10µl of enzyme extract to a mixture composed of 50 mM sodium phosphate pH 6.0, 0.1 mM FA and 5 mM H_2O_2 and the reaction.

3.5.3. Detection of AOX by western blot analysis (Chapter 4.1.)

As a complement to the respiration measurements, AOX protein from mitochondria isolated from *A. thaliana* seedlings (Chapter 3, section 3.3.) was detected by immunoblotting. Proteins (30 µg per lane) were separated by SDS-PAGE and electroblotted onto Hybond ECL membrane (GE Healthcare). The AOX protein was immunochemically detected using the anti-AOX1A antibody (Agrisera) and the anti-mouse IgG conjugated with horseradish peroxidase (Sigma) as primary and secondary antibodies, respectively. Briefly, the membranes were first blocked with 1% (w/v) BSA in TBS buffer overnight at 4 ºC, and then incubated for 24 hours with the primary antibody diluted up to 1:1000 (v/v) in TBS-T buffer (0.05% Tween-20, 150 mM NaCl and 10 mM Tris pH 8.0) with 5% BSA. After washing three times with TBS-T buffer, the membranes were incubated with the secondary antibody for 1 hour. Finally, AOX protein was detected using a chemiluminescence HRP kit purchased from Bio-Rad, using LAS-4000 (Fujifilm; GE Healthcare) image analyzer.

3.6. Proteomic analysis using iTRAQ approach (Chapter 4.4.)

A comparative proteomic analysis of *M. truncatula* roots using the isobaric Tags for Relative and Absolute Quantitation (iTRAQ) approach was performed (Unwin *et al.* 2010). The experiment was carried out with two-three biological replicates in each experimental condition. The specific procedures for proteins extraction, sample preparation, iTRAQ-based proteomic workflows (Figure 3.9) and mass spectrometry used are explained below.

3.6.1. Protein extraction

Total proteins of *M. truncatula* roots were obtained from frozen tissues (0.3 g) previously ground using mortar and pestle, and with the addition of proteases inhibitor. Powdered samples were homogenated with 500µl of extraction buffer containing 7 M urea, 2 M thiourea, 4% (w/v) CHAPS, 2% (v/v) TritonX-100 and 50 mM DTT. The homogenate was transferred to eppendorfs tubes and centrifugated at 10000 *g* for 10 min at 4 ºC. Consecutively, supernatants containing total root proteins were recovered and conserved at -80 ºC until use.

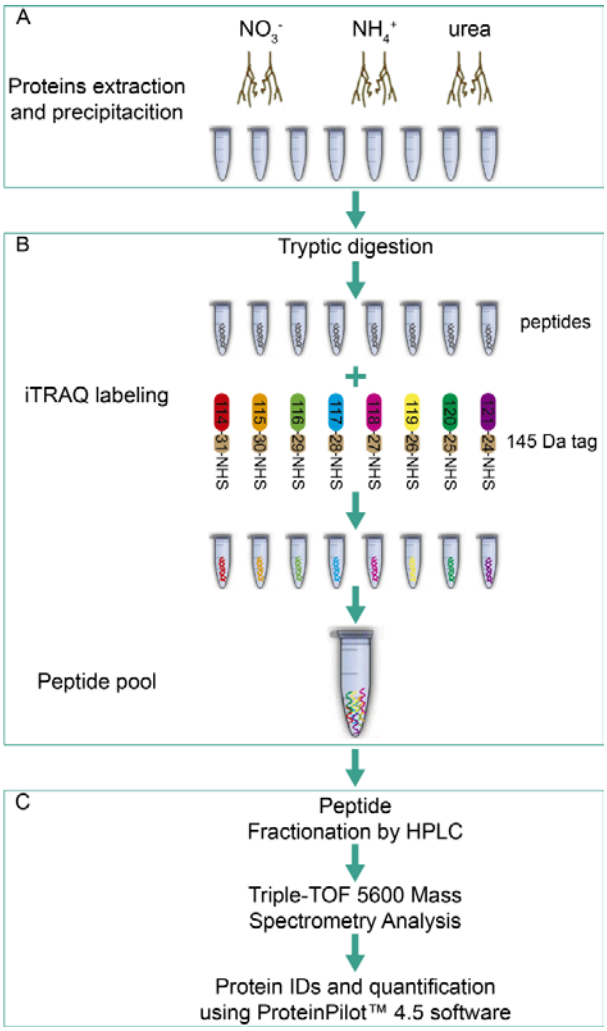

Figure 3.9. iTRAQ based proteomic analysis. The workflow followed for the proteomic analysis of NO_3^-, NH_4^+, and urea *M. truncatula* fed roots using iTRAQ approach was divided into 3 phases. (**A**) Extraction and precipitation of total roots proteins; (**B**) digestion of proteins with trypsin, labeling and mixing of peptides; and (**C**) labeled peptides pool fractionation, peptides analysis, proteins identification and quantification.

3.6.2. Peptide labeling

Root protein extracts (150 μg) were precipitated with methanol/chloroform, and the obtained pellets were resuspended in a mixutre of 7 M urea, 2 M thiourea and 4% (v/v) CHAPS. Protein content of each extract was quantified with the Bradford assay kit (Bio-Rad) prior to label the samples. As described next, samples iTRAQ labeling was performed according to the manufacturer's protocol (ABSciex). Briefly, a total of 100 μg of protein from each sample was reduced with 50 mM tris(2-carboxyethyl) phosphine (TCEP) at 60 °C for 1 h, and cysteine residues were alkylated with 200 mM

methylmethanethiosulfonate (MMTS) at room temperature for 15 min. Trypsin (Promega; 1:20, w/v) was used to protein enzymatic cleavage at 37 ºC for 16 h and each tryptic digest was labelled with one isobaric amine-reactive tag by incubation during 1 h. Finally, each set of labelled samples were independently pooled and evaporated until reach a volume lower than 40 µl in a vacuum centrifuge.

3.6.3. Peptide fractionation by HPLC

In order to increase proteome coverage, peptide fractionation was performed before characterize proteins. The peptide pool was injected to an Ettan LC system with a X-Terra RP18 pre-column (2.1 x 20mm) and a high pH stable X-Terra RP18 column (C18; 2.1mm x 150mm; 3.5µm) (Waters) at a flow rate of 40 µl/min. Peptides were eluted with a mobile phase B of 5–65% linear gradient over 35 min (A, 5 mM ammonium bicarbonate in water at pH 9.8; B, 5 mM ammonium bicarbonate in acetonitrile at pH 9.8). Then, 11 fractions were collected, evaporated under vacuum and reconstituted into 20 µl of 2% acetonitrile, 0.1% formic acid, 98% milli-Q H_2O prior to mass spectrometric analysis.

3.6.4. Mass spectrometry analysis

Peptides mixtures contained in each fraction were separated by reverse phase chromatography using an Eksigent nanoLC ultra 2D pump fitted with a 75 µm inner diameter column (Eksigent 0.075 x 25cm). First of all, samples were loaded for desalting and concentration into a 0.5 cm length and 300 µm inner-diameter pre-column packed with the same chemistry as the separating column. Mobile phases were 0.1% formic acid (FA) in 100% water as buffer A and 0.1% FA in 100% acetonitrile as buffer B. Column gradient was developed in a 237 min two step gradient from 5% B to 25% B in 180 min and 25% B to 40% B in 30 min. Column was equilibrated in 95% B for 10 min and 5% B for 15 min. During all process, pre-column was in line with column and flow maintained all along the gradient at 300 nl/min. Eluting peptides from the column were analyzed using an AB Sciex 5600 TripleTOF™ system. Data was acquired upon a survey scan performed in a mass range from 350 m/z up to 1250 m/z in a scan time of 250 ms. Top 35 peaks were selected for fragmentation. Minimum accumulation time for MS/MS was set to 100 ms giving a total cycle time of 3.8 s. Product ions were scanned in a mass range from 100 m/z up to 1700 m/z and excluded for further fragmentation during 15 s. After MS/MS analysis, data files were processed using ProteinPilot™ 4.5 software from AB Sciex which uses the algorithm Paragon™ (v.4.5.0.0.1654) (Shilov *et al.* 2007) for database search and Progroup™ for data grouping and searched against Uniprot *M.truncatula* database. False discovery rate

(FDR) was performed using a non-lineal fitting method and displayed results were those reporting a 1% global FDR or better.

3.6.5. Data analysis

Raw data (.wiff, AB Sciex) were analyzed with *MaxQuant* software (Cox and Mann, 2008). For peak list generation, default AB Sciex Q-TOF instrument parameters were used except the main search peptide tolerance and MS/MS match tolerance, which were set to 0.01 Da and increased up to 50 ppm respectively. A contaminant database (.fasta) was used for filtering out contaminants. Peak lists were searched against JCVI database (http://www.jcvi.org/medicago) of *Medicago truncatula* protein sequences, and Andromeda was used as a search engine (Cox *et al.* 2011). Methionine oxidation was set as variable modification, and the carbamidomethylation of cysteine residues was set as fixed modification. Reporter ion intensities were bias corrected for the overlapping isotope contributions from the iTRAQ tags according to the certificate of analysis provided by the reagent manufacturer (ABsciex). The peptide and protein selection criteria for relative quantitation were performed as follows. Maximum false discovery rates (FDR) were set to 0.01 at protein and peptide levels. Analyses were limited to peptides of six or more amino acids in length, and considering a maximum of two missed cleavages.

Relative protein abundance output data files were managed using R scripts or Matlab for subsequent statistical analyses and representation. Proteins identified by site (identification based only on a modification), reverse proteins (identified by decoy database) and potential contaminants were filtered out. Among the identified peptides, some of them were excluded from the quantitative analysis for one of the following reasons: (i) The peaks corresponding to the iTRAQ labels were not detected; (ii) the peptides were identified with low identification confidence (<1.0%); (iii) the sum of the signal-to-noise ratio for all of the peak pairs was <6 for the peptide ratios. Only proteins with more than one identified peptide were used for quantification. For possible quantification data rescue, up to one missing value for each group was rescued replacing it by the mean of the rest in-group samples.

Data were normalized and transformed for later comparison using quantiles normalization and log2 transform respectively. The Limma Bioconductor software package in R was used for ANOVA analyses. Significant and differential data were selected by a *p*-value lower than 0.01, fold changes of <0.77 (down-regulation) and >1.3 (up-regulation) in linear scale. Thus, proteins with iTRAQ ratios below 0.77 were considered to be underexpressed, whereas those above 1.3 were considered to be

overexpressed. These parameters were used for differential expression threshold with volcano and profile plots.

3.6.6. Proteomic data analysis

The analysis of the proteomic information was performed using bioinformatic tools. Hence, the functional classification of the differentially accumulated proteins was realized according to the Gen Onthology Annoatation (GOA) consortium and using the browser QuickGo (https://www.ebi.ac.uk/QuickGO/) developed by the European Bioinformatics Institute (EMBL-EBI) (Binns *et al.*, 2009). Proteins were also clustered into orthologous groups using the database eggNOG 4.5 (Huerta-Cepas *et al.* 2016). Moreover, the identified proteins were studied with the Kyoto Encyclopedia of Genes and Genomes (KEGG) and the enriched metabolic pathways were analyzed with the pathway mapping tool KOBAS 3.0 (http://kobas.cbi.pku.edu.cn/).

3.7 Statistical analysis

The data obtained in this research was analyzed statistically using the mean as a measure of central tendency and the standard error (SE) as a measure of dispersion. All data were tested for normality (Kolmogorov-Smirnof test) and homogeneity of variances (Levene (used usually for n>8) or Cochran test (used for low n) and log-transformed if necessary. Differences among treatments were evaluated with one-way ANOVA and post-hoc Student-Newman-Keuls or non-parametric T3-Dunnet test. The resulting *p* values were considered to be statistically significant at $\alpha = 0.05$.

In Chapter 4.2, relationships between studied parameters were analyzed using linear regressions (Fig 4.14 and 4.18), and *p*-values, coefficients and regression lines are indicated whenever significant at $\alpha = 0.05$.

Statistical analyses were performed with IBM SPSS Statistics for Windows, Version 21.0. Armonk, NY: IBM Corp.

Chapter 4:

RESULTS

4.1. Effect of inorganic phosphate deprivation in *Arabidopsis thaliana* seedlings

With the goal to fulfill the specific aim 1 (Chapter 2) the effect of the inorganic phosphate deprivation as stress for *A. thaliana* was investigated. In the following section below, the results for the growth of WT and mutan seedlings in axenic culture with or without inorganic phosphate are shown in detail.

4.1.1. Sensitivity of the *nia* mutant to low Pi

Omitting Pi from the growth medium reduced the total Pi content of both WT and *nia* seedlings, showing that the treatment was sufficient to cause the onset of P-deficiency (Fig. 4.1). The overall growth of WT seedlings was unaffected by the absence of Pi from the growth medium over 15 days, with no significant difference in size between plants grown on media containing 0 or 1 mM Pi (Fig. 4.2C). In contrast the growth of the *nia* mutants was significantly slower after 8 days in the absence of external Pi, and the effect was even more marked after 15 days (Fig. 4.2B).

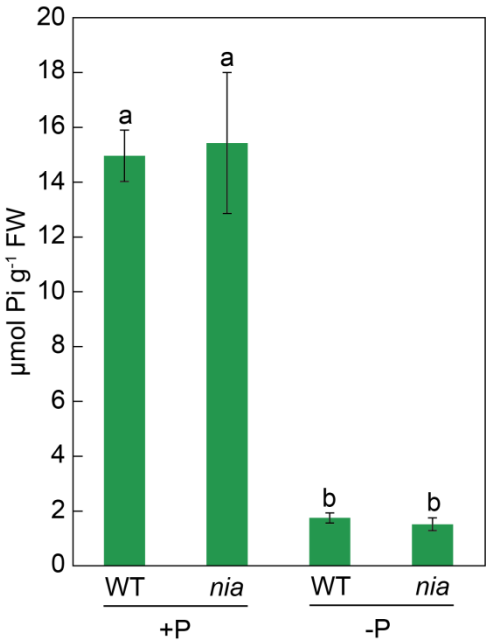

Figure 4.1. ***Effect of Pi supply on the Pi content in Arabidopsis seedlings.*** Pi was quantified in the roots of 15 days old WT and *nia* seedlings grown on a medium containing 0 or 1 mM Pi. The values are the mean ± S.E. (n = 4). Different lowercase letters denote statistically significant differences at α=0.05 using the Student-Newman-Keuls test.

Measurements of root/shoot ratios showed that omitting Pi from the growth medium increased the ratio for WT plants at days 8 and 15, but had no effect on the *nia* seedlings by day 15 (Fig. 4.2D and 4.2E). Thus the *nia* mutant is more sensitive to

Pi deprivation than the WT plant, indicating the impairment of mechanisms that could contribute to adaptation to low Pi in the mutant.

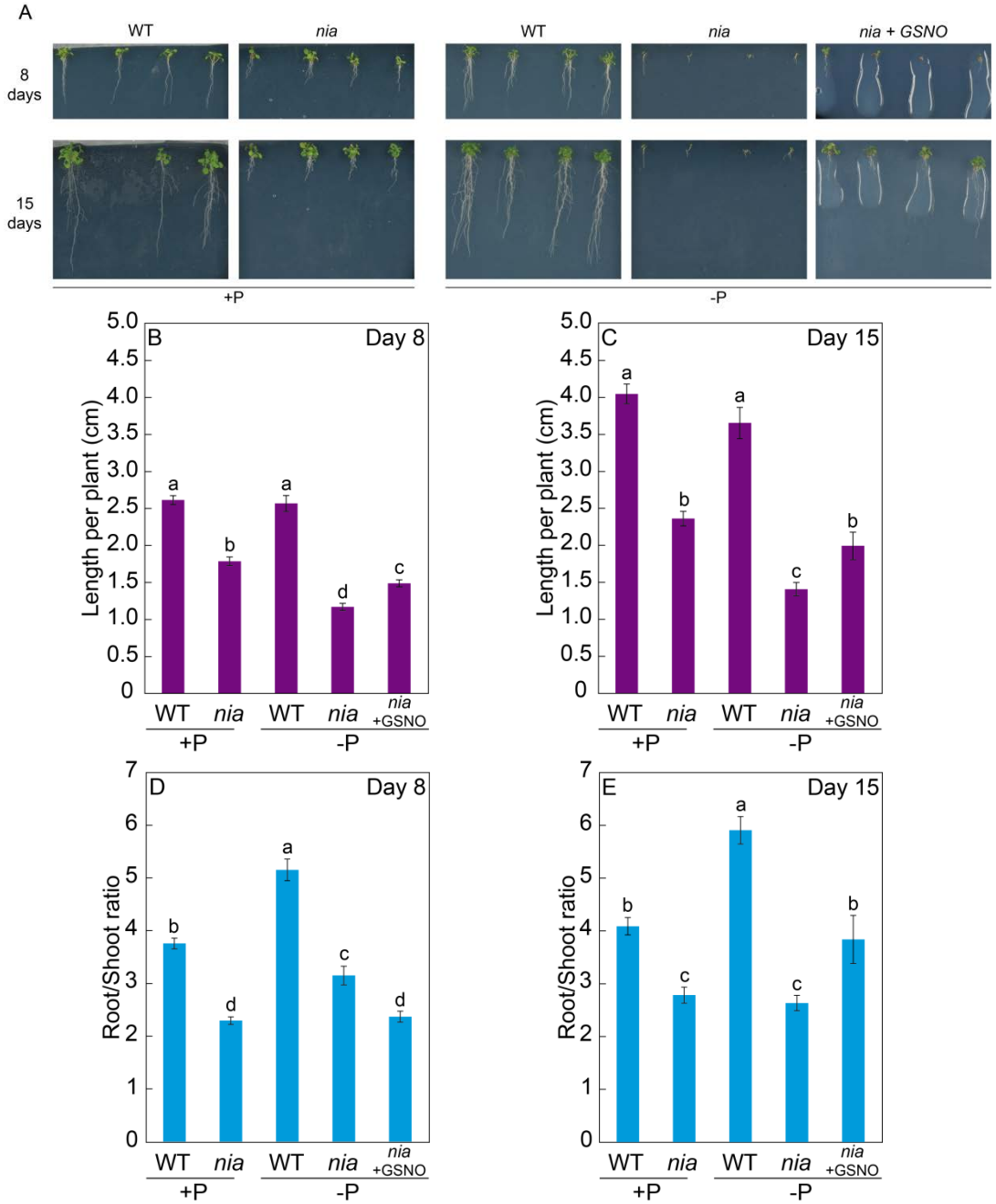

Figure 4.2. ***Effect of Pi supply on root growth of Arabidopsis seedlings.*** (**A**) Representative images of 8 (upper row) and 15 (lower row) days old WT and *nia* seedlings grown on a medium containing 0 or 1 mM Pi. For the GSNO treatment, 200 µM GSNO was added to the growth medium. Length of WT and *nia* plants grown with or without Pi at 8 days (**B**) and 15 days (**C**). Root/shoot ratios of WT and *nia* plants grown with or without Pi at 8 days (**D**) and 15 days (**E**). The values are the mean ± S.E. (n = 32). Different lowercase letters denote statistically significant differences at α=0.05 after the T3-Dunnet test.

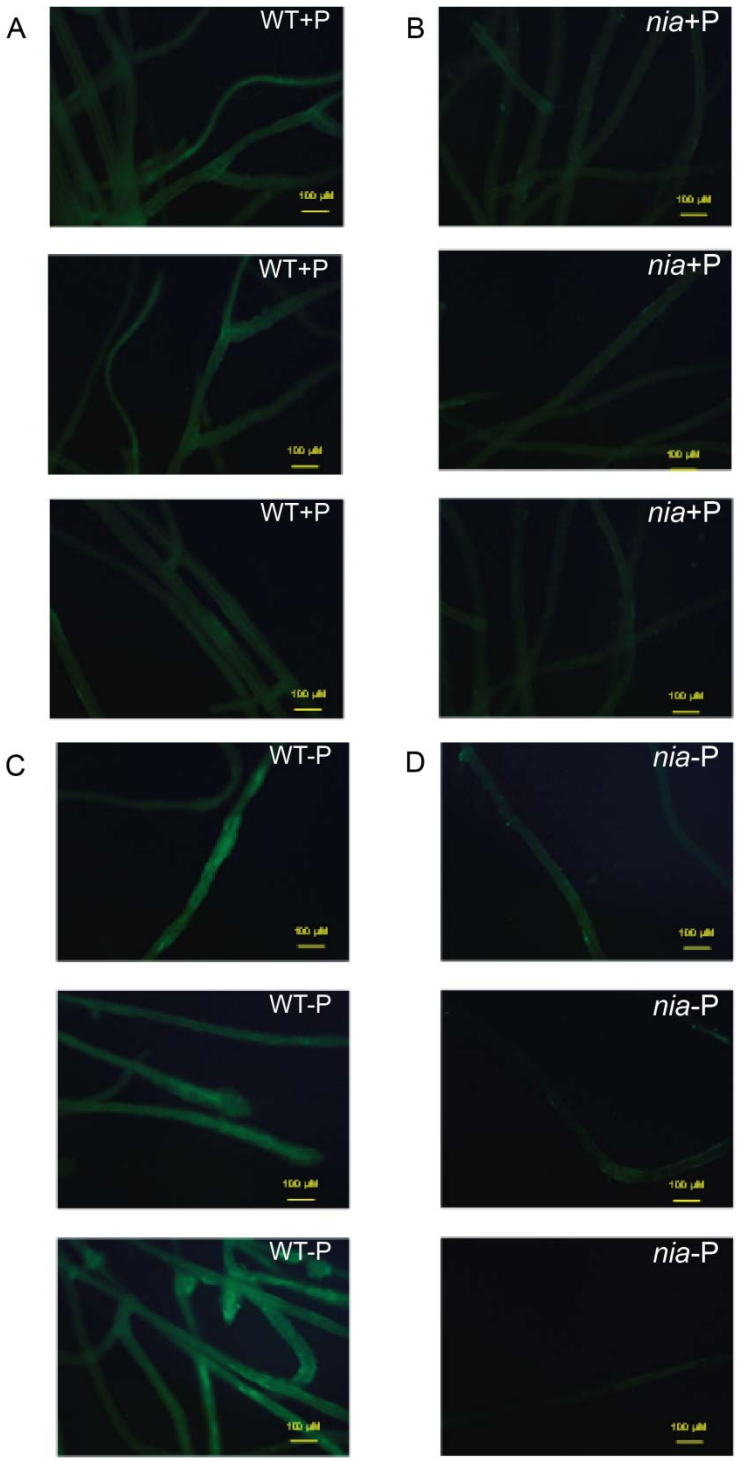

Figure 4.3. ***Effect of Pi supply on DAF-2DA fluorescence of Arabidopsis roots.*** DAF-2DA fluorescence images of 14 days old roots grown with 1mM Pi of WT(**A**) and *nia* (**B**) seedlings, and with 0 mM Pi of WT (**C**) and *nia* (**D**) seedlings. Fluorescence was excited at 495 nm and observed at 515 nm.

4.1.2. NO production by WT and nia as a response to low Pi

The effect of low Pi on NO production was measured using the fluorophore DAF-2DA. The advantage of this cell-permeant dye is that it diffuses to NO producing sites and reacts with NO to form a highly fluorescent product. WT roots had higher levels of NO than the *nia* mutant when the seedlings were grown on 1 mM Pi, but while the NO level increased substantially in the WT roots grown on 0 mM Pi, the level decreased slightly in the roots of the *nia* mutant (Fig. 4.3; Fig. 4.4A).

Similar results were obtained when NO production was analysed with the gas phase Griess reagent assay. These measurements showed that the rate of NO production increased substantially in WT roots grown on 0 mM Pi, whereas there was no change in the roots of the *nia* mutant (Fig. 4.4B). It is good practice to measure NO by more than one method (Gupta and Igamberdiev, 2013) and here the two assays show that Pi deprivation increased the capacity for NO production and the endogenous NO level in *Arabidopsis* roots.

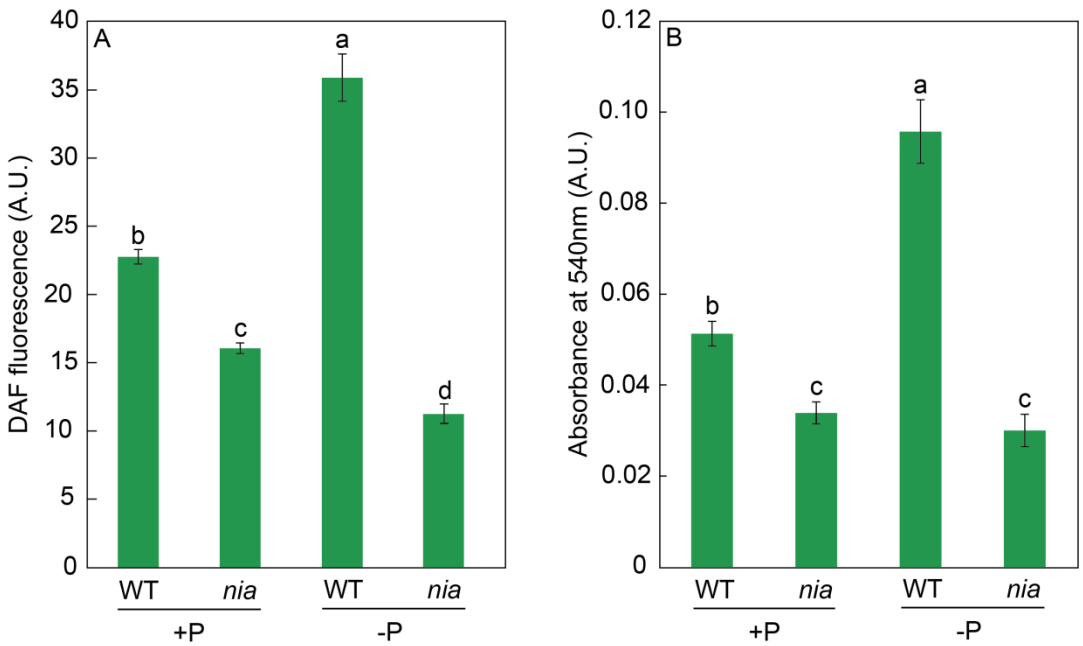

Figure 4.4. ***Effect of Pi supply on the NO level in Arabidopsis roots.*** NO was quantified in the roots of 14 days old WT and *nia* seedlings grown on a medium containing 0 or 1 mM Pi by: (**A**) DAF-2DA fluorescence; and (**B**) a gas phase Griess reagent assay. The values are means ± S.E. (n=3). Different lowercase letters denote statistically significant differences at α=0.05 using the Student-Newman-Keuls test

As a result of nitrite reductase (NiR) activity of the NR enzyme or the action of the mitochondrial electron transport chain, NO can be produced from nitrite. In that

way, nitrite levels were determined in *Arabidopsis* roots to determine whether the origin of NO was by the action of the NiR. Hence, in agreement with NO production, WT roots, but not *nia* mutants, showed an increase on nitrite levels when seedlings were grown whitout supplying Pi (Figure 4.5) supporting the idea that Pi deprivation could downregulate the NiR activity.

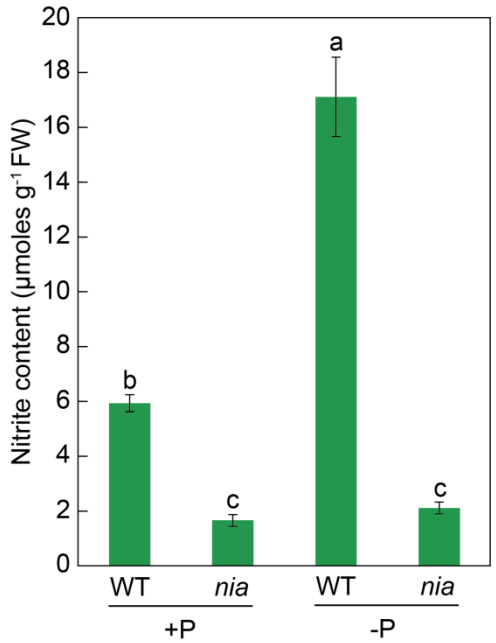

Figure 4.5. ***Effect of Pi supply on nitrite levels in Arabidopsis roots.*** The nitrite level was measured by the Griess reagent assay in the roots of 14 days old WT and *nia* seedlings grown on a medium containing either 0 (-P) or 1 mM (+P) Pi. The values are the mean ± S.E. (n = 3). Different lowercase letters denote statistically significant differences at α=0.05 using the Student-Newman-Keuls test.

4.1.3. Effect of low Pi on respiration

The respiration rate of WT and *nia* seedlings was the same for plants grown with 1 mM Pi (Fig. 4.6A, Fig. 4.6B). In contrast there was a marked difference ($p<0.05$) between the lines grown on 0 mM Pi, with the respiration rate of the *nia* mutant dropping to about 50% of the WT value (Fig. 4.6C, Fig. 4.6D). The capacity of the AOX pathway was investigated by the sequential addition of KCN and SHAM. The addition of SHAM had a greater effect on the respiration rate of WT seedlings grown on 0 mM Pi, reducing the KCN-independent respiration rate by 2.0 µmol O_2 g FW^{-1} h^{-1} at 1 mM Pi and by 2.9 µmol O_2 g FW^{-1} h^{-1} at 0 mM Pi (Fig. 4.6A, Fig. 4.6C); whereas the *nia* seedlings only showed an effect of SHAM on the seedlings were grown on 1 mM Pi, reducing the respiration rate by 2.5 µmol O_2 g FW^{-1} h^{-1} (Fig. 4.6B, Fig. 4.6D). The contrast between the WT and *nia* lines – specifically the absence of an effect of

SHAM on the *nia* seedlings grown on 0 mM Pi - suggests that there could be a positive correlation between NO production and AOX induction during Pi deprivation. Note that the residual respiration rates in the presence of both KCN and SHAM were generally high in these experiments, but they did not decrease when the inhibitor concentrations were increased to 2 mM KCN and 5 mM SHAM indicating that the high values could not be attributed to poor penetration by the inhibitors (data not shown).

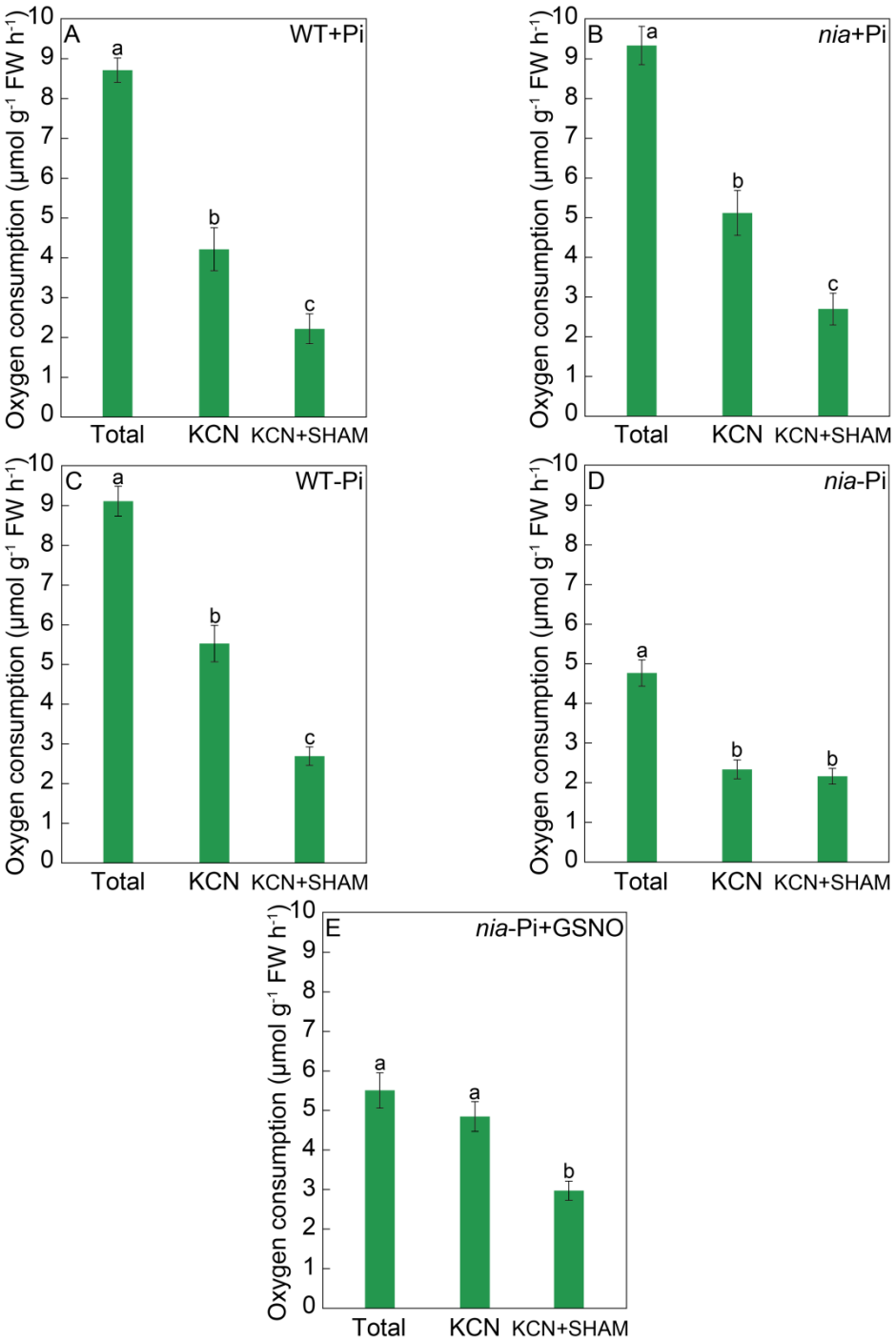

Figure 4.6. ***Effect of Pi supply on the respiration rate of Arabidopsis seedlings.*** Oxygen consumption rates of 14 days old seedlings were measured for WT (**A**) and *nia* (**B**) seedlings grown on 1 mM Pi; WT (**C**) and *nia* (**D**) seedlings grown on 0 mM Pi; and *nia* seedlings grown on 0 mM Pi plus 200 µM GSNO (**E**). The measurements were repeated after the addition of 1 mM KCN, and again after adding 2 mM SHAM. The values are the mean ± S.E. (n = 6-9). Different lowercase letters denote statistically significant differences at α=0.05 after the T3-Dunnet test.

4.1.4. Effect of low Pi on AOX protein level

There was a substantial increase in the AOX level in WT plants grown on 0 mM Pi (Fig. 4.7), which correlated with the increased capacity of the AOX pathway and the effect of SHAM on the respiration rate of the KCN-treated seedlings (Fig. 4.6A, Fig. 4.6C). However, Pi deprivation had no effect on the AOX protein level in the *nia* mutant (Fig. 4.7), suggesting that the induction of AOX under low Pi required an increase in NO.

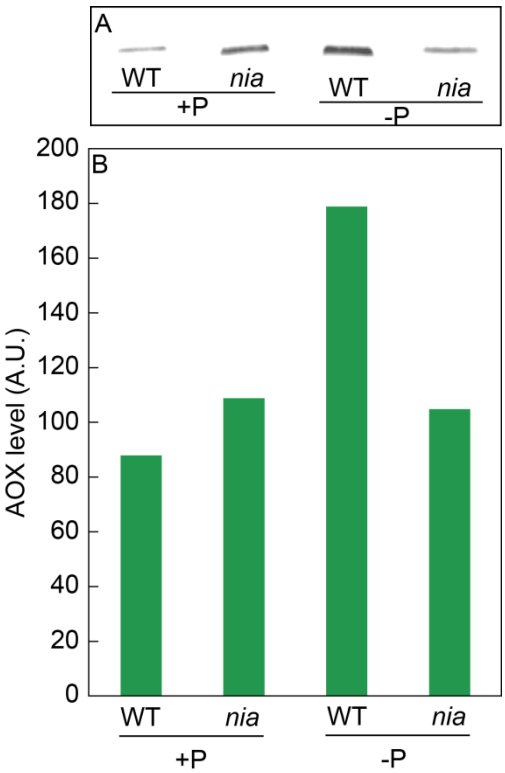

Figure 4.7. ***Effect of Pi supply on the AOX level in Arabidopsis seedlings.*** Immunoblotting of AOX mitochondrial protein from *Arabidopsis* WT and *nia* seedling using a polyclonal anti-AOX antibody.
(**A**) Inmunodetection of the 35-kDa band corresponding to the AOX1A protein present in the mitochondrial protein fraction from 15 days old WT and *nia* seedlings grown in the presence or absence of 1 mM Pi.
(**B**) Quantification of AOX1 bands using Image J software (n = 2).
Mitochondria were isolated from two weeks old liquid seedling culture grown in the presence or absence of 1mM phosphate.

4.1.5. Effect of s-nitrosoglutathione (GSNO) on growth and AOX capacity of nia mutants under low Pi

To confirm the involvement of NO in the response to low Pi in the growth medium *nia* mutant plants were grown on a medium containing 200 μM GSNO. This compound is an effective and reliable NO donor (Mur *et al.*, 2013) and its inclusion in the medium improved the growth of the plants on 0 mM Pi (Fig. 4.2B and 4.2C) and increased the root/shoot ratio (Fig. 4.2D and 4.2E). GSNO also increased the effect of SHAM on the respiration of the *nia* seedlings (Fig. 4.6D and 4.6E) suggesting that NO is indeed required for AOX induction and growth under low Pi conditions.

4.1.6. Superoxide and hydrogen peroxide production under low Pi conditions

Alternative oxidase helps to minimise ROS production under conditions that lead to over-reduction of ubiquinone (Maxwell *et al.,* 1999). While only low levels of superoxide were detected in WT and *nia* roots grown on 1 mM Pi, the level increased in *nia* plants grown on 0 mM Pi (Fig. 4.8A and 4.9A). Thus the inability of the *nia* mutant to induce AOX under low Pi conditions has a deleterious effect on one of the mechanisms controlling ROS levels in the roots. Increased levels of superoxide can increase H_2O_2, but DAB staining showed no change in root H_2O_2 levels in all treatments (Fig. 4.8B and 4.9B).

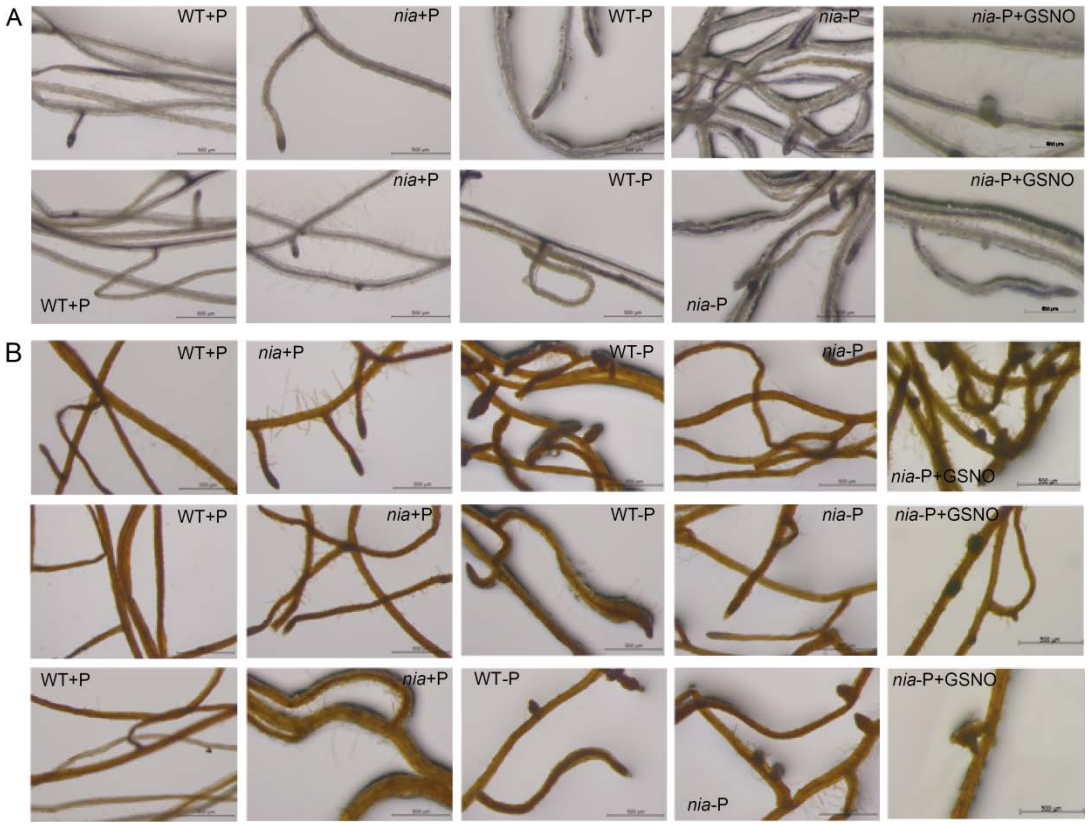

Figure 4.8. ***Effect of Pi supply on superoxide and hydrogen peroxide levels in Arabidopsis roots.*** Representative images of (**A**) superoxide detection by NBT staining and (**B**) H_2O_2 detection by DAB staining of 15 days old *Arabidopsis* WT and *nia* roots grown on the presence or absence of 1mM Pi.

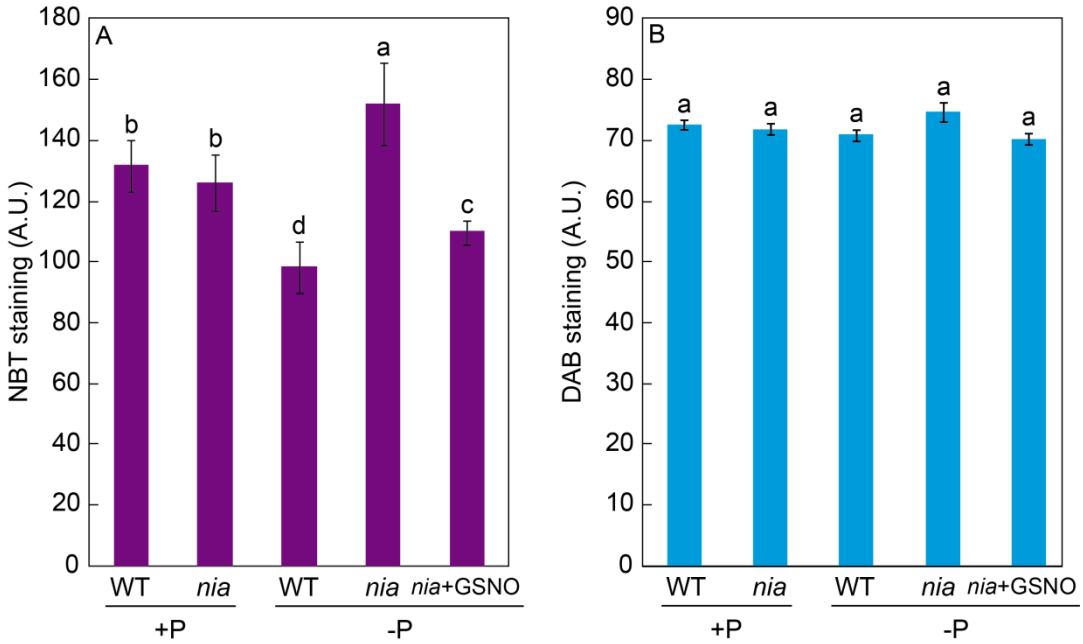

Figure 4.9. ***Effect of Pi supply on superoxide and H_2O_2 levels in Arabidopsis roots.*** Relative quantification of (**A**) NBT staining for superoxide; and (**B**) DAB staining for H_2O_2 on the roots of 14 days old WT and *nia* seedlings grown on a medium containing 0 or 1 mM Pi. 200 μM GSNO was used for the NO donor treatment. Image intensities were quantified by image J software. The values are the mean ± S.E. (n = 3). Different lowercase letters denote statistically significant differences at α=0.05 after the Student-Newman-Keuls test.

4.2. Response of *Medicago truncatula* to ammonium and urea nutrition under axenic conditions

In order to achieve part of the specific objective 2 (Chapter 2), the physiological response of *Medicago truncatula* to different nitrogen nutrition was studied. The standardization of the growing method and the characterization of the differential effect of ammonia and urea respect to nitrate are described below.

4.2.1. Physiological response *Medicago truncatula* to ammonium and urea nutrition under axenic conditions

4.2.1.1. Effect of N-source on pH

A differentially N-supplemented medium was used to grow *Medicago truncatula* plants under axenic conditions with NO_3^-, NH_4^+, or urea for 15 days. The growth medium, containing 1.5 mM of phosphate buffer, exhibited a significant buffering capacity, similar to that of Murashige and Skoog medium, which contains 1.25 mM of phosphate. Hence, the pH of the growth medium during the experiment changed little for the plants grown using nitrate. However, in the plants grown with NH_4^+ as the sole source of N there was a significant decrease in pH, with pH levels of 5.2 and 4.5 being observed for the 1mM and 25mM ammonium treatments, respectively. Intermediate decreases were found associated with urea nutrition at both doses (Fig. 4.10).

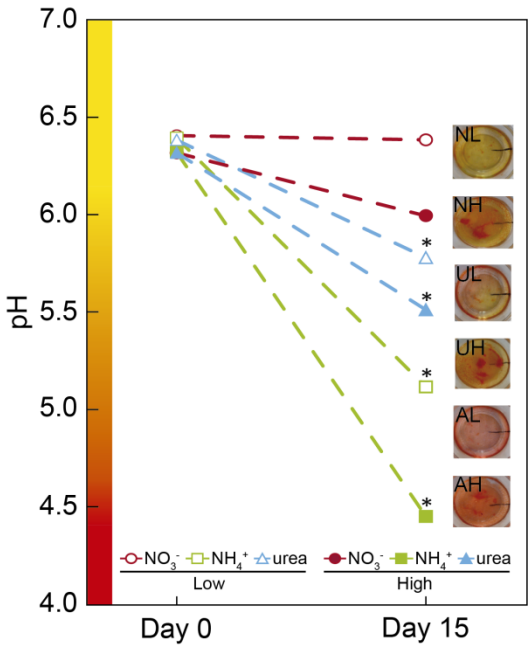

Figure 4.10. ***Effects of NO_3^-, NH_4^+, and urea on pH.*** pH on days 0 and 15 of the experiment under the different treatments: low doses of NO_3^-, NH_4^+, and urea (opened circle, square and triangle, respectively) and high doses of NO_3^-, NH_4^+, and urea (closed circle, square and triangle, respectively). The values are the mean ±S.E (n=15). Photographs of the pH indicator methyl red on day 15 of the experiment for each of the treatments are shown (NL, AL, UL: low doses of NO_3^-, NH_4^+, and urea, respectively, and HH, AH, UH: high doses of NO_3^-, NH_4^+, and urea, respectively).

4.2.1.2. Growth and root system architecture of seedlings under the different N-sources

Treatment with either NH_4^+ or urea at a low dose caused a significant reduction of the fresh weight of the shoots of *M. truncatula* seedlings compared with NO_3^- treatment (Fig. 4.12A). At a high dose, only the plants fed with urea showed reduced shoot growth, which was related to the differential root/shoot biomass ratio, with greater investment in the roots being observed under this type of nutrition (Fig. 4.12D). Interestingly, NH_4^+ had a negative effect on fresh weight at a low dose, but not a high dose, where a different root/shoot ratio may influence changes in fresh weight. Root growth was only affected under NH_4^+ nutrition at a low N concentration (Fig. 4.12B). The differences were not significant for dry matter in either the roots or the shoots (Fig. 4.11A and 4.12B). In terms of the total biomass (Fig. 4.12C), both low and high doses of NH_4^+ decreased the growth per plant, which was also reduced under high-dose urea-fed plants.

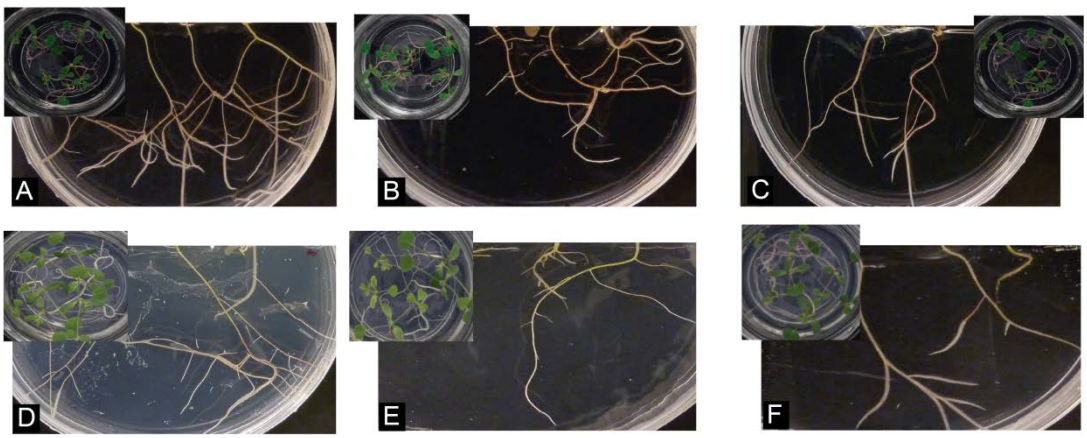

Figure 4.11. ***Effects of NO_3^-, NH_4^+, and urea on the root system architecture.*** Representative image of plants grown under low dose of NO_3^- (**A**), NH_4^+ (**B**), and urea (**C**) and high doses of NO_3^- (**D**), NH_4^+ (**E**), and urea (**F**) at day 14.

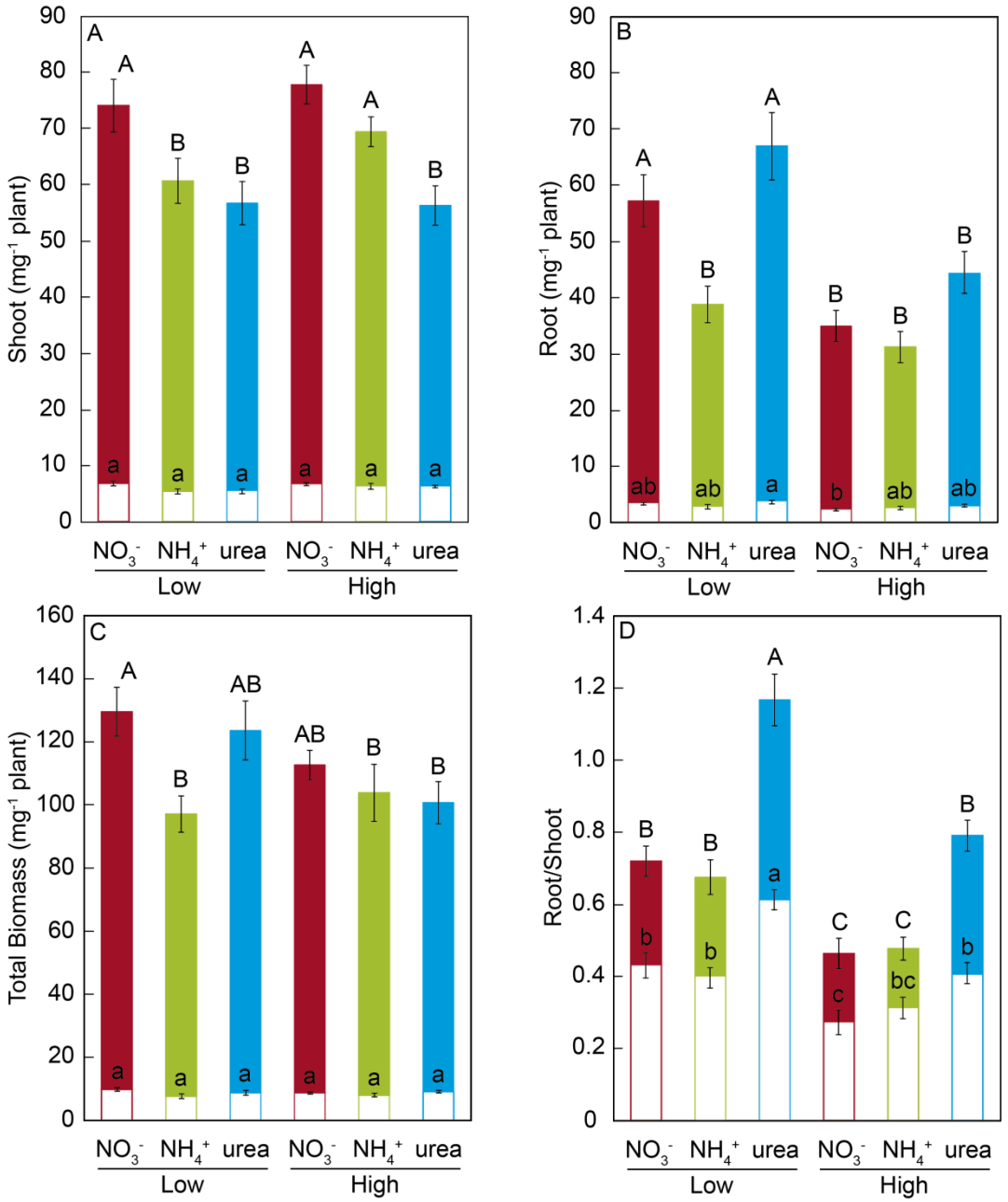

Figure 4.12. ***Effects of NO_3^-, NH_4^+, and urea on biomass.*** Distribution of the plant biomass of shoots (**A**) and roots (**B**), total biomass (**C**), and the root/shoot ratio (**D**) expressed on the basis of the fresh weight (colored bars) and dry weight (white bars) (mg) per plant subjected to the different treatments (low and high doses of NO_3^-, NH_4^+, and urea). The values are the mean ± S.E. (n = 15). Different letters (capital letters for fresh weight and lowercase letters for dry weight) denote statistically significant differences at $\alpha = 0.05$ using the Student–Newman–Keuls test. To standardize the variances, one data point was replaced by the mean of the group for the root fresh weight, and 1 degree of freedom was subtracted from the residual (Winer et al., 1991).

Significant changes in the architecture of the roots occurred during development (Fig. 4.13, Fig. 4.14 and Table 4.1). We confirmed that there was a significant change in the main root elongation rate in each of the treatments, with a delay in growth being observed during the first 4 days in plants grown under a high dose of NH_4^+ (Fig. 4.13A). Interestingly, in the plants fed with urea at a low dose, enhancement of the elongation of the main root was observed after the first 4 days of growth. All treatments reduced the main root elongation rate after the 8th day of growth. The differences in lateral root growth and elongation were also evident and significant at the end of the experiment. In both the NH_4^+- and urea-fed plants, the accumulated lateral root growth was lower than in the NO_3^--fed plants (Figs. 4.13B and Fig. 4.13C).

Table 4.1. ***Phenotypic evaluation of the effects of various N treatments on the root system architecture in 15-day old M. truncatula seedlings, grown under low and high doses of NO_3^-, NH_4^+, and urea.***

Treatment		Primary root length (cm)	Primary root surface (cm^2)	Lateral root length (cm)	Lateral root surface (cm^2)
Low	**N**	9.6±0.2^{a}	2.2±0.1^{a}	3.6±0.3^{a}	0.6±0.1^{a}
	A	6.6±1.2^{a}	1.5±0.3^{a}	1.2±0.2^{bd}	0.2±0.0^{b}
	U	7.5±0.2^{a}	1.5±0.2^{a}	3.0±0.9^{c}	0.6±0.2^{a}
High	**N**	11.1±1.1^{a}	1.8±0.3^{a}	1.2±0.3^{bd}	0.1±0.0^{b}
	A	2.0±0.3^{b}	1.8±0.2^{a}	0.7±0.1^{d}	0.1±0.0^{b}
	U	6.9±1.6^{a}	1.5±0.2^{a}	2.2±0.4^{bc}	0.6±0.1^{a}

The analyses of root system architecture were performed using SmartRoot software. This software converts pixel data into cm units. The data are the means ± SD based on 4 or 5 independent biological replicates. Different small letters denote statistically significant differences at $\alpha = 0.05$ using the Student-Newman-Keuls test.

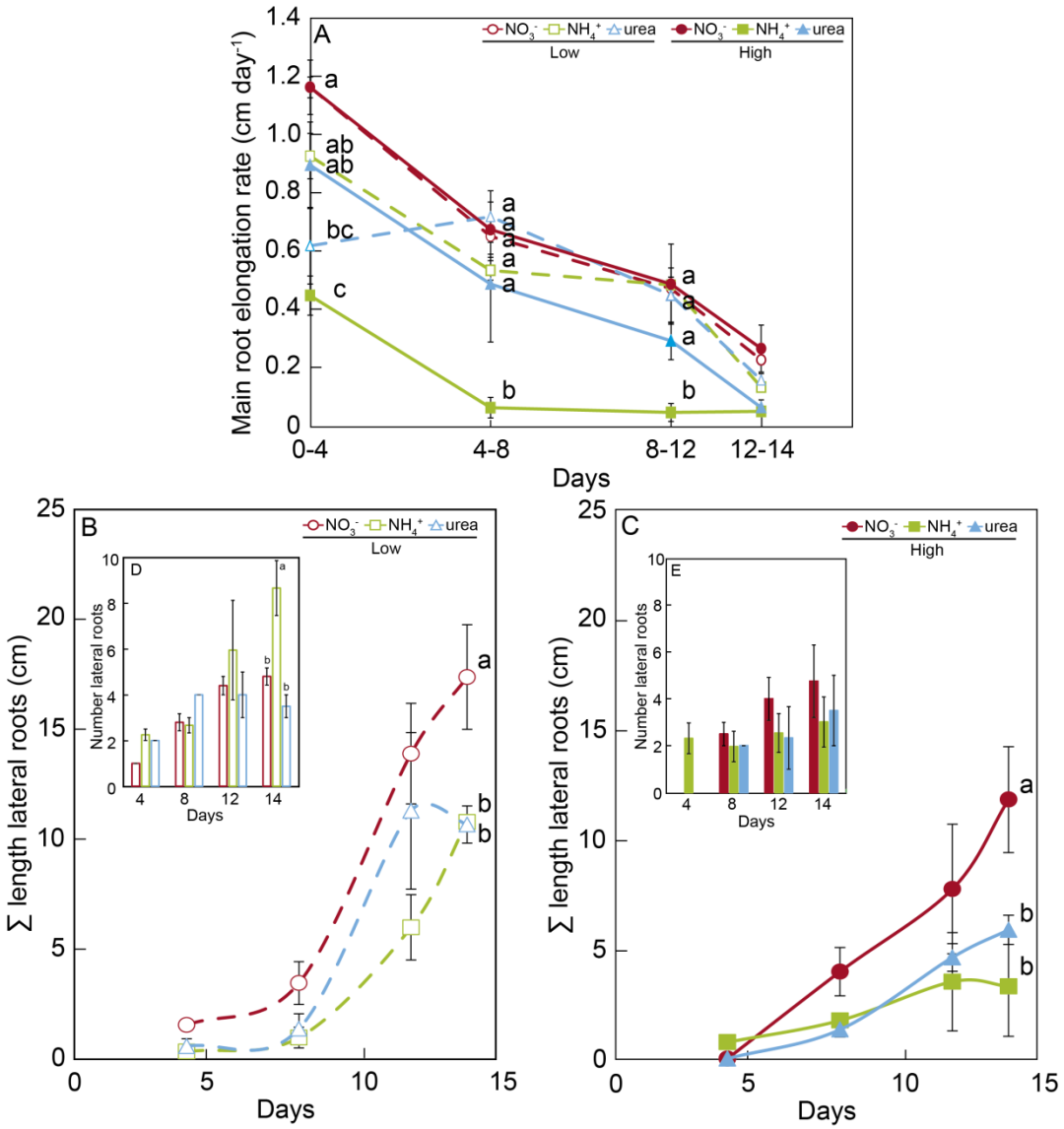

Figure 4.13. ***Effects of NO_3^-, NH_4^+, and urea on the root system architecture.*** Main root elongation rate (**A**) and accumulated (Σ) lateral root length under a low dose (**B**) and high dose (**C**). Insert panels show the changes in the number of lateral roots under each treatment for a low dose (**D**) and high dose (**E**). The values are the mean of 5-3 ± S.E. An analysis of variance (ANOVA) was performed in (**A**) considering the treatment as a fixed factor. Different lowercase letters denote statistically significant differences at $\alpha = 0.05$ using the Student-Newman-Keuls test. An absence of letters indicates that there were no significant differences.

This differential accumulated lateral growth in the low-dose treatments was due to a greater number of lateral roots growing more slowly in NH_4^+-treated roots and to the presence of fewer lateral roots in urea-fed roots (Fig. 4.13D). No significant differences in the number of lateral roots were found for the high-dose treatment (Fig. 4.13E). Moreover, a remarkable relationship was observed regarding the length of the lateral roots and the position of insertion from the root base, with opposite patterns being recorded in the NH_4^+- and NO_3^--grown plants, as illustrated in Figure 4.14. No significant relationship was detected in the urea-fed plants, probably due to the low number of lateral roots (data not shown; $p = 0.075$).These differences in plant growth in relation to the type of nutrition might reflect disparities in N uptake and/or assimilation, but they may also be related to differential hormone signaling.

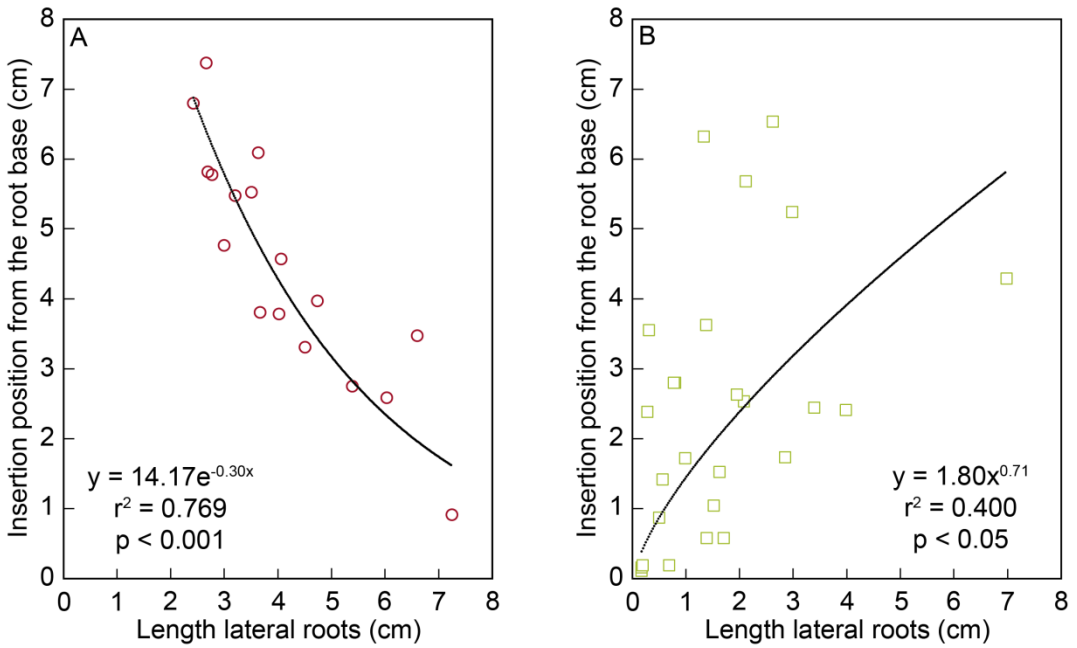

Figure 4.14. ***Effects of NO_3^- and NH_4^+, on the root system architecture.*** Relationship of the insertion position from the root base with length of lateral roots for a low dose of NO_3^- (**A**) and a low dose of NH_4^+ (**B**).

Accordingly, the free IAA content was analyzed. The NH_4^+ (low and high doses) -fed plants showed a decrease in IAA content in the roots compared with NO_3^--grown plants (Fig. 4.15). The decrease in the IAA content was even more pronounced and significant when analyzed based on dry weight (data no shown). However, the most remarkable decrease was observed in the shoots under 25 mM NH_4^+. In contrast, urea did not alter IAA contents at the shoot level but did provoke a decrease in IAA at the root level at a low-dose treatment compared with NO_3^- treatment. Indeed, the decrease

was remarkably higher in the presence of urea at low dose than was observed for NH_4^+.

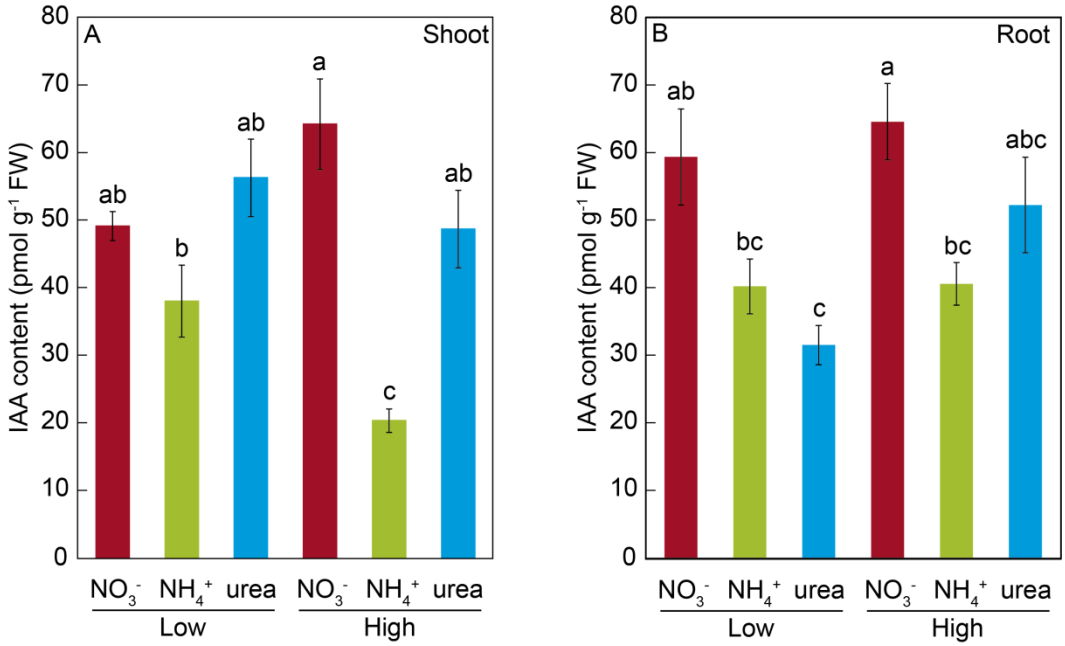

Figure 4.15. ***Effects of NO_3^-, NH_4^+, and urea on the IAA concentration.*** High and low doses of NO_3^-, NH_4^+, and urea altered the IAA concentration (pmoles g^{-1} fresh weight) of *M. truncatula* seedlings. The values are the mean ± S.E. (n = 3). Different lowercase letters denote statistically significant differences at $\alpha = 0.05$ after the Student–Newman–Keul test.

4.2.1.3. Stress indicators

Photosystem II is considered to play a key role in the response of photosynthesis to environmental stress (as may be the case for NH_4^+ or ureic nutrition), and OJIP monitoring is a method for investigating the events occurring in photosystem II. This technique allows *in vivo* evaluation of plant performance in terms of biophysical parameters quantifying photosynthetic energy conservation (Strasser et al., 2000; 2004).

The induction of relative variable fluorescence (Fig. 4.16) and the parameters derived from this curve (Table 4.2) showed no remarkable differences between the treatments at low doses. However, there was a clear effect of a high dose of N nutrition, as indicated by the relative amplitude of the J–I phase (1 ms-10 ms) plotted on a logarithmic time scale for NH_4^+ compared with the NO_3^- and urea treatments (Fig. 4.16).

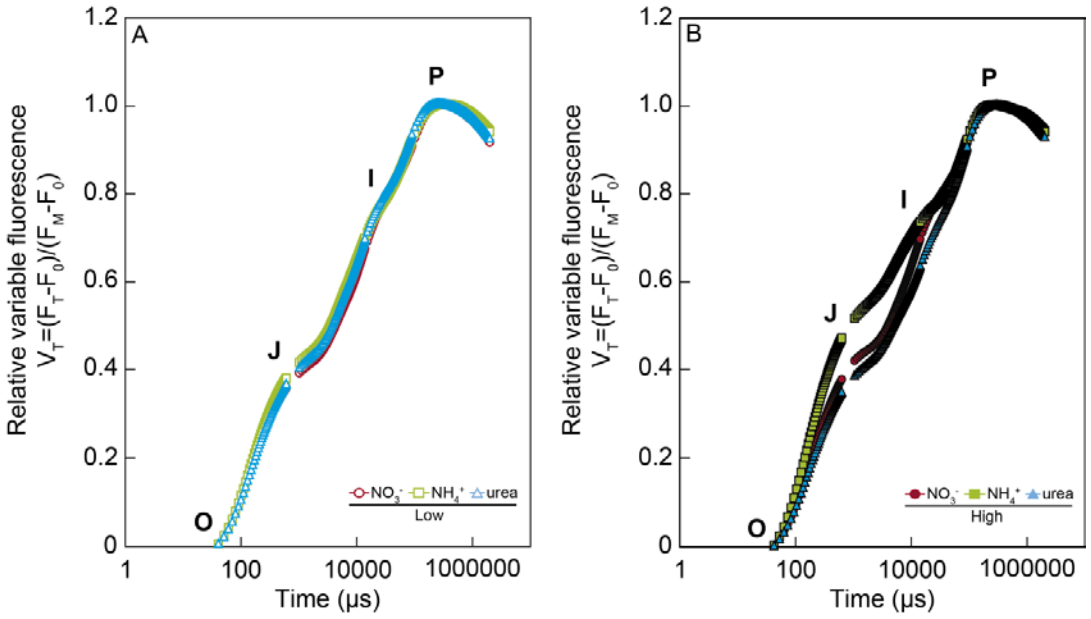

Figure 4.16. ***Effects of NO_3^-, NH_4^+, and urea on fast chlorophyll a fluorescence transients (OJIP) from dark-adapted leaves of M. truncatula plants grown under the different treatments at low (A) and high doses (B).*** Each transient is plotted on a logarithmic time scale from 40 µs and 1 s and expressed as the relative variable fluorescence (V_t) after double normalization of Fo and Fm. The values are the means (n = 3-4).

Much more pronounced differences between treatments were revealed by the parameters derived after further analyses of the curves of fluorescence according to the OJIP test (see the Material and methods; Table 3.4). Indeed, the relative variable Chl fluorescence at 2 ms (V_j) was significantly lower under high NH_4^+ doses. Curiously, the maximum quantum yield of the primary photochemistry (φ_{Po}) and the quantum yield for energy dissipation (φ_{Do}) were significantly higher under urea at a high dose, while the efficiency with which a trapped exciton could move an electron into the electron transport chain (ψ_o) and the quantum yield of electron transport (φ_{Eo}) were significantly lower under NH_4^+ at a high dose. Regarding the specific changes per reaction center (RC), only the electron transport flux per RC (ET_o/RC) was affected in high-dose NH_4^+-fed plants. The parameter Pi_{Abs}, which combines (i) the RC density expressed on an absorption basis, (ii) the quantum yield of primary photochemistry, and (iii) the ability to feed electrons into the electron chain between photosystem II and I (Cascio et al., 2010), exhibited a significantly higher value under a high dose of urea, which was even higher than the value observed under NO_3^-. Conversely, Pi_{Abs} showed the lowest values under NH_4^+ at both doses (presenting a lower value in the high-dose treatment; Table 4.2). Moreover, slight differences in chlorophylls content (SPAD units) were observed, with a significant decrease being recorded in plants fed

with 25 mM NH_4^+. No differences in the total protein content were detected. (Table 4.3).

Regarding antioxidants, there were no significant changes in the size and general oxidation state of the antioxidant pools in the roots. On the contrary, NH_4^+- and urea-supplied plants presented a lower reduced pool of GSH+hGSH in the shoots. On the other hand, there were detectable differences in the ASC oxidation pool in shoots, with higher contents being recorded in urea-grown seedlings (Table 4.3).

Table 4.2. ***Numerical values for fluorescence parameters derived from the chlorophyll a fast florescence transients in the leaves of M. truncatula: (i) normalized data as V_j and V_i, (ii) quantum yields and flux ratios as φ_{Po}, Ψ_o, φ_{Eo}, (iii) performance index ($Pi_{\_Abs}$), and (iv) specific energy fluxes per Q_A^- reducing photosystem II centers as ABS/RC, TR_0/RC, ET_0/RC, and DI_0/RC.***

Parameter		Low N supply			High N supply		
		Nitrate	Ammonium	Urea	Nitrate	Ammonium	Urea
Normalized data	V_j	0.42±0.02^{b}	0.45±0.01^{b}	0.44±0.02^{b}	0.45±0.03^{b}	0.56±0.04^{a}	0.42±0.02^{b}
	V_i	0.78±0.03	0.78±0.02	0.79±0.01	0.79±0.01	0.78±0.02	0.74±0.00
Quantum yields and flux ratios	φ_{Po}	0.74±0.00^{b}	0.75±0.00^{ab}	0.76±0.01^{ab}	0.76±0.00^{ab}	0.74±0.00^{b}	0.77±0.00^{a}
	Ψ_o	0.58±0.02^{a}	0.55±0.01^{a}	0.56±0.02^{a}	0.55±0.03^{a}	0.44±0.04^{b}	0.58±0.02^{a}
	φ_{Eo}	0.43±0.01^{a}	0.42±0.00^{a}	0.43±0.02^{a}	0.42±0.02^{a}	0.33±0.03^{b}	0.44±0.02^{a}
	φ_{Do}	0.26±0.00^{a}	0.25±0.00^{ab}	0.24±0.01^{ab}	0.24±0.00^{ab}	0.26±0.00^{a}	0.23±0.00^{b}
	$Pi_{\_Abs}$	1.12±00.07^{ab}	1.06±0.04^{ab}	1.22±0.15^{ab}	1.19±0.14^{ab}	0.67±0.12^{b}	1.39±0.16^{a}
Specific energy fluxes	ABS/RC	3.58±0.04	3.54±0.12	3.39±0.08	3.32±0.03	3.54±0.17	3.29±0.07
	TR_o/RC	2.67±0.04	2.66±0.07	2.57±0.04	2.53±0.08	2.63±0.11	2.52±0.04
	ET_o/RC	1.54±0.03^{a}	1.47±0.06^{a}	1.44±0.03^{a}	1.39±0.0^{a}	1.17±0.14^{b}	1.46±0.04^{a}
	DI_o/RC	0.92±0.01	0.88±0.05	0.82±0.04	0.79±0.01	0.92±0.06	0.77±0.03

Definitions and formulae are given in Materials and Methods, Table 3.4. The values are the means ± S.E. from independent measurements (n = 3-4). An analysis of variance (ANOVA) was performed, considering treatments as fixed factors. Different superscripted letters denote statistically significant differences at α = 0.05 after Student-Newman-Keuls test. An absence of letter indicates that there were no significant differences.

Regarding SOD activity (Fig. 4.17), four isozymes were found in both the leaves and roots (MnSOD, FeSOD, cytosolic-CuZnSOD and plastidial-CuZnSOD). However, the response was different between the two tissues. In the roots (Fig. 4.17A), no or very slight differences were observed for the isoenzyme MnSOD, indicating that a special level of protection for mitochondria-associated superoxide production was not required under any of the tested conditions. On the other hand, cyt-CuZnSOD was somewhat affected by the type of nutrition, increasing under low and high urea, but showing no significant increases under NH_4^+ treatment. Increases (although not significant) could also be observed for FeSOD in plants grown under high N doses (NO_3^- and NH_4^+).

Table 4.3. ***Chlorophylls by SPAD units, ascorbate (ASC), and glutathione+homoglutathione (GSH+ hGSH) redox status and protein content in tissues (shoots and roots) of M. truncatula plants grown using NO_3^-, NH_4^+, and urea media as the only N source.***

	Tissue	n	Low N supply			High N supply		
			Nitrate	Ammonium	Urea	Nitrate	Ammonium	Urea
Chlorophylls (SPAD units)	Leaves	14	29.1±1.2^{abc}	25.9±1.5^{bc}	26.3±1.6^{bc}	30.8±1.0^{a}	25.4±1.1^{c}	29.7±1.6^{ab}
ASC/(DHA+ASC)	Shoot	4	0.48±0.02^{b}	0.53±0.03$^{ab'}$	0.57±0.04^{a}	0.62±0.02^{a}	0.53±0.00^{ab}	0.58±0.02^{a}
	Root	4	0.60±0.00^{a}	0.57±0.0^{ab}	0.57±0.02^{ab}	0.54±0.02^{b}	0.55±0.01^{ab}	0.56±0.01^{ab}
(GSH+hGSH)/ (GSSG+hGSSG+GSH +hGSH)	Shoot	4	1.37±014^{a}	1.29±0.21^{a}	1.00±0.01^{ab}	1.39±0.25^{a}	0.77±0.25^{ab}	0.43±0.02^{b}
	Root	4	0.76±0.14^{a}	0.95±0.21^{a}	0.58±0.06^{a}	0.73±0.07^{a}	0.83±0.28^{a}	0.54±0.06^{a}
Protein content (mg/g^{-1} DW)	Shoot	8	10.4±2.0	9.6±1.6	8.2±1.7	12.5±2.0	12.5±1.8	11.4±1.8
	Root	5	8.6±1.3	8.4±1.1	8.1±1.8	11.1±1.3	10.1±1.1	8.7±1.1

The values represent the mean ± SE (n = 4-14). Different superscripted letters denote statistically significant differences at α = 0.05 using Student-Newman-Keuls test. An absence of letters indicates that were no significantly differences.

Unlike FeSODs from determinate nodule-forming legume plants, such as soybean, cowpea, or *Lotus japonicum*, where FeSOD members occur in the plastids or cytosol, the FeSODs of the *Medicago* family are plastidial proteins (Moran et al., 2003; Asensio et al., 2012). Additionally, plastid-associated CuZnSOD was significantly induced in plants fed with high NH_4^+ and low or high urea. On the whole, it appears that plastidial enzymes are more affected, and ureic nutrition appears to impact a

greater number of SOD isoenzymes. Conversely, no important changes were observed in the shoots (Fig. 4.17B), with the exception of a decrease of cyt-CuZnSOD activity under high NO_3^- treatment. Overall, these results suggest that small adjustments in the antioxidant pool may prevent major perturbations in redox ratios under differential N nutrition.

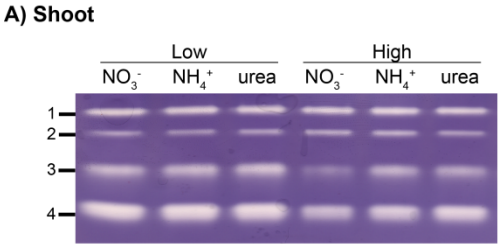

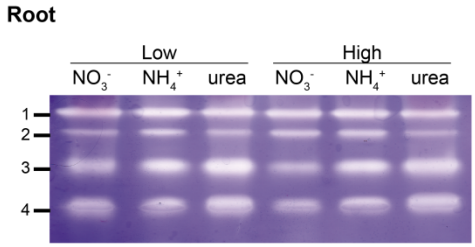

	Low			High		
	NO_3^-	NH_4^+	urea	NO_3^-	NH_4^+	urea
MnSOD	100	116±22	111±22	187±11	100±13	100±13
FeSOD	100	115±51	89±31	84±24	112±6	86±7
cyt-CuZnSOD	100^a	101±5^a	108±10^a	57±13^b	85±11^a	86±14^a
pl-CuZnSOD	100^a	91±3^{ab}	100±7^a	65±11^b	67±5^b	86±8^{ab}

	Low			High		
	NO_3^-	NH_4^+	urea	NO_3^-	NH_4^+	urea
MnSOD	100	108±5	114±15	112±7	118±11	122±17
FeSOD	100	126±14	117±35	150±14	146±22	111±32
cyt-CuZnSOD	100	107±21	155±25	97±14	126±17	134±23
pl-CuZnSOD	100^b	121±9^b	199±45^a	137±10^{ab}	161±37^{ab}	166±30^{ab}

Figure 4.17. ***Effect of NO_3^-, NH_4^+, and urea on superoxide dismutase activity in roots (A) and leaves (B) of 2-week-old Medicago truncatula plants grown under axenic conditions with NO_3^-, NH_4^+, or urea as the exclusive source of N.*** The gels are representative examples of three replicate experiments. The densitometry results of the isoenzyme bands are expressed in the lower panel as percentages relative to the corresponding control reference bands (1mM NO_3^-). All lanes of the 15% native-PAGE gel were loaded with 30 µg of protein. The values are means ± S.E. (n=3). Different letters denote statistically significant differences at $\alpha = 0.05$ using the Student-Newman-Keuls test. To standardize the variances, one data point was replaced with the mean for the group for shoot cyt-CuZnSOD, and root pl-CuZnSOD, and consequently, 1 degree of freedom was subtracted from the residual in each case (Winer et al., 1991). An absence of letters indicates that there were no significant differences.

Our study also demonstrated interesting relationships among the studied parameters (Fig. 4.18). Pi_{Abs} (a parameter obtained from the induction of chlorophyll *a*) showed a significant positive relationship with the shoot IAA content ($r^2 = 0.653$; $p < 0.05$; Fig. 4.18C). Moreover, the shoot IAA content exhibited a significant positive relationship with the total length of the plant ($r^2 = 0.815$; $p < 0.05$), as did the total IAA content with the total length of the plant (data not shown; $r^2 = 0.7785$; $p < 0.05$). There was also a tendency for a greater length to be correlated with a higher performance index, although not significantly ($r^2 = 0.617$; Fig. 4.18B). Interestingly, total biomass on a fresh basis was not correlated with IAA content (Fig. 4.18D), nor was the root IAA content correlated with root length (data not shown). Taken together, these findings suggested that NO_3^-- and urea-fed seedlings showed higher performance index than NH_4^+-fed plants, which was clearly correlated with higher IAA contents, potentially resulting in better length growth for these plants.

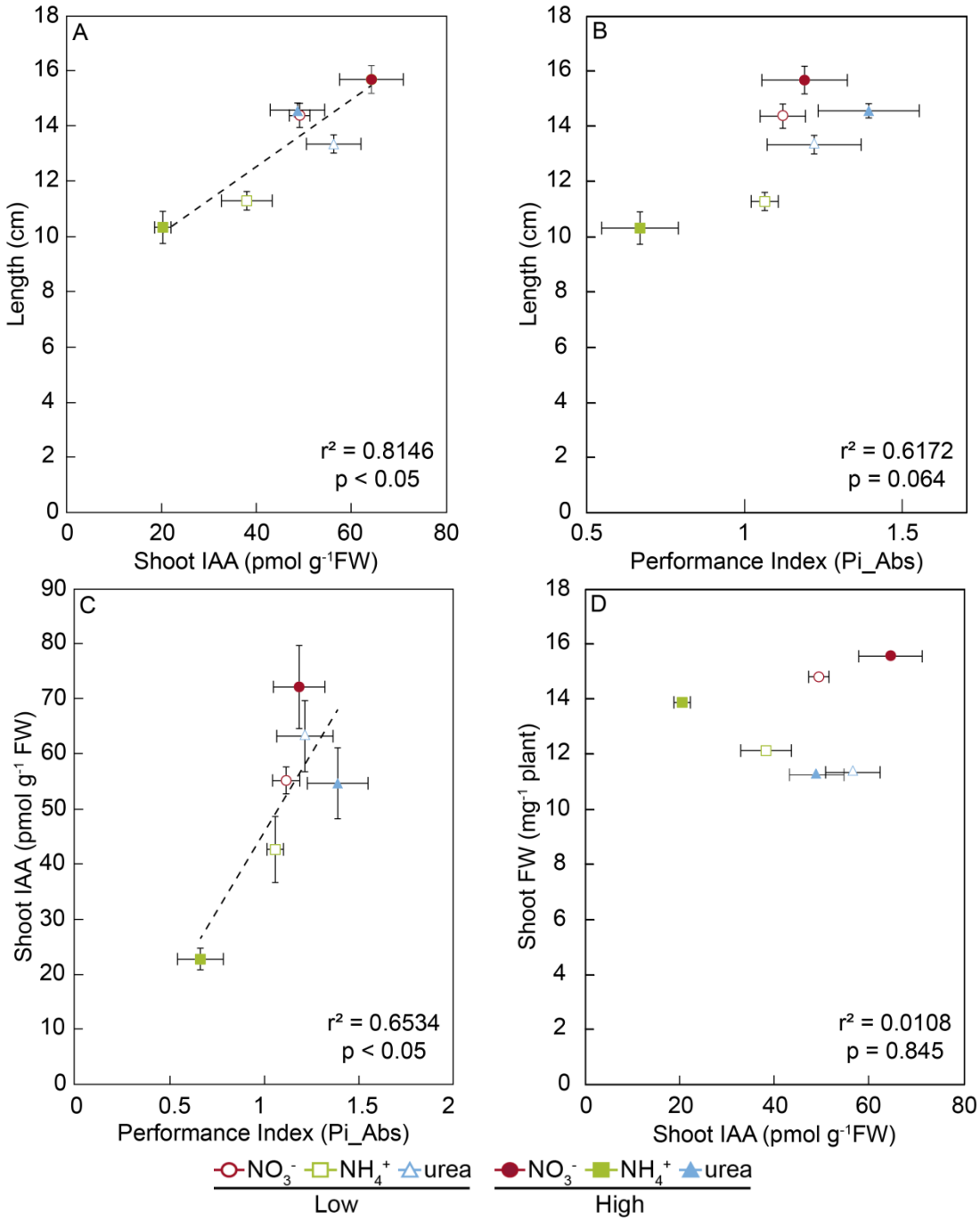

Figure 4.18. ***Relationships under the effects of NO_3^-, NH_4^+, and urea.*** Relationship of the total plant length with the shoot IAA content (**A**) and performance index (**B**). Relationship of the shoot IAA content with performance index (**C**) and with shoot fresh weight (**D**). Points shown are means (n = 4) ± SE for the plants.

4.3. Nitrogen metabolism and signaling in *Medicago truncatula* seedlings grown under ammonium and urea nutrition

In this chapter, in line with the specific aim 2 of this thesis (Chapter 2), the effect of differential nitrogen nutrition (nitrate, ammonium and urea) in the nitrogen metabolism and signaling of *M. truncatula* was investigated. The results obtained for the several metabolites and molecules analyzed are described in the following sections:

4.3.1. Effect of N-source on cations and anions content in *Medicago truncatula* grown under axenic conditions

Medicago truncatula plants were grown in a differentially N-supplemented medium under axenic conditions. The nature of those N sources may lead to differences in the internal content of ions in the distinct tissues of plants. Thus, the cations (C^+) and anions (A^-) content were determined by ion chromatography (Table 4.4). In general terms, both total C^+ and A^- contents were higher in roots than in shoots. The NO_3^--fed plants at high dose, exhibited the highest level of C^+ in both tissues and the highest content of A^- in roots. Plants supplied with high dose of NH_4^+ presented the highest value of A^- in shoots. Regarding the ratio between C^+ and A^- content, no differences were found in roots, whereas plants grown with high dose of NH_4^+ exhibited the lowest content in shoots. In addition, those plants showed almost the same ratio C^+/A^- in both tissues.

Table 4.4. ***Cations (C^+), anions (A^-) content (mmol g^{-1} DW), and cations/anions ratio (C^+/A^-) in 15-days old* M. truncatula *seedlings* grown in *NO_3^- (N), NH_4^+ (A), and urea(U) under axenic conditions.***

Treatment		Shoot			Root		
		C^+	A^-	C^+/A^-	C^+	A^-	C^+/A^-
Low	N	2.54 ± 0.22^{ab}	1.53 ± 0.13^{bc}	1.67 ± 0.07^{ab}	3.47 ± 0.26^{b}	2.63 ± 0.09^{c}	1.33 ± 0.11
	A	2.69 ± 0.15^{ab}	1.77 ± 0.07^{bc}	1.53 ± 0.08^{ab}	3.01 ± 0.17^{b}	2.69 ± 0.07^{c}	1.12 ± 0.07
	U	2.54 ± 0.22^{ab}	1.21 ± 0.17^{c}	2.33 ± 0.45^{a}	3.23 ± 0.11^{b}	3.11 ± 0.10^{bc}	1.05 ± 0.05
High	N	3.25 ± 0.15^{a}	2.13 ± 0.20^{ab}	1.57 ± 0.13^{ab}	4.46 ± 0.15^{a}	4.40 ± 0.29^{a}	1.04 ± 0.10
	A	2.98 ± 0.10^{a}	2.61 ± 0.13^{a}	1.15 ± 0.07^{b}	3.01 ± 0.19^{b}	2.58 ± 0.10^{c}	1.18 ± 0.12
	U	2.19 ± 0.17^{b}	1.60 ± 0.24^{bc}	1.53 ± 0.27^{ab}	3.50 ± 0.15^{b}	3.32 ± 0.14^{b}	1.06 ± 0.07

The values represent the mean ± S.E. (n = 5). Different superscripted letters denote statistically significant differences at $\alpha = 0.05$ using the Student-Newman-Keuls test. An absence of letters indicates that there were no significant differences.

In relation to the specific C^+ analyzed, Mg^{+2} showed significantly larger amounts in both tissues of plants grown at high dose of NO_3^-, being the content of this C^+ related with the dose of N in a dependent manner, in shoots, as well as, in roots (Fig. 4.19A, E). Nitrate was supplied to the growth medium as $Ca(NO_3)_2$ and hence, as it

could be expected, roots of NO_3^--fed plants significantly accumulated more Ca^{2+} at both doses of N. Regarding the shoots content, no remarkable differences were found (Fig. 4.19B, F). Besides, K^+ content was significantly higher on NO_3^--fed roots, but despite that nutrition led to the highest value in shoots, this K^+ level was only significantly different in shoots from high urea treatment (Fig. 4.19C, G). Finally, the Na^+, in both plant tissues, decreased as N doses became higher but not clear tendencies were detected between treatments. At shoot level, plants grown with low dose of NO_3^- exhibited the highest value compared with all the treatments at high dose. In roots, the increase of N dose significantly affected the accumulation of Na^+(decreasing) in NO_3^-- and NH_4^+-fed plants (Fig. 4.19D, H).

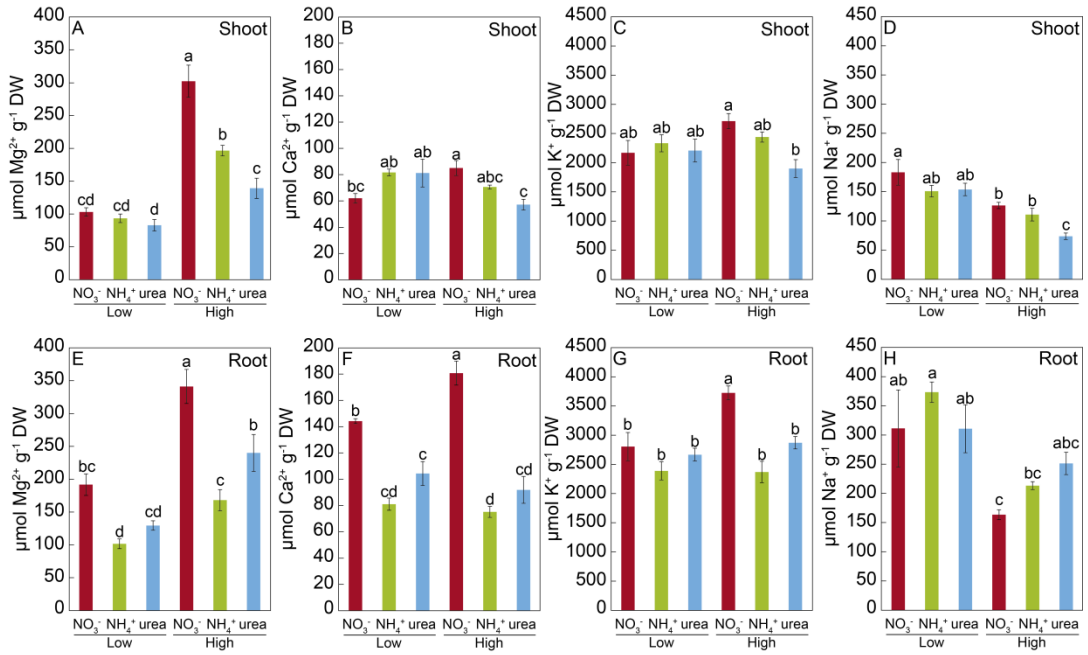

Figure 4.19 ***Effects of NO_3^-, NH_4^+, and urea on the cations content.*** High and low doses of NO_3^-, NH_4^+, and urea affected the amount of Mg^{2+} (**A**, **E**), Ca^{2+} (**B**, **F**), K^+ (**C**, **G**), and Na^+ (**D**, **H**) (µmol g^{-1} dry weight) accumulated on *M. truncatula* seedlings. The values are the mean ± S.E. (n = 5). Different letters denote statistically significant differences at $\alpha = 0.05$ using the Student-Newman-Keuls test.

Regarding the A^- content in *M. truncatula* seedlings (Fig. 4.20), NH_4^+-fed plants accumulated significantly higher quantities of SO_4^{2-} (Fig. 4.20A, D) in both tissues. The amount of SO_4^{2-} found in plants grown at high doses of NH_4^+ and urea was nearly 5-fold higher than such A^- at low dose of N (Fig. 4.20A, D). The differences between both doses is the consequence of the application of $CaSO_4$ on NH_4^+ and ureic treatments to compensate the Ca^{2+} concentration on culture media (see Chapter 3, section 3.1.2 and Table 3.3). Concerning the Cl^- anion, both tissues showed a similar pattern, and NH_4^+-fed plants presented significant higher values, reaching similar

content at high and low dose. In the other hand, NO_3^--fed plants significantly accumulated less amount of the Cl^- ion (Fig. 4.20 C, F). Ultimately, the PO_4^{3-} content was significantly higher in roots form ureic nutrition. In shoots, no remarkable differences were found in the PO_4^{3-} amount and similar levels were reached at both doses of N for every studied treatment (Fig. 4.20B, E).

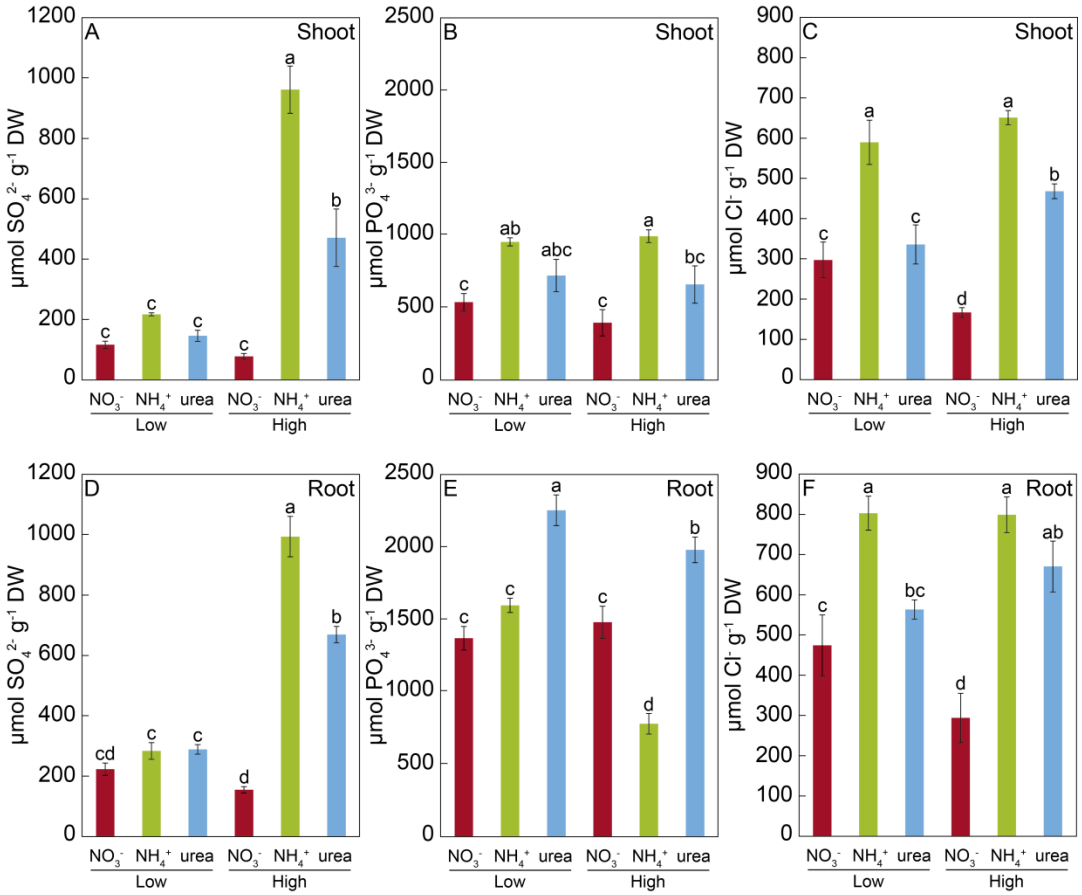

Figure 4.20 ***Effects of NO_3^-, NH_4^+, and urea on the anions content.*** High and low doses of NO_3^-, NH_4^+, and urea affected the amount of SO_4^{2-} (**A**, **D**), PO_4^{3-} (**B**, **E**), and Cl^- (**C**, **F**) (µmol g^{-1} dry weight) accumulated on *M. truncatula* seedlings. The values are the mean ± S.E. (n = 5). Different letters denote statistically significant differences at $\alpha = 0.05$ using the Student-Newman-Keuls test.

The uptake and assimilation of different N sources may imply differences in the distribution and accumulation of the N compounds along the whole plant. Hence, the content of NO_3^- and NH_4^+ ions were also measured as first molecules of the N signaling metabolism (Fig. 4.21). As it might be expected, NH_4^+ internal content was higher in NH_4^+-fed seedlings, being significantly higher at high N dose. At low doses of N, the NH_4^+ quantity was significant different among treatments in roots, but not in shoots (Fig. 4.21A, B).

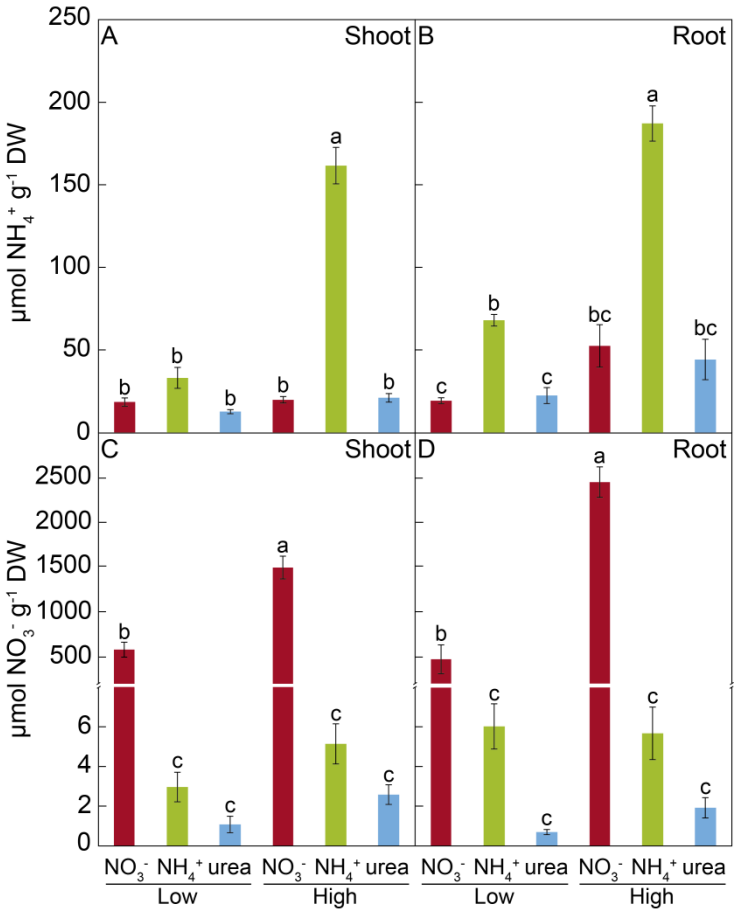

Figure 4.21 E*ffects of NO_3^-, NH_4^+, and urea on the NH_4^+ and NO_3^- internal content*. Accumulation of NH_4^+ (**A**, **B)**, and NO_3^- (**C**, **D)** on shoots and roots of *M. truncatula* seedlings grown under axenic conditions. The values are the mean ± S.E. (n = 5). Different letters denote statistically significant differences at α = 0.05 using the Student-Newman-Keuls test.

Accordingly, NO_3^- content was much more elevated in NO_3^-- fed plants than those cultivated in either NH_4^+ or urea (Fig. 4.21 C, D). Ammonium roots showed similar quantities of NO_3^- at both doses; while slightly higher content was found in shoots cultured at high dose. The same tendency was observed in both tissues of urea-fed plants, which accumulated a little more NO_3^- at high dose of N. However, the anion nitrite (NO_2^-) was not detected, although the same chromatography detection technique was used. In this sense, the colorimetric Griess method was also assayed and NO_2^- was neither detected (data not shown). In relation with those key metabolites of N assimilation, we tried to measure the nitrate reductase (NR) activity of *M. truncatula* seedling but, we were not able to detect it.

Nitric oxide (NO) is the first reactive nitrogen species generated under various stresses, and eventually plays a key role in signalling. Besides, NO could be originated

by different metabolic pathways, which include production from NO_2^- either by action of the NR or the nitrite:NO reductase (NiNOR) enzymes, among others. Thus, the effect of the different N sources studied on NO production was detected by imaging fluorescence. Images of the roots were taken and further analysed to quantify the relative fluorescence emited when NO reacts with the cell permeable fluorophore DAF-2DA probe (Figure 4.22).

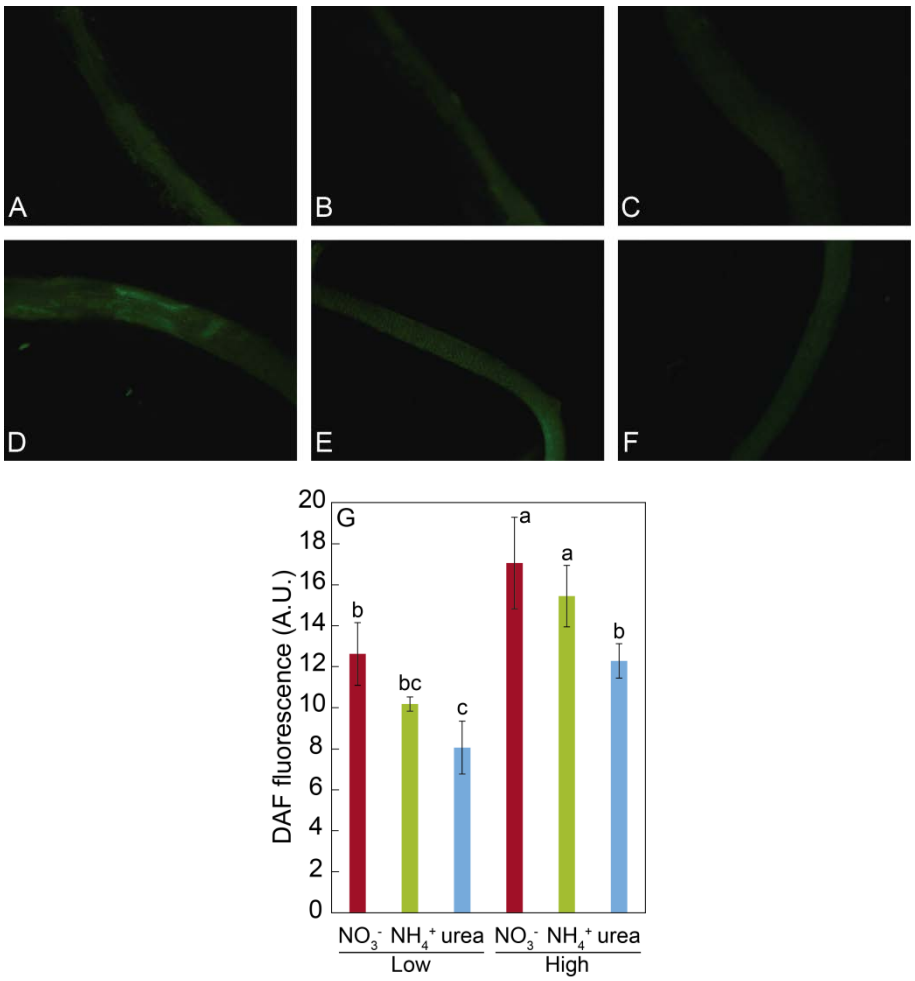

Figure 4.22. ***Effects of NO_3^-, NH_4^+, and urea on the NO level of*** **M. truncatula** ***roots after DAF staining.*** Representative images of NO fluorescence of 15 days old roots grown with low dose of NO_3^- (**A**), NH_4^+ (**B**), and urea (**C**) and high dose of NO_3^- (**D**), NH_4^+ (**E**), and urea (**F**); and realtive quantification of NO from the images (**G**). The values are the mean ± S.E. (n = 3-7). Different letters denote statistically significant differences at $\alpha = 0.05$ using the Student-Newman-Keuls test.

In agreement with nitrate contents, NO was accumulated in a dose-dependent maner based on the N contained in the nutrient medium; and high NO_3^-- and NH_4^+-

fed roots also exhibited significantly higher contents of NO (Fig. 4.22G). Urea treatment also showed the lowest production of NO.

4.3.2. Effect of N-source on the amino acids content on *Medicago truncatula* grown under axenic conditions

Total amino acids were significantly higher in NH_4^+-fed plants in both tissues at high N dose. Nitrate and urea showed a similar content of amino acids in both tissues and doses (Fig. 4.23).

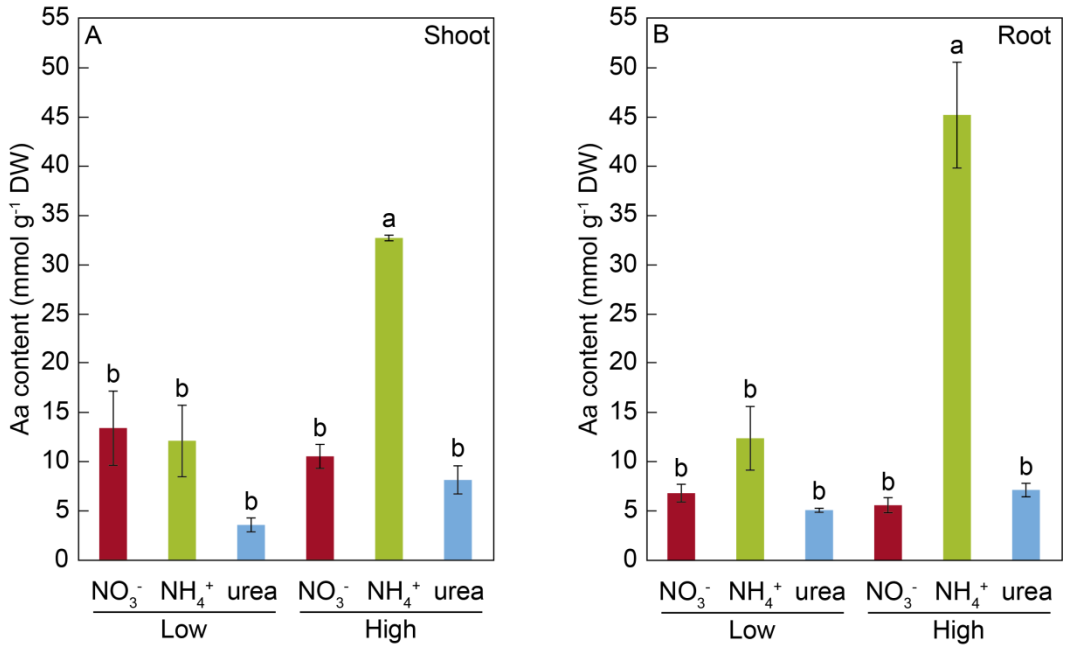

Figure 4.23. ***Effects of NO_3^-, NH_4^+, and urea on the Aa content.*** Total amino acids content of shoots (**A**), and roots (**B**) of 15-days old *M. truncatula* seedlings grown under axenic conditions. The values are the mean ± S.E. (n = 4). Different letters denote statistically significant differences at α = 0.05 using the Student-Newman-Keuls test.

The influence of the N-source on the soluble amino acids was analyzed individually, and the most remarkable obtained results are described below. First of all, a representation of the shoots and roots amino acids profiles is showed in Figures 4.24 and 4.25, respectively. At low concentrations of N, shoots suffered a significant decrease of alanine (Ala) and γ-amino-butyric acid (GABA) at both NH_4^+ and ureic treatments, while ureic shoots also exhibited a significantly lower content of serine (Ser) (Fig. 4.24A). In roots, a significant increase in methionine (Met) and arginine (Arg) accumulation was observed when N was supplied as NH_4^+ (Fig. 4.25A).

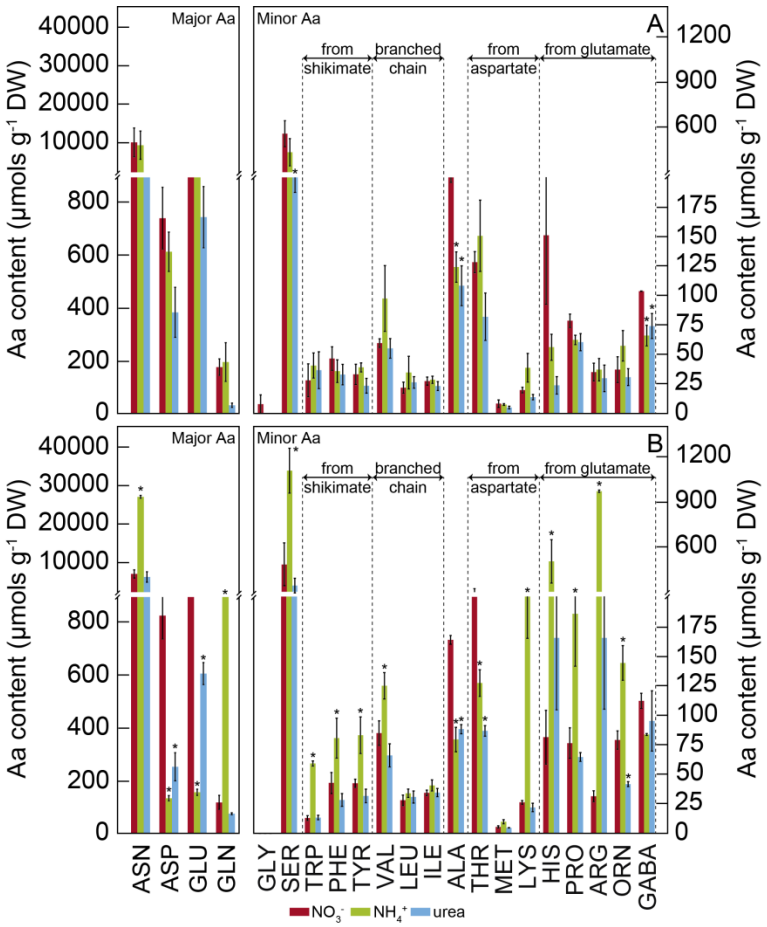

Figure 4.24. ***Effects of NO_3^-, NH_4^+, and urea on the shoots Aa content.*** Amino acids profiles of shoots from *M. truncatula* plants grown under the different treatments at low (**A**) and high (**B**) doses of N. The values are the mean ± S.E. (n = 4). An asterisk (*) denotes a significant difference between the pointed treatment and NO_3^- conditions at α = 0.05 after using the Student-Newman- Keuls test.

On the other hand, high N concentration produced changes in a larger number of amino acids in both plant tissues. The majority of Aa contents significantly increased under NH_4^+ nutrition, and most of them also enhanced when cultured with urea. Those changes implicated a redistribution of N from amino acids under high N conditions by increasing the ratio of C_4 to C_5 amino acids. The huge difference among high NH_4^+ treatment and the other nutritions, resides in the amino acids asparagine (Asn) and glutamine (Gln), which for instance showed values over 10 and 30-fold higher respectively in roots (Fig. 4.25B). In addition, both amino acids together represented around the 90% of the total amino acids present in either tissues of seedling subjected to this treatment. Furthermore, the forms with lower ratio C/N, as Asn and the amino acids derived from glutamate (Glu), Gln and Arg, sharply increased in both tissues of NH_4^+-fed plants. Moreover, roots from urea grown cultures

accumulated significantly lower amounts of Arg than those grown on nitric and NH_4^+ media; nevertheless Ala and GABA were significantly higher in those roots (Fig. 4.25B). By the contrary, NO_3^--grown plants differentially accumulated higher amounts of aspartate (Asp) and Glu in shoots, but not in roots (Fig. 4.24B and 4.25B). Additionally, Ala and threonine (Thr) also showed higher values in shoots from nitric medium. It should be noted that at shoot level, the content of leucine (Leu), isoleucine (Ile), Met, and GABA did not change, while glycine (Gly) was not detected (Fig. 4.24B).

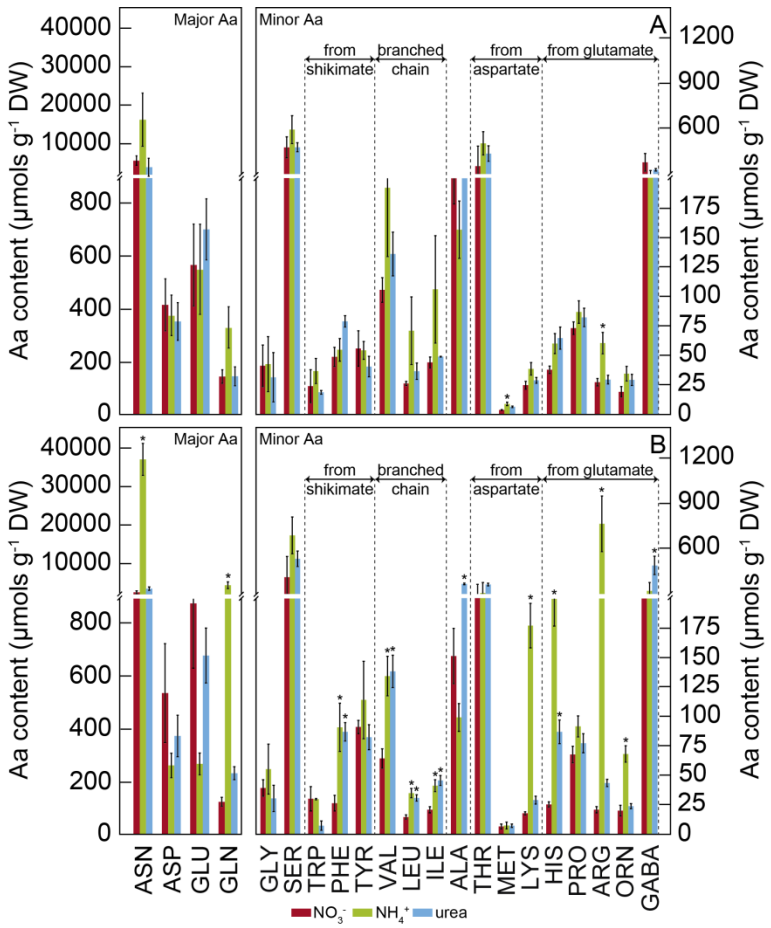

Figure 4.25. ***Effects of NO_3^-, NH_4^+, and urea on the roots Aa content.*** Amino acids profiles of roots from *M. truncatula* plants grown under the different treatments at low (**A**) and high (**B**) doses of N. The values are the mean ± S.E. (n = 4). An asterisk (*) denotes a significant difference between the pointed treatment and NO_3^- conditions at $\alpha = 0.05$ after using the Student-Newman- Keuls test.

The relative content of amino acids was also determined (Tables 4.5 and 4.6). At low doses of N, we detected that the distribution of Aa abundance was differentially assigned in urea-fed shoots since the relative content of Asp, Glu, Ile, Thr, Met, Pro

and GABA was significantly higher under this treatment. At the same time, the relevance of Asn was lower in those ureic roots (Table 4.5). However, in roots no remarkable differences on the participation of each Aa were found. But we showed that in the ureic roots Phe was the solely Aa that accumulates at relatively high content, whereas Ala and GABA were found to participate in a less proportion in NH_4^+-feed roots (Table 4.6).

Table 4.5. ***Relative amino acids content (%) in*** **M. truncatula** ***shoots*** **grown using** ***NO_3^-, NH_4^+, and urea as the only N source.***

Amino acid	Low			High		
	NO_3^-	NH_4^+	Urea	NO_3^-	NH_4^+	Urea
ASN	64.93±10.24^{ab}	66.56±9.89^{ab}	40.14±6.95^{b}	62.84±3.45^{ab}	81.78±0.81^{a}	70.39±5.12^{ab}
ASP	7.83±2.93^{ab}	6.34±1.37^{ab}	11.51±2.61^{a}	8.44±1.82^{ab}	0.42±0.04^{b}	3.59±1.03^{ab}
GLU	12.42±4.44^{ab}	10.94±3.69^{ab}	22.35±3.18^{a}	13.05±1.39^{ab}	0.46±0.04^{b}	8.61±2.12^{b}
GLN	1.47±0.24^{b}	1.72±0.60^{ab}	0.91±0.18^{b}	1.08±0.16^{b}	4.54±0.59^{a}	1.00±0.20^{b}
GLY	0.04±0.04	0.00±0.00	0.00±0.00	0.00±0.00	0.00±0.00	0.00±0.00
SER	4.85±0.92	4.8±1.37	6.73±0.94	4.23±1.15	3.72±0.41	4.41±0.54
TRP	0.16±0.06	0.44±0.18	1.02±0.35	0.13±0.02	0.18±0.01	0.19±0.07
PHE	0.38±0.06	0.47±0.28	0.92±0.09	0.41±0.07	0.29±0.05	0.43±0.17
TYR	0.27±0.05	0.45±0.17	0.66±0.13	0.42±0.07	0.29±0.04	0.43±0.10
VAL	0.70±0.21	1.38±0.85	1.62±0.21	0.84±0.13	0.41±0.03	0.94±0.26
LEU	0.19±0.05	0.54±0.37	0.79±0.13	0.29±0.07	0.11±0.01	0.44±0.13
ILE	0.31±0.08^{b}	0.22±0.06^{b}	0.70±0.12^{a}	0.34±0.05^{b}	0.14±0.01^{b}	0.47±0.09^{ab}
ALA	2.13±0.64^{ab}	1.26±0.27^{ab}	3.35±0.85^{a}	1.73±0.29^{ab}	0.27±0.01^{b}	0.97±0.12^{ab}
THR	1.24±0.35^{ab}	1.53±0.48^{ab}	2.28±0.16^{a}	2.72±0.67^{a}	0.42±0.02^{b}	1.23±0.32^{ab}
MET	0.07±0.02^{b}	0.08±0.03^{b}	0.14±0.01^{a}	0.05±0.00^{b}	0.03±0.01^{b}	0.07±0.02^{b}
LYS	0.18±0.04^{b}	0.38±0.14^{b}	0.41±0.05^{b}	0.26±0.03^{b}	0.73±0.12^{a}	0.29±0.06^{b}
HIS	1.01±0.14	0.68±0.11	0.67±0.18	0.73±0.18	1.92±0.30	1.97±0.57
PRO	0.75±0.21^{b}	0.86±0.32^{b}	1.84±0.29^{a}	0.77±0.17^{b}	0.65±0.17^{b}	0.92±0.24^{b}
ARG	0.36±0.15^{ab}	0.53±0.24^{ab}	0.76±0.14^{ab}	0.32±0.02^{ab}	2.97±0.00^{a}	1.81±0.47^{b}
ORN	0.36±0.15	0.64±0.25	0.90±0.15	0.77±0.08	0.48±0.02	0.57±0.13
GABA	0.92±0.38^{ab}	0.75±0.27^{ab}	2.29±0.53^{a}	1.14±0.21^{ab}	0.26±0.00^{b}	1.53±0.70^{ab}

The values represent the mean ± S.E. (n = 4). Different superscripted letters denote statistically significant differences at $\alpha = 0.05$ using the Student-Newman-Keuls test. An absence of letters indicates that there were no significant differences.

In the other hand, in shoots grown at high doses of N, Ala, Thr and some of the amino acids related to the urea cycle, such as Asp, Glu or GABA, presented significant lower relative content when subjected to ammonium nutrition. On the contrary, the same treatment showed the lowest relative content of Lys, while Arg exhibited the same trend in shoots from ureic cultures (Table 4.5). Furthermore, we observed that

most of the Aa presented the lowest relative content in roots from NH_4^+ cultures, with the exception of those with lowest C/N ratio (Asn, Gln and Arg), whose proportion was significantly higher. At high dose of urea, the relative content of Ala and Phe was the highest, similarly to the tendency observed in low ureic roots. Finally, the relative content of Tyr was the only that was significantly higher under nitrate treatment (Table 4.6).

Table 4.6. ***Relative amino acids content (%) in* M. truncatula *roots* grown using *NO_3, NH_4^+, and urea as the only N source.***

Aa (%)	Low NO_3^-	Low NH_4^+	Low Urea	High NO_3^-	High NH_4^+	High Urea
ASN	54.48±1.02^{b}	63.27±10.45^{b}	43.44±8.23^{b}	45.70±3.06^{b}	82.27±0.89^{a}	48.88±3.22^{b}
ASP	6.15±1.22^{ab}	3.81±1.34^{ab}	6.23±1.64^{ab}	9.24 ± 2.25^{a}	0.58±0.06^{b}	5.08±0.73^{ab}
GLU	8.22±1.87^{ab}	5.49±2.25^{bc}	12.25±2.74^{ab}	15.10±2.43^{a}	0.62±0.11^{c}	9.61±1.25^{ab}
GLN	2.06±0.13^{b}	2.73±0.12^{b}	2.25±0.14^{b}	2.24 ± 0.03^{b}	9.37±0.96^{a}	3.49±0.79^{b}
GLY	0.68±0.35	0.38±0.23	0.42±0.24	0.72 ± 0.13	0.13±0.04	0.42±0.14
SER	7.26±1.09^{a}	6.44±2.16^{a}	8.11±0.80^{a}	7.81 ± 2.23^{a}	1.52±0.19^{b}	7.49±0.34^{a}
TRP	0.37±0.22	0.45±0.23	0.32±0.05	0.49 ± 0.12	0.07±0.01	0.09±0.05
PHE	0.71±0.07^{b}	0.60±0.22^{b}	1.36±0.20^{a}	0.48 ± 0.11^{b}	0.20±0.04^{b}	1.26±0.18^{a}
TYR	0.81±0.15^{bc}	0.57±0.20^{bc}	0.72±0.20^{bc}	1.69±0.15^{a}	0.26±0.08^{c}	1.16±0.11^{b}
VAL	1.58±0.09	2.34±1.14	2.24±0.14	1.16±0.16	0.30±0.02	1.94±0.07
LEU	0.40±0.06	0.91±0.50	0.58±0.02	0.26±0.01	0.08±0.01	0.43±0.03
ILE	0.66±0.08	1.43±0.85	0.96±0.04	0.37±0.02	0.10±0.02	0.64±0.02
ALA	3.18±0.45^{bc}	1.42±0.22^{d}	3.93±0.46^{ab}	2.69±0.12^{c}	0.23±0.05^{c}	4.73±0.22^{a}
THR	5.09±1.48^{a}	4.81±1.23^{a}	7.60±1.41^{a}	5.12±0.68^{a}	0.72±0.21^{b}	5.22±0.45^{a}
MET	0.06±0.01	0.09±0.03	0.11±0.02	0.12±0.04	0.02±0.01	0.09±0.01
LYS	0.37±0.05	0.41±0.17	0.49±0.07	0.32±0.03	0.40±0.03	0.40±0.03
HIS	0.60±0.13	0.65±0.27	1.15±0.24	0.46±0.05	0.48±0.13	1.27±0.22
PRO	1.11±0.11^{a}	0.93±0.30^{a}	1.38±0.14^{a}	1.24±0.09^{a}	0.21±0.02^{b}	1.10±0.10^{a}
ARG	0.40±0.04^{b}	0.61±0.19^{b}	0.48±0.05^{b}	0.37±0.01^{b}	1.61±0.25^{a}	0.61±0.03^{b}
ORN	0.29±0.09^{ab}	0.33±0.08^{ab}	0.49±0.09^{a}	0.38±0.09^{ab}	0.15±0.01^{b}	0.33±0.02^{ab}
GABA	5.54±0.42^{a}	2.43±0.59^{b}	5.73±0.81^{a}	5.39±0.82^{a}	0.71±0.07^{b}	6.92±0.76^{a}

The values represent the mean ± S.E. (n = 4). Different superscripted letters denote statistically significant differences at $\alpha = 0.05$ using the Student-Newman-Keuls test. An absence of letters indicates that there were no significant differences.

4.3.3. Effect of N-source on xanthine dehydrogenase and ureides in *Medicago truncatula* grown under axenic conditions

Nitrogen metabolism in plants also comprises the mobilization of N from one another nitrogenous compounds. Hence, the end products of purine degradation

glyoxylate and ammonia are recycled into other nitrogenous molecules, which will be used next for plant growth and development. In the catabolism of purines the first common metabolite is xanthine that should be degraded by xanthine dehydrogenase (XDH) in the cytosol. Then, the XDH activity in of *M. truncatula* seedlings was measured in both shoots and roots, and no differences were observed in shoots (Fig. 4.26A). In roots, low NO_3^--fed plants showed significantly higher XDH activity, when comparing with roots grown at high dose of urea (Fig. 4.26B).

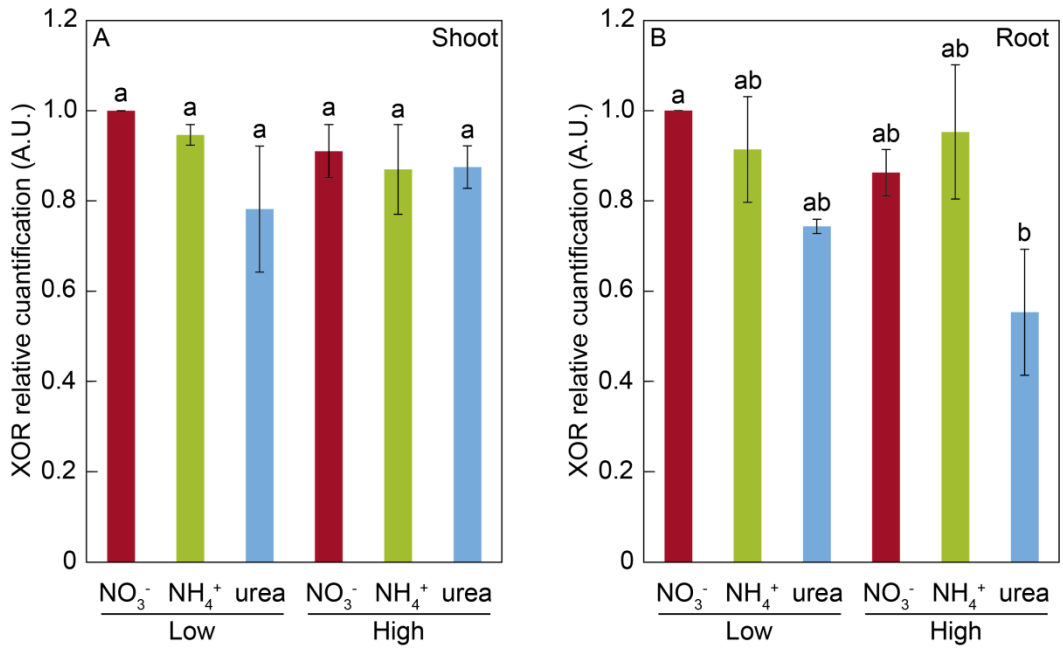

Figure 4.26. ***Effects of NO_3^-, NH_4^+, and urea on the XDH activity.*** Xanthine dehydrogenase activity was detected in shoots (**A**) and roots (**B**) of 15-days old *M. truncatula* seedlings by native-PAGE. The gels were analysed and the results are showed as densiometry relative to the corresponding control reference band (1mM NO_3^-). The values are the mean ± S.E. (n = 3-4). Different letters denote statistically significant differences at $\alpha = 0.05$ using the Student-Newman-Keuls test. To standardize the variances, one data point was replaced with the mean for the group for root low urea, and consequently, 1 degree of freedom was subtracted from the residual in that case (Winer *et al.*, 1991).

As a consequence of xanthine degradation, urate is produced and it is imported into the peroxisome, where it is successively transformed by the action of urate oxidase and allantoin synthase to form allantoin. Then, once allantoin is transported to the endoplasmic reticulum, the catabolism of ureides is initiated. Thus, the different N sources did not affect the total ureides content of *M. truncatula* shoots, but NO_3^--fed roots showed significant higher amount of total ureides at high doses than those grown under NH_4^+ and urea at low N concentration (Fig. 4.27A and B).

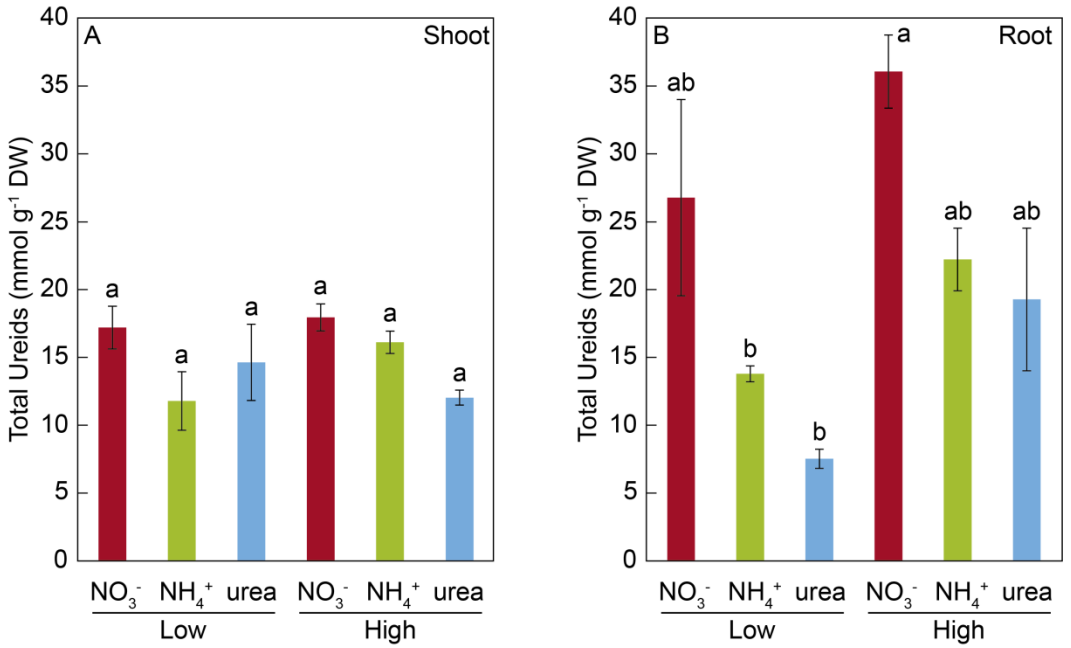

Figure 4.27. ***Effects of NO_3^-, NH_4^+, and urea on the toatal uredis content.*** Total ureides content of shoots (**A**), and roots (**B**) of 15-days old *M. truncatula* seedlings grown under axenic conditions. The values are the mean ± S.E. (n = 4). Different letters denote statistically significant differences at $\alpha = 0.05$ using the Student-Newman-Keuls test.

Regarding each specific ureide response to each of the treatments applied here, no differences were found in allantoate and allantoin in shoots. Note that allantoin was only detected under low urea dose in shoots (Fig. 4.28A and B). Ureidoglycolate amount was significantly lower in low NH_4^+ shoots than that accumulated at high dose treatments (Fig. 4.28C). In roots, allantoin content was significantly higher in nitrate fed plants at high dose. On the contrary, very little allantoin was accumulated on high NH_4^+-fed roots (Fig. 4.28D). Roots grown at high doses of NO_3^- and NH_4^+ showed significant higher quantities of allantoate, and the lowest amount was observed in ureic roots (Fig. 4.28E). Ureidoglycolate was significantly lower in NH_4^+-fed roots at high dose (Fig. 4.28F). In addition, glyoxylate was under detection limit in all cases and tissues.

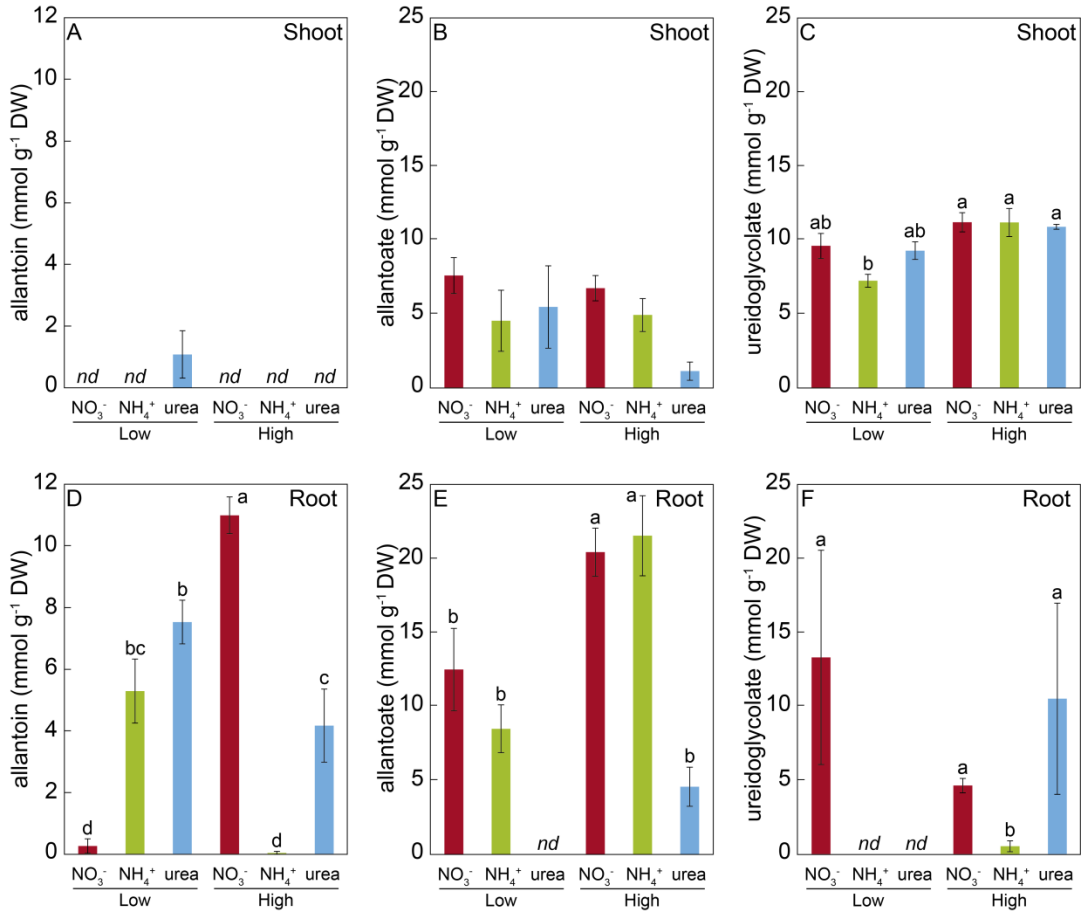

Figure 4.28 E*ffects of NO₃, NH₄⁺, and urea on the ureides content*. Accumulation of allantoin (**A**, **D)**, allantoate (**B**, **E**), and ureidoglycolate (**C**, **F)** on shoots and roots of *M. truncatula* seedlings grown under axenic conditions. The values are the mean ± S.E. (n = 4). Different letters denote statistically significant differences at $\alpha = 0.05$ using the Student-Newman-Keuls test. An absence of letters indicates that there were no significant differences. To standardize the variances, two data point were replaced with the mean for the group for root allantoin, and consequently, 2 degrees of freedom was subtracted from the residual in that case (Winer *et al.*, 1991).

4.3.4. Reactive oxigen species: hydrogen peroxide and superoxide

Reactive oxygen species (ROS) such as hydrogen peroxide (H_2O_2) and superoxide anion (O_2^-) are molecules of great interest as signaling molecules. We analyse, therefore, the produccion of these reactive species, in order to identify the possible oxidative stress produced by the nutrition of ammoium or urea.

Reactive oxygen species on roots from plants grown under low and high dose of N were detected by DAB and NBT staining (for H_2O_2 and O_2^-detection and quantification respectevely). No differences were found for H_2O_2 (Fig. 4.29G). However, the O_2^- showed a significant higher amount in roots grown at high dose of N

than those cultured at low dose. Ammonium and ureic nutrition had not a differential effect respect to NO_3^- on the production of O_2^- anion in each of the dosis (Fig. 4.30G).

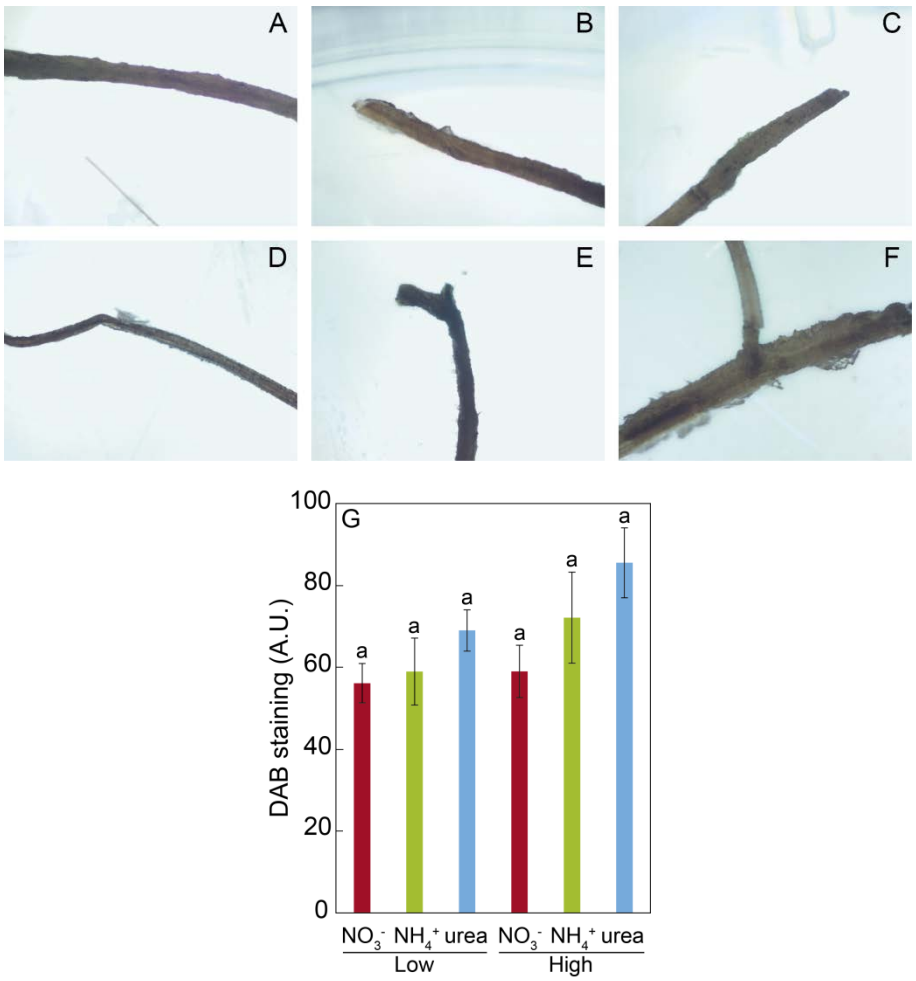

Figure 4.29. ***Effects of NO_3^-, NH_4^+, and urea on hydrogen peroxide levels of* M. truncatula *roots analysed after DAB staining.*** Representative images of DAB staining of 15 days old roots grown with low dose of NO_3^- (**A**), NH_4^+ (**B**), and urea (**C**) and high dose of NO_3^- (**D**), NH_4^+ (**E**), and urea (**F**); and relative quantification of H_2O_2 from the images (**G**). The values are the mean ± S.E. (n = 10-12). Different letters denote statistically significant differences at $\alpha = 0.05$ using the Student-Newman-Keuls test.

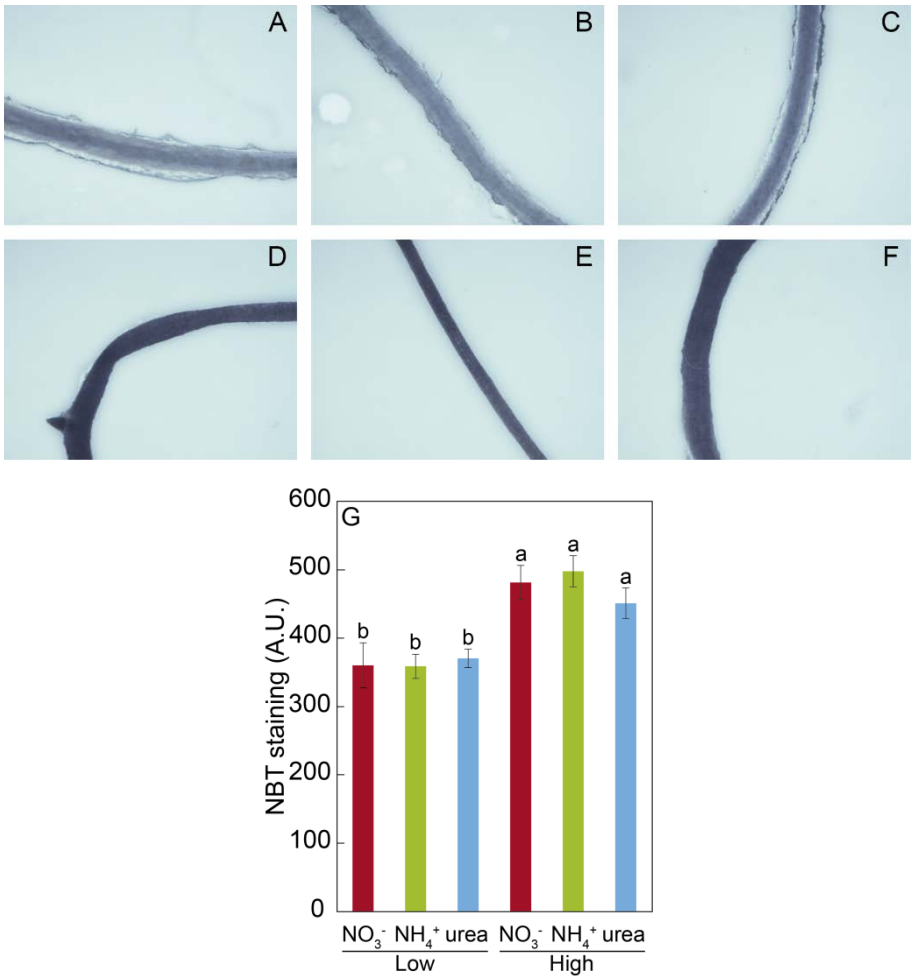

Figure 4.30. ***Effects of NO_3^-, NH_4^+, and urea on superoxide levels of*** **M. truncatula** ***roots analysed after NBT staining.*** Representative images of NBT staining of 15 days old roots grown with low dose of NO_3^- (**A**), NH_4^+ (**B**), and urea (**C**) and high dose of NO_3^- (**D**), NH_4^+ (**E**), and urea (**F**); and relative quantification of O_2^- from the images (**G**). The values are the mean ± S.E. (n = 10-12). Different letters denote statistically significant differences at $\alpha = 0.05$ using the Student-Newman-Keuls test.

4.4. Proteomic analysis of *Medicago truncatula* roots in response to nitrate, ammonium and ureic nutrition

4.4.1. Identification and quantification of root proteins using iTRAQ-mass spectrometry

In this study, we analyzed the root proteome of *Medicago truncatula* plants grown for 15 days in axenic medium containing either nitrate, ammonium or urea as the sole N source using iTRAQ-mass spectrometry (see Chapter 3, section 3.1.2). Following low-scoring spectra filtering, we identified 1533 distinct proteins on the basis of 5799 unique peptides, exhibiting at least two matches at the respective entire protein sequence and a false discovery rate (FDR) lower than 1%. Out of those, 1126 root proteins were quantified, which clustered into groups of homologs by aligning all proteins with highly significant alignment scores (Fig. 4.31). The final dendrogram depicted in the figure demonstrated a strong correlation among the replicates for any of the three nutritional treatments and further showed that proteins identified upon urea treatment were more similar to the nitrate protein cluster, while, the ammonium cluster represented as outgroup.

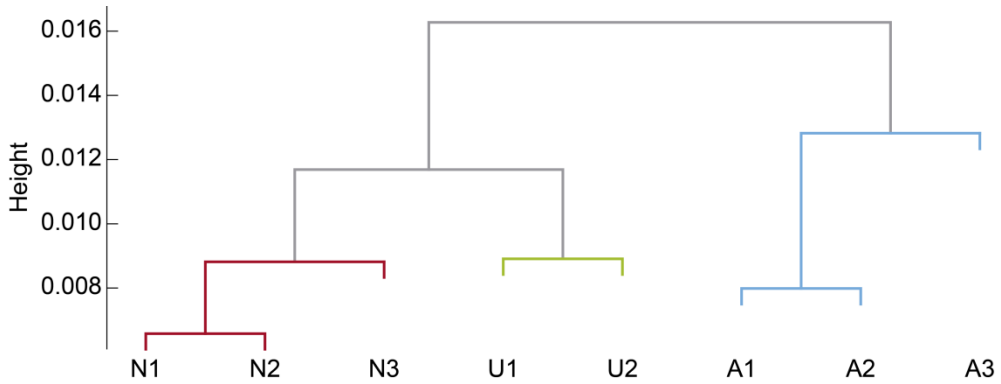

Figure 4.31. ***Cluster dendrogram of 1,126 quantified proteins showing the distance among clusters.*** Classification of quantified proteins of nitrate- (N1, N2, N3), urea- (U1, U2), and ammonium-fed (A1, A2, A3) roots grouped into clusters.

4.4.2. Differentially accumulated proteins

In order to identify differentially expressed proteins, the differences among the averages of quantified data from biological replicates were used to calculate the fold change between treatments. Based on a significance level of $p < 0.01$ and a 1.3-fold change cut off, differentially accumulated proteins were identified with respect to control conditions (nitrate). Using this criteria, a total of 61 differentially expressed proteins were identified from all three N regimes. Using the iTRAQ score, we

calculated the variation of the expression of each protein at a given treatment, relative to the level of such protein in the three treatments. This analysis was performed using the z-score and the relative expression level of each differential protein for each treatment illustrated in the heat-map (Fig. 4.32).

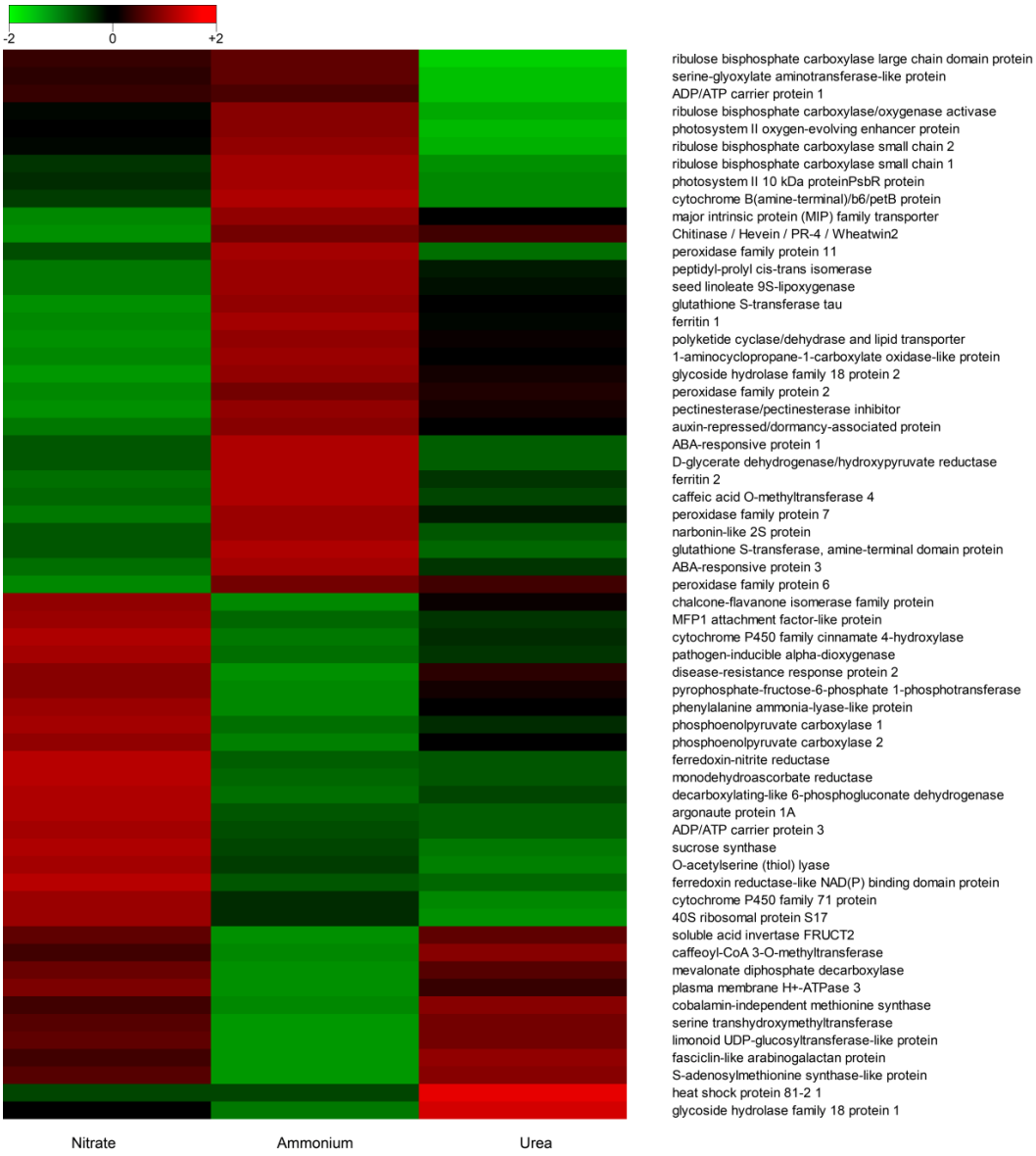

Figure 4.32. ***Heat map from iTRAQ data analysis.*** The heat map illustrates the differential expression of 61 significantly accumulated proteins of *M. truncatula* roots grown in nitrate, ammonium, and urea under axenic conditions. Relative intensity (z-score) was used to generate the map where columns in *X*-axis indicate the proteins identified in each treatment, and each row of *Y*-axis is an individual protein. The color code depicted on top of the panel indicates the z-score, which fluctuates from a minimum of -2 (green) to a maximum of 2 (red). Black color indicates no change in protein abundance.

Accordingly with the heat map above depicted, z-scores for NO_3^-- and NH_4^+ -fed plants were quite contrasting in general, showing opposite patterns. Thus, proteins that exhibited a low z-score in NO_3^--fed roots fundamentally were up-regulated under NH_4^+ nutrition, and *vice versa*. However, proteins from ureic roots were mainly down-regulated relative to those from NO_3^--fed seedlings, with some exceptions (Fig. 4.32).

Compared to control conditions, NH_4^+ produced a total of 53 differentially expressed proteins, 26 of them were significantly up-regulated (49%), while, 27 were significantly found to down-regulate (51%). Furthermore, urea-grown roots showed a pattern that involved a lower number of proteins (a total of 29), with about two thirds of those 29 identified proteins down-regulated (69%), being one third up-regulated (31%) (Fig. 4.33A).

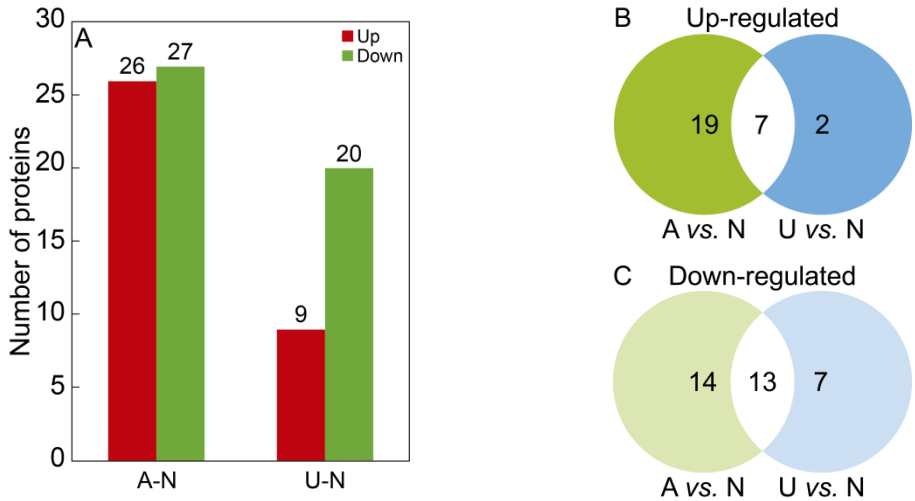

Figure 4.33. ***Accumulation of differentially identified proteins***. The identified proteins of *M. truncatula* roots grown under NH_4^+ and urea nutrition differentially accumulated when comparing to NO_3^- nutrition respectively. Histogram representing the up- and down-accumulation of the 61 differentially expressed proteins when comparing NH_4^+ *vs.* NO_3^-, and urea *vs.* NO_3^- nutrition. Venn diagram showing the shared up- (**B**) and down- (**C**) regulated proteins between nitrate and NH_4^+ and nitrate and urea treatments.

Additionally, the comparison of the share up- and down- regulated proteins of NH_4^+ *vs.* NO_3^- (Fig. 4.33B) and urea *vs.* NO_3^- (Fig. 4.33B) showed that out of the 21 differentially proteins, the amount of down-regulated proteins was higher (13 proteins) than those that were up-regulated (7 proteins). Interestingly, the ribulose bisphosphate carboxylase/oxygenase (RuBisCo) activase was the only protein that was identified as a differential protein in both NH_4^+ and urea in respect to NO_3^- nutrition. However, its expression showed an opposite effect: in NH_4^+-fed roots, RuBisCo activase was found to be up-regulated whereas it was down-regulated in urea-grown roots (Table 4.7).

4.4.3. Functional classification of the differentially accumulated proteins

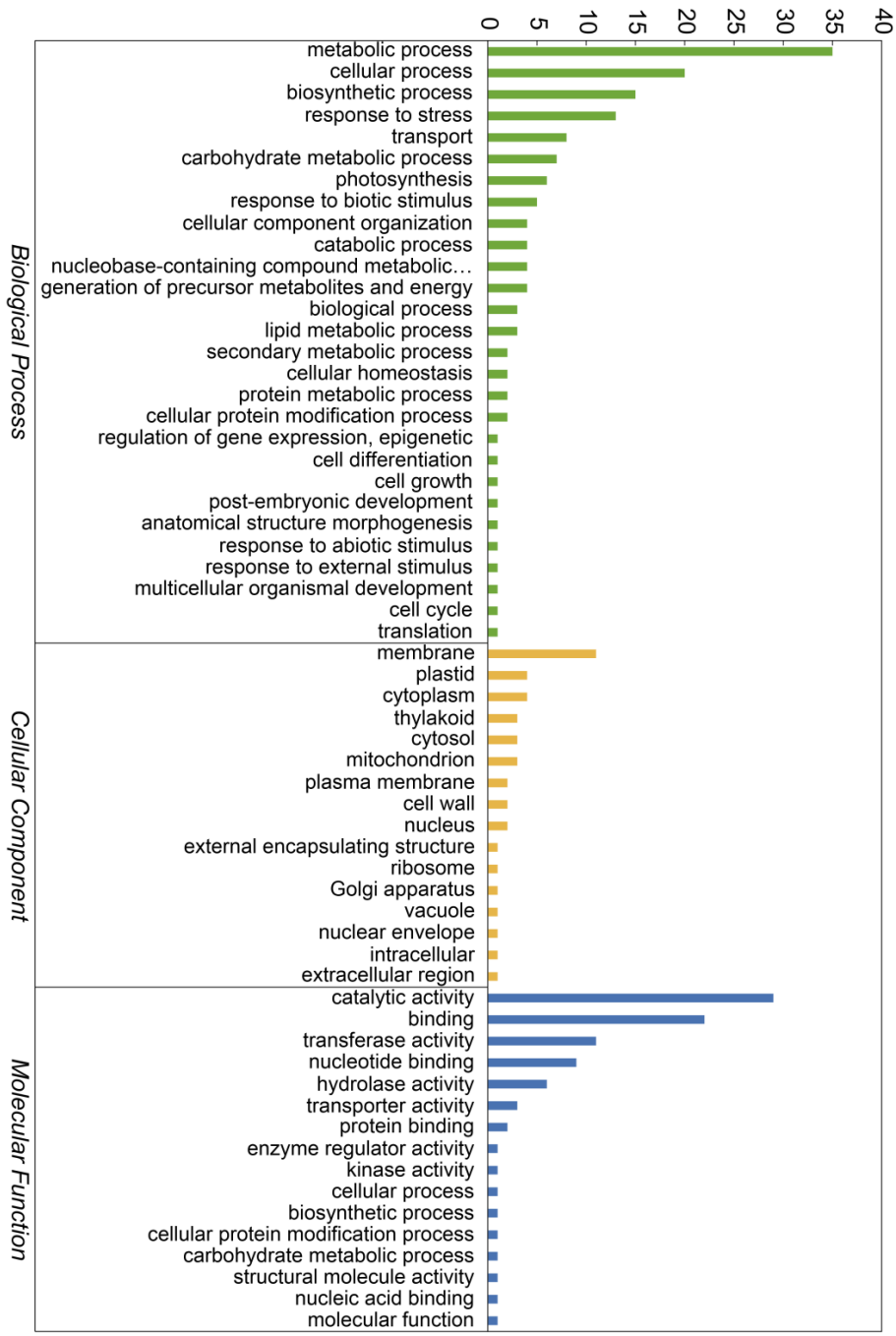

Figure 4.34. ***Gen Onthology (GO) categories assigned to*** **M. truncatula** ***root proteins***. The 61 differentially identified proteins when comparing NH_4^+ and urea nutrition to NO_3^- treatment were categorized according to the annotation of GO Slim. The number of proteins associated to each category is displayed on *Y*-axis, while the different categories are represented on *X*-axis based on biological process, cellular component, and molecular function.

According to the Gene Ontology (GO) from the Gene Ontology Consortium, the differentially expressed proteins were classified on the basis of biological processes, molecular function and cellular component by GO Slim (Fig. 4.34). Most of the proteins were involved in metabolic, cellular and biosynthetic processes. In addition, around 33% of the studied proteins were implicated in the response of both biotic and abiotic stimulus. Moreover, based on the molecular function properties, the 61 proteins were mainly classified into binding (51%) and catalytic (48%) activity. Further, the 18% and 10% of the proteins also have transferase and hydrolase activities. With respect to their cellular localization, differentially accumulated proteins were mostly associated with membranes (Fig. 4.34).

Meanwhile, these proteins were also classified in 13 different functional categories in accordance with the "euKaryotic Orthologous Group of proteins" (KOG) (Fig. 4.35). The results showed that the proteins were assigned as follows in descending order: carbohydrate transport and metabolism (18 proteins), energy production and conservation (8 proteins), post-translational modifications (5), secondary metabolites biosynthesis (5), inorganic ion (5), amino acids (4) transport and metabolism, and another 8 proteins with an already unknown function. In the rest of the functions less than 6 proteins were implicated.

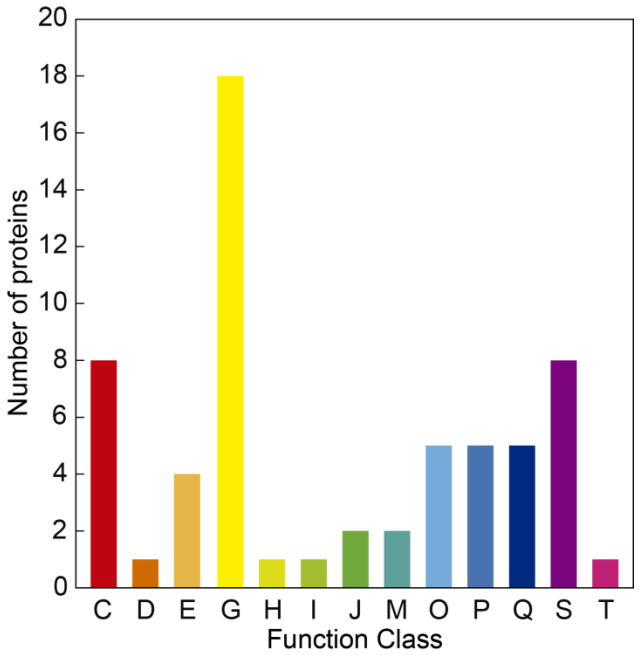

Figure 4.35. ***Functional classification of 61 identified root proteins by KOG.*** Proteins were grouped by the following function class: C) energy production and conversion. D) cell cycle control, cell division, chromosome partitioning. E) Amino acid transport and metabolism. G) carbohydrate transport and metabolism. H) coenzyme transport and metabolism. I) lipid transport and metabolism. J) translation, ribosomal structure and biogenesis. M) cell wall/membrane/envelope biogenesis. O) post-translational modification, protein turnover, chaperones. P) inorganic ion transport and metabolism. Q) secondary metabolites biosynthesis, transport and catabolism. S) unknown. functions T) signal transduction mechanisms.

The KOG classification also evidenced that carbohydrate transport and metabolism-related proteins in NH_4^+-fed roots underwent highest changes among all

categories (Fig. 4.36A). This group of proteins is related to the energy production. A group of proteins associated with post-translational modifications and protein turnover ("O" group) were also shown to be enriched. As shown in Table 4.7, those proteins were a Tau class glutathione s-transferase (Tau GST), glutathione S-transferase amine-terminal domain protein, peptidyl-prolyl cis-trans isomerase, and the RuBisCo activase. It should be mentioned that all the proteins were found up-regulated compared with NO_3^- treatment. Additionally, we found that proteins, which belong to the amino acid, coenzyme and lipid metabolisms, together with secondary metabolites and cell wall/membrane biosynthesis, were all down-regulated in those NH_4^+ treated plants (Fig. 4.36A).

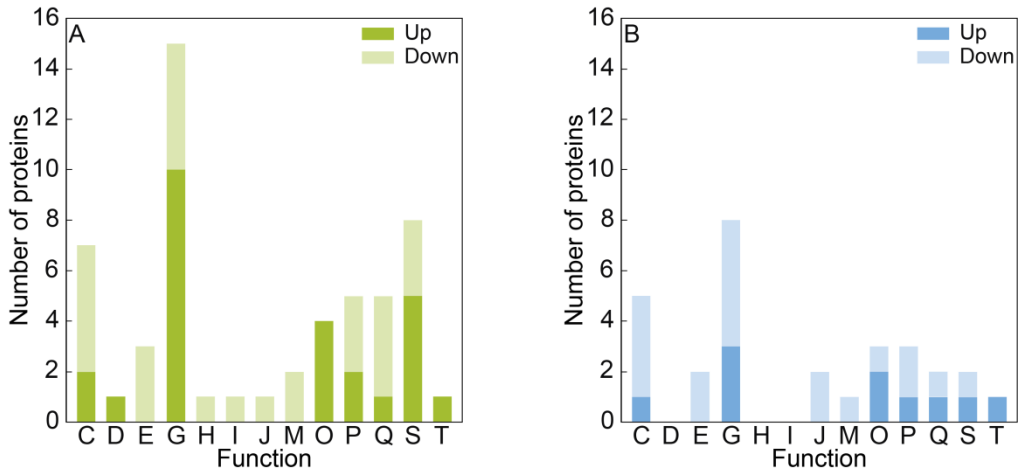

Figure 4.36. ***Effect of NH_4^+ and urea nutrition on the KOG classification.*** The differentially expressed proteins of *M. truncatula* roots were clustered according to the KOG classification separately for each comparison. KOG assignment of significantly up- and down-regulated proteins from NH_4^+ *vs.* NO_3^- (**A**), and urea *vs.* NO_3^- (**B**).

On the other hand, proteins from ureic nutrition implies changes in a fewer number of functional classes than NH_4^+ nutrition, being half of them related to carbohydrates and energy metabolism. Groups E, J and M showed a down-regulation of all their proteins (Fig. 4.36B). Besides, as showed in Figure 4.35, only one protein was assigned to the signal transduction mechanisms. This protein was a chitinase (Medtr7g115220.1), whose relative expression increased when subjecting plants to either NH_4^+ or urea treatments (Fig. 4.36BA and 4.36B).

Also in agreement with KOG clustering, the information obtained from iTRAQ analysis of the total significantly identified proteins was supplementary depicted in Table 4.7. In this table, more complete information of every protein implicated in each of the groups is shown.

Table 4.7. ***Differentially identified proteins in response to NO_3^-, NH_4^+, and urea nutrition.*** The 61 differentially identified proteins with a confidence interval (CI) >99% of *M. truncatula* roots grown in axenic culture under different N sources were grouped in accordance with KOG classification.

Uniprot ID	Protein Name	Accesion	UP[1]	Score[2]	FC1[3]	FC2[4]	*p*Val[5]
Energy production and conversion **(C)**							
G7JQB0	Cytochrome B(amine-terminal)/ b6/petB protein	Medtr4g034790	2	16.46	**1.643**	0.843	0.0002
A0A072UGE8	D-glycerate dehydrogenase /hydroxypyruvate reductase	Medtr6g007170	6	54.48	**1.518**	0.982	0.0007
G7LDP4	ADP/ATP carrier protein 1	Medtr8g036880	9	16.98	1.022	**0.695**	0.0044
A0A072UXU6	ADP/ATP carrier protein 3	Medtr4g078545	7	23.30	**0.705**	**0.693**	0.0055
G7IH71	Phosphoenolpyruvate carboxylase 1	Medtr2g076670	25	323.31	**0.682**	**0.752**	0.0014
A0A072VRK6	Limonoid UDP-glucosyltransferase-like protein	Medtr1g107285	3	23.587	**0.627**	1.033	0.0005
G7IKU6	Ferredoxin reductase-like NAD(P) binding domain protein	Medtr2g030200	5	55.54	**0.361**	**0.340**	0.0000
G7IU25	Phosphoenolpyruvate carboxylase 2	Medtr2g092930	11	10.97	**0.331**	**0.574**	0.0011
Cell cycle control, cell division chromosome partitioning **(D)**							
G7K511	Caffeic acid O-methyltransferase 4	Medtr5g098170	2	12.94	**1.475**	1.053	0.0014
Amino acid transport and metabolism **(E)**							
G7J014	Serine-glyoxylate aminotransferase-like protein	Medtr3g053890	5	50.33	1.054	**0.682**	0.0019
G7JNN9	O-acetylserine (thiol) lyase	Medtr4g087520	6	78.63	**0.753**	**0.687**	0.0039
G7LH57	Serine transhydroxymethyltransferase	Medtr8g081510	9	18.62	**0.680**	1.035	0.0010
G7L0I7	Cobalamin-independent methionine synthase	Medtr7g086300	37	323.31	**0.635**	1.141	0.0034

[1] Number of peptides that are unique in the cited protein.[2] Quality of the identification of the preotein represented as the sume of the individual SCORE of each peptide that conform the protein. [3] Difference on the intensity of the protein expresed as the fold change when comparing NH_4^+ *vs.* NO_3^- nutrition. [4] Difference on the intensity of the protein expresed as the fold change when comparing urea *vs.* NO_3^- nutrition. FC were depicted in red color for up-regulated proteins and in green color for down-regulated proteins. [5] p-value of ANOVA test

Table 4.7. *Continuation*

Uniprot ID	Protein Name	Accesion	UP[1]	Score[2]	FC1[3]	FC2[4]	*p*Val[5]
***Carbohydrate transport and metabolism* (G)**							
A4UN77	Peroxidase family protein 2	Medtr2g029750	9	323.31	**1.674**	**1.448**	0.0079
A0A072TLJ8	Glycoside hydrolase family 18 protein 2	Medtr0002s1060	15	179.97	**1.532**	**1.315**	0.0002
Q946J9	Major intrinsic protein transporter	Medtr5g082070	5	15.58	**1.485**	1.241	0.0026
G7IG38	Narbonin-like 2S protein	Medtr0062s0090	4	26.03	**1.453**	0.997	0.0075
G7IJU5	Peroxidase family protein 6	Medtr2g029850	5	169.31	**1.419**	**1.340**	0.0084
G7IJV0	Peroxidase family protein 7	Medtr2g029910	2	43.96	**1.411**	1.135	0.0080
B7FHB2	Ribulose bisphosphate carboxylase small chain 1	Medtr6g018310	10	185.68	**1.403**	0.852	0.0003
Q2HRX3	Pectinesterase/pectinesterase inhibitor	Medtr7g050980	9	89.38	**1.393**	1.231	0.0019
A0A072UAE2	Peroxidase family protein 11	Medtr6g043240	10	256.16	**1.391**	0.955	0.0020
G7IJ45	Photosystem II 10 kDa proteinPsbR protein	Medtr2g064650	3	17.38	**1.344**	0.867	0.0018
A0A072TXF3	Ribulose bisphosphate carboxylase small chain 2	Medtr7g007220	8	64.95	1.298	**0.728**	0.0008
G7ZVI4	Photosystem II oxygen-evolving enhancer protein	Medtr8g078870	10	154.31	1.213	**0.722**	0.0011
G7JG19	Ribulose bisphosphate carboxylase large chain domain protein	Medtr4g051270	23	323.31	1.063	**0.595**	0.0001
G7ZXA1	Glycoside hydrolase family 18 protein 1	Medtr0062s0170	10	174.32	0.810	**1.407**	0.0002
A0A072TUR1	Decarboxylating-like 6-phosphogluconate dehydrogenase	Medtr8g099185	11	80.481	**0.736**	**0.768**	0.0008
A0A072V0J5	Soluble acid invertase FRUCT2	Medtr4g101630	6	64.33	**0.731**	1.004	0.0072
A0A072V1H8	Chalcone-flavanone isomerase family protein	Medtr3g093980	3	26.17	**0.713**	0.870	0.0027
Q2HTG9	Pyrophosphate-fructose-6-phosphate 1-phosphotransferase	Medtr2g025020	5	36.30	**0.695**	0.884	0.0042
A0A072VRK6	Limonoid UDP-glucosyltransferase-like protein	Medtr1g107285	3	23.587	**0.627**	1.033	0.0005
***Coenzyme transport and metabolism* (H)**							
A4PU48	*S*-adenosylmethionine synthase-like protein	Medtr7g110310	14	131.47	**0.759**	1.052	0.0009
***Lipid transport and metabolism* (I)**							
A0A072W240	Mevalonate diphosphate decarboxylase	Medtr1g112230	4	42.34	**0.732**	0.984	0.0059

[1] Number of peptides that are unique in the cited protein.[2] Quality of the identification of the preotein represented as the sume of the individual SCORE of each peptide that conform the protein. [3] Difference on the intensity of the protein expresed as the fold change when comparing NH_4^+ *vs.* NO_3^- nutrition. [4] Difference on the intensity of the protein expresed as the fold change when comparing urea *vs.* NO_3^- nutrition. FC were depicted in red color for up-regulated proteins and in green color for down-regulated proteins. [5] p-value of ANOVA test

Table 4.7. *Continuation*

Uniprot ID	Protein Name	Accesion	UP[1]	Score[2]	FC1[3]	FC2[4]	*p*Val[5]
***Translation, ribosomal and biogenesis* (J)**							
I3SPL5	40S ribosomal protein S17	Medtr1g058250	3	25.39	0.821	**0.735**	0.0050
A0A072UAR8	Argonaute protein 1A	Medtr6g477980	2	43.28	**0.602**	**0.592**	0.0005
***Cell wall/membrane/envelope biogenesis* (M)**							
G7K0M1	Fasciclin-like arabinogalactan protein	Medtr5g098420	2	13.56	**0.684**	1.124	0.0003
Q9T0M6	Sucrose synthase	Medtr4g124660	28	323.31	**0.638**	**0.578**	0.0003
***Post-translational modification, protein turnover and chaperones* (O)**							
G7JPE9	Glutathione S-transferase, amine-terminal domain protein	Medtr4g059730	4	41.67	**1.801**	0.954	0.0002
A0A072VLL6	Glutathione S-transferase tau	Medtr1g067180	5	50.89	**1.713**	**1.365**	0.0005
A0A072VNE4	Peptidyl-prolyl cis-trans isomerase	Medtr1g085560	4	33.04	**1.351**	1.114	0.0068
A0A072UYT5	RuBisCO activase	Medtr3g068030	24	323.31	**1.301**	**0.726**	0.0035
G7K4R2	Heat shock protein 81-2 1	Medtr5g096460	45	323.31	1.000	**1.321**	0.0033
***Inorganic ion transport and metabolism* (P)**							
G7JLS7	Ferritin 1	Medtr4g014540	6	50.15	**2.732**	**1.544**	0.0000
G7K283	Ferritin 2	Medtr5g083170	5	29.15	**1.527**	1.092	0.0010
G7JUD2	Plasma membrane H+-ATPase 3	Medtr4g127710	23	293.12	**0.734**	0.931	0.0043
A0A072U5J4	Monodehydroascorbate reductase	Medtr8g098910	8	94.56	**0.560**	**0.580**	0.0000
G7JL79	Ferredoxin-nitrite reductase	Medtr4g086020	5	32.44	**0.312**	**0.326**	0.0000
***Secondary metabolites biosynthesis, transport and catabolism* (Q)**							
A0A072VEZ8	1-aminocyclopropane-1-carboxylate oxidase-like protein	Medtr1g032220	2	11.58	**1.824**	**1.353**	0.0001
Q2MJ09	Cytochrome P450 family cinnamate 4-hydroxylase	Medtr5g075450	3	18.81	**0.765**	0.828	0.0028
G7KEE9	Cytochrome P450 family 71 protein	Medtr5g072980	4	44.29	**0.724**	**0.621**	0.0031
A0A072U4G3	Phenylalanine ammonia-lyase-like protein	Medtr7g101395	2	12.48	**0.690**	0.822	0.0015
G7K511	Caffeic acid O-methyltransferase 4	Medtr5g098170	2	12.94	**0.663**	1.130	0.0033

[1] Number of peptides that are unique in the cited protein.[2] Quality of the identification of the preotein represented as the sume of the individual SCORE of each peptide that conform the protein. [3] Difference on the intensity of the protein expresed as the fold change when comparing NH_4^+ *vs.* NO_3^- nutrition. [4] Difference on the intensity of the protein expresed as the fold change when comparing urea *vs.* NO_3^- nutrition. FC were depicted in red color for up-regulated proteins and in green color for down-regulated proteins. [5] p-value of ANOVA test

Table 4.7. *Continuation*

Uniprot ID	Protein Name	Accesion	UP[1]	Score[2]	FC1[3]	FC2[4]	*p*Val[5]
***Function unknown* (S)**							
G7IMZ3	ABA-responsive protein 1	Medtr2g035190	11	30.55	**1.785**	0.991	0.0007
A0A072V3F7	Auxin-repressed/dormancy-associated protein	Medtr2g014240	4	78.68	**1.566**	1.251	0.0088
I3T9Y8	Polyketide cyclase/dehydrase and lipid transporter	Medtr1g030820	14	206.99	**1.447**	1.243	0.0016
G7LI99	Seed linoleate 9S-lipoxygenase	Medtr8g018420	26	323.31	**1.420**	1.154	0.0072
G7INA7	ABA-responsive protein 3	Medtr2g035220	11	38.92	**1.384**	1.084	0.0021
G7IMY7	Disease-resistance response protein 2	Medtr2g035120	9	103.35	**0.664**	0.892	0.0009
A0A072U6C1	Pathogen-inducible alpha-dioxygenase	Medtr6g007763	5	7.18	**0.648**	**0.714**	0.0013
A0A072V335	MFP1 attachment factor-like protein	Medtr3g102500	2	28.59	**0.625**	**0.692**	0.0043
***Signal transduction mechanisms* (T)**							
A0A072U5A4	Chitinase / Hevein / PR-4 / Wheatwin2	Medtr7g115220	2	40.86	1.436	1.353	0.0064

[1] Number of peptides that are unique in the cited protein.[2] Quality of the identification of the preotein represented as the sume of the individual SCORE of each peptide that conform the protein. [3] Difference on the intensity of the protein expresed as the fold change when comparing NH_4^+ *vs.* NO_3^- nutrition. [4] Difference on the intensity of the protein expresed as the fold change when comparing urea *vs.* NO_3^- nutrition. FC were depicted in red color for up-regulated proteins and in green color for down-regulated proteins. [5] p-value of ANOVA test

4.3.4. Enrichment pathways

Furthermore, we determined the role of the 61 proteins in the Kyoto Encyclopedia of Genes and Genomes (KEGG) database to identify pathways enriched in our set of differentially accumulated proteins. As shown in Table 4.8, using a *p*-value threshold of $\leq$ 0.01, proteins from NH_4^+ treatment were mainly implicated in metabolic processes, such as the biosynthesis of secondary metabolites and the carbon metabolism, as well as, the metabolism of some amino acids. Proteins from urea grown roots were enriched in just 4 pathways that were specially related to carbon metabolism.

Table 4.8. ***Pathway enrichment analysis of differentially accumulated proteins in ammonium and urea nutrition compared with nitrate with a p-value ≤ 0.01 identified using the KOBAS 3.0 database .*** Enriched pathways were ordered in descending order of significance.

Path ID	Pathway Name	Proteins[1]	*p*-value[2]
Ammonium vs. Nitrate nutrition			
mtr01100	Metabolic pathways	26	$7.39e^{-18}$
mtr01110	Biosynthesis of secondary metabolites	15	$7.07e_{-10}$
mtr00940	Phenylpropanoid biosynthesis	8	$4.66e^{-08}$
mtr01200	Carbon metabolism	7	$8.62e^{-07}$
mtr00360	Phenylalanine metabolism	3	$1.02e^{-03}$
mtr00630	Glyoxylate and dicarboxylate metabolism	3	$2.35e^{-03}$
mtr00710	Carbon fixation in photosynthetic organisms	3	$2.35e^{-03}$
mtr01230	Biosynthesis of amino acids	4	$2.35e^{-03}$
mtr00270	Cysteine and methionine metabolism	3	$3.73e^{-03}$
mtr00480	Glutathione metabolism	3	$4.37e^{-03}$
mtr00945	Stilbenoid, diarylheptanoid and gingerol biosynthesis	2	$6.02e^{-03}$
mtr00195	Photosynthesis	3	$6.02e^{-03}$
Urea vs. Nitrate nutrition			
mtr01200	Carbon metabolism	7	$1.97e^{-08}$
mtr01100	Metabolic pathways	13	$1.97e^{-08}$
mtr00710	Carbon fixation in photosynthetic organisms	4	$7.96e^{-06}$
mtr00630	Glyoxylate and dicarboxylate metabolism	3	$4.40e^{-04}$

[1] Number of proteins identified that take part in that pathway
[2] *p*-value after the Fisher's exact test corrected by FDR as described in Benjamini and Yekutieli (2001)

Since NH_4^+ nutrition involved mainly shifting of the production of estructural metabolites, as phenylpropanoids, including the stilbenoids and gingerol, the study of the implicated proteins is described hereunder.

As showed in Table 4.9, a batch of 8 proteins were differently regulated into the phenylpropanoids pathway. If we look at it in detail, we found that peroxidase (POD) and caffeic acid O-methyltransferase (COMT) activities were up-accumulated, whereas, caffeoyl-CoA 3-O-methyltransferase (CCOMT), Cytochrome P450 family cinnamate 4-hydroxylase (CyP450 C4H), and phenylalanine ammonia-lyase-like protein (PAL) were down-accumulated in NH_4^+ roots. The CCOMT and CyP450 C4H activities also belong to the stilbenoid, diarylheptanoid and gingerol biosynthesis pathway, which end products include phenolic compounds, glycosides, and curcumins from the ginger family too. The involvement of these 8 differentially identified proteins in phephylpropanoid biosynthesys is shown in Figure 4.37.

On the other hand, amino acids biosynthesis was another remarkable enriched pathway that included 4 proteins from the 53 differentially identified proteins when growing plants under NH_4^+ nutrition (Table 4.8). All of them were down-regulated (Table 4.9), and three of those proteins found, cobalamin-independent methionine synthase, O-acetylserine (thiol) lyase and S-adenosylmethionine synthase-like protein, also belong to the cysteine and methionine metabolism (mtr00270).

Table 4.9. Differentially identified proteins implied in the phenylpropanoids and amino acids biosynthesis pathway. The protein name, the accession and the identification from UniProt is provided. UniProt ID was depicted in red color for up-regulated proteins and in green color for down-regulated proteins.

Protein Name	Accesion	UniProt ID
Phenylpropanoids biosinthesys		
Caffeic acid O-methyltransferase	gi|657386071|	G7K511
Caffeoyl-CoA 3-O-methyltransferase (CCOMT)	gi|355508982|	G7JK14
Cytochrome P450 family cinnamate 4-hydroxylase (CyP450 C4H)	gi|355517372|	Q2MJ09
Peroxidase family protein 11	gi|657382113|	A0A072UAE2
Peroxidase family protein 2	gi|355483535|	A4UN77
Peroxidase family protein 6	gi|355483545|	G7IJU5
Peroxidase family protein 7	gi|355483550|	G7IJV0
Phenylalanine ammonia-lyase-like protein (PAL)	gi|657379705|	A0A072U4G3
Amino acids biosynthesis		
Cobalamin-independent methionine synthase	gi|355499692|	G7L0I7
O-acetylserine (thiol) lyase	gi|657389197|	G7JNN9
S-adenosylmethionine synthase-like protein	gi|355501050|	A4PU48
Serine transhydroxymethyltransferase	gi|355523623|	G7LH57

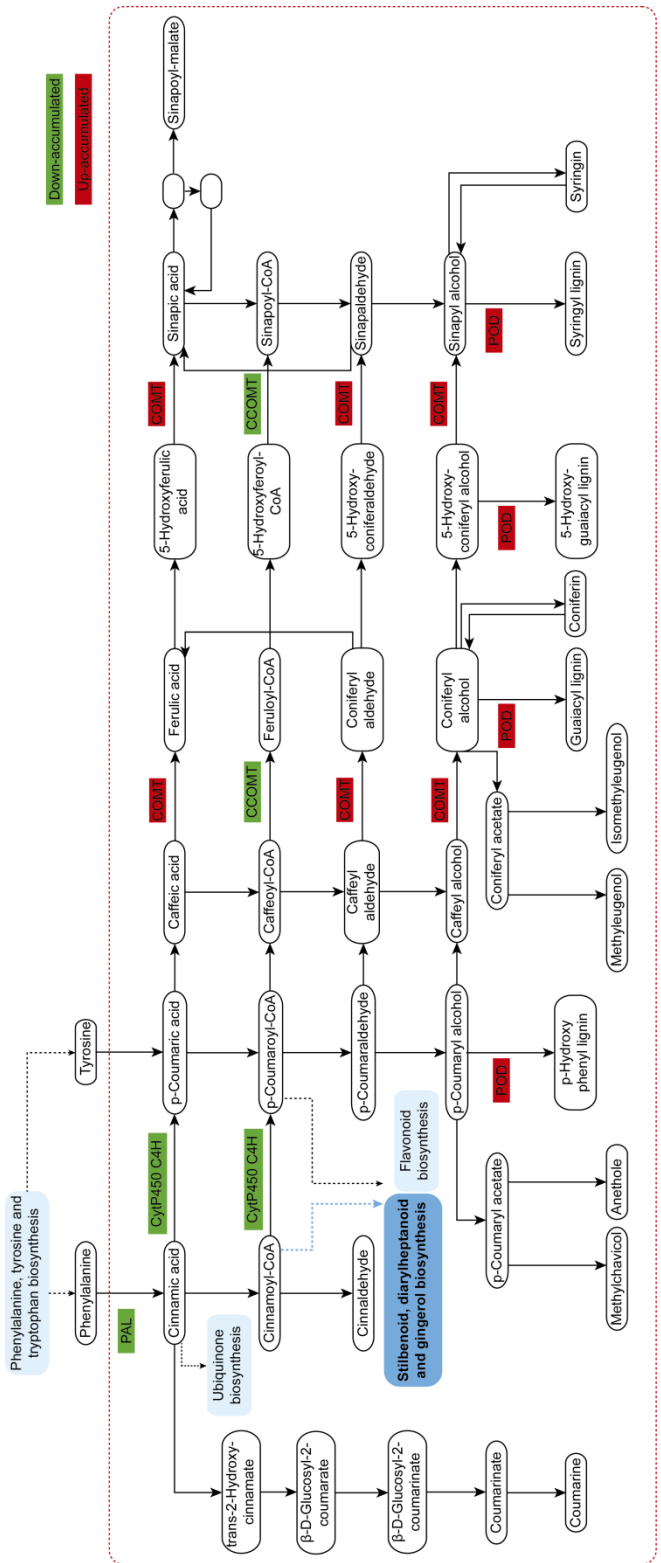

Figure 4.37. ***Effects of NH_4^+ nutrition on phenylpropanoid biosynthesis pathway.*** The biosinthesys of phenylpropanoids pathway was significantly enriched on NH_4^+-fed *M. truncatula* roots relative to nitric roots, and the expression of the 8 affected proteins is ilustrated. The proteins name backgroun is red or green for up-and down-regulation, respectively.

4.4.5. Peroxidase activity in roots of *Medicago truncatula*

Our data indicate that peroxidase activity (POD) was up-regulated, and taking into account that this activity might play an important role for cell wall formation, their implication on the tolerance to NH_4^+ nutrition in *M. truncatula* plants was hypothesized. Hence, in order to confirm the data obtained by iTRAQ analysis, the guaiacol peroxidase (GPX), and ferulic acid dependent peroxidase (FPX) activities were determined in root tissues (Fig. 4.38).

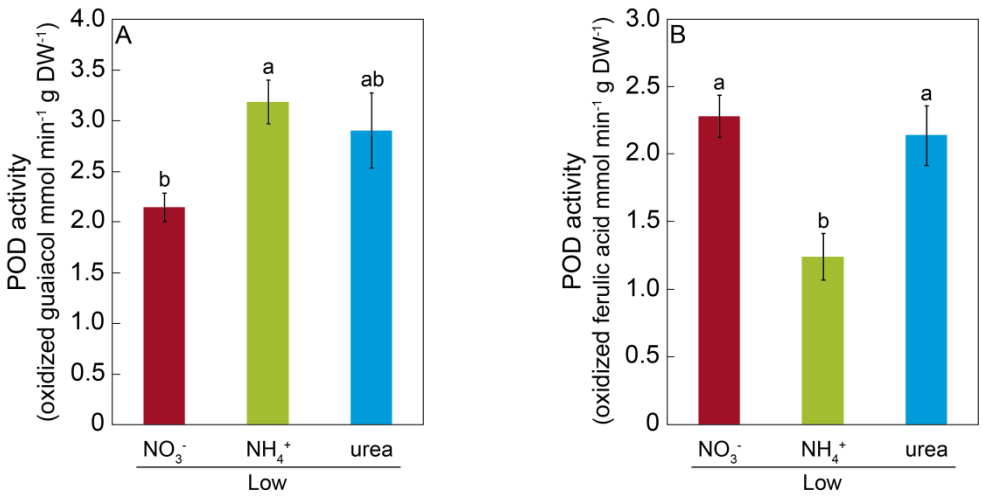

Figure 4.38. ***Peroxidase activity of*** **M. truncatula** ***roots.*** The differential effect of low doses of NO_3^-, NH_4^+, and urea as the sole N source on 15-days old *M. truncatula* roots grown under axenic conditions on GPX (**A**) and FPX (**B**) activities was assayed by measuring the oxidation of guaiacol and ferulic acid. The values are the mean ± S.E. (n = 3). Different letters denote statistically significant differences at α = 0.05 using the Student-Newman-Keuls test.

GPX activity, an approach to determine the total peroxidase activity, is frequently used. The data we obtained (Fig. 3.8A) matched with the proteomics results displayed previously (Tables 4.7 and 4.9). In particular, GPX was significantly higher in ammonium-fed roots, whereas not significant differences were found between nitrate and urea-–grown roots. Moreover, FPX activity was also lower in ammonium roots (Fig. 4.38B), which correlates with the highest accumulation of COMT protein when comparing this treatment respect to the others.

Chapter 5:

DISCUSSION

5.1. Effect of inorganic phosphate deprivation in *Arabidopsis thaliana* seedlings

Understanding the mechanisms that allow plants to acclimate to Pi deprivation is a prerequisite for optimising Pi use efficiency in crop plants (Wu *et al.*, 2013). This task is important because current agronomic practice relies heavily on the use of the finite and dwindling reserves of rock phosphate to compensate for low Pi availability in the soil (Cordell *et al.*, 2011). Induction of AOX, which is commonly observed in response to Pi starvation, provides additional flexibility in the coordination of the TCA cycle and respiration under Pi-limiting conditions, and the experiments reported here show that this acclimatory response is mediated by NO. The same molecule has been observed to act upstream of AOX induction during the response of tomato leaves to tobacco mosaic virus (Fu *et al.*, 2010), and it is likely, although yet to be established, that the increase in NO triggers a signal transduction pathway that culminates in increased AOX gene expression. In principle, NO can be synthesised by several oxidative and reductive pathways in plants (Gupta *et al.*, 2011; Yu *et al.*, 2014), but the lower NO levels in the *nia* mutants, and the failure to increase the level in a growth medium lacking Pi, demonstrate the importance of the NR pathway for NO production under these conditions. Given that the formation of cluster roots by white lupin during Pi deficiency is also regulated by NO (Wang *et al.*, 2010), it may be concluded that Pi deficiency is another example of an abiotic stress that elicits responses that depend on NO.

The nitrite produced by NR can either be further metabolised by NR to NO (Rockel *et al.*, 2002), or it can be reduced to NO by the mitochondrial electron transport chain (Gupta *et al.*, 2005). NO production can be limited by the availability of nitrite (Planchet *et al.*, 2005) and interestingly it has been found that Pi starvation caused a four-fold down regulation of nitrite reductase (NiR) gene expression in roots of Arabidopsis (Wu *et al.*, 2003). This is likely to result in reduced NiR activity, elevated nitrite levels and hence increased NO production in WT plants during Pi starvation. In agreement with this prediction, nitrite levels were found to increase in WT roots, but not the *nia* mutants, when seedlings were grown in a medium lacking Pi (Fig. 4.5).

AOX reduces the production of ROS in plant mitochondria, including superoxide (Cvetkovska and Vanlerberghe, 2012), and under stress conditions the induction of the alternative pathway leads to reduced ROS levels (Van Aken *et al.*, 2009). In keeping with this, the failure to elevate NO in the *nia* mutant grown on the Pi-free medium resulted in higher levels of superoxide than the WT, reflecting both the very low respiratory capacity of the AOX pathway in the *nia* seedlings under these

conditions (Fig. 4.6D) and the inability of the mutant to increase the AOX level in response to the stress. The increased capacity of the alternative pathway in the *nia* mutant grown with the NO donor (Fig. 4.6E) emphasises the pivotal role for NO in the recruitment of the alternative pathway under Pi deficiency.

Observations on barley seedlings overexpressing a non-symbiotic haemoglobin-1 to scavenge NO led to the conclusion that the NO level regulates respiration, internal oxygen, carbohydrate consumption and ROS levels in aerobic barley roots (Gupta *et al.*, 2014). COX is inhibited by competitive binding of NO to the Fe^{2+}-heme group at the O_2-binding site (Cleeter et al., 1994) and the inverse correlation between NO and oxygen consumption in barley roots was attributed to decreased inhibition of COX by NO (Gupta *et al.*, 2014). The interpretation of the changes in oxygen consumption observed during P-deficiency is less straightforward because of the induction of the AOX pathway (Rychter and Mikulska, 1990; Wanke *et al.*, 1998). Thus the increased NO levels observed in WT grown in a Pi-free medium did not cause the expected inhibition of respiration (Fig. 4.6A), presumably reflecting the NO-induced expression of AOX and an increased contribution of the alternative pathway to respiration. Moreover total respiration in the *nia* mutant was indistinguishable from the WT when the plants were grown on 1 mM Pi, despite the lower NO level, and the rate decreased when the plants were grown on 0 mM Pi even though the NO level remained low. Thus while the *nia* mutant data provide evidence that NO is required for the increase in the AOX level when seedlings are grown under Pi-limiting conditions, it seems that the NO level is not a major factor in determining the respiratory behavior of the mutant. The increase in superoxide level observed in the *nia* mutant roots under Pi deficiency (Fig. 4.9A), with the potential for oxidative damage and lipid peroxidation to the mitochondria (Taylor et al., 2002), might also be relevant, and the decrease in superoxide in response to incubation with the NO donor strengthens the conclusion that NO stimulates the AOX pathway when Pi availability is reduced.

It has been shown previously that AOX plays an important role in the response of plants to cold, drought stress, hypoxia, ozone injury and Pi deficiency (Van Aken *et al.*, 2009; Plaxton and Tran, 2011; Gupta *et al.*, 2012). The pathway that leads to increased AOX activity under Pi deficiency has yet to be fully elucidated, but it is now clear that NO provides the signal that triggers the process.

5.2. Response of *Medicago truncatula* to ammonium and urea nutrition under axenic conditions

5.2.1. The Importance of pH Control

Growing crop plants using NH_4^+ or urea as the only N source under axenic conditions is a poorly examined method. Few studies are performed under these conditions, especially in plants grown with urea (Gerendás *et al.*, 1998; Wang *et al.*, 2013; Yang *et al.*, 2015), and it is therefore a challenging task. Appropriate control of the pH in the medium after the sterilization process is important to achieve the correct growth of plants and appropriate evaluation of urea or NH_4^+ nutrition treatments because the autoclaving process may change the pH of the solution when certain nutrients are autoclaved together (Chapter 3). Moreover, it is widely known that the pH of the medium may have an effect on nutrient assimilation during the development of seedlings. Our system standardized the control of pH during the preparation of the media and the development of the seedlings using the routine color indicator methyl red (Fig. 4.10). Our results showed that the pH did not decrease greatly under all tested conditions, except at a very high dose of NH_4^+, where the pH could drop to 4.5. Under this condition, the plants showed a maximum quantum yield of primary photochemistry similar to the rest of the treatments (φ_{Po}; Table 4.2). In contrast, in non-buffered full-strength solutions containing NH_4^+, pH values lower than 4.0 can occur, which renders the solution unsuitable for healthy growth (Zaccheo *et al.*, 2006).

5.2.2. How are the shoots and roots affected by NH_4^+ and urea nutrition?

One of the most dramatic plant adaptations for ensuring adequate N acquisition is the modulation of the RSA (Forde and Lorenzo, 2001; Hodge, 2004; Smith and De Smet, 2012; Forde, 2014). A detailed description of root development under NH_4^+ nutrition has not yet been provided, and only a few studies have described the changes in the RSA under urea nutrition (Yang *et al.*, 2015; Zanin *et al.*, 2015). Our results obtained in both NH_4^+- and urea-fed plants at both tested doses (Fig. 4.12A-C; Fig. 4.13A-C) agree with the phenotype described under NH_4^+ stress in the majority of plants (Britto and Kronzucker, 2002). These changes imply the existence of shortened roots, with a significant reduction of the primary root, which is explained by the inhibition of cell elongation (Li *et al.*, 2010) and the suppression of lateral root elongation (Li *et al.*, 2010, 2011; Rogato *et al.*, 2010). Inhibition of lateral root length was also observed under a high NO_3^- supply (Fig. 4.13C; Walch-Liu *et al.*, 2006). Interestingly, we found a negative correlation for NO_3^--grown roots (Fig. 4.14A) and a

positive relationship for NH_4^+-grown roots (Fig. 4.14B) when relating the position of insertion from the base of the lateral roots to their lengths. The absence of a relationship in urea-fed plants was probably due to the small number of lateral roots in these plants (Fig. 4.13D), as reported for urea-grown Arabidopsis plants (Yang *et al.*, 2015). Conversely, Zanin *et al.* (2015) described a significant increase in the total density and area of urea-fed maize roots. Our results did not show a decrease in dry weight in any of the treatments, probably due to the low biomass originating from axenic cultures. Other species described as tolerant to NH_4^+ nutrition, such as *M. truncatula,* have not been found to show any decrease in dry matter contents when grown with NH_4^+ as the only N source (Domínguez-Valdivia *et al.*, 2008; Cruz *et al.*, 2011). Although there were no significant changes in biomass, the root/shoot ratio was significantly altered under different N sources, as previously demonstrated for high and low N doses (Ariz *et al.*, 2011a). The urea-treated plants showed significant growth reduction on a fresh weight basis, compared with the plants grown under NO_3^- nutrition, but to a lesser extent than the NH_4^+-grown seedlings, as described for a number of plant species (Houdusse *et al.*, 2005; Mérigout *et al.*, 2008; Garnica *et al.*, 2010; Yang *et al.*, 2015). Indeed, various authors have reported that plants fed with urea suffer from N deficiency due to an extremely low urea uptake rate (Arkoun *et al.*, 2012; Wang *et al.*, 2013). However, the recent description of efficient urea transporters (Kojima *et al.*, 2007; Wang *et al.*, 2008; Zanin *et al.*, 2014; Liu *et al.*, 2015) confirms the possibility that plants may use urea the sole nitrogen source, with the compound being assimilated and translocated by plants (Mérigout *et al.*, 2008). The unchanged total biomass of urea- and NO_3^--fed plants (Fig. 4.12C) showed that urea is taken up by the roots without hydrolysis in our experimental system, as the axenic conditions prevented any microbial-based conversion of the supplied N forms during the course of the experiments. Furthermore, no urea degradation was found to occur in the nutrient media, as no NH_4^+ was detected through ion chromatography in samples of the agar media collected randomly at the end of plant growth (data not shown). Finally, the similar protein contents of the root tissues after exposure to the different N sources indicated efficient assimilation of urea and NH_4^+ in our plants (Table 4.3). Accordingly, Cao *et al.* (2010) reported that urea-grown plants were subject to a more inefficient N distribution than to inefficient urea uptake, and it was subsequently reported that plants are able to use urea (Zanin *et al.*, 2015).

5.2.3. How is the IAA pool affected by NH_4^+ and urea nutrition?

Phenotypic changes, beyond simple morphological transformation, may imply more profound regulation regarding hormone-related signals (Guo *et al.*, 2009; Bartoli *et al.*, 2013). Accordingly, auxin levels have been reported to regulate the elongation of the main and lateral roots during development (Péret *et al.*, 2009; Li *et al.*, 2011). In the present study, we did not observe inhibition of IAA levels in the roots under a high NO_3^- supply (Fig. 4.15B), as has been described in other studies (Tian *et al.*, 2008; Tamura *et al.*, 2010), which may likely explain why the primary length was not inhibited under a high NO_3^- supply in our experiments (Fig. 4.13A). Conversely, in NH_4^+-fed-plants, a suppression of root IAA contents has been described (Kudoyarova *et al.*, 1997; Li *et al.*, 2011), as observed in the present work (Fig. 4.15B). In urea-supplied plants, transcriptomic data have also shown a marked phytohormonal imbalance, although auxin-regulated gene categories were not affected (Yang *et al.*, 2015). This may be explained by the absence of NO_3^-, in urea- and NH_4^+-grown seedlings. Nitrate is essential for the uptake of IAA into root cells and therefore for auxin signaling (Krouk *et al.*, 2010). Thus, in treatments with a complete absence of NO_3^-, the length of lateral roots may be altered due to the absence of signaling related to the NO_3^--auxin interplay in the roots (Krouk *et al.*, 2010). On the other hand, the correlation found between total length and the shoot IAA pool in *M. truncatula* (Fig. 4.18A) suggests that exogenous IAA could complement the NH_4^+ and urea phenotype. Accordingly, IAA was added to the growth medium at 20 μM. However, it did not promote root development (data not shown). Barth *et al.* (2010) and Yang *et al.* (2015) also concluded that plants grown with exogenous IAA did not show any symptoms of growth recovery from NH_4^+ toxicity or urea nutrition, respectively. The shoots of NO_3^--fed plants presented higher IAA levels than those of urea-fed plants (at high doses), in contrast to what was observed by Mercier *et al.* (1997), who reported that urea-treated plants presented higher IAA levels than those grown with NO_3^-. Nitrate may be not as important in the shoots as in the roots, as we observed that the IAA contents were positively correlated withplant length and the performance index, indicating differences in regulation and effects for both the roots and shoots. Taking into account that the suppression of auxin signaling is considered to enhance stress tolerance (biotic and abiotic) (Park *et al.*, 2007), the decline of IAA contents observed under urea and NH_4^+ nutrition (more pronounced) suggests that both treatments may modify auxin contents, suggesting a trade-off mechanism for enhancing tolerance toward these conditions.

5.2.4. Do urea and NH_4^+ nutrition induce s tress in *M. truncatula*?

Although the toxic effect of NH_4^+ at the whole-plant level is widely known (Britto and Kronzucker, 2002; Bittsánszky *et al.*, 2015), the toxic effect of urea is still a matter of debate. The effects of NH_4^+ on the photosynthetic machinery have been described in several species, such as spinach (Lasa *et al.*, 2002), maize (Foyer *et al.*, 1994), and *Synechocystis* (Drath *et al.*, 2008). The similar maximum quantum yield of the primary photochemistry observed in all of the treatments (φ_{P_o}) revealed that the photosynthetic apparatus of *M. truncatula* was not photoinhibited under different types of nutrition, as shown in other studies (Podgórska *et al.*, 2013; Bittsánszky *et al.*, 2015). However, a detailed analysis of the kinetic transients of chlorophyll *a* fluorescence indicated that NH_4^+ at a high dose was associated as the most sensitive phenotype, due to the lower value of Pi_{Abs} (Fig. 4.16; Table 4.2). Paradoxically, urea, which has been reported to share similar assimilation pathways in *Arabidopsis* (Mérigout *et al.*, 2008), had the opposite effect. Not only did urea-treated *M. truncatula* plants maintain their photosynthetic capacity, but the biophysical parameters of the photosynthetic apparatus also indicated that urea-grown plants displayed a dose-dependent improvement in energy conservation from absorbed photons to reduction, which was even better than that observed in NO_3^--grown plants. Urea applied at the leaf level has been reported to increase leaf CO_2 assimilation in N-deficient plants (Del Amor and Cuadra-Crespo, 2011). However, transcriptomic data indicated down-regulation of genes involved in photosynthesis (Yang *et al.*, 2015). The investigation of whether oxidative stress is involved in NH_4^+ tolerance/toxicity has led to contradictory conclusions. Ammonium does not give rise to oxidative stress in pea and spinach plants (Domínguez-Valdivia *et al.*, 2008). However, it does generate stress in aquatic plants (Nimptsch and Pflugmacher, 2007), tobacco (Skopelitis *et al.*, 2006), and *Arabidopsis* (Patterson *et al.*, 2010). Most plants exhibit more oxidized states for both antioxidants when NH_4^+ is supplied (Podgórska and Szal, 2015). However, we did not find clear differences in the redox status of ASC and GSH+hGSG (Table 4.3), and mitochondria-associated superoxide production was not specifically increased under any of the conditions, in contrast to the findings of other studies conducted in *A. thaliana,* in which mitochondrial Mn-dependent SOD has been shown to be particularly upregulated when NH_4^+ is supplied (Podgórska *et al.*, 2013; Podgórska and Szal, 2015). Our results suggested that plastidial enzymes were more affected by both NH_4^+ and urea, while urea nutrition impacted the greatest number of SOD isoenzymes, which suggests that production of ROS occurs in this situation. This observation is consistent with a transcriptomic analysis performed in urea-fed *Arabidopsis* plants, in which FeSOD genes were found to be overexpressed (Mérigout *et*

al., 2008). In our model, the legume *M.truncatula* did not appear to suffer from NH_4^+ toxicity, as the leaves did not show any chlorotic symptoms, which are the main markers of NH_4^+ toxicity (Britto and Kronzucker, 2002). This finding agrees with the fact that legume plants are relatively tolerant to NH_4^+, as demonstrated by the growth ratio between NO_3^- and NH_4^+ conditions (Ariz *et al.*, 2011a).Overall, NH_4^+ treatment leads to "mild" perturbation under this system, with differential effects on the photosynthetic machinery.

5.3. Nitrogen metabolism and signaling in *Medicago truncatula* seedlings grown under ammonium and urea nutrition

5.3.1. Low doses of ammonium and urea did not affect plant metabolism and signaling

Ammonium sensitivity of plants is a worldwide problem, constraining crop production. Prolonged application of ammonium as the sole nitrogen source may result in physiological and morphological disorders that lead to toxicity and decreased plant growth (Esteban *et al.*, 2016b). However, the threshold in which ammonium (or urea) is toxic or not depends on various factors as plant species, variety (in crops) (as examples, see Dominguez-Valdivia *et al.*, 2008; Cruz *et al.*, 2011; Li *et al.*, 2011; Sarasketa *et al.*, 2014), and environmental factors (such as temperature, soil pH, CO_2 concentration or light intensity) (Setién *et al.*, 2013; Vega-Mas *et al.*, 2015). In the bibliography, the other model species, *Arabidopsis thaliana*, is described as the most sensitive to ammonium nutrition, even at low dose (Li *et al.*; 2014; Esteban *et al.*, 2016). However, our species, *M. truncatula* seems to be more tolerant because the concentration of N referred in this work as low dose (1 mM) do not produce toxic effects in seedlings of *M. truncatula* (Chapter 4.2), as other species as pea or clover. We have measured several metabolites related with the N metabolism, and others molecules that act as signals to maintain the plant performance, including internal anions content or reactive species (ROS, RNS). No remarkable differences were found among treatments of low dose and tissues, indicating that plants are able to modulate their metabolism and show a broad tolerance in relation to the N source present in the medium. Overall, it might be indicating that plant roots exhibit high specialized mechanisms to sense and respond with an integrated signaling system when different N sources are detected.

5.3.2. *Medicago truncatula* seedlings differentially store and transport N depending on the N source in the growth medium.

Although some differences exist between species, the N compounds synthesized in the roots (after N assimilation) are transported along the plant, mainly in the form of amides and ureides (Marschner, 2012). In general terms, these organic N-compounds transfer the N from source organs to sink tissues, and also acts as transient storage during periods of high N availability. The compounds used for long-distance transports or storage differ among plant families; even between species within a family such as legumes (Hawkesford *et al.*, 2012). Thus, the difference between the transport of amides or ureides lies on the nodule structure that each legume forms in symbiosis.

For instance, legumes with indeterminate nodules such as species of the genus *Pissum*, *Trifolium* or *Medicago* (temperate legumes), are known as amide-exporters, since they principally transport the organic N as the amino acids asparagine and glutamine (Lea *et al.*, 2007). However, tropical legumes, characterized by determined nodules, such as soybean, cowpea and common bean, transport primarily the N, as the ureides allantoin and allantoate (Smith and Atkins 2002; Pélissier *et al.*, 2004). Ureides synthesis mainly occurs in the root nodules, but the use of axenic conditions, as our experimental design, impeded the formation of them; nevertheless non-nodulated plants are still able to produce ureides but in a lower proportion (McClure and Israel, 1979; Pélissier and Tegeder, 2007). Furthermore, the N compounds preferably transported can differ within the same specie depending on whether the plant has been nodulated or not (do Amarante *et al.*, 2006). In our work, the content of amino acids (including Asn and Gln) and ureides were measured and differences in the way that the seedlings store and transport N were detected among treatments. Based on the Asn accumulation (Fig. 4.24 and 4.25) and the total ureides content (Fig. 4.27), our results indicate that high NO_3^--based nutrition in *Medicago truncatula* preferably transported ureides, whereas NH_4^+-grown plants might be using the amides as long-distance transport of N. An increase of total ureides content in both roots and shoots of non-nodulated common bean was observed in 10mM NO_3^--fed plants under drought conditions (Alamillo *et al.*, 2010). These results reinforce the hypothesis that increasing the NO_3^- concentration triggers a redistribution of N from amides (Fig. 4.24 and 4.25), the usual *Medicago* preference, to ureides (Fig. 4.27); and as ureides present lower C/N ratio, this fact might be indicating that those nitric plans effectively regulates the C/N balance. Accordingly, studies with non-nodulated soybean and pea plants showed that a typical characteristic of high NH_4^+ concentrations is the higher accumulation of lower C/N ratio amino acids such as Asn or Arg (Ueda *et al.*, 2008; Ariz *et al.*, 2013). This finding agrees with the high content of Asn and Gln found under high NH_4^+ nutrition in *M. truncatula* in our experiments, which could be indicating a higher C requirement of those plants due to a lower photosynthetic efficiency (Chapter 4.2, Fig. 4.16; Table 4.2). Such increase from the C/N ratio of ureides (1) to a higher ratio of Asn (2) and Gln (2.5) provide an extra C to plants, improving the C/N balance of the plant. Accordingly, the exposure to high-light irradiance also provide an extra C to pea plants grown under 10 mM NH_4^+ increasing the ratio of C5 (Glu+Gln) to C4 (Asp+Asn) amino acids, which reverted the C-starvation symptoms observed under such NH_4^+ nutrition (Ariz *et al.*, 2013).

Furthermore, studies on alfalfa showed that the application of either 20 or 100mM NH_4^+ increased the accumulation of allantoin in shoots and roots (Wang *et al.*, 2015). Interestingly, we also detected a remarkable increase of allantoin in *M. truncatula*

roots at low doses of NH_4^+ and even in urea-grown seedlings, but not at high doses (Fig. 4.28A and B). As a significant increase of Asn and Gln was detected in high NH_4^+-fed roots (Fig. 4.25); taking together, these findings suggest that *M. truncatula* subjected to NH_4^+ or urea transports organic N as both amides and ureides at low doses, while an excess of N leads to a higher amides content as transient storage.

Altogether, it reinforces our previous hypothesis that *M. truncatula* grown under NH_4^+ and urea preferably transport/store the organic N as amides, whereas nitrate seedlings use ureides.

On the other hand, the GABA shunt allows a direct link between the N and the C metabolism (Fait *et al.*, 2008). Moreover, under certain stress situations, as a response plants accumulates GABA that it is related to plant growth regulation (Kinnersley and Turano, 2000), but how GABA exerts this function is unknown. An increase in total Aa (Fig. 4.23) and the Arg relative content was accompanied by a decrease of the relative contents of GABA shunt amino acids, mainly Glu, Ala and GABA, (Table 4.6) in *M. truncatula* roots grown at high doses of NH_4^+. The same results were found in pea roots, where the supply of 10mM NH_4^+ also produces the same change in the participation of each Aa (Ariz *et al.*, 2013). Recently, a study with wheat roots subjected to pH and aluminum stress demonstrated that an accumulation of GABA down-regulated the aluminum transporters, and consequently the role of GABA as a signaling molecule was proposed (Ramesh *et al.*, 2015). Hence, we propose that the activation of the GABA shunt pathway under high NH_4^+ nutrition should be related to the re-establishment of the C/N balance and the control of NH_4^+ uptake by direct regulation of NH_4^+ transporters.

5.3.3. Urea fed plants effectively uptake and metabolize urea

In natural soil, urea is hydrolyzed by soil microorganisms, and then enters into the plant as NH_4^+, or NO_3^- after nitrification. Since the experimental design present in this thesis avoids the hydrolysis of urea, it might enter into the plant through transporters. In the past, the toxicity due to urea fertilization was related to high internal accumulation of NH_4^+ (Court *et al.*, 1962), but this theory was questioned in several reports, where no symptoms related to ammonium toxicity were observed in *A. thaliana*, wheat, maize and rice when supplying urea as the sole source of N (Krogmeier *et al.*, 1989; Merigout *et al.*, 2008a and 2008b; Cao *et al.*, 2010; Yang *et al.*, 2015). Furthermore, the accumulation of urea has been proposed to produce a shift in the "urea cycle" that might lead to toxicity (Gérendas *et al.*, 1998). The low internal content of NH_4^+ found under urea nutrition was similar to the content exhibited by NO_3^--fed

seedlings at both doses of N (Fig.4.21A and B), suggesting that plants effectively metabolize all the absorbed urea without an over-accumulation of NH_4^+.

Total amino acids content was also not affected by urea treatment compared to NO_3^- nutrition (Fig. 4.23), contrary with the lower accumulation observed in rice (Gérendas *et al.*, 1998). The imbalance of amino acids profiles with a higher accumulation of Asn and Gln was pointed out as the cause of the reduced plant performance in rice (Cao *et al.*, 2010). Contradictory, urea nutrition did not affect the amino acids relative content on *M. truncatula* grown at both doses of N (Table 4.5 and 4.6). Although ureic plants exhibited a reduced biomass (Fig. 4.12), they were indeed photosynthetically more efficient (Fig. 4.16; Table 4.2); then we are able to suggest that *M. truncatula* effectively metabolize and transport urea along the plant even when supplied as high doses.

This hypothesis may be supported by the fact that *M. truncatula* roots only uptake the urea they need. It has been described that the presence of urea up-regulates the expression of the high-affinity urea transporter gene AtDUR3 (Kojima *et al.* 2007), but not the genes involved in urea metabolism (Witte CP, 2011). In fact, the expression of these transporters in *A. thaliana* showed that the urea uptake increased with increasing urea concentrations (Wang *et al.*, 2015). Likewise, urea can enters in the plant through aquaporins, also known as major intrinsic proteins (MIPs), but Yang and colleagues (2015) proved that urea nutrition did not regulate its expression. However, the proteomic study developed in this thesis (Chapter 4.4 and Chapter 5.4) showed an up-regulation of one MIP (Table 4.7). In *A. thaliana* plants exposed to urea, the symptoms of toxicity observed were more related with N deficiencies than N toxicity. Indeed, repression of those aquaporins expression was detected (Yang *et al.*, 2015). Then, we suggest that the role of MIPs in the transport across roots might play an essential role in the sensing and optimal uptake of urea in *M. truncatula* even at high doses of urea (without any symptom of toxicity).

5.3.4. Are ureides and allantoin implicated in the stress response in *Medicago truncatula* seedlings?

The accumulation of ureids in roots under NH_4^+, darkness, drought or salinity has been reported in *Arabidopsis*, *Phaseolus vulgaris* and *Salicornia europea* among other species (Brychkova *et al.*, 2008; Alamillo *et al.*, 2010; Wu *et al.*, 2012). Moreover, it has also been proposed that the increase of allantoin contents might play protective roles under some abiotic stress (Sagi *et al.*, 1998; Watanabe *et al.*, 2014; Lescano *et al.*, 2016). In *Arabidopsis*, an induction of the expression of genes involved in allantoin synthesis together with a strongly repression of the unique gene encoding allantoinase (AtALN)

was observed under salt stress. As a consequence, salt treated seedlings showed higher allantoin and lower allantoic acid contents; while the use of knockout, knockdown and salt-inducible mutants for AtALN showed that under salt stress conditions the accumulation of allantoin is essential for salt stress tolerance (Lescano *et al.*, 2016). Watanabe *et al.* (2014), using also the knockout AtALN mutant, demonstrated that the accumulation of allantoin increased the tolerance to water stress by regulating the production of ABA. On the contrary, in the present work, increasing the dose of N provoked the opposite effect under both NH_4^+ and urea nutrition. Hence, in roots, while the amount of allantoate increased with the dose, allantoin accumulation was lower (Fig. 4.28D and E). This is in agreement with a study with soybean, in which the inhibitory effect of Asn on the allantoate amidohydrolase was demonstrated, and the increase of allantoate after the supply of ammonium was related to this fact since no XDH activity was detected (Lukaszewski *et al.*, 1992). Thus, the higher allantoate content found under high NH_4^+ in our experiments (Fig. 4.28E) might be due to the elevated content of Asn found in those NH_4^+-fed roots (Fig. 4.25). A study in ryegrass compared the effect of NO_3^- and NH_4^+ nutrition on ureides metabolism, and also analyzed the effect of salinity under nitric nutrition (Sagi *et al.*, 1998). They observed that an increase on the level of salinity produced a simultaneous increase of allantoin and allantoate in nitric roots. This observation agrees with our nitrate fed plants, where both ureides increased in a dependent manner with the dose of N (Fig. 4.28D and E). Moreover, Sagi *et al.* also detected that the supply of 4.5 mM NH_4^+ decreased the content of allantoin and increased the allantoate accumulation comparing with 4.5 mM NO_3^--fed roots. Interestingly, in our experiments, the supply of NH_4^+ leads to the opposite effect at low N dose. Thus, Sagi *et al.* conclude that the increase of purines metabolism may constitute part of the mechanisms of plant adaptation to salt stress. However, in our case, since an enhancement on XDH activity was not observed at neither NH_4^+ nor high N dose, we suggest that ureides might be acting as protective molecules under high nitrate, while their role when the N source differs from NO_3^- at both doses needs to be elucidated in the future.

Taken all as a whole, the different results found in the bibliography and in our results might be indicating that the protective role of ureides against stress situation may differ among species and, in our case, among the different N source supplied.

5.3.5. NO role in NH_4^+ tolerance in *M. truncatula roots*

Nitric oxide participates in plant growth and development, energy metabolism and signaling processes (Wendehenne *et al.*, 2004; Baudouin, 2011, Gupta *et al.*, 2011). Besides, it also plays an essential role in the modulation of plant response to certain abiotic stresses (e.g. Song *et al.*, 2017). An increase in NO levels has been demonstrated to play a protective role under several stresses including heavy metal toxicity (Leterrier *et al.*, 2012; Sun *et al.*, 2014; Singh *et al.*, 2015); iron deficiency (Graziano and Lamattina, 2007; Song *et al.*, 2017), phosphate deficiency, as presented in the present thesis (Chapter 4.1 and Chapter 5.1); and salt and drought stresses (Fan *et al.*, 2013; Shi *et al.*, 2014; Liu *et al.*, 2015) by inducing transcriptional changes as a response. Accordingly, ammonium-fed roots produced high amounts of NO, especially at high N dose, reaching even similar levels than roots from NO_3^- cultures (Fig. 4.22F). This fact suggests that the tolerance of *M. truncatula* to NH_4^+ may well be mediated by the enhanced NO production. In this context, NO is known to exert considerable effects on the acclimation of plants to variable nitrogen sources and availability (Gupta *et al.,* 2011).

The accumulation of NO has also been proposed to regulate several genes involved in N uptake and assimilation, such as high-affinity NH_4^+ and NO_3^- transporters or the enzyme NR. Under NH_4^+ and urea, it seems plausible the idea that plants do not need the reduction of NO_3^- into NH_4^+, and consequently the production of NO might be originated from NO_3^- by the action of NR. However, we could not detect NR in any of the treatments in our experimental designs; so we are not able to assume this hypothesis. A crucial role of NO in regulating NR activity is suggested in above results, but the direction of the effect largely depends on experimental conditions (Jin *et al.*, 2009). For instance, NR was inhibited by NO in leaves of wheat (Rosales *et al.*, 2010), whereas an activation of this activity was observed in cabbage (Du *et al.*, 2008). In the photosynthetic green algae *Chlamydomonas reinhardtii*, the down-regulation of NR and high-affinity NH_4^+ and NO_3^- uptake was induced by NO under NH_4^+ nutrition (Sanz-Luque *et al.*, 2013). In our results, urea-grown plants exhibited lower amounts of NO_3^- and NO (Fig. 4.21 and 4.22), whereas NH_4^+ leads to an enhanced production of NO at high doses (Fig. 4.22). Thus, in the present thesis NR could be repressed by high levels of NO.

The question arisen next is which is the origin for the NO production? The localization of NO production determines its involvement on the different plant processes, hence different pathways and sites for NO production has been proposed

(Planchet and Kaiser, 2006; Gupta *et al.*, 2011). Here, we propose three ways for our experimental design and based in our results.

(i) Arginase-dependent pathway: arginine level on NH_4^+-fed roots was significantly higher than in the other treatments (Fig. 4.25). The enhanced NO detected, therefore, it might be uncoupled from arginase-dependent pathway. The assumption fits with the results obtained in *A. thaliana* seedlings, where the level of NO did not increase when Arg was supplied exogenously (Tun *et al.*, 2006). However, this hypothesis disagrees with an improved root development mediated by an increase of NO level observed in *A. thalinana* arginase deficient mutants (Flores *et al.*, 2008). Therefore, since NR- or arginase-linked synthesis of NO are not considered as the origin of NO in our system, another pathway for its production should be investigated. (ii) Polyamines (PA) pathway: Polyamines have been proposed to mediate the production of NO in response to various stresses (Diao *et al.*, 2016; Zhou *et al.*, 2016). For instance, the induction of NO synthesis by the external supply of PA was studied in *A. thaliana*, showing that both spermine and spermidine increased NO biosynthesis in roots and in primary leaves (Tun *et al.*, 2006). In tomato plants, an enhanced antioxidant response to chilling injury was induced by an increased production of NO by exogenous spermidine (Diao *et al.*, 2016). Moreover, an accumulation of NO induced by putrescine was pointed out to mediate the response to Fe deficiency by remobilization of Fe from root cell wall hemicellulose in *Arabidopsis* (Fang *et al.*, 2016). In pea plants, high light irradiance reversed the toxic effects of high NH_4^+ nutrition, but the high accumulation of putrescine observed in the same plants was related to toxicity (Ariz *et al.*, 2013). In light of these results found in the bibliography, our plants might be increasing the production of NO due to an increase of PA. In future studies, we will measure PA to corroborate this hypothesis.

(iii) By XDH: This activity is able to catalyze the reduction of NO_2^- to NO in the presence of either NADH or xanthine as reducing substrate (Godber *et al.*, 2000). In addition, an increase of this activity has been linked to NH_4^+ applied as sole N source in pea plants (Zdunek-Zastocka and Lips, 2003). In the present work, since no NO_2^- was detected the XDH activity might be involved in the production of NO and a complete reduction of it might be occurring. However, no significance differences on XDH were found among treatments (Fig. 4.26). In this aspect, three hypotheses are proposed: i) the higher content of NO_3^- exhibited by NO_3^--fed plants could produce more NO_2^- and consequently, an induction of XDH to detoxify the elevated NO_2^- produced. Then, the possible enhancement of XDH by NH_4^+ described previously has not been observed because under NO_3^- it also is enhanced. ii) Under high NH_4^+ dose, the increase of XDH should be occurring; however, the amounts of NO produced

might inhibited the XDH. iii) The XDH activity is not involved in the production of NO. In a recent review, the possible role of XDH to reduce nitrite to NO has been argued (Cantu-Medellin and Kelley, 2013). They exposed that the low oxygen concentration, as well as, the low internal content of NO_2^- usually found inside cells difficult the production of NO by this activity.

In this context, we suggest that NO might be playing an important role in the tolerance of *M. truncatula* to high NH_4^+ nutrition, nevertheless the mechanism and the signals that stimulate its production remain still unclear, especially when NH_4^+ is supplied as the sole N source.

5.4. Proteomic characterization of *Medicago truncatula* roots in response to nitrate, ammonium and ureic nutrition

In this study, we have studied the differential early response of *M. truncatula* roots proteome grown under NO_3^-, NH_4^+ or urea axenic mediums. The analysis revealed that roots subjected to these N forms expressed a distinct proteome, depending on the nutrition on which the seedlings have been grown (see details below).

5.4.1. Urea showed higher similarity to nitrate than to ammonium proteome

Urea nutrition has been described to produce similar toxic effects on plants, but with less intensity than those caused by NH_4^+ (Houdusse *et al.*, 2005; Arkun *et al.*, 2012). However, in our study, when we clustered the effect of the differential N nutrition, higher similarity was found between proteins from NO_3^-- and urea-grown roots than between NH_4^+- and NO_3^--grown roots (Fig. 4.31). Besides, urea-fed roots produced lower number of differentially expressed proteins when comparing to those grown on NO_3^-. All together, these findings were in agreement with the results previously described and discussed in this thesis (Chapter 4.2 and Chapter 5.2), where we demonstrated that urea did not exhibit a toxic effect in the legume *M. truncatula*, since plants growth is maintained, and even a higher photosynthethical efficiency (based of chlorophyll *a* fluorescence and OJIP test) is obtained.

5.4.2 No symptoms of toxicity for ammonium based nutrition

Ammonium toxicity depends on several aspects, as external NH_4^+ concentration, environmental factors, including soil pH, temperature and light intensity. Even the genotype of the species influences in the response; since the sensitive/tolerance to NH_4^+ can be different among varieties (Esteban *et al.*, 2016). Plant biomass and other physiological parameters are commonly used to evidence a stressful situation, but in this study no symptoms of toxicity for NH_4^+ were detected (Chapter 4.2 and Chapter 5.2). The reason might be related to either the N concentration supplied, the known relative tolerance of legumes to NH_4^+ or to the careful control of the grown medium pH (Chapter 4.2), as observed in *Arabidopsis* (Sarasketa *et al.*, 2016). In this study, the supply of N as NH_4^+ principally altered the biosynthesis of carbohydrates, secondary metabolites and amino acids suggesting that the correct plant performance might be the result of an adequate metabolic reorganization as response to the N source (but without any symptom of toxicity). This observation is in agreement with the results obtained in several proteomic studies of *A. thaliana (*a highly sensitive species to NH_4^+), in which distinct proteins phosphorilation patterns and an enhancement of the

glucosinolates metabolism were detected, when comparing NH_4^+- against NO_3^-- fed plants (Engelsberger and Schulze, 2012; Marino *et al.*, 2016; Menz *et al.*, 2016).

5.4.3 Carbon metabolism related processes

Interestingly, *M. truncatula* roots differentially accumulated RuBisco proteins in both ammonia- and urea-fed roots. Moreover, urea-fed roots differentially modulate the processes related to carbon metabolism, where photosynthesis is involved. A decline in RuBisco and RuBisco activase abundance was observed in those ureic roots, and contrastingly, ammonia fed roots up-regulates RuBisco.

The detection of these proteins in our roots may be related to the grown system used in this study (agar in pots), which permits the light reaching the roots tissues. Although the presence of RuBisco in non-photosynthetic tissues becomes surprising, it has been previously observed in other non-photosynthetic tissues, as *Arabidopsis* roots (Mooney *et al.*, 2006), oilseed rape embryos (Schwender *et al.*, 2004) and pods, developing seeds and embryos of legumes (Furbank *et al.*, 2004 ; Allen *et al.*, 2009). In rice, the RuBisco small subunit homolog OsRbcS1 was exclusively expressed in non-photosynthetic organs (Morita *et al.*, 2014). Moreover, the identification of that rice gene in several species was performed and high homology was found in immature tomato fruit, grape, nodules of *Lotus japonicus*, Setaria *italica* and *Selaginella moellendorffii* (Morita *et al.*, 2016). Then, we propose that the function of this protein in roots might be different from RuBisco found in photosynthetic tissues. Accordingly, a non-Calvin cycle, CO_2-scanvenging role for RuBisco has been demonstrated in *Brassica napus* embryos (Schwender *et al.*, 2004). Due to its unusual presence on roots, no studies on the effect of stress situations on RuBisco have been conducted. Thus, the discussion of this interesting finding has been difficult to perform, and the comparison has been made focusing in leaves.

Concomitantly to the RuBisco down-regulation found in urea-fed roots, a down-regulation of RuBisco activity has also been observed in pea plants subjected to elevated CO_2 (Rivere-Rolland *et al.*, 1996). Studies in cotton, wheat and maize also evidenced that high temperatures produce a diminution in RuBisco (Feller *et al.*, 1998; Crafts-Brandner and Salvucci, 2000). Likewise, under drought stress this activity suffers a depression in leaves of *Arabidopsis*, rice and tobacco (reviewed in Parry *et al.*, 2008). Nevertheless, NH_4^+ increased the accumulation of RuBisco and it correlates with the activation observed in leaves of barley as a response to drought and heat stress (Rollins *et al.*, 2013).

In addition, it is known that phosphoenolpyruvate carboxylases (PEPC) play a key role during C4 photosynthesis; however it also participates in a wide range of processes in non-photosynthetic tissues (Izui *et al.*, 2004). Different isoforms of PEPC are expressed in a tissue-specific manner, thus PEPC2 is a housekeeping gen present in all organs, whereas PEPC1, PEPC3 and PEPC4 genes have been found in roots and/or flowers. In roots of *A. thaliana*, an up-regulation of PEPC1, PEPC3 and PEPC4 was found under salt stress (Sanchez *et al.*, 2006). In the NH_4^+-tolerant species *Pissum sativum*, PEPC was 3-fold higher in NH_4^+ than in NO_3^- fed roots (Lasa *et al.*, 2002). Stresses such as drought, salt and cold increased PEPC activity (Doubnerová and Ryšlaváa, 2011), and an enhanced PEPC activity was also observed in roots of *Lupinus* spp. under phosphate starvation (Peñaloza *et al.*, 2005; Le Roux *et al.*, 2006) and drought stressed roots of wheat (Mansour *et al.*, 2000). However, we found a down-regulation of PEPC1 and PEPC2 in *M. truncatula* roots grown in both N sources. The regulation of non-photosynthetic linked PEPC, but not of RuBisco kept the same direction in both treatments; therefore, we suggest that the regulation of PEPC activity might be a key factor for the metabolic adaptation of plants to NH_4^+ and urea nutrition.

5.4.4. Membrane proteins are key players in the sensing of N forms different from nitrate

The plasma membrane H^+-ATPase plays a central role in nutrient uptake, intracellular pH regulation and cell growth, especially in processes of adaptation to stress conditions (Morsomme and Boutry, 2000) Hence, several studies have described that the amount of H^+-ATPase is increased under different stresses, suggesting that it might be a resistance key element. For instance, the involvement of H^+-ATPase activity in salt tolerance has been largely demonstrated by the study of halophytes and salt sensitive plants (Kalampanayil and Wimmers, 2001; Lopez-Perez *et al.*, 2009; Sahu and Shaw, 2009; Shen *et al.*, 2011). A short exposure to Cd and Cu produced the inhibition of plasma membrane H^+-ATPase activity, while a long-term treatment with those heavy metals led to increased activity in cucumber roots (Kabala *et al.*, 2008). Although NH_4^+ or urea are not stressful condition for *M. truncatula* under our experimental design (see Chapter 4.2), the down-regulation of the H^+-ATPase activity under NH_4^+ and urea nutrition more than a relation with an stressful condition, may be related with the external pH. An increase in H^+-ATPase when external pH decreases, has been proposed as the reason why rice prefers ammonia instead to NO_3^- (Zhu *et al.*, 2009). Also in rice, it has been suggested that an enhancement of this activity under NH_4^+ might be responsible for stimulating the uptake of phosphorus (Zeng *et al.*, 2012). In contrast, in our results the down-regulation might be related with the

alkalinization of the intracellular pH experimented by NH_4^+-fed plants. This observation is consistent with the H+-ATPase activity increase observed in tobacco plants, where an enhancement of this activity has been related to the alkalinization of the cytosol in response to situations in which its acidification takes place (Bobik *et al.*, 2010).

Besides, major intrinsic proteins (MIPs), also known as aquaporins, were found up-regulated in NH_4^+ and urea nutrition compared to NO_3^-. Aquaporins facilitate the transport of neutral molecules across cell membranes in higher plants, but they are also connected with N metabolism (Liu *et al.*, 2003; Loque *et al.*, 2005; Bienert *et al.*, 2011; 2014). In that sense, it has been shown that different subfamilies of MIPs are able to transport NH_3 and urea maintaining the balance of these molecules between the cytoplasm and vacuole (Loque *et al.*, 2005; Wallace *et al.*, 2005; Wang *et al.*, 2016). The results obtained in this thesis showed that NH_4^+ and urea differentially regulated MIPs in *M. truncatula* roots compared to NO_3^-. This idea is consistent with the up-regulation of tonoplast and plasma membrane aquaporins (TIP and PIP) found in rice supplied with NH_4^+ (Ding *et al.*, 2015). In maize and *Arabidopsis*, the up-regulation of several TIPs and NIPs has been related to urea transport and with the maintaining of urea concentrations in the tonoplast (Gu *et al.*, 2012; Yang *et al.*, 2015). However, the growth of *Phaseolus vulgaris* using a split root system showed that lower expression of PIP genes in roots supplied with NH_4^+ than those supplied with NO_3^- (Guo *et al.*, 2007). Hence, we suggest that the uptake of N mediated by aquaporins in roots may be regulated by the N source supplied and the species preference. Moreover, we propose that the up-regulation found in *M. truncatula* roots may be related with the mobilization of both, NH_4^+ and urea, across the different cell compartments as mechanism of tolerance since at external low concentrations of N the uptake of N should be produced by high-affinity mechanisms. Additionally, as part of these aquaporins could be transporting NH_4^+ or urea, such increase of MIPs might be associated with an effective regulation of water flow across the plasma membrane and the tonoplast.

Furthermore, the up-regulation of aquaporins may underlie the alkalinization of the intracellular pH under NH_4^+ nutrition. Thus, it has been revealed that NH_4^+ induces a greater input of NH_3 gas which, as mentioned earlier, can be transported through different MIP families (Loque *et al.*, 2005; Wallace *et al.*, 2005; Wang *et al.*, 2016). This input of NH_3 as gaseous and neutral form would produce cellular alkalinization when it is protonated inside the cell (Ariz *et al.*, 2011; Esteban *et al.*, 2016). Interestingly, species that allow a lower uptake of NH_3 show greater tolerance of this type of nutrition (Ariz *et al.*, 2011b). Therefore, our results highlight the role that

MIPs have under NH_4^+ nutrition, as well as under urea, since the nitrogenous product after its assimilation is also NH_4^+.

Overall, our results indicate that membrane proteins might play an important role in the sensing and uptake of N forms different from NO_3^-. In addition, as it could be expected the transport together with the metabolism of inorganic ions was also altered when growing plants under ammonium or urea.

5.4.5. Ammonium modulates phenylpropanoids metabolism

Phenylpropanoids (PP) and their derivatives are common secondary metabolites that control different physiological aspects to adapt to the environmental conditions. These compounds are involved in processes, such as seed dispersal, pigmentation, auxin transport or protection against abiotic stress (Valdés-López and Hernández, 2014), but the bulk of the PP play cell wall structural roles (Cheyniert *et al.*, 2013). For instance, an increase in phenolic compounds and their subsequent incorporation into the cell wall has been described under cold stress, nutrient deficiencies, UV-radiation, high light or wounding among others (e.g. Dixon and Paiva, 1995; Griffith and Yaish, 2004).

The primary activities involved in the PP pathway as PAL (phenylalanine ammonia lyase), TAL (tyrosine ammonia lyase) and CytP450-C4H (Cytochrome P450 family cinnamate 4-hydroxylase) are encoded by large gene families, whereas the activities occurring down-stream of PAL have been described as small gene families in various species (Hamberger *et al.*, 2007). Peroxidases also are key players on PP metabolism since they have been proposed as the source of radical formation and random coupling to form lignin from monolignols (Hatfield and Vermerris, 2001; Boerjan *et al.*, 2003). It is largely known that class III peroxidases (CIII PODs), mainly located in cell wall (Welinder, 1992), both consume and generate ROS (Liszkay *et al.*, 2003). Besides to their role in biological processes, CIII PODs are involved in cell wall dynamics during plant growth (Cosgrove, 2005). Concretely, cell expansion is associated to cell wall loosening and stiffening, and it is proposed that CIII PODs can control the balance between both due to their dual role of generate and regulate the level of ROS (Francoz *et al.*, 20015).

In the present work, the proteins identified by i-TRAQ showed a modulation of phenylpropanoids (PP) biosynthesis, where four peroxidases isoenzymes were remarkably involved. Under NH_4^+ nutrition, our data showed an up-regulation of the total and specific POD activities (Table 4.7 and Fig. 4.38). However, no differences in hydrogen peroxide contents among treatments were found (see Chapter 4.3, Fig. 4.29),

suggesting that POD might be implicated on the tolerance to NH_4^+ nutrition in *M. truncatula* rather than to the regulation of hydrogen peroxide levels. In addition, the PAL protein is the first enzyme affecting both the PP and stilbenoid and gingerol biosynthesis. Since in our analysis this protein, and the other two proteins identified from both pathways Caffeoyl-CoA 3-O-methyltransferase (CCOMT) and CyP450 C4H were found down-accumulated, we propose that the production of stilbenoid and gingerol from cinnamic acid might be repressed. This hypothesis may be supported by the higher Caffeic acid O-methyltransferase (COMT) accumulation found that might be acting immediately after the cinnamic acid degradation, increasing the production of PP. The higher POD activity also supports this theory since it is involved in the final synthetic step of phenolic compounds such as p-hydroxy phenyl lignin, guaiacyl lignin or syringyl lignin. Furthermore, COMT catalyzes the conversion of caffeic acid to ferulic acid (FA) and next 5-hydroxyferulic acid to sinapic acid. Thus, the low FA-dependent POD activity detected in NH_4^+-fed roots (Fig. 4.38B) together with the highest accumulation of COMT protein in those roots might be indicating that an accumulation of FA may be occurring. Its polymerization might enhance the cell wall rigidity and strength and as a consequence a stunted root growth (see Chapter 4.2, Table 4.1). In accordance with this suggestion, the inhibition of root growth was associated to an increase in POD in cowpea under salinity (Maia *et al.*, 2013). In cotton and wheat, higher levels of this activity were found in drought tolerant than in drought sensitive cultivars (Secenji *et al.*, 2010; Ranjan *et al.*, 2012). In sweet potato, it has been identified the gene SWPA4 that codes for a peroxidase isoform, which is strongly induced by abiotic stresses. Hence, its overexpression in tobacco has been proposed as the explanation why those transgenic plants exhibit an increased tolerance against salt and drought stress (Kim *et al.*, 2008). In addition, a POD-mediated cell-wall stiffening has been proposed to be involved in NH_4^+- and ABA-inhibited root growth of rice seedlings (Lin and Kao, 1999; 2001).

In relation with our findings, an increase in cell wall-bound POD activities followed by a higher content of lignin has been suggested as the reason why soybean roots copes with flavonoids induced stress. Specifically, the study of flavonoids stress induced by its exogenous application has also shown a decrease in PAL activity as well as in the content of phenolic compounds (Bido *et al.*, 2010). Moreover, the hypothesized increase of FA content is in agreement with the reduction of root growth observed after application of FA in pea, wheat, canola and soybean (Patterson, 1981; Vaughan and Ord, 1990; Devi and Prasad, 1996; Baleroni *et al.*, 2000).

Therefore, current proteomic data points out that NH_4^+ nutrition modulates the phenylpropanoids metabolim, by increasing cell wall linked peroxidase activities, which

lead to form a complex network, where probably an increase on lignin content enables a stiffening of root cell walls (accompanied by a stunted growth, Chapter 4.2).

In the light of these observations, the present study suggests that mechanism of tolerance to NH_4^+ and urea triggers important protein changes. These mechanisms include regulation of groups of proteins in the metabolism of C to reorganize the assimilation of N. Also, membrane proteins at the plasma membrane and tonoplast are remarkably changed, which is crucial for the modulation of the NH_4^+ uptake, pH controlling and energy consumption. Finally, the modification of the PP metabolism seems to reinforce the idea of an important role of the cell wall during the NH_4^+ and urea tolerance.

Chapter 6:

CONCLUSION AND PERSPECTIVES

DRAWING MAIN CONCLUSIONS

(i) *Arabidopsis thaliana* and phosphate deprivation:

1. Phosphate deprivation increased NO production in WT *Arabidopsis* roots, the AOX level and the capacity of the alternative pathway to consume electrons in WT seedlings.
2. The same treatment failed to stimulate NO production and AOX expression in the *nia* mutant, and the plants had an altered growth phenotype.
3. The NO donor S-nitrosoglutathione rescued the growth phenotype of the *nia* mutants under phosphate deprivation to some extent, and it also increased the respiratory capacity of AOX.
4. NO is required for the induction of the AOX pathway when seedlings are grown under phosphate-limiting conditions.

(ii) *Medicago truncatula* and differential effect of distinct nitrogen sources and doses:

1. Low N doses from different sources had no remarkable effects on *M. truncatula*, with the exception of the differential phenotypic root response. High dose of both ammonium and urea caused great changes in plant length, auxin contents and physiological measurements.
2. Both the indole-3-acetic acid pool and performance index are important components of the response of *M. truncatula* under ammonium or urea as the sole N source.
3. The re-distribution of assimilated N as amino acids and ureides depends on the dose and the source of N supplied to *M. truncatula*. High content

of amides as transport and transient storage of N alleviates an excess of N at high dose of both ammonium and urea.

4. An enhanced production of NO in roots triggers the adaptation of *M. truncatula* to high ammonium.
5. Root proteome of urea-grown seedlings had more similarity with nitrate seedlings than ammonium.
6. Membrane proteins were key players in the sensing of differential N forms.
7. *Medicago truncatula* tolerates ammonium and urea as the only N source.

PERSPECTIVES

The role of NO in signaling under several stress situations has been largely studied and demonstrated (as has been explained during this work) (Mur *et al.* 2013). Although different pathways for NO production have been proposed in plants, its oxidative origin remains still unclear since a NOS-like activity has not been discovered (Gupta *et al.*, 2011). Laboratory results have been probed that NO is produced when plants are grown under NH_4^+ as the sole source of N. However, how it is produced and which role is playing in the tolerance to NH_4^+ is an open window for future research. Recently, it has been described that GABA acts in the signaling against stressful conditions regulating anion transporters (Ramesh*et al.*, 2015). Besides, an increase of GABA contents due to an impaired NO production under NH_4^+ nutrition was proposed as the reason why leaves of tobacco lowered the hypersensitive response (Gupta *et al.* 2013). In addition, the accumulation of PA has also been proposed to induce the production of NO (Wimalasekera *et al.*, 2011; Diao *et al.* 2017) and *viceversa*, an enhanced production of NO under NO_3^- nutrition was described to induce the PA biosynthesis in response to pathogen infection (Gupta *et al.* 2013). Moreover, plants under NH_4^+ nutrition modulate the phenylpropanoids

metabolism. This thesis has established important pieces of the puzzle of ammonium toxicity/tolerance as the important elements (e.g. IAA, NO, membrane proteins…) for tolerance. However, which is the signal that triggers the switching of the cell wall it is still unknown.

In the last decade, important advances in the knowledge of NH_4^+ toxicity and its amelioration have occurred, but further efforts are necessary to elucidate the different aspects of its uptake, transport, storage and assimilation in plants. Thus, unraveling the link existing among GABA shunt, PA biosynthesis, the NO, and the modulation of cell wall composition in relation with NH_4^+ nutrition in tolerant plants might contribute to a better understand about the management of NH_4^+ by plants.

Chapter 7:

REFERENCES

Abramoff MD, Magalhaes PJ, Ram SJ. 2004. Image Processing with ImageJ. Biophotonics International 11 (7): 36-42.

Alamillo JM, Díaz-Leal JL, Sánchez-Moran MV, Pineda M. 2010. Molecular analysis of ureide accumulation under drought stress in *Phaseolus vulgaris* L. Plant Cell & Environment 33: 1828-1837. doi:10.1111/j.1365-3040.2010.02187.x

Allen AE, Dupont CL, Oborník M, Horák A, Nunes-Nesi A, McCrow JP, Zheng H, Johnson DA, Hu H, Fernie AR, Bowler C. 2011. Evolution and metabolic significance of the urea cycle in photosynthetic diatoms. Nature 473: 203-207.

Allen DK, Ohlrogge JB, Shachar-Hill Y. 2009. The role of light in soybean seed filling metabolism. Plant J. 58: 220-234.

Ariz I, Artola E, Cabrera-Asensio A, Cruchaga S, Aparicio-Tejo PM, Moran J.F. 2011a. High irradiance increases NH_4^+ tolerancein *Pisum sativum*: higher carbon and energy availability improve ion balance but not N assimilation. J Plant Physiol. 168: 1009-1015.doi:10.1016/j.jplph.2010.11.022.

Ariz I, Asensio CA, Zamarreño AM, García-Mina JM, Aparicio-Tejo PM, Moran JF. 2013. Changes in the C/N balance caused by increasing external ammonium concentrations are driven by carbon and energy availabilities during ammonium nutrition in pea plants: the key roles of asparagine synthetase and anaplerotic enzymes. Physiol. Plant. 148: 522-537.

Ariz I, Cruz C, Moran JF, González-Moro MB, García-Olaverri C, González-Murua C, *et al.* 2011b. Depletion of the heaviest stable N isotope is associated with NH_4^+/NH_3 toxicity in NH_4^+-fed plants. BMC. Plant. Biol. 11: 83. doi: 10.1186/1471-2229-11-83

Arkoun M, Sarda X, Jannin L, Laîné P, Etienne P, García-Mina JM, *et al.* 2012. Hydroponics versus field lysimeter studies of urea, ammonium and nitrate uptake by oilseed rape (*Brassica napus* L.). J. Exp. Bot. 63: 5245–5258.doi: 10.1093/jxb/ers183

Arnon DI, Stout PR. 1939. The essentiality of certain elements in minute quantity for plant with special reference to copper. Plant Physio 14 (2): 371-375.

Arora D, Jain P, Singh N, Kaur H, Bhatla SC. 2016. Mechanisms of nitric oxide crosstalk with reactive oxygen species scavenging enzymes during abiotic stress tolerance in plants. Free Radic. Res. 50: 291–303.

Asada K. 2006. Production and scavenging of reactive oxygen species in chloroplasts and their functions. Plant Physiology 141 (2): 391-396. doi:10.1104/pp.106.082040.

Asensio AC, Gil-Monreal M, Pires L, Gogorcena Y, Aparicio-Tejo PM, Moran JF. 2012. Two Fe-superoxide dismutase families respond differently to stress and senescence in legumes. J Plant Phys 169: 1253-1260. doi:10.1016/j.jplph.2012.04.019.

Asensio AC, Marino D, James EK, Ariz I, Arrese-Igor C, Aparicio-Tejo PM, *et al.* 2011. Expression and localization of a *Rhizobium*-derived cambialistic superoxide dismutase in pea (*Pisum sativum*) nodules subjected to oxidative stress. Mol. Plant Microbe Interact. 24: 1247-1257. doi:10.1094/MPMI-10-10-0253.

Baleroni CRS, Ferrarese MLL, Braccini AL, Scapim CA, Ferrarese-Filho O. 2000. Effects of ferulic and p-coumaric acids on canola (*Brassica napus* L. cv. Hyola 401) seed germination. Seed Sci Tecnol 28:201-207.

Balkos KD, Britto DT, Kronzucker HJ. 2010. Optimization of ammonium acquisition and metabolism by potassium in rice (*Oryza sativa* L. cv. IR-72). Plant Cell Environ. 33: 23-34.

Barth C, Gouzd ZA, Steele HP, Imperio RM. 2010. A mutation in GDP-mannose pyrophosphorylase causes conditional hypersensitivity to ammonium, resulting in *Arabidopsis* root growth inhibition, altered ammonium metabolism, and hormone homeostasis. J. Exp. Bot. 61: 379-394. doi: 10.1093/jxb/erp310

Bartoli CG, Casalongué CA, Simontacchi M, Marquez-García B, Foyer CH. 2013. Interactions between hormone and redox signalling pathways in the control of growth and cross tolerance to stress. Environ. Exp. Bot. 94: 73-88. doi: 10.1016/j.envexpbot.2012.05.003

Baudouin E. 2011. The language of nitric oxide signaling. Plant Biology 13: 233-242. doi:10.1111/j.1438-8677.2010.00403.x

Beauchamp C, Fridovich I. 1971. Superoxide dismutase improved assays and an assay applicable to acrylamide gels. Anal. Biochem. 44: 276-287. doi: 10.1016/0003-2697(71)90370-8

Benjamini Y, Yekutieli D. 2001. The control of the false discovery rate in multiple testing under dependency. The Annals of Statistics 29(4): 1165-1188.

Bertl A, Kaldenhoff R. (2007) Function of a separate NH_3-pore in aquaporin TIP2;2 from wheat, FEBS Lett. 581: 5413-5417.

Bido GS, Ferrarese MLL, Marchiosi R, Ferrarese-Filho O. 2010. Naringenin inhibits the growth and stimulates the lignification of soybean root. Brazilian Archives of Biology and Technology 53 (3): 533-542.

Bienert GP, Bienert MD, Jahn TP, Boutry M, Chaumont F. 2011. Solanaceae XIPs are plasma membrane aquaporins that facilitate the transport of many uncharged substrates. Plant J. 66: 306-317.

Bienert GP, Chaumont F. 2014. Aquaporin-facilitated transmembrane diffusion of hydrogen peroxide. Biochim. Biophys. Acta 1840: 1596-1604.

Binns D, Dimmer E, Huntley R, Barrell D, O'Donovan C, Apweiler R. 2009. QuickGO: a web-based tool for Gene Ontology searching. Bioinformatics 25(22): 3045-6.

Bittsánszky A, Pilinszky K., Gyulaib G, Komives T. 2015. Overcoming ammonium toxicity. Plant Sci. 231, 184-190. doi: 10.1016/j.plantsci.2014.12.005

Bobik K, Boutry M, Duby G. 2010. Activation of the plasma membrane H^+-ATPase by acid stress. Plant Signaling & Behavior 56: 681-683.

Boerjan W, Ralph J, Baucher M. 2003. Lignin biosynthesis. Annu. Rev. Plant Biol. 54: 519-46.

Bozzo GG, Dunn EL, Plaxton WC. 2006. Differential synthesis of phosphate-starvation inducible purple acid phosphatase isozymes in tomato (*Lycopersicon esculentum*) suspension cells and seedlings. Plant Cell and Environment 29: 303-313.

Bradford MM. 1976. A rapid and sensitive method for the quantitation of microgram quantities of protein utilizing the principle of protein-dye binding. Anal Biochem 72: 248-254.

Britto DT, Kronzucker HJ. 2002. NH_4^+ toxicity in higher plants: a critical review. J. Plant Physiol. 159: 567-584. doi: 10.1078/0176-1617-0774

Brown GC, Borutaite V. 2007. Nitric oxide and mitochondrial respiration in the heart. Cardiovasc Res 75 (2): 283-90.

Brunori M, Forte E, Arese M, Mastronicola D, Giuffré A, Sarti P. 2006. Nitric oxide and the respiratory enzyme. Biochim Biophys Acta 1757: 1144-1154.

Brychkova G, Alikulov Z, Fluhr R, Sagi M. 2008. A critical role for ureides in dark and senescence-induced purine remobilization is unmasked in the Atxdh1 *Arabidopsis* mutant. Plant J. 54: 496-509.

Cantu-Medellin N, Kelley EE. 2013. Xanthine oxidoreductase-catalyzed reduction of nitrite to nitric oxide: insights regarding where, when and how. Nitric oxide : biology and chemistry (official journal of the Nitric Oxide Society) 34: 19-26. doi:10.1016/j.niox.2013.02.081.

Cao FQ, Werner AK, Danhcke K, Romeis T, Liu LH, Witte CP. 2010. Identification and characterization of proteins involved in rice urea and arginine catabolism. Plant Phys. 154, 98–108. doi: 10.1104/pp.110.160929

Cao Y, Glass AD, Crawford NM. 1993. Ammonium inhibition of *Arabidopsis* root growth can be reversed by potassium and by auxin resistance mutations aux1, axr1, and axr2. Plant Physiol. 102: 983-989.

Carter EL, Flugga N, Boer JL, *et al.* (2009) Interplay of metal ions and urease. Metallomics 1: 207-221.

Cascio C, Schaub M, Novak K, Desotgiu R, Bussotti F, Strasser RJ. 2010. Foliar responses to ozone of *Fagus sylvatica* L. seedlings grown in shaded and in full sunlight conditions. Environ. Exp. Bot. 68, 188-197. doi:10.1016/j.envexpbot.2009.10.003

Cecconi D, Orzetti S, Vandelle E, Rinalducci S, Zolla L, Delledonne M. 2009. Protein nitration during defense response in *Arabidopsis thaliana*. Electrophoresis 30: 2460-2468.

Chaki M, Valderrama R, Fernández-Ocaña AM, Carreras A, Gomez-Rodríguez MV, López-Jaramillo J, Begara-Morales JC, Sánchez-Calvo B, Luque F, Leterrier M, Corpas FJ, Barroso JB. 2011. High temperature triggers the metabolism of *S*-nitrosothiols in sunflower mediating a process of nitrosative stress which provokes the inhibition of ferredoxin-NADP reductase by tyrosine nitration. Plant, Cell &Environment 34: 1803-1818.

Cheynier V, Comte G, Davies KM, Lattanzio V, Martens S. 2013. Plant phenolics: recent advances on their biosynthesis, genetics, and ecophysiology. Plant Physiology and Biochemistry 72: 1-20.

Clark Jr LC, Wolf R, Granger D, Taylor Z. 1953. Continuous recording of blood oxygen tensions by polarography. Journal of Applied Physiology 6 (3): 189–93.

Cleeter MWJ, Cooper JM, Darley-Usmar VM, Moncada S, Schapira AHV. 1994. Reversible inhibition of cytochrome c oxidase, the terminal enzyme of the mitochondrial respiratory chain, by nitric oxide: implications for neurodegenerative diseases. *FEBS Letters* 345, 50–54.

Cona A, Rea G, Angelini R, Federico R, Tavladoraki P. 2006. Functions of amine oxidases in plant development and defense. Trends Plant Sci. 11: 80-88.

Cordell D, Rosemarin A, Schröder JJ, Smit AL. 2011. Towards global phosphorus security: a systems framework for phosphorus recovery and reuse options. *Chemosphere* 84: 747-758.

Cordoba-Pedregosa M, Gonzalez-Reyes JA, Canadillas M, Navas P, Cordoba F. 1996. Role of apoplastic and cell-wall peroxidases on the stimulation of root elongation by ascorbate. Plant Physiology 112 (3): 1119-1125.

Corpas FJ, Barroso JB, del Río LA. 2001. Peroxisomes as a source of reactive oxygen species and nitric oxide signal molecules in plant cells. Trends Plant Sci 6: 145-150.

Cosgrove DJ. 2005. Growth of the plant cell wall. Nat. Rev. Mol. Cell Biol. 6: 850-861.

Coskun D, Britto DT, Li M, Becker A, Kronzucker HJ. 2013. Rapid ammonia gas transport accounts for futile transmembrane cycling under NH_3/NH_4^+ toxicity in plant roots. Plant Physiol. 163: 1859-1867.

Costa E, Pérez J, Kreft JU. 2006. Why is metabolic labour divided in nitrification? Trends Microbiol. 14: 213-219.

Court MN, Stephen RC, Waid JS. 1962. Nitrite toxicity arising from the use of urea as fertilizer. Nature 194: 1263-1265.

Court MN, Stephen RC, Waid JS. 1964. Toxicity as a cause of the inefficiency of urea as a fertilizer. J Soil Sci 15: 42-48.

Cox J, Mann M. 2008. MaxQuant enables high peptide identification rates, individualized p.p.b.-range mass accuracies and proteome-wide protein quantification. Nature Biotechnology 26 (12): 1367-72. doi: 10.1038/nbt.1511.

Cox J, Neuhauser N, Michalski A, Scheltema RA, Olsen JV, Mann M. 2011. Andromeda: a peptide search engine integrated into the MaxQuant environment. J Proteome Res 10 (4): 1794-805. doi: 10.1021/pr101065j.

Crafts-Brandner SJ, Salvucci ME. 2000. Rubisco activase constrains the photosynthetic potential of leaves at high temperature and CO_2. Proceedings of the National Academy of Sciences USA 97: 13430-13435.

Cruz C, Domínguez-Valdivia MD, Aparicio-Tejo JM, Lamsfus C, Bio A, Martins-Loução AM, *et al.* 2011. Intra-specific variation in pea responses to

ammonium nutrition leads to different degrees of tolerance. Environ. Exp. Bot. 70: 233-243. doi: 10.1016/j.envexpbot.2010.09.014

Cvetkovska M, Vanlerberghe GC. 2012. Alternative oxidase modulates leaf mitochondrial concentrations of superoxide and nitric oxide. *New Phytologist* 195: 32-39.

Das K., Roychoudhury A. 2014. Reactive oxygen species (ROS) and response of antioxidants as ROS-scavengers during environmental stress in plants. Front. Environ. Sci. 2: 53.

Davey MW, Dekempeneer E, Keulemans J. 2003. Rocket-powered high-performance liquid chromatographic analysis of plant ascorbate and glutathione. Anal Biochem 316: 74-81. doi: 10.1016/S0003-2697(03)00047-2.

Day DA, Neuburger M, Douce R. 1985. Biochemical characterization of chlorophyll-free mitochondria from pea leaves. Aus J of Plant Physiol 12: 219– 228.

De Saussure NT. 1804. Recherches Chimiques sur la Végétation.

Dean JV, Harper JE. 1988. The conversion of nitrite to nitrogen oxide(s) by the constitutive NAD(P)H-nitrate reductase enzyme from soybean . Plant Physiology 88 (2): 389-395.

Del Amor, F. M., and Cuadra-Crespo, P. 2011. Gas exchange and antioxidant response of sweet pepper to foliar urea spray as affected by ambient temperature. Sci. Hortic. 127: 334-340. doi: 10.1016/j.scienta.2010.10.028

Devi RS, Prasad MNV. 1996. Ferulic acid mediated changes in oxidative enzymes of maize seedlings: implications in growth. Biol Plant 38: 387-395.

Diao QN, Song YJ, Shi DM, Qi HY. 2017. Nitric oxide induced by polyamines involves antioxidant systems against chilling stress in tomato (*Lycopersicon esculentum* Mill.) seedling. Journal of Zhejiang University Science B. 17 (12): 916-930. doi:10.1631/jzus.B1600102.

Ding L, Gao CM, Li YR, Li Y, Zhu YY, Xu GH, Shen QR, Kaldenhoff R, Kai L, Guo SW. 2015. The enhanced drought tolerance of rice plants under ammonium is related to aquaporin (AQP). Plant Sci. 234: 14-21.

Dixon RA, Paiva N. 1995. Stressed induced phenylpropanoid metabolism. Plant Cell. 7: 1085-97.

do Amarante L, Lima JD, Sodek L. .2006. Growth and stress conditions cause similar changes in xylem amino acids for different legume species.Environ Exp Bot 58: 123-129.

Domínguez-Valdivia, M. D., Aparicio-Tejo, P. M., Lamsfus, C., Cruz, C., Martins-Loução, M. A., and Moran, J. F. 2008.. Nitrogen nutrition and antioxidant metabolism in ammonium-tolerant and sensitive plants. Physiol. Plant 132: 359-369. doi: 10.1111/j.1399-3054.2007.01022.x

Doubnerova V, Ryslava H. 2011. What can enzymes of C4 photosynthesis do for C3 plants under stress? Plant Sci 180: 575-583.

Drath M, Kloft N, Batschauer A, Marin K, Novak J, Forchhammer K. 2008. Ammonia triggers photodamage of photosystem II in the cyanobacterium *Synechocystis* sp. strain PCC 6803. Plant Phys. 147: 206-215. doi: 10.1104/pp.108.117218

Du S, Zhang Y, Lin X, Wang Y, Tang C. 2008. Regulation of nitrate reductase by nitric oxide in Chinese cabbage pakchoi (*Brassica chinensis* L.). Plant Cell and Environment 31: 195-204.

Engelsberger WR, Schulze WX. 2012. Nitrate and ammonium lead to distinct global dynamic phosphorylation patterns when resupplied to nitrogen-starved *Arabidopsis* seedlings. Plant J. 69: 978-995.

Epstein E. 1999. "The discovery of the essential elements. In: Discoveries" in Plant Biology 3. S.D. Kung and S.F. Yang, eds. World Scientific Publishing, Singapore.

Esteban R, Ariz I, Cruz C, Moran JF. 2016. Review: Mechanisms of ammonium toxicity and the quest for tolerance. Plant Science 248: 92-101. http://dx.doi.org/10.1016/j.plantsci.2016.04.008.

Fan HF, Du CX, Guo SR. 2013. Nitric oxide enhances salt tolerance in cucumber seedlings by regulating free polyamine content. Environmental and Experimental Botany 86: 52-59.

Fang XZ, Bin Wang, Wen Feng Song, Shao Jian Zheng, and Ren Fang Shen. 2016. Putrescine alleviates iron deficiency via NO-dependent reutilization of root cell-wall Fe in *Arabidopsis*. Plant Physiol. 170: 558-567. doi:10.1104/pp.15.01617

Feller U, Crafts-Brandner SJ, Salvucci ME. 1998. Moderately high temperatures inhibit ribulose-1,5-bisphosphate carboxylase/oxygenase (RuBisco) activase-mediated activation of RuBisco. Plant Physiology 116: 539-546.

Fischer G, Nachtergaele FO. Prieler S, van Velthuizen H, Verelst L, Wiberg D. 2008. Global Agro-Ecological Zones Assessment for Agriculture (GAEZ 2008).

Flores T, Todd CD, Tovar-Mendez A, *et al.* 2008. Arginase-negative mutants of *Arabidopsis* exhibit increased nitric oxide signaling in root development. Plant Physiology 147(4): 1936-1946.

Foreman J, Demidchik V, Bothwell JH, Mylona P, Miedema H, Torres MA, Linstead P, Costa S, Brownlee C, Jones JD, Davies JM, Dolan L. 2003. Reactive oxygen species produced by NADPH oxidase regulate plant cell growth. Nature 422: 442-446.

Foyer CH, Noctor G, Lelandais M, Lescure JC, Valadier MH, Boutin JP, *et al.* 1994. Short-term effects of nitrate, nitrite and ammonium assimilation on photosynthesis, carbon partitioning and protein phosphorylation in maize. Planta 192: 211-220.

Fu LJ, Shi K, Gu M, Zhou YH, Dong DK, Liang WS, Song FM, Yu JQ. 2010. Systemic induction and role of mitochondrial alternative oxidase and nitric oxide in a compatible tomato-*Tobacco mosaic virus* interaction. Molecular Plant-Microbe Interactions 23: 39-48.

Furbank RT, White R, Palta JA, Turner NC. 2004. Internal recycling of respiratory CO_2 in pods of chickpea (*Cicer arietinum* L.): the role of pod wall, seed coat, and embryo. J. Exp. Bot. 55: 1687-1696.

Garnica M, Houdusse F, Zamarreño AM, Garcia-Mina JM. 2010. Nitrate modifies the assimilation pattern of ammonium and urea in wheat seedlings. J. Sci. Food Agric. 90: 357-369. doi: 10.1002/jsfa.3811

Gerendás J, Zhu Z, Bendixen R, Ratcliffe RG, Sattelmacher B. 1997. Physiological and biochemical processes related to ammonium toxicity in higher plants. Z. Pflanzenernaehr. Bodenk. 160: 239-251. doi:10.1002/jpln.19971600218

Gerendás, J., Zhu, Z., and Sattelmacher, B. (1998). Influence of N and Ni supply on nitrogen metabolism and urease activity in rice (*Oryza sativa* L.) J. Exp. Bot. 49: 1545-1554. doi: 10.1093/jxb/49.326.1545

Godber BL, Doel JJ, Sapkota GP, Blake DR, Stevens CR, Eisenthal R, Harrison R. 2000. Reduction of nitrite to nitric oxide catalysed by xanthine oxidoreductase. J Biol Chem 275: 7757-7763.

González EM, Cabrerizo PM, Royuela M, Aparicio-Tejo PM, Arrese-Igor C. 2001. Nitrate reduction in tendrils of semi-leafless pea. Physiol Plant 111 (3): 329-335.

Gonzàlez-Meler MA, Giles L, Thomas RB, Siedow JN. 2001 Metabolic regulation of leaf respiration and alternative oxidase activity in response to phosphate supply. Plant Cell Environ 24: 205–215.

Graziano M. Lamattina L. 2007. Nitric oxide accumulation is required for molecular and physiological responses to iron deficiency in tomato roots. The Plant Journal 52: 949-960. doi:10.1111/j.1365-313X.2007.03283.x

Griffith M, Yaish MWF. 2004. Antifreeze proteins in overwintering plants: a tale of two activities. Trends Plant Sci. 9: 399-405. doi: 10.1016/j.tplants.2004.06.007

Groß F, Durner J, Gaupels F. 2013. Nitric oxide, antioxidants and pro-oxidants in plant defence responses. Frontiers in Plant Science 4: 419. doi: 10.3389/fpls.2013.00419.

Gu RL, Chen XL, Zhou YL, Yuan LX. 2012. Isolation and characterization of three maize aquaporin genes, ZmNIP2;1, ZmNIP2;4 and ZmTIP4;4 involved in urea transport. BMB Rep 45: 96-101.

Guo K, Kong WW, Yang ZM. 2009. Carbon monoxide promotes root hair development in tomato. Plant Cell Environ. 32: 1033-1045. doi: 10.1111/j.1365-3040.2009.01986.x

Guo SW, Kaldenhoff R, Uehlein N, Sattelmacher B, Brueck H. 2007. Relationship between water and nitrogen uptake in nitrate- and ammonium-supplied Phaseolus vulgaris L. plants. J. Plant Nutr. Soil Sci. 170: 73-80.

Gupta KJ, Brotman Y, Mur LAJ. 2014b. Localisation and quantification of reactive oxygen species and nitric oxide in *Arabidopsis* roots in response to fungal infection. BIO-PROTOCOLS Press.

Gupta KJ, Brotman Y, Segu S, *et al.* 2013. The form of nitrogen nutrition affects resistance against Pseudomonas syringae pv. phaseolicola in tobacco. Journal of Experimental Botany. 64 (2): 553-568. doi:10.1093/jxb/ers348.

Gupta KJ, Fernie AR, Kaiser WM, van Dongen JT. 2011. On the origins of nitric oxide. Trends in Plant Science 16: 160-168.

Gupta KJ, Hebelstrup KH, Kruger NJ, Ratcliffe RG. 2014. Nitric oxide is required for homeostasis of oxygen and reactive oxygen species in barley roots under aerobic conditions. Molecular Plant 7: 747-750.

Gupta KJ, Igamberdiev AU. 2013. Recommendations of using at least two different methods for measuring NO. Frontiers in Plant Science: 58.

Gupta KJ, Shah JK, Brotman Y, Jahnke K, Willmitzer L, Kaiser WM, Bauwe H, Igamberdiev AU. 2012. Inhibition of aconitase by nitric oxide leads to induction of the alternative oxidase and to a shift of metabolism towards biosynthesis of amino acids. Journal of Experimental Botany 63: 1773-1784.

Gupta KJ, Stoimenova M, Kaiser WM. 2005. In higher plants, only root mitochondria, but not leaf mitochondria reduce nitrite to NO, in vitro and in situ. Journal of Experimental Botany 56: 2601-2609.

Halliwell B, Gutteridge JMC. 2007. Free radicals in biology and medicine. Ed. Clarendon Press, Oxford, UK.

Hamberger B, Ellis M, Friedmann M, de Azevedo Sousa C, Barbazuk, B, Douglas C. 2007. Genome-wide analyses of phenylpropanoid-related genes in *Populus trichocarpa*, *Arabidopsis thaliana*, and *Oryza sativa*: the *Populus* lignin toolbox and conservation and diversification of angiosperm gene families. Can J. Bot. 85: 1182-1201.

Hatfield R, Vermerris W. 2001. Lignin formation in plants. The dilemma of linkage specificity. Plant Physiol. 126: 1351-1357.

Hawkesford M, Horst W, Kichey T, Lambers H, Schjoerring J, Skrumsager Møller I, White P. Functions of macronutrients. In Marschner's Mineral Nutrition of Higher Plants (3rd Ed.), Academic Press, London. pp 135-190.

Hodge A. 2004. The plastic plant: root responses to heterogeneous supplies of nutrients. New Phytologist 162: 9-24. doi: 10.1111/j.1469-8137.2004.01015.x

Holford ICR. 1997. Soil phosphorus: its measurement and its uptake by plants. Aust J Soil Res 35: 227-239.

Hollocher TC. 1981. Oxidation of ammonia by *Nitrosomonas europaea*. J Biol Chem 256: 10834-10836.

Holzmeister C, Gaupels F, Geerlof A, Sarioglu H, Sattler M, Durner J, *et al.* 2015. Differential inhibition of *Arabidopsis* superoxide dismutases by peroxynitrite-mediated tyrosine nitration. J. Exp.Bot. 66: 989-999.

Houdusse F, Zamarreño AM, Garnica M, García-Mina JM. 2005. The importance of nitrate in ameliorating the effects of ammonium and urea nutrition on plant development: the relationships with free polyamines and plant proline contents. Funct. Plant Biol. 32: 1057–1067. doi: 10.1071/FP05042

Huerta-Cepas J, Szklarczyk D, Forslund K, *et al.* 2016. eggNOG 4.5: a hierarchical orthology framework with improved functional annotations for eukaryotic,

prokaryotic and viral sequences. Nucleic Acids Research 44(Database issue): D286-D293. doi:10.1093/nar/gkv1248.

Izui K, Matsumura H, Furumoto T, Kai Y. 2004. Phosphoenolpyruvate carboxylase: a new era of structural biology. Annu Rev Plant Biol 55: 69-84.

Jambunathan N. 2010. Determination and detection of reactive oxygen species (ROS), lipid peroxidation, and electrolyte leakage in plants. Methods in Molecular Biology 639: 291-297.

Jardim-Messeder D, Caverzan A, Rauber R, Ferreira ES, Margis-Pinheiro M, Galina A. 2015. Succinate dehydrogenase (mitochondrial complex II) is a source of reactive oxygen species in plants and regulates development and stress responses. New Phytologist 208: 776-789.

Jásik J, Boggetti B, Baluška F, *et al.* 2013. PIN2 turnover in *Arabidopsis* root epidermal cells explored by the photoconvertible protein dendra2. PLoS ONE 8: e61403

Jauregui I, Aroca R, Garnica M, Zamarreño AM, García-Mina JM, Serret MD, *et al.* 2015. Nitrogen assimilation and transpiration: key processes conditioning responsiveness of wheat to elevated CO_2 and temperature. Physiol. Plant. 155: 338-354. doi: 10.1111/ppl.12345

Jin CW, Du ST, Zhang YS, Lin XY, Tang CX. 2009. Differential regulatory role of nitric oxide in mediating nitrate reductase activity in roots of tomato (*Solanum lycocarpum*). Annals of Botany 104: 9-17.

Juszczuk IM, Wagner AM, Rychter AM. 2001. Regulation of alternative oxidase activity during phosphate deficiency in bean roots (*Phaseolus vulgaris*). Physiol. Plant. 113: 185-192.

Kabała K, Janicka-Russak M, Burzyński M, Kłobus G. 2008. Comparison of heavy metal effect on the proton pumps of plasma membrane and tonoplast in cucumber root cells. Journal of Plant Physiology 165: 278-288.

Kaiser WM, Planchet E, Rümer S. 2011. Nitrate reductase and nitric oxide. In: Nitrogen metabolism in plants in the post-genomic era. Annu Plant Rev 42: 127-145.

Kalaji HM, Schansker G, Ladle RJ, *et al.* 2014. Frequently asked questions about in vivo chlorophyll fluorescence: practical issues. Photosynth Res 122: 121. doi: 10.1007/s11120-014-0024-6

Kalampanayil BD, Wimmers LE. 2001. Identification and characterization of a salt-stress-induced plasma membrane H^+-ATPase in tomato. Plant, Cell & Environment, 24: 999-1000. doi: 10.1046/j.1365-3040.2001.00743.x

Kärkönen A, Kuchitsu K. 2015. Reactive oxygen species in cell wall metabolism and development in plants. Phytochem 112: 22-32.

Kempinski CF, Haffar R, Barth C. 2011. Toward the mechanism of NH_4^+ sensitivity mediated by *Arabidopsis* GDP-mannose pyrophosphorylase. Plant Cell Environ. 34: 847-858.

Kim YH, Kim CY, Song WK, Park DS, Kwon SY, Lee HS, *et al.* 2008. Overexpression of sweetpotato swpa4 peroxidase results in increased hydrogen peroxide production and enhances stress tolerance in tobacco. Planta 227: 867-881. 10.1007/s00425-007-0663-3

Kinnersley AM, Turano FJ. 2000. Gamma aminobutyric acid (GABA) and plant responses to stress. Crit. Rev. Plant Sci. 19: 479-509.

Kirscht A, Kaptan SS, Bienert GP, *et al.* 2016. Crystal structure of an ammonia-permeable aquaporin. Dutzler R, ed. PLoS Biology 14(3): e1002411.

Kojima H, Sakurai K, Kikuchi K, Kawahara S, Kirino Y, Nagoshi H, Hirata Y, Nagano T. 1998. Development of a fluorescent indicator for nitric oxide based on the fluorescein chromophore. Chemical and Pharmaceutical Bulletin 46: 373-375.

Kojima S, Bohner A, Gassert B, Yuan L, von Wirén N. 2007. AtDUR3 represents the major transporter for high-affinity urea transport across the plasma membrane of nitrogen-deficient *Arabidopsis* roots. Plant J. 52: 30-40. doi: 10.1111/j.1365-13X.2007.03223.x

Krogmeier MJ, McCarty GW, Bremner JM. 1989. Phytotoxicity of foliar-applied urea. Proc. Natl Acad. Sci. USA 86: 8189-8191.

Krouk G, Lacombe B, Bielach A, Perrine-Walker F, Malinska K, Mounier E, Hoyerova K, Tillard P, Leon S, Ljung K, Zazimalova E, Benkova E, Nacry P, Gojon A. 2010. Nitrate-regulated auxin transport by NRT1.1 defines a mechanism for nutrient sensing in plants. Dev. Cell 18: 927-937. doi: 10.1016/j.devcel.2010.05.008

Kudoyarova GR, Farkhutdinov RG, Veselov SY. 1997. Comparison of the effects of nitrate and ammonium forms of nitrogen on auxin content in roots and the growth of plants under different temperature conditions. Plant Growth Regul. 23: 207-208. doi: 10.1023/A:1005990725068

Lam HM, Coschigano KT, Oliveira IC, Melo-Oliveira R, Coruzzi G M. 1996. The molecular genetics of nitrogen assimilation into amino acids in higher plants. Annu. Rev. Plant Physiology Plant Mol. Biol. 47: 569-593.

Lasa B, Frechilla S, Aparicio-Tejo PM, Lamsfus C. 2002. Role of glutamate dehydrogenase and phosphoenolpyruvate carboxylase activity in ammonium nutrition tolerance in roots. Plant Physiol. Biochem. 40: 969-976. doi: 10.1016/S0981-9428(02)01451-1

Le Roux MR, Ward CL, Botha FC, Valentine AJ. 2006. Routes of pyruvate synthesis in phosphorus-deficient lupin roots and nodules. New Phytol., 169: 399-408.

Lea P, Miflin B. 2011. Nitrogen assimilation and its relevance to crop improvement. In Annual Plant Reviews Volume 42: Nitrogen Metabolism in Plants in the Post-Genomic Era (eds C. H. Foyer and H. Zhang), Wiley-Blackwell, Oxford, UK. pp 1-40.

Lescano CI, Martini C, González CA. *et al.* 2016. Allantoin accumulation mediated by allantoinase downregulation and transport by ureide permease confers salt stress tolerance to *Arabidopsis* plants. Plant Mol Biol 91: 581.

Leterrier M, Airaki M, Palma JM, Chaki M, Barroso JB, Corpas FJ. 2012. Arsenic triggers the nitric oxide (NO) and S-nitrosoglutathione (GSNO) metabolism in *Arabidopsis*. Environ. Pollut. 166: 136-143. doi: 10.1016/j.envpol.2012.03.012.

Li B, Li G, Kronzucker HJ, Baluška F, Shi W. 2014. Ammonium stress in *Arabidopsis*: signaling, genetic loci, and physiological targets. Trends Plant Sci 19: 107-114.

Li B, Li Q, Su Y, Chen H, Xiong L, Mi G, *et al.* 2011. Shoot supplied ammonium targets the root auxin influx carrier AUX1 and inhibits lateral root emergence in *Arabidopsis*. Plant Cell Environ. 34: 933-946. doi: 10.1111/j.1365-3040.2011.02295.x

Li B, W. Shi, Y. Su. 2011. The differing responses of two Arabidopsis ecotypes to ammonium are modulated by the photoperiod regime. Acta Physiol. Plant. 33: 325-334.

Li Q, Li BH, Kronzucker HJ, Shi WM. 2010 Root growth inhibition by NH_4^+ in *Arabidopsis* is mediated by the root tip and is linked to NH_4^+ efflux and GMPase activity. Plant Cell Environ. 33: 1529-1542. doi: 10.1111/j.1365-3040.2010.02162.x

Lima JE, Kojima S, Takahashi H, von Wirén N. 2010. Ammonium triggers lateral root branching in *Arabidopsis* in an ammonium transporter1;3-dependent manner. Plant Cell. 22: 3621-3633.

Lin CC, Kao CH. 1999. NaCl induced changes in ionically bound peroxidase activity in roots of rice seedlings. Plant Soil 216: 147-153.

Ling Q, Huang W, Jarvis P. 2011. Use of a SPAD-502 meter to measure leaf chlorophyll concentration in *Arabidopsis thaliana*. Photosynth Research 107: 209. doi: 10.1007/s11120-010-9606-0

Liszkay A, Kenk B, Schopfer P. 2003. Evidence for the involvement of cell wall peroxidase in the generation of hydroxyl radicals mediating extension growth. Planta 217: 658-667.

Liu GW, Sun AL, Li DQ, Athman A, Gilliham M, Liu LH. 2015. Molecular identification and functional analysis of a maize (*Zea mays*) DUR3 homolog that transports urea with high affinity. Planta 241: 861-874. doi: 10.1007/s00425-014-2219-7.

Liu LH, Ludewig U, Gassert B, Frommer WB, von Wiren N. 2003. Urea transport by nitrogen-regulated tonoplast intrinsic proteins in *Arabidopsis*. Plant Physiol. 133: 1220-1228.

Liu Y, Lai N, Gao K, Chen F, Yuan L, Mi G. 2013. Ammonium inhibits primary root growth by reducing the length of meristem and elongation zone and decreasing elemental expansion rate in the root apex in *Arabidopsis thaliana*. Muday G, ed. PLoS ONE 8(4): e61031.

Lobet G, Pagès L, Draye X. 2011. A novel image analysis toolbox enabling quantitative analysis of root system architecture. Plant Phys. 157: 29–39. doi: 10.1104/pp.111.179895.

López-Pérez L, Martínez- Ballesta MC, Maurel C, Carvajal M. 2009. Changes in plasma membrane lipids, aquaporins and proton pump of broccoli roots, as an adaptation mechanism to salinity. Phytochemistry 70: 492-500.

Loque D, Ludewig U, Yuan LX, von Wiren N. 2005. Tonoplast intrinsic proteins AtTIP2;1 and AtTIP2;3 facilitate NH_3 transport into the vacuole. Plant Physiol. 137: 671-680.

Loque D, Tillard P, Gojon A, Lepetit M. 2003. Gene expression of the NO_3^- transporter NRT1.1 and the nitrate reductase NIA1 is repressed in *Arabidopsis* roots by NO_2^-, the product of NO_3^- reduction. Plant Physiol 132: 958-967.

Lukaszewski KM, Blevins DG, Randall DD. 1992. Asparagine and boric acid cause allantoate accumulation in soybean leaves by inhibiting manganese-dependent allantoate amidohydrolase . Plant Physiology 99 (4): 1670-1676.

Maia JM, Voigt EL, Ferreira-Silva SLA, Fontenele V, Macedo CEC, Silveira JAG. 2013. Differences in cowpea root growth triggered by salinity and dehydration are associated with oxidative modulation involving types I and III peroxidases and apoplastic ascorbate. J. Plant Growth Regul. 32: 376-387. doi: 10.1007/s00344-012-9308-2

Mansour MMF, Al-Mutawa MM 2000. Protoplasmic characteristics of wheat cultivars differing in drought tolerance. Physiol Plant 6: 35-43.

Marino D, Ariz I, Lasa B, *et al.* 2016. Quantitative proteomics reveals the importance of nitrogen source to control glucosinolate metabolism in *Arabidopsis thaliana* and *Brassica oleracea*. Journal of Experimental Botany 67 (11): 3313-3323. doi:10.1093/jxb/erw147.

Marschner H. 2012. Mineral Nutrition of Higher Plants, 3rd ed. Academic Press, London. https://doi.org/10.1016/B978-0-12-384905-2.00030-3.

Mata-Pérez C, Begara-Morales JC, Chaki M, Sánchez-Calvo B, Valderrama R, Padilla MN, Barroso JB. 2016. Protein tyrosine nitration during development and abiotic stress response in plants. Frontiers in Plant Science 7: 1699

Maxwell DP, Wang Y, McIntosh L. 1999. The alternative oxidase lowers mitochondrial reactive oxygen production in plant cells. Proceedings of the National Academy of Sciences USA 96: 8271–8276.

McClure PR, Israel DW. 1979. Transport of nitrogen in the xylem of soybean plants. Plant Physiology 64: 411-416.

Medici OL, Azevedo RA, Smith RJ, Lea PJ. 2004. The influence of nitrogen supply on antioxidant enzymes in plant roots. Funct. Plant Biol. 31: 1-9.

Mengel K, Kirkby EA. 1987. Principles of plant nutrition. 4th Ed. International Potash Institute, IPI, Bern, Switzerland. 685p.

Menz J, Li Z, Schulze WX, Ludewig U. 2016. Early nitrogen-deprivation responses in *Arabidopsis* roots reveal distinct differences on transcriptome and phospho-proteome levels between nitrate and ammonium nutrition. Plant J 88: 717-734. doi:10.1111/tpj.13272

Mercier H, Kerbauy GB, Sotta B, Miginiac E. 1997. Effects of NO_3^-, NH_4^+ and urea nutrition on endogenous levels of IAA and four cytokinins in two epiphytic bromeliads. Plant Cell Environ. 20: 387-392. doi: 10.1046/j.1365-3040.1997.d01-72.x

Mérigout P, Lelandais M, Bitton F, Renou JP, Briand, X, Meyer C, *et al.* 2008. Physiological and transcriptomic aspects of urea uptake and assimilation in *Arabidopsis* plants. Plant Phys. 147: 1225-1238. doi: 10.1104/pp.108.119339

Meyer C, Stitt M. 2001. Nitrate reductase and signaling. In: Lea PJ, Morot-Gaudry J-F, eds. Plant nitrogen. New York: Springer, 37-59.

Millar AH, Whelan J, Soole KL, Day DA. 2011. Organization and regulation of mitochondrial respiration in plants. Annual Review of Plant Biology 62: 79-104.

Minocha R, Majumdar R, Minocha SC. 2014. Polyamines and abiotic stress in plants: a complex relationship. Frontiers in Plant Science. 5: 175. doi:10.3389/fpls.2014.00175.

Mittler R. 2002. Oxidative stress, antioxidants and stress tolerance. Trends in Plant Science 7 (9): 405-410.

Moller IM. 2001. Plant mitochondria and oxidative stress: electron transport, NADPH turnover, and metabolism of reactive oxygen species. Annu Rev Plant Physiol Plant Mol Biol 52: 561-591.

Mooney BP, Miernyk JA, Michael Greenlief C, Thelen JJ. 2006. Using quantitative proteomics of *Arabidopsis* roots and leaves to predict metabolic activity. Physiologia Plantarum, 128: 237-250. doi:10.1111/j.1399-3054.2006.00746.x

Moran JF, James EK, Rubio MC, Sarath G, Klucas RV, Becana M. 2003. Functional characterization and expression of a cytosolic iron-superoxide dismutase from cowpea (*Vigna unguiculata*) root nodules. Plant Physiol. 133: 773-782. doi: 10.1104/pp.103.023010.

Morita K, Hatanaka T, Misoo S, Fukayama H. 2014. Unusual small subunit that is not expressed in photosynthetic cells alters the catalytic properties of RuBisco in rice. Plant Physiol. 164: 69-79.

Morsomme P, Boutry M. 2000. The plant plasma membrane H^+-ATPase: structure, function and regulation. Biochim Biophys Acta, Biomembr. 1465 (1-2): 1-16. doi: 10.1016/S0005-2736(00)00128-0

Müller K, Linkies A, Vreeburg RAM, Fry SC, Krieger-Liszkay A, Leubner-Metzger G. 2009. In vivo cell wall loosening by hydroxyl radicals during cress seed germination and elongation growth. Plant Physiol. 150: 1855-1865.

Mur LAJ, Mandon J, Persijn S, Cristescu SM, Moshkov IE, Novikova GV, Hall MA, Harren FJM, Hebelstrup KH, Gupta KJ. 2013. Nitric oxide in plants: an assessment of the current state of knowledge. AoB Plants 5, pls052.

Nimptsch J, Pflugmacher S. 2007. Ammonia triggers the promotion of oxidative stress in the aquatic macrophyte *Myriophyllum mattogrossense*. Chemosphere 66: 708-714. doi: 10.1016/j.chemosphere.2006.07.064

Novo-Uzal E, Fernández-Pérez F, Herrero J, Gutiérrez J, Gómez-Ros LV, Bernal MA, Díaz J, Cuello J, Pomar F, Pedreño MA. (2013) From *Zinnia* to *Arabidopsis*: approaching the involvement of peroxidases in lignification. J. Exp. Bot. 64: 3499-3518.

Oaks A. 1994. Primary nitrogen assimilation in higher plants and its regulation. Can. J. Bot. 72: 739-750.

Pantoja O. 2012. High Affinity Ammonium Transporters: Molecular Mechanism of Action. Frontiers in plant science 3: 34. doi:10.3389/fpls.2012.00034.

Park JE, Park JY, Kim YS, Staswick PE, Jeon J, Yun J, *et al.* 2007. GH3-mediated auxin homeostasis links growth regulation with stress adaptation response in *Arabidopsis*. J. Bio Chem. 282: 10036-10046. doi: 10.1104/pp.103.023010

Parry MAJ, Keys AJ, Madgwick PJ, Carmo-Silva AE, Andralojc PJ. 2008. Rubisco regulation: a role for inhibitors. J Exp Bot 59 (7): 1569-1580. doi: 10.1093/jxb/ern084

Parsons HL, Yip JYH, Vanlerberghe GC. 1999. Increased respiratory restriction during phosphate-limited growth in transgenic tobacco cells lacking alternative oxidase. Plant Physiology 121: 1309–1320.

Passardi F, Penel C, Dunand C. 2004. Performing the paradoxical: how plant peroxidases modify the cell wall. Trends Plant Sci. 9: 534-540.

Patterson DT. 1981. Effects of allelopathic chemicals on growth and physiological responses of soybean (*Glycine max* L). Weed Sci 29: 53-59.

Patterson K, Cakmak T, Cooper A, Lager I, Rasmusson AG, Escobar MA. 2010. Distinct signaling pathways and transcriptome response signatures differentiate ammonium and nitrate-supplied plants. Plant Cell Environ. 33: 1486-1501. doi: 10.1111/j.1365-3040.2010.02158.x

Pélissier HC, Frerich A, Desimone M, Schumacher K, Tegeder M. 2004. PvUPS1, an allantoin transporter in nodulated roots of French bean. Plant Physiology. 134 (2): 664-675. doi:10.1104/pp.103.033365.

Pélissier HC, Tegeder M. 2007. PvUPS1 plays a role in source-sink transport of allantoin in French bean (*Phaseolus vulgaris*). Funct. Plant Biol. 34: 282-291.

Peñaloza E, Muñoz G, Salvo-Garrido H, Silva H, Corcuera LJ. 2005. Phosphate deficiency regulates phosphoenolpyruvate carboxylase expression in proteoid root clusters of white lupin. J Exp Bot 56 (409): 145-153. doi: 10.1093/jxb/eri008

Péret B, de Rybel B, Casimiro I, Benková E, Swaruup R, Laplaze L, *et al.* 2009. *Arabidopsis* lateral root development: an emerging story. Trends Plant Sci. 14: 399-408. doi: 10.1016/j.tplants.2009.05.002

Pinton R, Tomasi N, Zanin L. 2016. Molecular and physiological interactions of urea and nitrate uptake in plants. Plant Signaling & Behavior 11(1): e1076603.

Planchet E, Gupta KJ, Sonoda M, Kaiser WM. 2005. Nitric oxide emission from tobacco leaves and cell suspensions: rate limiting factors and evidence for the involvement of mitochondrial electron transport. The Plant Journal 41: 732-743.

Planchet E, Kaiser WM. 2006. Nitric Oxide Production in Plants: Facts and Fictions. Plant Signaling & Behavior. 1 (2): 46-51.

Plaxton WC, Tran HT. 2011. Metabolic adaptations of phosphate-starved plants. Plant Physiology 156: 1006-1015.

Podgórska A, Gieczewska K, Łukawska-Kuz´ma K, Rasmusson AG, Gardeström P, Szal B. 2013. Long-term ammonium nutrition of *Arabidopsis* increases the extrachloroplastic NAD(P)H/NAD(P)$^+$ ratio and mitochondrial reactive oxygen species level in leaves but does not impair photosynthetic capacity. Plant Cell Environ. 36: 2034-2045. doi: 10.1111/pce.12113

Podgórska A, Szal B. 2015. "The role of reactive oxygen species under ammonium nutrition," in Reactive Oxygen and Nitrogen Species Signaling and Communication in Plants, eds K. J. Gupta and A. U. Igamberdiev (Dordrecht: Springer), 133–153.

Polacco JC, Holland MA. 1993. Roles of urease in plant cells. Int Rev Cytol 145: 65-103.

Qin, C. Qian W, Wang W, *et al.* 2008. GDP-mannose pyrophosphorylase is a genetic determinant of ammonium sensitivity in *Arabidopsis thaliana*. Proc. Natl. Acad. Sci. U.S.A. 105: 18308-18313.

Radi R. 2004. Nitric oxide, oxidants, and protein tyrosine nitration. Proc. Natl. Acad. Sci. 101: 4003-4008.

Raghothama KG. 1999. Phosphate acquisition. Annu Rev Plant Physiol. Plant Mol Bio l50: 665-693.

Ramesh SA, Tyerman SD, Xu B, *et al.* 2015. GABA signalling modulates plant growth by directly regulating the activity of plant-specific anion transporters. Nature Communications 6: 78-79. doi:10.1038/ncomms8879.

Ranjan A, Pandey N, Lakhwani D, Dubey NK, Pathre UV, Sawant SV. 2012. Comparative transcriptomic analysis of roots of contrasting *Gossypium herbaceum* genotypes revealing adaptation to drought. BMC Genomics 13: 680. 10.1186/1471-2164-13-680

Rasband WS. ImageJ, U. S. National Institutes of Health, Bethesda, Maryland, USA, https://imagej.nih.gov/ij/, 1997-2016.

Rhoads DM, Umbach AL, Subbaiah CC, Siedow JN. 2006. Mitochondrial reactive oxygen species. Contribution to oxidative stress and interorganellar signaling. Plant Physiology 141 (2): 357-366. doi:10.1104/pp.106.079129.

Richardson AD, Duigan SP, Berlyn GP. 2002. An evaluation of non-invasive methods to estimate foliar chlorophyll content. New Phytologist 153: 185-194. doi: 10.1046/j.0028-646X.2001.00289.x

Riviere-Rolland H, Contard P, Betsche T. 1996. Adaptation of pea to elevated atmospheric CO_2: Rubisco, phosphoenolpyruvate carboxylase and chloroplast phosphate translocator at different levels of nitrogen and phosphorus nutrition. Plant, Cell & Environment 19: 109-117. doi:10.1111/j.1365-3040.1996.tb00232.x

Rockel P, Strube F, Rockel A, Wildt J, Kaiser WM. 2002. Regulation of nitric oxide (NO) production by plant nitrate reductase in vivo and in vitro. Journal of Experimental Botany 53: 103-110.

Rogato A, D'Apuzzo E, Barbulova A, *et al.* 2010. Characterization of a developmental root response caused by external ammonium supply in *Lotus japonicus*. Plant Physiology 154(2): 784-795. doi: 10.1104/pp.110.160309

Rollins JA, Habte E, Templer SE, Colby T, Schmidt J, von Korff M. 2013. Leaf proteome alterations in the context of physiological and morphological responses to drought and heat stress in barley (*Hordeum vulgare* L.). J Exp Boty 64 (11): 3201-12. doi: 10.1093/jxb/ert158

Roosta HR, Schjoerring JK. 2007. Effects of ammonium toxicity on nitrogen metabolism and elemental profile of cucumber plants. J. Plant Nutr. 30: 1933-1951.

Rosales EP, Iannone MF, Groppa MD, Benavides MP. 2010. Nitric oxide inhibits nitrate reductase activity in wheat leaves. Plant Physiology and Biochemistry 49: 124-130.

Rychter AM, Chauveau M, Bomsel JL, Lance C. (1992) The effect of phosphate deficiency on mitochondrial activity and adenylate levels in bean roots. Physiologia Plantarum 84: 80-86.

Rychter AM, Mikulska M. 1990. The relationship between phosphate status and cyanide resistant respiration in bean roots. Physiologia Plantarum 79: 663–667.

Sagi M, Fluhr R. 2006. Production of reactive oxygen species by plant NADPH oxidases. Plant Physiology 141 (2): 336-340. doi:10.1104/pp.106.078089.

Sagi M, Omarov RT, Lips SH (1998) The Mo-hydroxylases xanthine dehydrogenase and aldehyde oxidase in ryegrass as affected by nitrogen and salinity. Plant Sci 135:125–135

Sahu B, ShawB. 2009. Salt-inducible isoform of plasma membrane H^+-ATPase gene in rice remains costitutively ezpressed in natural halophyte *Suaeda maritima*. Journal of Plant Physiology 166: 1077-1089.

Sánchez R, Flores A, Cejudo FJ. 2006. *Arabidopsis* phosphoenolpyruvate carboxylase genes encode immunologically unrelated polypeptides and are differentially expressed in response to drought and salt stress. Planta 223: 901-909.

Sarasketa A, González-Moro MB, González-Murua C, Marino D. 2014. Exploring ammonium tolerance in a large panel of *Arabidopsis thaliana* natural accessions. J. Exp. Bot. 65: 6023-6033.

Schachtman DP, Reid RJ, Ayling S. 1998. Phosphorus uptake by plants: from soil to cell. Plant Physiology 116 (2): 447-453.

Schneider CA, Rasband WS, Eliceiri KW. 2012. "NIH Image to ImageJ: 25 years of image analysis". Nature Methods 9: 671-675.

Schwender J, Goffman F, Ohlrogge JB, Shachar-Hill Y. 2004. Rubisco without the Calvin cycle improves the carbon efficiency of developing green seeds. Nature 432: 779-782.

Secenji M, Lendvai A, Miskolczi P, Kocsy G, Galle A, Szucs A, *et al.* 2010. Differences in root functions during long-term drought adaptation: comparison of active gene sets of two wheat genotypes. Plant Biol. 12: 871-882. 10.1111/j.1438-8677.2009.00295.x

Setién I, Fuertes-Mendizabal T, González A, Aparicio-Tejo PM, González-Murua C, González-Moro MB, Estavillo JM. 2013. High irradiance improves ammonium tolerance in wheatplants by increasing N assimilation, J. Plant Physiol. 170: 758-771.

Shen P, Wang R, Zhang W. 2011. Rice phospholipase Dα is involved in salt tolerance by the mediation of H^+-ATPase activity and transcription. Journal of Integrative Plant Biology 534: 289-299.

Shilov IV, Seymour SL, Patel AA, Loboda A, Tang WH, Keating SP, Hunter CL, Nuwaysir LM, Schaeffer DA. 2007. The Paragon Algorithm, a next generation search engine that uses sequence temperature values and feature probabilities to identify peptides from tandem mass spectra. Mol Cell Proteomics 6 (9): 1638-55.

Siegel LM, Wilkerson JQ. 1989. Structure and function of spinach ferredoxin-nitrite reductase. In Molecular and Genetic Aspects of Nitrate Assimilation, J. L. Wray and J. R. Kinghorn, eds., Oxford Science, Oxford, pp. 263-283.

Sieger SM, Kristensen BK, Robson CA, Amirsadeghi S, Eng EWY, Abdel-Mesih A, Møller IM, Vanlerberghe GC. 2005. The role of alternative oxidase in modulating carbon use efficiency and growth during macronutrient stress in tobacco cells. J. Exp. Bot. 56: 1499-1515.

Singh AP, Dixit G, Kumar A, *et al.* 2015. Nitric oxide alleviated arsenic toxicity by modulation of antioxidants and thiol metabolism in rice (*Oryza sativa* L.). Frontiers in Plant Science 6: 1272. doi:10.3389/fpls.2015.01272.

Skopelitis DS, Paranychianakis NV, Paschalidis K A, Pliakonis ED, Delis ID, Yakoumakis DI, *et al.* 2006. Abiotic stress generates ROS that signal expression of anionic glutamate dehydrogenases to form glutamate for proline synthesis in Tobacco and Grapevine. Plant Cell 10: 2767-2781. doi: 10.1105/tpc.105.038323

Smith FW. 2002. The phosphate uptake mechanism. Plant and Soil 245: 105. doi:10.1023/A:1020660023284

Smith PMC, Winter H, Storer PJ, Bussell JD, Schuller KA, Atkins CA. 2002. Effect of short-term N_2 deficiency on expression of the ureide pathway in cowpea root nodules. Plant Physiology 129 (3): 1216-1221. doi:10.1104/pp.010714.

Smith S, De Smet I. 2012. Root system architecture: insights from *Arabidopsis* and cereal crops. Philos Trans. R. Soc. Lond. B. Biol. Sci. 367, 1441–1452. doi: 10.1098/rstb.2011.0234

Song Y, Dong Y, Kong J, Tian X, Bai X, Xu L. 2017. Effects of root addition and foliar application of nitric oxide and salicylic acid in alleviating iron deficiency induced chlorosis of peanut seedlings. Journal of Plant Nutrition 40 (1): 63-81.

Stasolla C, Yeung EC. 2007. Cellular ascorbic acid regulates the activity of major peroxidases in the apical poles of germinating white spruce (*Picea glauca*) somatic embryos. Plant Physiol Biochem 45: 188-198.

Stirbet A, Govindjee. 2011. Chlorophyll *a* fluorescence induction: a personal perspective of the thermal phase, the J-I-P rise. Photosynth Res 113: 15-61. doi: 10.1007/s11120-012-9754-5.

Stoimenova M, Igamberdiev AU, Gupta KJ, Hill RD. 2007. Nitrite-driven anaerobic ATP synthesis in barley and rice root mitochondria. Planta 226: 465-474.

Strasser RJ, Srivastava A, Tsimilli-Michael M. 2000. "The fluorescence transient as a tool to characterize and screen photosynthetic samples" in Probing Photosynthesis: Mechanism, Regulation and Adaptation, eds M. Yunus, U. Pathre, and P. Mohanty (London: Taylor and Francis), 443-48.

Strasser RJ, Tsimilli-Michael M, Srivastava A. 2004. "Analysis of the chlorophyll fluorescence transient," in Chlorophyll *a* Fluorescence: A Signature of Photosynthesis. Advances in Photosynthesis and Respiration, eds G. C. Papageorgiou and Govindjee (Dordrecht: Springer), 321-362.

Sun C, Lu L, Liu L, Liu W, Yu Y, Liu X, *et al.* 2014. Nitrate reductase–mediated early nitric oxide burst alleviates oxidative damage induced by aluminum through enhancement of antioxidant defenses in roots of wheat (*Triticum aestivum*). New Phytol. 201: 1240-1250.

Sweetlove LJ, Taylor NL, Leaver CJ. 2007. Isolation of intact, functional mitocondria from the model plant Arabidopsis thaliana. Methods in Molecular Biology 372: 125-136.

Szczerba MW, Britto DT, Balkos KD, Kronzucker HJ. 2008. Alleviation of rapid, futile ammonium cycling at the plasma membrane by potassium reveals K^+ -sensitive and -insensitive components of NH_4^+ transport. J. Exp. Bot. 59: 303-313.

Tamura W, Hidaka Y, Tabuchi M, Kojima S, Hayakawa T, Sato T, *et al.* 2010. Reverse genetics approach to characterize a function of NADH-glutamate synthase1 in rice plants. Amino Acids 39: 1003-1012. doi: 10.1007/s00726-010-0531-5

Tang H, Krishnakumar V, Bidwell S, *et al.* 2014. An improved genome release (version Mt4.0) for the model legume *Medicago truncatula*. BMC Genomics 15: 312. doi:10.1186/1471-2164-15-312.

Taylor NL, Day DA, Millar AH. 2002. Environmental stress causes oxidative damage to plant mitochondria leading to inhibition of glycine decarboxylase. Journal of Biological Chemistry 277: 42663-42668.

Tian Q, Chen F, Liu J, Zhang F, Mi G. 2008. Inhibition of maize root growth by high nitrate supply is correlated with reduced IAA levels in roots. J. Plant Physiol. 165: 942-951. doi: 10.1016/j.jplph.2007.02.011.

Tischner R, Kaiser WM. 2007. "Nitrate assimilation in plants" in: Biology of the nitrogen cycle. Bothe H, Ferguson SJ, Newton WE, Eds. Elsevier BV, Oxford, UK. pp 283-301.

Tun NN, Santa-Catarina C, Begum T, Silveira V, Handro W, Floh EIS, Scherer GFE. 2006. Polyamines induce rapid biosynthesis of nitric oxide (NO) in *Arabidopsis thaliana* seedlings. Plant Cell Physiol 47 (3): 346-354. doi: 10.1093/pcp/pci252

Ueda S, Ikeda M, Yamakawa T. 2008. Provision of carbon skeletons for amide synthesis in non-nodulated soybean and pea roots in response to the source of nitrogen supply. Soil Sci Plant Nutr 54: 732-737.

Unwin RD, Griffiths JR, Whetton AD. 2010. Simultaneous analysis of relative protein expression levels across multiple samples using iTRAQ isobaric tags with 2D nano LC-MS/MS. Nat Protoc 5 (9): 1574-82. doi: 10.1038/nprot.2010.123

Valdés-López O, Hernández G. 2014. Phenylpropanoids as master regulators: state of the art and perspectives in common bean (*Phaseolus vulgaris*). Frontiers in Plant Science 5: 336. doi:10.3389/fpls.2014.00336.

Van Aken O, Giraud E, Clifton R, Whelan J. 2009. Alternative oxidase: a target and regulator of stress responses. Physiologia Plantarum 137: 354-361.

Van Kessel MAHJ, Speth DR, Albertsen M, *et al.* 2015. Complete nitrification by a single microorganism. Nature 528(7583): 555-559.

Vance CP, Uhde-Stone C, Allan DL. 2003. Phosphorus acquisition and use: critical adaptations by plants for securing a nonrenewable resource. New Phytologist 157: 423-447.

Vaughan D Ord B. 1990. Influence of phenolic acids on morphological changes in roots of *Pisum sativum*. J Sci Food Agric 52: 289-299.

Vega-Mas I, Marino D, Sánchez-Zabala J, González-Murua C, Estavillo JM, González-Moro MB. 2015. CO_2 enrichment modulates ammonium nutrition in tomato adjusting carbon and nitrogen metabolism to stomatal conductance. Plant Sci.241: 32-44.

Vijayraghavan V, Soole K. 2010. Effect of short- and long-term phosphate stress on the non-phosphorylating pathway of mitochondrial electron transport in *Arabidopsis thaliana*. Funct. Plant Biol 37: 455-466.

Vogels GD, Van der Drift C. 1970. Differential analyses of glyoxylate derivatives. Anal Biochem 33 (1): 143-57.

Walch-Liu P, Ivanov II, Filleur S, Gan Y, Remans T, Forde BG. 2006. Nitrogen regulation of root branching. Ann. Bot. Lond. 97: 875-881. doi: 10.1093/aob/mcj601

Wallace IS, Roberts DM. 2005. Distinct transport selectivity of two structural subclasses of the nodulin-like intrinsic protein family of plant aquaglyceroporin channels. Biochemistry 44: 16826-16834.

Wang BL, Tang XY, Cheng LY, Zhang AZ, Zhang WH, Zhang FS, Liu JQ, Cao Y, Allan DL, Vance CP, Shen JB. 2010. Nitric oxide is involved in phosphorus deficiency-induced cluster-root development and citrate exudation in white lupin. New Phytologist 187: 1112-1123.

Wang J, Zhao J, Tian J, Liao H. 2014. Control of phosphate homeostasis through gene regulation in crops. Current Opinion in Plant Biology 21: 59-66.

Wang L, Jiang L, Mika N, Shigeyuki T, Cheng X. 2015. Excessive ammonia inhibited transcription of MsU2 gene and furthermore affected accumulation distribution of allantoin and amino acids in alfalfa *Medicago sativa*. Journal of Integrative Agriculture 14: 1269-1282. doi: 10.1016/S2095-3119(14)60908-4.

Wang M, Ding L, Gao L, Li Y, Shen Q, Guo S. 2016. The interactions of aquaporins and mineral nutrients in higher plants. Rouached H, ed. International Journal of Molecular Sciences. 17 (8): 1229. doi:10.3390/ijms17081229.

Wang WH, Kohler B, Cao FQ, Liu GW, Gong YY, Sheng S, *et al.* 2012. Rice DUR3 mediates high-affinity urea transport and plays an effective role in improvement of urea acquisition and utilization when expressed in *Arabidopsis*. New Phytol. 193: 432-444.

Wang WH, Köhler B, Cao FQ, Liu LH. 2008. Molecular and physiological aspects of urea transport in higher plants. Plant Sci. 175: 467-477. doi: 10.1016/j.plantsci.2008.05.018

Wang WH, Liu GW, Cao FQ, Cheng XY, Liu BW, Liu LH. 2013. Inadequate root uptake may represent a major component limiting rice to use urea as sole nitrogen source for growth. Plant Soil 363: 191-200. doi: 10.1007/s11104-012-1305-5

Wanke M, Ciereszko I, Podbielkowska M, Rychter AM. 1998. Response to phosphate deficiency in bean (*Phaseolus vulgaris* L.) roots. Respiratory metabolism, sugar localization and changes in ultrastructure of bean root cells. Annals of Botany 82: 809-819.

Watanabe S, Matsumoto M, Hakomori Y, Takagi H, Shimada H, Sakamoto A. 2014. The purine metabolite allantoin enhances abiotic stress tolerance through synergistic activation of abscisic acid metabolism. Plant Cell Environ 37: 1022-1036.

Watson CJ, Miller H, Poland P, *et al.* 1994. Soil properties and the ability of the urease inhibitor N-(N-butyl) thiophosphoric triamide (nbtpt) to reduce ammonia volatilization from surface-applied urea. Soil Biol. Biochem. 26: 1165-1171.

Welinder KG. 1992. Plant peroxidases: structure–function relationships. In: Penel, C., Gaspar, T., Greppin, H. (Eds.), Plant Peroxidases. University of Geneva, Switzerland, pp. 1-24.

Wendehenne D, Durner J, Klessig DF. 2004. Nitric oxide: a new player in plant signaling and defence responses. Curr Opin Plant Biol 7 (4): 449-55.

Wiesler F. 1997. Agronomical and physiological aspects of ammonium and nitrate nutrition of plants. Z. Pflanzenerna¨hr. Bodenkd. 160: 227–238.

Wimalasekera R, Tebartz F, Scherer GFE. 2011. Polyamines, polyamine oxidases and nitric oxide in development, abiotic and biotic stresses. Plant Science 181 (5): 593-603.

Winer BJ, Brown DR, Michels KM. 1991. Statistical Principles in Experimental Design, 3rd Ed. New York, NY: McGraw-Hill.

Wissuwa M, Gamat G, Ismail AM. 2005. Is root growth under phosphorus deficiency affected by source or sink limitations? J Exp Bot. 56 (417): 1943-50.

Witte CP, Tiller SA, Taylor MA, Davies HV. 2002. Leaf urea metabolism in potato. Urease activity profile and patterns of recovery and distribution of ^{15}N after

foliar urea application in wild-type and urease-antisense transgenics. Plant Physiology 128 (3): 1129-1136. doi:10.1104/pp.010506.

Witte CP. 2011. Urea metabolism in plants. Plant Science 180 (3): 431-438.

Wu J, Mao X, Cai T, Luo J, Wei L. 2006. KOBAS server: a web-based platform for automated annotation and pathway identification. Nucleic Acids Res 34 (Web Server issue): W720-W724. doi:10.1093/nar/gkl167.

Wu P, Ma L, Hou X, Wang M, Wu Y, Liu F, Deng XW. 2003. Phosphate starvation triggers distinct alterations of genome expression in *Arabidopsis* roots and leaves Plant Physiology 132: 1260-1271.

Wu P, Shou H, Xu G, Lian X. 2013. Improvement of phosphorus efficiency in rice on the basis of understanding phosphate signaling and homeostasis. Current Opinion in Plant Biology 16: 205-212.

Wu ZM, Tan XM, Chen HZ, Han RC, Shi QH, Pan XH. 2012. Effects of molybdenum nutrition on the total yield of *Salicornia europaea* under different nitrogen solution. Pratacult. Sci. 7: 022.

Xie C, Mao X, Huang J, *et al.* 2011 KOBAS 2.0: a web server for annotation and identification of enriched pathways and diseases. Nucleic Acids Research 39 (Web Server issue): W316-W322. doi:10.1093/nar/gkr483.

Xie Y, *et al.* 2014. Heme-heme oxygenase 1 system is involved in ammonium tolerance by regulating antioxidant defence in *Oryza sativa.* Plant Cell Environ.38: 129-143.

Yamasaki H and Sakihama Y. 2000. Simultaneous production of nitric oxide and peroxynitrite by plant nitrate reductase: in vitro evidence for the NR-dependent formation of active nitrogen species. FEBS Letters 468. doi: 10.1016/S0014-5793(00)01203-5

Yang H, Menz J, Häussermann I, Benz M, Fijiwara T, Ludewig U. 2015. High and low affinity urea root uptake: involvement of NIP5;1. Plant Cell Physiol. 56: 1588-1597. doi: 10.1093/pcp/pcv067

Yu M, Lamattina L, Spoel SH, Loake GJ. 2014. Nitric oxide function in plant biology: a redox cue in deconvolution. New Phytologist 202: 1142-1156.

Zabalza A, Gaston S, Sandalio LM, del Rio LM, Royuela M. 2007. Oxidative stress is not related to the mode of action of herbicides that inhibit acetolactate synthase. Environ Experimental Botany 59: 150-159. doi: 10.1016/j.envexpbot.2005.11.003.

Zaccheo P, Crippa L, Di Muzio Pasta V. 2006. Ammonium nutrition as a strategy for cadmium mobilization. Plant Soil 283: 43-56. doi: 10.1007/s11104-005-4791-x

Zanin L, Tomasi N, Wirdnam C, Meier S, Komarova NY, Mimmo T, *et al.* 2014. Isolation and functional characterization of a high affinity urea transporter from roots of *Zea mays*. BMC Plant Biol. 14: 222. doi: 10.1186/s12870-014-0222-6

Zanin L, Zamboni A, Monte R, Tomasi N, Varanini Z, Cesco S, *et al.* 2015.. Transcriptomic analysis highlights reciprocal interactions of urea and nitrate for nitrogen acquisition by maize roots. Plant Cell Physiol. 56: 532-548. doi: 10.1093/pcp/pcu202

Zdunek-Zastocka E, Lips HS. 2003. Is xanthine dehydrogenase involved in response of pea plants (*Pisum sativum* L.) to salinity or ammonium treatment? Acta Physiol Plant 25: 395-401.

Zeng H, Liu G, Kinoshita T, Zhang R, Zhu Y, Shen Q, Xu G. 2012. Stimulation of phosphorus uptake by ammonium nutrition involves plasma membrane H^+ ATPase in rice roots, Plant and Soil 357: 1-2, 205

Zheng X, He K, Kleist T, Chen F, Luan S. 2015. Anion channel SLAH3 functions in nitrate-dependent alleviation of ammonium toxicity in *Arabidopsis*. Plant Cell Environ. 38: 474-486.

Zhou C, Liu Z, Zhu L, Ma Z, Wang J, Zhu J. 2016. Exogenous melatonin improves plant iron deficiency tolerance via increased accumulation of polyamine-mediated nitric oxide. Iriti M, ed. International Journal of Molecular Sciences 17 (11): 1777. doi:10.3390/ijms17111777.

Zhou Z, Metcalf AE, Lovatt CJ, Hyman BC. 2000. Alfalfa (*Medicago sativa*) carbamoylphosphate synthetase gene structure records the deep lineage of plants. Gene 243: 105-114.

Zhu Y, Di T, Xu G, Chen X, Zeng H, Yan F, Shen Q. 2009. Adaptation of plasma membrane H^+-ATPase of rice roots to low pH as related to ammonium nutrition. Plant, Cell & Environment 32: 1428-1440. doi: 10.1111/j.1365-3040.2009.02009.x

Zorov DB, Juhaszova M, Sollott SJ. 2014. Mitochondrial reactive oxygen species (ROS) and ROS-induced ROS release. Physiological Reviews. 94(3): 909-950.

Zou N, Li B, Chen H, Su Y, Kronzucker HJ, Xiong L, Baluška F, Shi W. 2013. GSA-1/ARG1 protects root gravitropism in *Arabidopsis* under ammonium stress. New Phytologist 200: 97-111.

Zou N, Li B, Dong G, Kronzucker HJ, Shi W. 2012. Ammonium-induced loss of root gravitropism is related to auxin distribution and TRH1 function, and is uncoupled from the inhibition of root elongation in *Arabidopsis*. J. Exp. Bot. 63: 3777-3788.

Zubek S, Turnau K, Tsimilli-Michael M, Strasser RT. 2009. Response of endangered plant species to inoculation with arbuscular mycorrhizal fungi and soil bacteria. Mycorrhiza 19: 113-123. doi: 10.1007/s00572-008-0209